MICROCLIMATE AND BUILDING ENERGY IN THE BUILT ENVIRONMENT:

A Study of Planning High-rise Building Groups at A City-Block Scale in China

By

Xi DENG

Welsh School of Architecture

Cardiff University

A thesis submitted for the degree of

Doctor of Philosophy

In Architecture

2018

DEDICATED TO

My Dear Mother

Associate Professor: Yunxiang YAN

[1953-2015]

Acknowledgements

Firstly, I would like to express my sincere gratitude to my supervisors Prof. Phil Jones, who has been supportive of my work, and Dr. Simon Lannon, who has provided expert guidance.

I would like to thank Miss Katrina Lewis, Dr. Shanshan Hou for their help during my study period.

Lastly, my great deep gratefulness to my family for their support and sacrifice.

Abstract

In the past two decades, most regions of China have gone into the process of rapid urbanisation. In response to the enormous pressure due to the booming economy and fast growth in urban population, large-scale high-rise building group appeared and dominated the civil construction industry. However, these city-block scale estate projects have been criticised for the low-level thermal comfort in poor designed indoor/outdoor spaces, and for its high energy consumption. Chengdu, a megacity in China, has been chosen as the research subject in consideration of its high urbanisation speed with a large number of estate projects at city-block scale and the deteriorating urban built environment. This study investigates the impact of multi-design variables on microclimates and the building energy performance of large-scale buildings through the application of GIS mapping and modellings. The relevant tools used in this study are ArcMap, ENVI-met, and SketchUp integrated with HTB2 and Virvil Plug-in.

The study makes contributions to the research on microclimate and building energy consumption in four aspects. Firstly, it fills the gap in the outdoor thermal comfort and building energy consumption study at city-block scale in China by building up a theoretical framework of planning and design the high-rise building group in China. Secondly, design guidelines are established to improve both the microclimate performance and the building energy performance. Thirdly, a new approach to observe the local temperature of multi-scale subjects in a long-time period is concluded, which provides a new option of a method to analysis microclimate conditions for building scale research. Lastly, this study offers implications to relevant stakeholders for understanding the evaluation of low-carbon development at city-block scale.

There are four phases in this study. In the first phase, document analysis is used to review the existing literature for discovering the research gaps, selecting potential measurements and technical tools, understanding the background and development history of the research subject. The second phase is the observation on microclimate condition. At this stage, on-site local urban heat island intensity is obtained by mapping the derived MODIS satellite data. In the third phase, multi-stage computational simulations will be used to calculate the microclimate performance and building energy performance accordingly. The former provides the predicted local meteorological data to be compared with data obtained from MODIS satellite, as well as the local air temperature of the target project sites for the adjusted simulation of the later which quantify the impact of variation in outdoor temperature. In the last phase, quantitative analysis and discussion are carried out for the results. Therefore, design guidelines of design strategy for mitigating building energy demand and optimising outdoor thermal comfort at city-block scale are concluded.

Contents

List of Figures

List of Tables

List of Abbreviations

GHG	Greenhouse Gas
HVAC	Heating, Ventilation, and Air Conditioning
UHI	Urban Heat Island
GIS	Geographic Information System
UBL	Urban Boundary Layer
UCL	Urban Canopy Layer
HDDs	Heating Degree Days
CDDs	Cooling Degree Days
SVF	Sky View Factor
H/W	Height- Width
LAI	Leaf Area Index
LAD	Leaf Area Density
NDVI	Normalised Difference Vegetation Index
MODIS	Moderate-Resolution Imaging Spectroradiometer
LST	Land Surface Temperature
FAR	Floor Area Ratio
BCR	Building Coverage Ratio
GCR	Green Coverage Ratio
DEM	Digital Elevation Model
D	Distance
TYPE	Project Type
PL	Plot Layout
HEIGHT	Building Height
H/A	Height to Floor Area Ratio
UHII	Urban Heat Island Intensity
HOPSCA	Hotel, Office, Park, Shopping Mall, Convention, and Apartment
COP	Coefficient of Performance
AC	Air Conditioning

Chapter One

INTRODUCTION

1.1 Background

1.1.1 New challenges in the built environment

Since the Industrial Evolution in the 19th Century, significant progress has been achieved in science and technology, which has led to sustained and rapid urbanisation resulting in urban expansion and a rapidly increasing global population. The global urbanisation rate is predicted to increase from 55 per cent of the world's 7.6 billion people in 2018 to 60 per cent of the future 8.1 billion in 2030 (UN-DESA 2008). However, as vast natural resources have been exploited in that process, concerns on the environmental issues are arising globally (Principles 2011). Characterising global climate change (Mideksa & Kallbekken 2010), global temperature change (Figure 1.1), directly or indirectly affects other issues, such as sea-level rising, extreme weather events, agriculture and food security, human health, and human settlements (IPCC 2001). The significant increase in greenhouse gas (GHG) emitted into the atmosphere (Figure 1.2) is considered as the dominant cause of global temperature change (Crowley 2000) (UN-HABITAT 2011). The GHGs, including carbon dioxide and nitrous oxide, absorb and emit radiation, thus warming the earth's surface and lower atmosphere. The urbanisation process with growth in economy and population is the most crucial driver of the increase in carbon dioxide emissions due to fossil fuel combustion (Figure 1.3), contributing more than 60% GHG emissions (IPCC 2014b) (Ponce de Leon Barido, D. and Marshall 2014) (Williams 2007). In particular, sectors allocated to cities, including city-based power stations, heavy industries, motor vehicles, residential and commercial buildings, and water and waste treatment, contribute 30.5 to 40.8 per cent of global GHG emissions (UN-HABITAT 2011). Therefore, the implementation of low carbon strategies in cities has become a significant action for global temperature change (Asia Pacific Energy Research Centre 2014).

In general, the amount of GHG emissions related to fossil fuel energy production, supply and use is up to nearly 70% of total emission globally (IPCC 2007) (Ebinger, Jane; Vergara 2011). Therefore, fossil energy is considered as a driver of climate

change (Ebinger, Jane; Vergara 2011). Moreover, as the primary consumers of energy consuming approximately 80% of all commercial energy produced (Jollands et al. 2008), cities are the keys for addressing the issue energy security as well (Dhakal 2009). In the meanwhile, urban energy efficiency is widely recognised as a cost-effective way to deal with the energy crisis and climate change (Ferrara et al. 2014). Because the significant amount of energy consumed and the carbon dioxide emitted by building sector is substantial (BPIE 2010), improving building energy performance, by decreasing the energy demand, has become an emphasis for researchers and designers (Delgarm et al. 2016). At a macro scale, the arrangement of city planning impacts on the carbon dioxide emissions produced by energy consumption through building heating and cooling (Liu & Sweeney 2012). At a building scale, being leading all end-users of building systems, the Heating, ventilation, and air conditioning (HVAC) system applied for heating, cooling and ventilation dominates a building's energy consumption: 50% to 70% of the total energy consumed for residential buildings and 40% to 60% of the total energy consumption of commercial buildings (Delgarm et al. 2016) (L. Xu et al. 2013). At a building component scale, the thermal properties of the building envelop significantly determine the gain and loss of heat flux (Raji et al. 2015). Accordingly, strategies toward to reducing energy demand have been well studied and implemented at multi-scales, including component scale (Lechtenböhmer & Schüring 2011), building scale (Li & Colombier 2009), neighbourhood scale (Kellett et al. 2013), and urban scale (De Jong et al. 2015).

"Urban areas contain buildings and environments with distinctive topography and bio-physical properties." ---- (Smith & Levermore 2008)

The local climate variation, regarding outdoor temperature change, affects energy sector on both demand side and supply side (Mideksa & Kallbekken 2010) (Schaeffer et al. 2012) (Ciscar & Dowling 2014). Higher temperatures can decrease the heating energy demand in winter but increase the cooling energy demand. As the basic unit of a city, city-block scale plays a vital role in local climate variation (Okeil 2010). *However,*

the existing research on outdoor temperature and building energy consumption at the city-block level is relatively low (Okeil 2010).

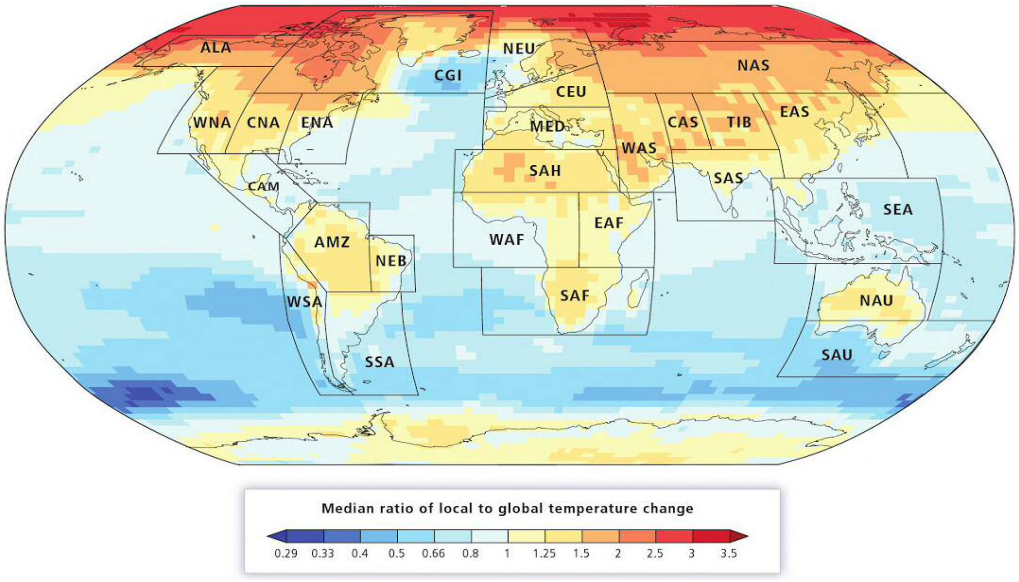

Figure 1. 1: Global temperature change
Source: (IPCC 2014)

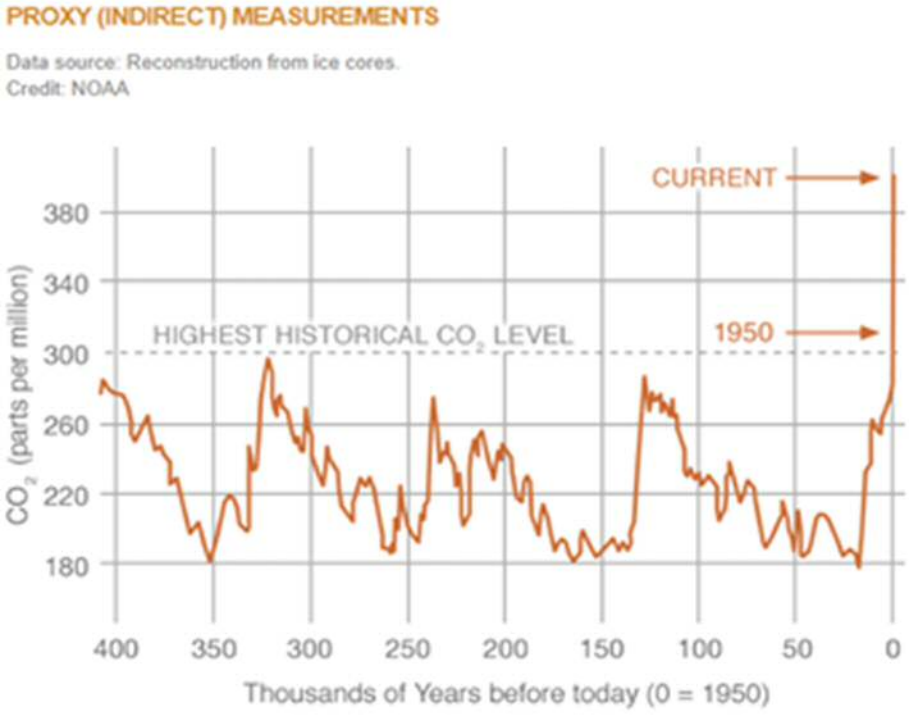

Figure 1. 2: the highest historical CO_2 level
Source: picture from http://climate.nasa.gov/vital-signs/carbon-dioxide/

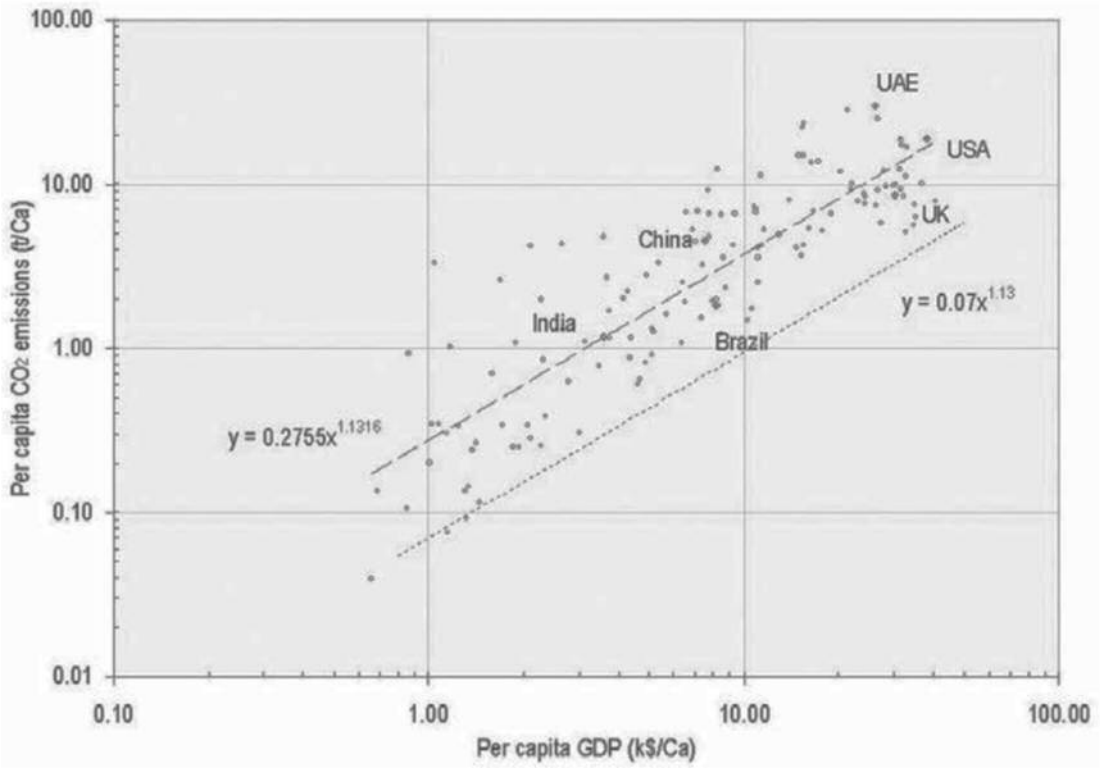

Figure 1. 3: Per capita GDP and per capita CO_2 emissions of most counties
Source: (Principles 2011)

1.1.2 The current situation in the construction industry in China

Like other countries, cities in China have become the primary area of carbon dioxide emissions in China (Chen, W.Z. and Lu 2010) (De-min 2011). Through the implementation of national policies, the concept of a low carbon city has emerged (Li et al. 2012). Though there have been a number of 'low-carbon' related city developments in Chinese cities (Yu 2014), obstacles remain when implementing low-carbon policies in the building industry. The lack of appropriate information and assessment systems has resulted in insufficient local measures for practical implementation strategies (Zhou et al. 2015); professionals, including urban planners, lack understanding of the nature of the low-carbon city concept when adapting it to climate change (Zhou 2015); too much attention paid on the relevant technologies rather than on the institutional development (Yu 2014).

During the period 2000 to 2014, the total energy consumption in China had been tripled, while the gap between production and consumption expanded (Figure 1.4). Cities

contribute 75% of total energy consumption (Dhakal 2009), and while more than one-fifth of total energy was consumed by buildings in 2009, the amount will reach 35% in 2020 (Long 2005). Just as being advocated in other European cities (CEC 1990), the concept of compact urban form was introduced and practised widely in China. In order to efficiently settle the rapidly increasing urban population (Table 1.1) within limited urban areas aiming for preventing extra urban expansions and protecting green fields (Chen et al. 2008). When this concept is reflected at city-block-scale, the real estate developments in the form of large-scale high-rise building groups, appear to dominate the civil construction industry (Wu 2012). This type of modern development is coupled with the boom of the urban population and rapid economic growth in China (Yin 2007) (CDMPB 2012).

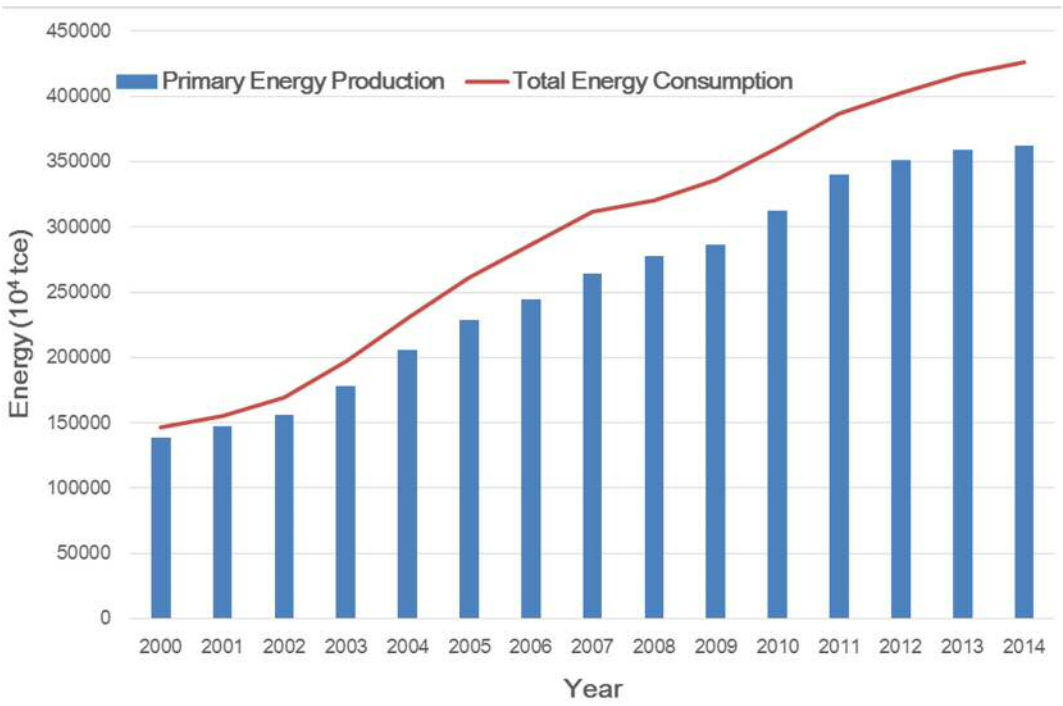

Figure 1. 4: Energy production and total energy consumption in China
Source: (National Bureau of Statistics 2015)

Table 1. 1: Total population and urbanisation rate in China

	1990	1995	2000	2005	2010	2014
Total Population	1,143 million	1,211 million	1,267 million	1,308 million	1,341 million	1,368 million
Urbanisation Rate	26.41%	29.04%	36.22%	42.99%	49.95%	54.77%

Source: compiled from National Bureau of Statistics

1.2 Research aim, research questions, and research objects

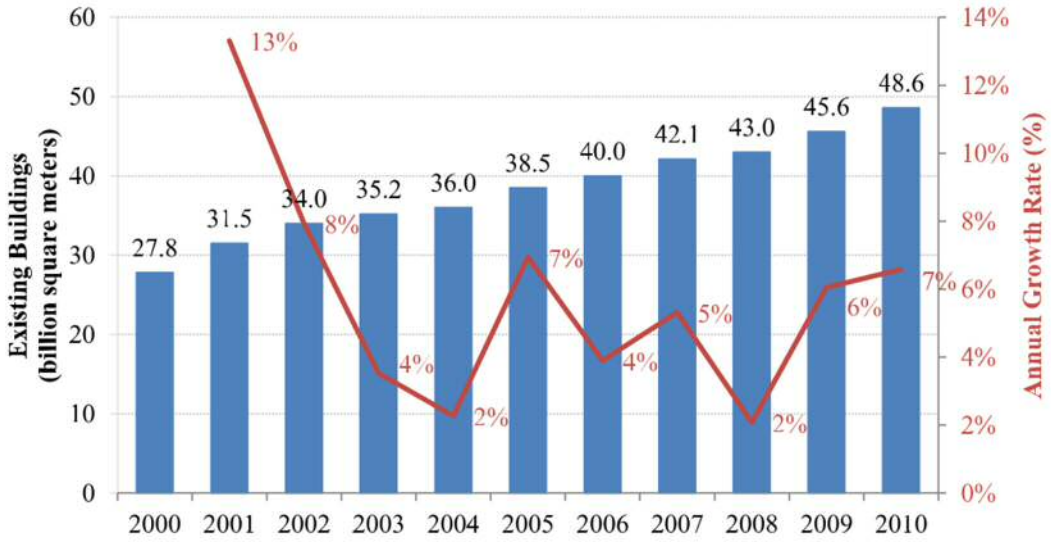

Figure 1. 5: Total building area and the growth rates in China
Source: (Li & Shui 2015)

The mainstream form of booming real estate development projects (Figure 1.5) in Chinese cities has been high-rise buildings. However, several relevant issues are raised: high energy consumption due to massive energy demand contributed from HVAC and other building services(Zhou 2006) (Zhang 2008) (J. Liu et al. 2009), physical and psychological illness caused by limited outdoor activities (Guo 2005) (Run et al. 2002), low livability in poor designed indoor (Ali-Toudert & Mayer 2006) (Zhang 2008) (Zhao 2010) and outdoor spaces (Niu 2004) (Zhou 2011). Nonetheless, many studies have reached conclusions on the impact of energy consumption and outdoor environmental performance. However, the existing literature on the relationship between urban form and outdoor spaces is relatively low. There is limited understanding of the configuration of settlements of building groups, including the surrounding open spaces and the physical properties of those relevant features, the influences on energy performance and outdoor thermal comfort, especially in the circumstances of Chinese cities. Accordingly, current design instructions for the building energy and outdoor livability issues in high-rise buildings are far from being mature and useful enough for achieving low carbon targets on both building energy performance and outdoor thermal performance. *Therefore, the systematic study of*

design strategies for mitigating building energy demand and optimising outdoor thermal comfort in city-block-scale building groups is urgently needed.

This leads to five critical research questions:

1. What is the historical background and development process of real estate projects with large-scale high-rise buildings in at the macro context in China, and what are the present situation of energy performance and outdoor thermal comfort?

2. How do the design features of the urban configuration of the real estate projects have impacts on microclimate condition?

3. What is the diurnal variation of air temperature and other microclimate variables on a summer day and a winter day, accordingly?

4. What are the building energy features of the city-block-scale building groups in China, and how do both the design features and microclimate condition of the urban configuration have impacts on building energy performance?

5. What is the relationship between the microclimate evaluations and building energy performance, what are best strategies planning in city-block-scale real estate projects in China from the perspectives of both mitigating the variation in microclimate and optimising building energy consumption?

6. What are indicators and guidelines for planning city-block-scale building groups?

In order to answer the research questions, this study aims ***to investigate the impact of multi-design variables on microclimates and the building energy performance of large-scale buildings in South-West China, through the application of GIS mapping and modelling***. It identifies the most appropriate 'design forms' for both buildings and outdoor spaces, which will explore the best energy performance as well as the minimised variation in microclimate. Therefore the study will secure the Low-

carbon targets of reducing energy demand and mitigating carbon dioxide emission intensity at estate scale in Chengdu, China.

In order to achieve the research aim, six objectives are derived:

1. *To understand the development low carbon city in the construction sector and the evolution of the real estate projects with large-scale buildings, and investigate the mechanisms of the impacts of design features of the city-block scale project on microclimate condition and building energy performance.*

2. *To explore the influence of design features of the urban configuration of the real estate projects on microclimate condition.*

3. *To understand the diurnal variation of air temperature and other microclimate variables on a summer day and a winter day, accordingly.*

4. *To identify building energy features of the city-block-scale building groups in China, to explore the influence of both design features of the urban configuration and microclimate on building energy performance.*

5. *To identify the issues of theoretical importance on both microclimate and building energy performance, find out best strategies planning in city-block-scale real estate projects in China from the perspectives of both mitigating the variation in microclimate and optimising building energy consumption.*

6. *To derive indicators and build up guidelines for the planning theory of city-block-scale building groups.*

1.3 Research methods and workflow

To answer the research questions and to achieve the aims and objectives, the following methods are summarised:

i) Literature review

The literature was carried out in three phases: Firstly, the literature on the general background of low carbon development and its core issues relevant to construction industry was analysed, in order to explore the research gaps. Secondly, potential technical measurements and technical tools were reviewed and analysed. Thirdly, history related research was reviewed. In this phase, fundamental information about the location of the research subject and history of the evolution of urban development within the city of Chengdu.

ii) Observation through remote sensor, inspection and survey

This method was applied to collect periodical urban heat island (UHI) data for 103 large-scale development projects through processed MODIS satellite data. The derived UHI maps were adopted into a geographic information system (GIS). By overlaying UHI intensity within the selected site area, temperature variation at microclimate scale was obtained. Moreover, the background of the selected projects was reviewed, including the information of location and development history. Through this method, several prototypes of the target architectures have been summarised, and construction parameters have been collected through investigations and surveys.

iii) Computational microclimate simulation and computational building energy simulation

This method was applied at two stages of this study accordingly. In the first stage, simulation of microclimate for target projects predicted meteorological data, including outdoor air temperature, relative humidity, and wind distribution. The simulation was created based on the information collected by literature analysis and survey at early stages of this study. In the second stage, the simulation was used to predict the energy

performance of building groups of target projects for two different cases. The two cases consisted of a ‘control group’ and a ‘sample group’ according to different outdoor temperature conditions.

The applied research methods will be carried out in four phases (Figure 1.6). In the first phrase, document analysis is used to review the existing literature. The method of observation is applied in the second phase; the derived microclimate data will be obtained. In the third phase, multi-stage computational simulations will be used to calculate the microclimate performance and building energy performance accordingly. Lastly, through the analysis and comparison of simulation results, better strategy packages to save energy for architectures are summarised; while in the last phase, quantitative analysis and discussion will be carried out for the results.

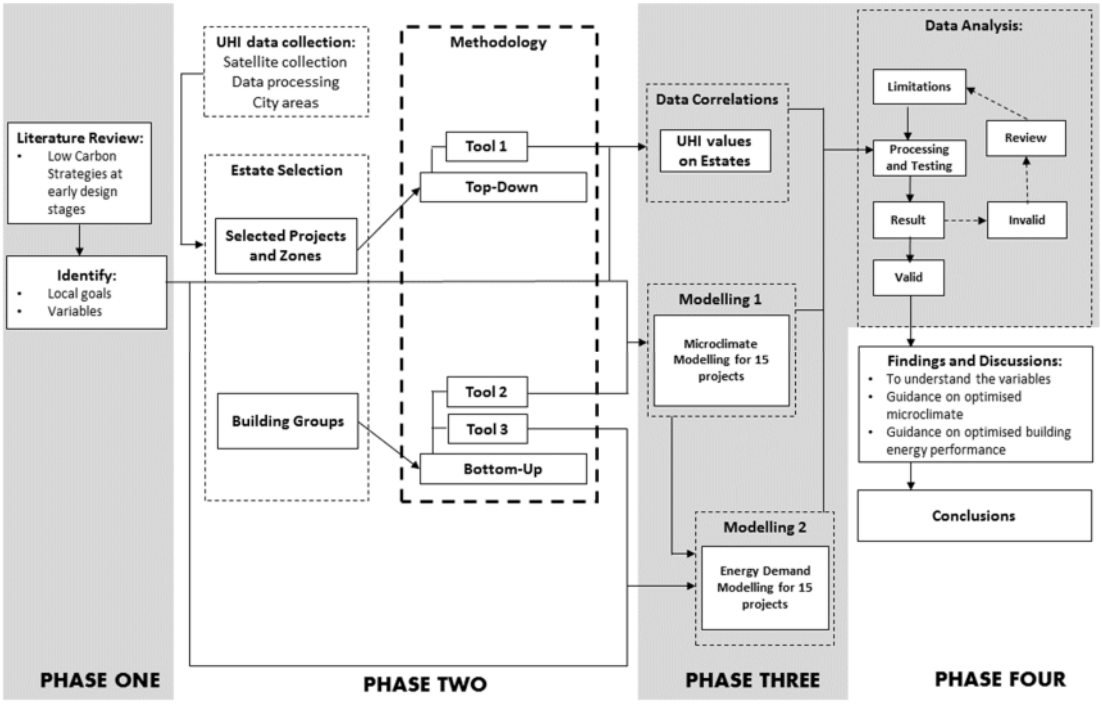

Figure 1. 6: Research workflow

1.4 Research contributions

The main contributions of this study are: (i) The study will fill the research gap by building up a theoretical framework of planning and design for the city-block-scale real estates with concerns on microclimate and building energy consumption in China. (ii) This study will make contributions to understand the mechanisms of development of city-block-scale high-rise buildings, to realise the advantage and disadvantages of existing design forms, and to establish design guidelines to improve both microclimate performance and building energy performance in the city-block-scale building groups. (iii) By using the periodical MODIS satellite data being converted into the UHI intensity map, a new approach to observe the local temperature in a long-time period for multi-scale subjects will be concluded. Both overall long-term conditions and specific details of urban air temperature can be obtained.

Moreover, due to its relatively high resolution of the processed UHI maps, local variation in terms of microclimate at any place within the urban area change will be investigated directly. This innovated methodology provides a new option of a method to analyse the microclimate conditions for building scale research subjects. Lastly, the study will provide a comprehensive understanding on microclimate and building energy consumption in large-scale building group real estates to the relevant stakeholders-scholars, policy-makers, designers and clients- and assist them to understand the evaluation of microclimate and building energy consumption, in order to achieve low-carbon development at city-block scale.

1.5 Thesis structure

This dissertation contains seven chapters, and it is organised as follows (Figure 1.7):

Chapter One: Introduction

Chapter Two: Literature Review

This chapter provides a theoretical framework for the whole research. Firstly, it comprises an introduction of Low-carbon Eco City, which reveals the core issues of the strategies in building industry. In addition, it includes reviews of the existing literature on urban microclimate, its most apparent phenomenon-UHI effect, and building energy performance at a city-block scale. Therefore, this chapter explores the research gaps and summarises the potential design features related to microclimate and building energy consumption.

Chapter Three Research framework and Methodology:

This chapter establishes the research framework and describes the methodology. Firstly, a city-block scale building group centred research framework is proposed, which builds the multi-method research strategy according to the research questions. Moreover, this chapter reviews research methods related to the analysis of urban climate at both the macro and the micro scale. Additionally, it investigates the simulation tools for both microclimate and building energy. Lastly, the background of research subjects, including the targets sites and the city, is introduced.

Chapter Four: Microclimate and remote sensing

This chapter presents the process of microclimate performance study at a city-block scale. It includes mapping UHI values obtained from remotes sensing, correlations between observed UHI values and design variables. Moreover, through analysing the results obtained from the correlations, potential design variables in planning high-rise buildings at city-block scale is investigated.

Chapter Five: Microclimate and simulations

This chapter focuses on analysing and predicting hourly microclimate performance at city-block scale. Firstly, the hourly data, including air temperature and other microclimate variables, obtained through simulation tools is presented. Secondly, this chapter investigates the relationship between the simulated results and design variables. Moreover, it compares the simulated air temperatures with the calculated temperatures which are derived from data obtained in Chapter Five, thereby validating the accuracy of the simulations.

Chapter Six: Building Energy and simulations

This chapter aims to simulate energy demand and derive the energy supply in two stages of simulations. In the first stage of the simulation process, prototypes will be set up to investigate the building energy performance and energy use. In the second stage, the outdoor environment regarding UHI values varied, and this is adopted by adjusting the weather data for the second simulation. Through the two stages of simulation, the impact of variation of outdoor microclimate on building energy performance will be investigated and analysed. Moreover, the influence of design factors on building energy performance will be discussed.

Chapter Seven: Conclusion and Recommendations

This chapter summarises the conclusions of all chapters, which examines the research aim, answers the research questions and achieves the research objects. Furthermore, a design guideline for planning city-block-scale buildings groups is presented. Lastly, it discusses the limitations of this research and makes recommendations for the future research work.

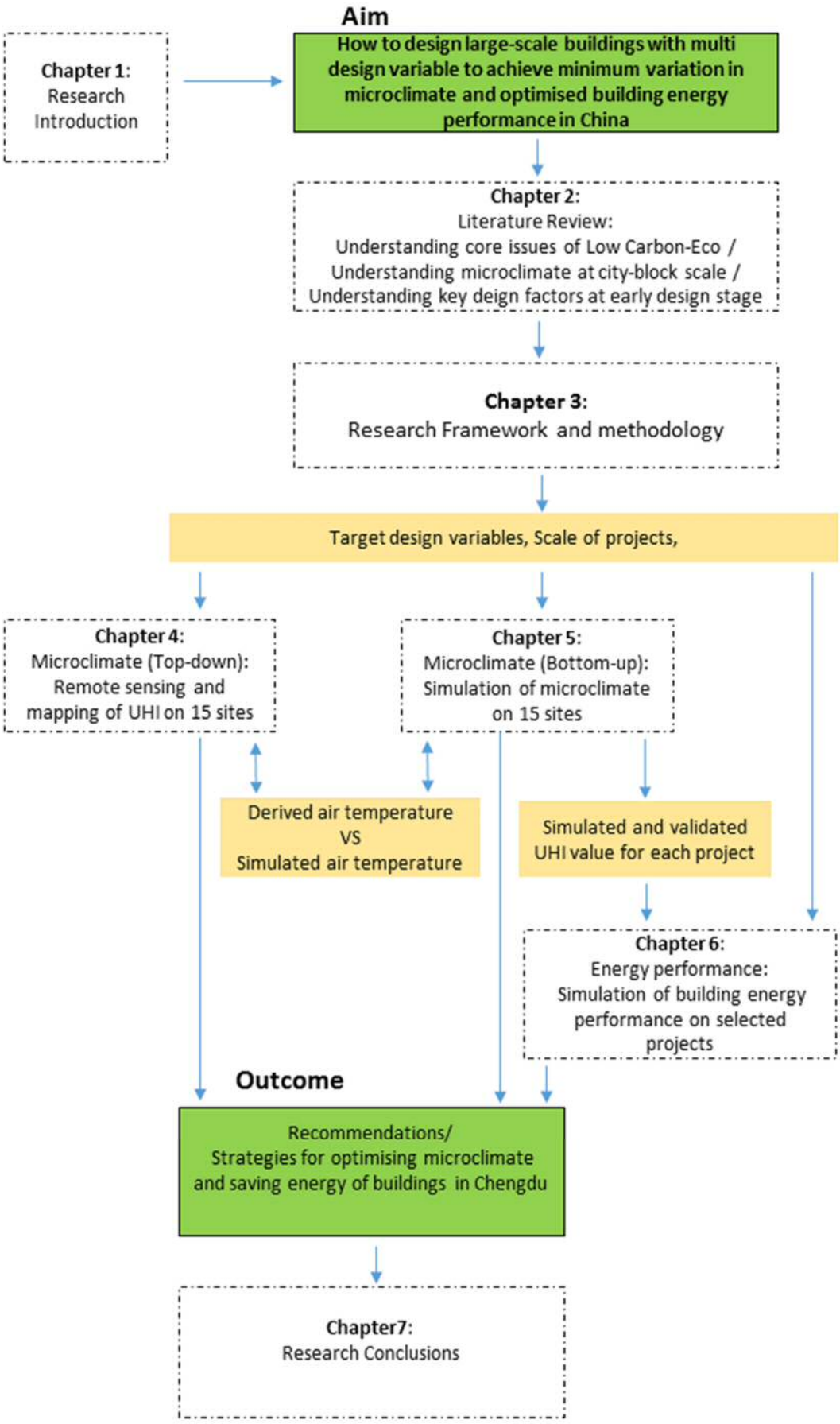

Figure 1. 7: Research structure

Chapter Two

LITERATURE REVIEW

2.1 Introduction

In this chapter, the following research question is answered:

> *'What is the historical background and development process of real estate projects with large-scale high-rise buildings in at the macro context in China, and what are the present situation of energy performance and outdoor thermal comfort?'*

This chapter provides a theoretical framework for the whole research. Firstly, it comprises an introduction of Low-carbon Eco City, which reveals the core issues of the strategies in building industry. In addition, it includes reviews of the existing literature on urban microclimate, its most apparent phenomenon-UHI effect, and building energy performance at a city-block scale. Moreover, it summarises the relevant parameters of urban form and design features were summarised at a city-block scale. Lastly, it reviews the development history of high-rise building groups in Chengdu, and local agendas of research on outdoor thermal comfort and building energy are also discussed. Therefore, this chapter explores the research gaps and summarises the potential design features related to microclimate and building energy consumption.

2.2 Behind the global agenda: energy and livability

2.2.1 Global actions toward climate change

Climate Change has distinctively effect on both natural and human systems (IPCC 2001) (IPCC 2014) considering its potential to be the urgent and irreversible threat to the planet (UNFCCC 2016). Even though the natural variation, including solar irradiance variation, is one of the main factors that cause the global warming effect, evidence (Schlesinger & Ramankutty 1992) (Fröhlich & Lean 1998)(Crowley 2000) indicate that greenhouse effect does exist, and GHG has dominated the global warming since the 20th Century. Therefore, just in case the situation is getting too worse, a series of actions have been taken to reduce the GHGs under the framework of the United Nations Framework Convention on Climate Change (UNFCCC) in recent twenty years (UNFCCC 2015).

Since the Reform and Opening Policies being implemented in 1978, China has been experiencing the rapid process of urbanisation for more than thirty years (Liu & Qin 2016), and the urbanisation rate reached 54.77% in 2014, respectively (China Statistical Bureau (CSB) 2015). With high energy-intensity and coal oriented energy structure, the urbanisation process in China consumes excessive fossil energy and emits a significant amount of CO_2 (Lin & Zhu 2017). Since 2005, China has become the world largest CO_2 emitter (Figure 2.1) (Liu 2015), even though the CO_2 emissions per capita in China is still lower than the most developed countries (Figure 2.2). As one of the main parties in the Framework, China has announced a series of policies at national level to emphasise the global temperature change (NDRC 2007) (State Council 2008) (State Council 2009) (Yuen 2009) (Liu & Qin 2016). In order to the implementation of the national policies, the concept of low carbon city has merged (Li et al. 2012) and becoming a hot topic in China. Till 2014, more than two hundred cities had announced or started their development strategy of eco-city, low carbon city, or low carbon-eco city (Yu 2014).

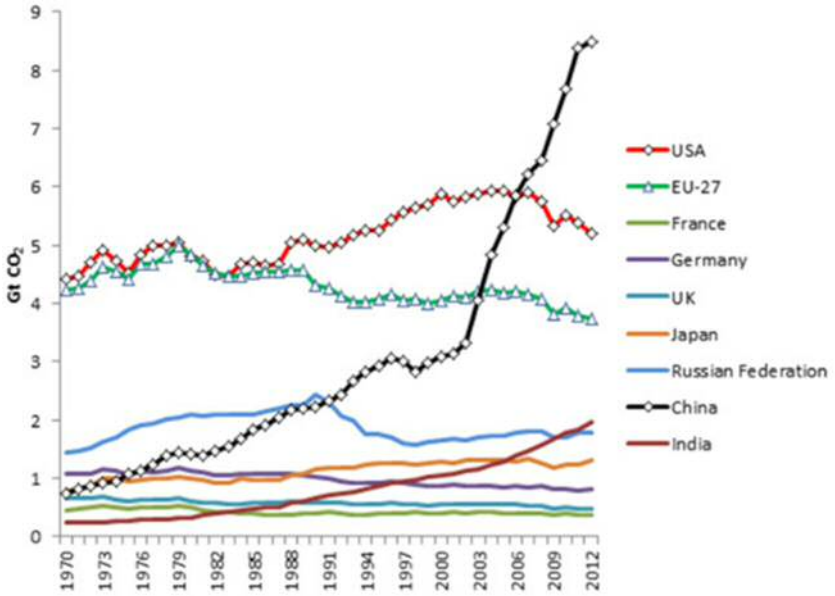

Figure 2. 1: Total CO2 emissions of major emitters in 1970-2012
Source: (Liu 2015)

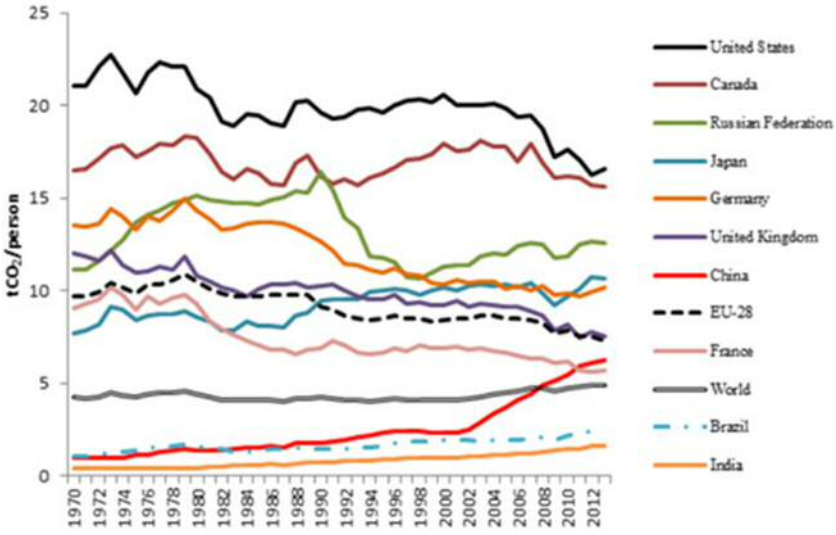

Figure 2. 2: CO2 emissions per capita of major emitters in 1970-2012
Source: (Liu 2015)

2.2.2 World-wide movements towards the low carbon-eco city

Since the early 20th century, many concepts have already been discussed, and theories have emerged for city development (Figure 2.1). These theories and models were proposed during the 20th century to create better, and livable cities and communities, each of them emphasised specific aspects and followed in different logistics, especially at the very beginning stage of each theory. Garden City (Daniels

2009) (Howard 1965) concerns the proportion of green area, residence, industry and agriculture, in order to adopt urban texture with social needs and regulations; Sustainable City focused on macro issues, such as development potential for next generations (Meadows 1998) (Rode & Burdett 2011); Eco city looked after the eco-system as a whole for a human being's living; while Low-carbon city addressed the economic topics, such as renewable energy, energy efficiency and more green transportation (Register 1993) (Yu 2014). As time goes on, different theories and models are being developed and integrated with further aspects, similar factors from each other are also adopted and broader the concerns of some theories. Due to a broader frame (de Jong et al. 2015) and much more interest has been burgeoning (Luederitz et al. 2013), sustainable development becomes the dominant principle in urban development, it sets goals and establishes targets for urban planning (Wan 2004). The very first proposal of low carbon development- 'UK Energy White Paper: Our Energy Future-Creating a Low Carbon Economy'- was issued by the UK government (Z. Liu et al. 2009). Since then, by making less energy-intensive an enhancing the implementation of renewables, low carbon development has been transforming the mode of economic production and consumption.

The concept of 'Low Carbon Eco City' extends the concept of the "Low-Carbon City" (Z. Liu et al. 2009) concerning features of harmony between environment and human beings, which combines 'Eco City' and 'Low Carbon City'. This concept has been merging since the 1980s, and the definition is still being revising (Qiu 2009b). It addresses the principle of energy-saving and environmentally friendly cities by emphasising low energy consumption, pollution and carbon emissions (Zhou et al. 2012b). Comparing to 'Sustainable City', 'Low Carbon Eco city' emphasises the importance of place and method of renewable energy harvest, as well as the reduction in energy per capita(de Jong et al. 2015). Therefore, as a comprehensive theory for city development, 'Low Carbon Eco City' is chosen to be a new target to achieve world-widely, it has become the mainstream of city development in China (Qiu 2009a). Moreover, 'Low-carbon Eco City' has been adopted with core issued disused in Garden

City and Eco City, which sets clear targets in CO_2 emission reduction and seeks a concrete development plan regardless of characteristics of development (Asia 2016).

Table 2. 1: Theories of city development

Concept or Theory	Background, Definition, and Major Content	Application to Low-Carbon Eco-Cities
Building to unify heaven and humanity	The ancient Chinese believed that humanity, society, and nature form a unified whole, each part similarly constituted and governed by the same laws.	Emphasizes the harmony between the city and surrounding environment.
Sustainable city	This concept calls for integrating into the planning and operation of cities the concept that development by this generation should not sacrifice the development potential of coming generations.	The sustainable city concept is helpful for establishing targets but does not reveal the interconnections between various subsystems.
Garden city	Initiated in 1898 by Sir Ebenezer Howard in the United Kingdom, garden cities were intended to be planned, self-contained communities surrounded by "greenbelts" (parks) and containing proportionate areas of residences, industry, and agriculture.	Supports the building of cities that optimize parks and green spaces.
Livable city	Stresses the quality of life in cities. Standard of living refers to the level of wealth, comfort, material goods, and necessities available to the socioeconomic classes in a city.	Focuses on living standard and the quality of urban development.
Eco-city	Ecological cities (eco-cities) enhance the well-being of citizens and society through integrated urban planning and management, harnessing the benefits of ecological systems while protecting and nurturing them for future generations. Eco-cities strive to function harmoniously with natural systems. They value their own ecological assets, as well as the regional and global ecosystems on which all people depend.	The concept of the eco-city is incorporated directly into the development of low-carbon eco-cities.
Low-carbon city	To address climate change, low-carbon cities decouple economic growth from the use of fossil fuel resources by shifting society and economy toward consumption that relies on renewable energy, energy efficiency, and green transportation.	This concept adds an awareness of carbon emissions and climate change to city development.
Low-carbon eco-city	This concept combines the low-carbon city and eco-city in support of energy-saving and environmentally friendly cities, with an emphasis on low energy consumption, pollution, and carbon emissions.	This concept underlies the theory and practice of a low-carbon eco-city.

Source :(Zhou et al. 2012b)

2.2.3 Vital issues among most indicator systems at building group building and scales: Energy performance of buildings and thermal performance of outdoor spaces

The indicator system has been made in low carbon eco-city in China (Yu 2014), however the policy-oriented index with macro targets leads to obstacles in implementing estate projects of building group for planners and designers: the missing of appropriate instructions and assessment systems result in insufficient local measures for practical implementation strategies (Zhou et al. 2015); professionals, including urban planners, lack understanding of the nature of the low-carbon city concept when adapting it to climate change (Zhou 2015). However, several issues

concerned with another independent indicator system from other urban development theories are still instructive for urban planners and architects.

Among the indicator systems of the real practised urban developments in China (Table 2.2) (Zhou et al. 2012a), the energy sector is widely concerned, which is often subcategorised into Energy Intensity, Carbon Intensity, Energy Security, Renewable and Clean Energy, and Sectorial Energy. Heating, cooling, and other electricity use are addressed in Sectorial Energy for commercial buildings and residential buildings. On the other hand, for public green areas and the outdoor built environment, the protection of land and natural system are focused on in the sector of Land Use, And the subcategory-Forestry and public green land - addresses the eco-system in both rural area and urban built-up spaces, respectively.

Table 2. 2: Issues covered in different indicator systems

Category	Energy	Water	Air	Waste	Transport	Economy	Land Use	Social Aspects
Chinese Society for Urban Studies	×	×	×	×	×	×	×	×
CAS/China City Sustainable Development Indicators	×	×	×			×	×	
CASS (Zhuang, Pan, and Zhu, 2011.)	×							
RUC (Zhang, Wen et al. 2008)						×		×
CAS (Wu and Wang, 2005)	×	×	×	×		×	×	×
MoC/MoHURD Eco-Garden City		×	×	×	×		×	
SEPA/MEP Ecological Province/City/ County	×	×	×	×			×	
Tianjin Eco-city	×	×	×	×	×		×	
Caofeidian	×	×	×	×	×		×	
Turpan New District			×					
Guiyang Eco-Civilization City	×	×	×	×	×	×	×	×
Totals	8	8	9	7	5	5	8	4

Source: (Zhou et al. 2012b)

In *the Concept of the Low-Carbon Town in the APEC Region* (Asia Pacific Energy Research Centre 2014), the measures of Low Carbon Town (LCT) are suggested (Figure 2.3), with sectors: 'Town Structure' and 'Buildings', for demand side, which is aiming to guide the urban planner and architects. Specifically, outdoor space environment and indoor energy efficiency are considered as core issues of measures to low carbon development at the schematic stage. Moreover, greenery in buildings (green roof and green wall) and outdoor spaces (tree planting) are specified in the Concept, which aims to CO_2 absorption and mitigation of urban heat island effect.

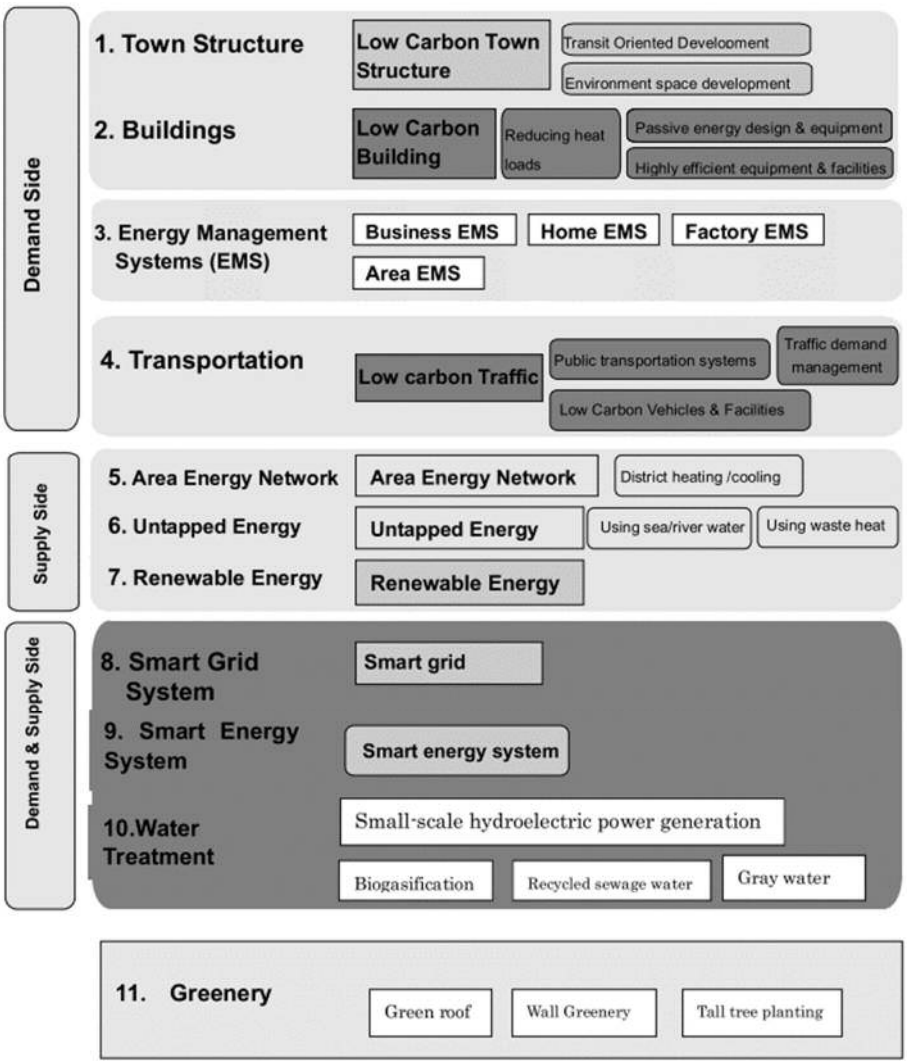

Figure 2. 3: Overview of low carbon measures
Source: (Asia Pacific Energy Research Centre 2014)

In the LEED rating system (U.S. Green Building Council (USGBC) 2016), energy performance and atmosphere are core issues and paid most attention to. The LEED version 4 establishes a priority on building energy efficiency and the reduction of CO_2 and other greenhouse gas emissions (Rastogi et al. 2017). Specifically, there are 4 prerequisites and 33 credits in the EA category, comparing to 1 prerequisite and 26 credits in the SS category. 'Minimum Energy Performance' and 'Optimise Energy Performance' are two of prerequisites required in the Energy and Atmosphere (EA) category. Whitelist 18 out of total 33 credits are awarded in 'Optimise Energy Performance' (Taylor 2010). 'Development Density and Community Connectivity', 'Maximise Open Space' 'Heat Island Effect' are also awarded credits to address

concerns on urban form and microclimate in Sustainable Sites (SS) category (Taylor 2010). Moreover, ecology and energy are emphasised in Green infrastructure and buildings in LEED for Neighbourhood Development (Haapio 2012).

Table 2. 3: Comparison of BREEAM and LEED

	BREEAM 2011		**LEED 2009**	
Certifying body	BRE – British Research Establishment		USGBC – U.S Green Building Council	
Scope of accredited buildings	Over 200,000 buildings		Nearly 45,000 commercial buildings Nearly 19,000 certified residential units and 75,000 registered residential unites	
Schemes	• New Construction • Refurbishment • Code for sustainable homes • Communities • In-use		• New construction and major renovations • Existing buildings • Commercial interiors • Core and shell • Schools • Retail • Healthcare • Homes • Neighborhood development	
Latest version	BREEAM New Construction 2.0:2011		LEED 2009 New Construction and Major Renovations	
Main parameter for reduction	Annual CO_2 emissions		Annual energy cost	
Categorises, available credits and weights	Management	22(w=12)	Sustainable site	26
	Health and Wellbeing	10(w=15)	Water efficiency	10
	Energy	30(w=19)	Energy and atmosphere	35
	Transport	9(w=8)	Materials and resources	14
	Water	9(w=6)	Indoor environmental quality	15
	Materials	12(w=12.5)	Innovation in design	6
	Waste	7(w=7.5)		
	Land use and ecology	10(w=10)		
	Pollution	13(w=10)		
	Innovation	10(w=10)		
Rating scale (%)	Outstanding	>85	Platinum	>80
	Excellent	70	Gold	60 – 79
	Very good	55	Silver	50 – 59
	Good	45	Certified	40 – 49
	Pass	30		

Source: (Schwartz & Raslan 2013)

In BREEAM system (Building Research Establishment (BRE) 2011), the energy use in buildings is focused aim to reducing CO_2 emissions (Schwartz & Raslan 2013) in the Climate and Energy category.15 out of a total 30 credits are assigned in Energy category, in which energy performance improvement is addressed in energy consumption, energy demand and CO_2 emissions. Moreover, the Ecology and Biodiversity category addresses the conservation of on-site ecology in BREEAM Communities (Haapio 2012).

In China, *the Evaluation Standard for Green Building* (China Ministry of Construction

2006) was introduced in 2006 as the first national assessment system of overall environmental performance for buildings of all functions. The Green Building Label system has three levels of labels- One Star, Two Stars, and Three Stars. In the system, Land Management & Outdoor Environment focuses on the mitigation of urban heat island effect planning of greenery infrastructure and Energy Efficiency & Use addresses building energy efficiency and the use of renewable energy.

Table 2. 4: Comparison of BREEAM Communities and LEED for Neighbourhood Development

BREEAM Communities	LEED for Neighborhood Development
Climate and energy – focuses on reducing the project's contribution to climate change Community – supports vibrant communities and encourages to integrate with surrounding areas Place shaping – provides a framework for the design and layout of the local area Ecology and biodiversity – aims at conserving the ecological value of the site Transportation – focuses on sustainable transportation options, and encouraging walking and cycling Resources – emphasises sustainable and efficient use of resources Business – aims at providing opportunities for local businesses and creating jobs in the region Buildings – focuses on the overall sustainability performance of buildings. (BREEAM, 2009) Criteria 51 criteria. All credits are equal. Values criteria from one to three points.	Smart location and linkage – favours development of cities and suburban areas. Development, revitalisation and services are important aspects. Protects areas, populations and water bodies. Neighborhood pattern and design – emphasises public transportation and reduction of auto dependency. Reaches for rich neighbourhood by increasing social interaction. Green infrastructure and buildings – devotes to decreasing environmental impact caused by construction and maintenance of buildings and infrastructure. Energy and water efficiency are emphasised. Additional categories: Innovation and design process Regional priority (LEED, 2009) Criteria 53 criteria. They are evaluated differently – some are worth 10 points, some only 1 point. From the main categories, the total is 100 points, and from additional categories it is possible to earn 10 extra points.

Source: (Haapio 2012)

2.2.4 Summary for design strategies of low-carbon eco development at city-block scale

'Block: row or mass of buildings connected together, as in a terrence, set against a street on the front and bounded by other streets, often mixed use'

-- (Curl 2006)

City-block scale is a subjective and relative concept, and the dimensions could range from 50m to 600m (Huang & Sun 2012) (Zang 2013). City-block is often divided into the isolated site by streets on its boundaries in most cases. Therefore, the urban canyon and building group are also classified in this scale (Kikegawa et al.

2006)(Kuang et al. 2015). And this scale is the usual size for land auction and development, especially in China (Yang 2008) (Huang & Sun 2012). ‘Superblock’, ‘Mega community’ with large-scale building group- housing estates and city complex with multi-function is increasingly frequently planned.

City-block scale is an intermediate, or mesoscale, between the macroscale and microscale. And the latter correspond to low carbon urban planning and low carbon buildings, respectively, which have been widely studied in terms of urban developments. Therefore, the city-block scale is a perfect subject for a low-carbon development project in practice, and the implementation strategies will combine the measures from both macro and micro. In the meanwhile, the research at this scale is a solid supplementary for the general framework of low carbon eco-development in the construction industry (Zang 2013). Specifically, Site Planning and- compact urban structure and breezeway, and Site Ecology- greenery in outdoor spaces are addressed from an urban planning perspective; Building energy efficiency- passive and low energy design, Greenery- a green roof, green wall, and site greening are focused on in a building scope. From stakeholders’ (owners and users) point of view, the living community is mostly at a city-block / neighbourhoods scale, and a bottom-up approach of planning a town/ city- identifying and promoting community initiatives with participation of stakeholders as a base or starting point for the urban planning solutions (Alexander et al. 1985) (Xing et al. 2017).

In summary, the building energy consumption and outdoor thermal environment are core issues for the low-carbon eco development at city-block scale for planners, designers, and stakeholders. Specifically, reducing energy consumption for heating, cooling and lighting in commercial and residential buildings, increasing the efficiency of building services, optimising the on-site microclimate are vital measures to achieve a reduction in energy and CO_2 emission at city-block scale.

2.3 Microclimate and urban heat island effect

2.3.1 Introduction

'The climate of a location is usually understood as comprising a number of physical aspects and includes temperature, the moisture content of the air, rain, wind, fog, snow, insolation, cloudiness and general air quality (as determined by various pollutants and particulate matter).' -- (Erell et al. 2011)

'Atmospheric processes present themselves on a continuum of temporal and spatial scales, ranging from an upper limit of 108 m and 107 s for atmospheric standing waves to 10-2 m and 10° s for the smallest turbulent eddies.'

-- (Steyn et al. 1981)

'Distinctly urban phenomena exist on length scales characteristic of buildings to those of a metropolitan region and beyond (100 to >105 m) and have timescales extending from the life of a plume to the life of a city (say 102 to >109 s).' -- *T. R. Oke* (1981)

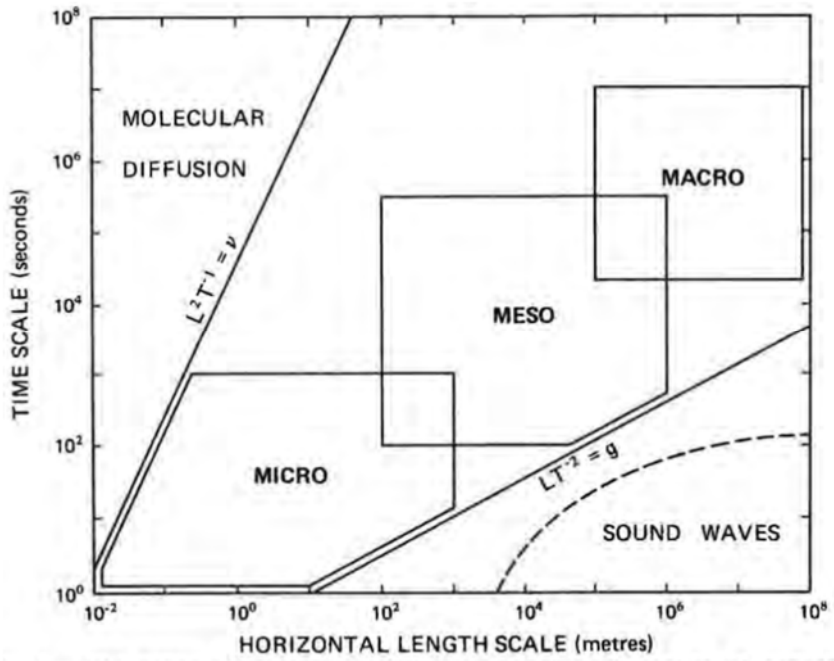

Figure 2. 4: The range of temporal and horizontal length scales of atmospheric processes

Source: (Steyn et al. 1981)

Study and discussion on the relationship between climate and urban environment started more than a century ago, but the research with theoretical systems has not been established until recent decades (Erell et al. 2011). In the early 1980s, based on the kinetic energy of atmospheric motions, the meteorology was defined into three scales: macro-scale, mesoscale and micro-scale (Figure 2.4) (Steyn et al. 1981). The classification of scale for climatology is based on a different logic from meteorology, which is the phenomenon instead of processes (Steyn et al. 1981). However, the microclimate can still be classified according to the same horizontal length scales applied in classification of scale in meteorology (Table 2.5), which is between 10^{-2} to 10^{3} m covering from single building/city-block to the neighbourhood (Erell et al. 2011). The other three larger scales are referred climate at city-level, regional level and state-level, respectively. Therefore, *microclimate can be defined as the prevailing climate at a micro-scale* (Erell et al. 2011).

Table 2. 5: Framework for urban climate classification

(a) TURBULENT BOUNDARY LAYERS

Layer	Flow Characteristics	Dimensions	Scale
I. Urban canopy (building) layer (UCL)	Highly turbulent, controlled by roughness elements	Same as H, typically 10m	Micro
Turbulent wake layer	Highly turbulent wakes and plumes, transition zone	2D – 3D, typically 20-40m	Micro
II. Urban boundary layer	Turbulent, includes surface and mixed layers	Depends on surface fluxes of heat and momentum. Typically – day 1km, night 0.2 km	Local and Meso

(b) URBAN MORPHOLOGY

Urban unites	Urban features	Urban climate phenomena	Dimensions			Scale
			H	W	L	
1.Building	Single building, tree or garden	Wake, plume or shadow	10m	10m	10m	Micro
2.Canyon	Urban street and bordering buildings or trees	Canyon shelter, circulation, shade, bioclimate	10m	30m	300m	Micro
3.Block (Neighbourhood)	City block, park, factory complex	Climate of parks, building clusters, cumulus, mini-breezes		0.5km	0.5km	Local
4.Land-use zone	Residential, commercial, Industrial etc.	Local climate incl. winds, cloud modification		5km	5km	Local
5.City	Urban area	Heat island, urban circulation, urban effects in general		25km	25km	Meso

Source: (Oke 1984)

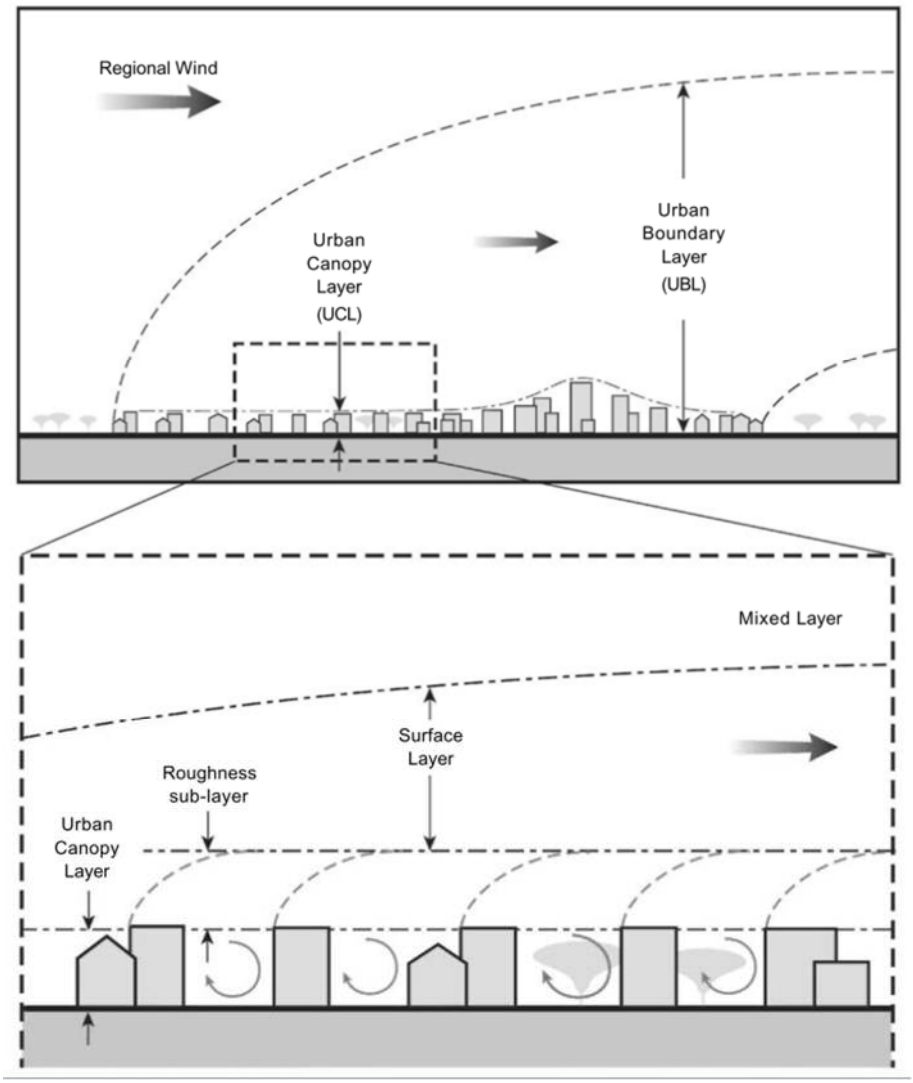

Figure 2. 5: Schematic section- different layers in the urban atmosphere
Source: (Erell et al. 2011)

On the other hand, in a vertical direction, the atmosphere in an urban area can be divided into several parts, and the lowest part is named the *urban boundary layer* (UBL) (Figure 2.5). The UBL is significantly influenced by the nature of the urban terrain, and four sub-layers can be further divided according to the vertical position relative to the full surface: Mix Layer, Surface Layer, Roughness sub-layer, and Urban Canopy Layer (UCL). UCL was considered as an independent layer rather than the lowest sub-layer of UBL in early studies (Oke 1982) (Oke 1984). Compared to other layers, the UCL is the at lowest level-below roof, which is made of trees, buildings, courtyards, gardens, lawns, etc. (Oke 1989) (Roth et al. 1989) (Oke 2011), where the microclimate is established with climate indicators, including air temperature, wind speed, relative

humidity, radiation intensity and so on (Li et al. 2012) (Deng 2016). At this scale, the design of space, physical properties of applied materials and vegetation as landscape modify the microclimate, which all become design parameters (Erell et al. 2011). *Therefore, the microclimate is an architectural issue, especially in terms of the study on both the outdoor thermal environment and building energy performance* (Erell et al. 2011).

2.3.2 Features of microclimate

Microclimate is not only a general name for the condition of all meteorological parameters at a micro-scale but also a description of the phenomena of a recurring dynamic process of physical interaction among the microclimate features (Deng 2016) (Li et al. 2012). In this section, the process of energy exchange occurred in microclimate will be introduced.

i) Surface energy balance

The First Law of Thermodynamics states that energy can be transformed from one form to another, keeping the total energy constant in an isolated system:

$$\Delta U = Q - W \tag{2.1}$$

Where ΔU is the internal energy, Q is the heat applied to the isolated system, W is the work done by the system.

While in the surface layer, the surface energy balance can be derived from the First Law of Thermodynamics above, which is:

$$E_{input} = E_{output} + E_{storage\ change} \tag{2.2}$$

The equation (2.2) (Oke 2002a) indicates that the energy input and output are not always equalled at all times. However, energy difference will occur due to energy accumulation or storage in components of the system in a short period. Due to the difficulty in assigning the values of the parameter in UCL, the smaller scale-urban

canyons is more appropriate for the measurement or modelling the energy balance in a microclimate.

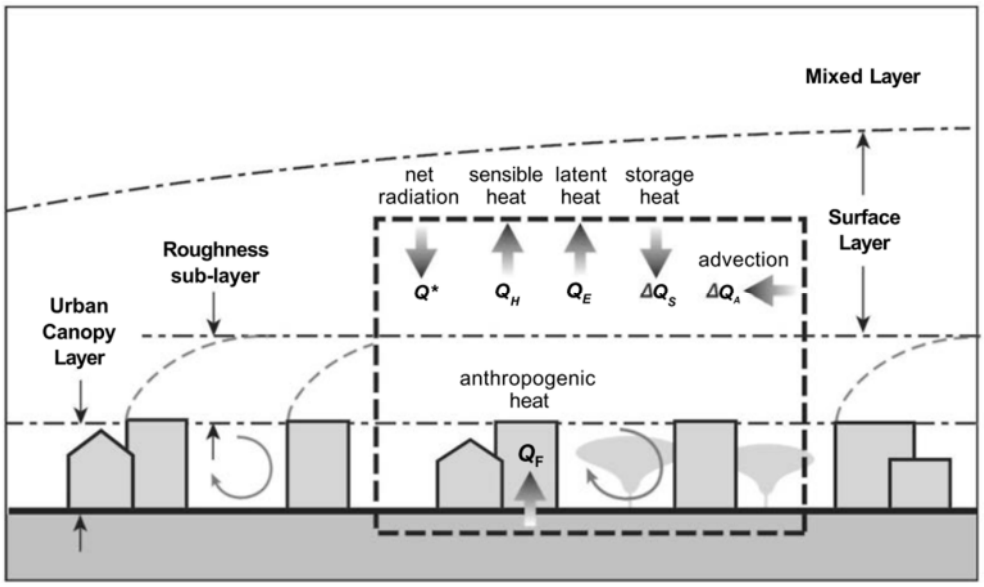

Figure 2. 6: Schematic section- surface energy balance
Source: (Erell et al. 2011)

The simplified equation of surface energy balance (SEB) is derived from the equation (2.3) (Oke 1982) (Figure 2.6):

$$Q^* + Q_F = Q_E + Q_H + \Delta Q_S + \Delta Q_A \qquad (2.3)$$

where Q^* is the net radiant flux, which is contributed the mostly by short-wave radiation exchange by and solely by long-wave radiation exchange at night; Q_F is the anthropogenic heat flux entering the UBL by human activities, including fuel use and heat released from electrical/thermal appliances; Q_E is the latent heat flux; Q_H is the sensible heat flux, ΔQ_S is the energy stored in the building components or outdoor surfaces; ΔQ_A is the heat advection, it depends on the parameters of wind and then the thermal condition of the outdoor spaces, which may be neglected in the dense urban area (Oke 1974).

ii) Solar radiation

The Sun is regarded as the sole source of radiant energy input to the Earth-

Atmosphere system (Oke 2002a). At the surface of the Earth, it is considered the primary source of energy in UCL, as well (Erell et al. 2011). The process of radiation exchange is occurring anywhere in the outdoor surface, and this process is affected by urbanisation *through building up the urban geometry interfering the transmission of radiance, varying in the thermal property (albedo and emissivity) of artificial construction materials, and producing the air pollutants* (Oke 1982). Moreover, the albedo (α) is the ratio- athe mount of reflected radiation out of total incoming radiation, it is defined as the reflectivity of hemispherical- and wavelength-integration, which applies to surfaces, including simple uniform, heterogeneous and complex ones (Taha 1997b). Typical albedo in most cities ranges from 0.10 to 0.20, but it exceeds to 0.30-0.45 in some North African towns (Taha 1997b). As shown in Table 2.6, albedo and emissivity vary in different natural materials, which are higher than average urban albedo. So the absorption of shortwave radiation in urthe ban surface is more efficient compared to that in rural terrain.

Table 2. 6: The Albedo and thermal emissivity of natural materials

Surface	Remarks	Albedo α	Emissivity ε
Soils	Dark, wet Light, dry	0·05– 0·40	0·98– 0·90
Desert		0·20–0·45	0·84–0·91
Grass	Long (1·0 m) Short (0·02 m)	0·16– 0·26	0·90– 0·95
Agricultural crops, tundra		0·18–0·25	0·90–0·99
Orchards		0·15–0·20	
Forests			
Deciduous	Bare Leaved	0·15– 0·20	0·97– 0·98
Coniferous		0·05–0·15	0·97–0·99
Water	Small zenith angle Large zenith angle	0·03–0·10 0·10–1·00	0·92–0·97 0·92–0·97
Snow	Old Fresh	0·40– 0·95	0·82– 0·99
Ice	Sea Glacier	0·30–0·45 0·20–0·40	0·92–0·97

Source: (Oke 2002a)

As shown in Figure 2.7, all radiation in the lower-layer is partially absorbed and stored in the air. A small amount of the incoming short-wave radiation- Flux 1 (directly from the Sun and reflected from the clouds)- is partly scattered back to upper layers, while the rest majority of the radiation- Flux 2- is transmitted to the surface. Most energy from Flux 2 is absorbed and stored in the surface, the rest radiation of Flux 3 is reflected in the atmosphere. Moreover, the most of Flux 3 is transmitted directly into upper layers, the rest part-Flux four is scattered again to the surface and absorbed by the surface buildings. However, due to the variation in the radiation received at the surface and lower urban albedo, the difference of net short-wave radiation between urban and rural is rather small (Oke 1982). On the other hand, the surface is emitting long-wave radiation- Flux 5- into the atmosphere, while the heated surface by absorbing short-wave radiation enhances the emissivity. Part of Flux 5 is absorbed by the low-layer atmosphere, and rest is transmitted into the upper layers. After patricianly absorbing Flux 6 from the upper layers, long-wave Flux 4 is stored in surface buildings. In addition, the air at lower-layer atmosphere together with the pollutants reemits long-wave radiations, and part of it- Flux 8- is trapped into the surface.

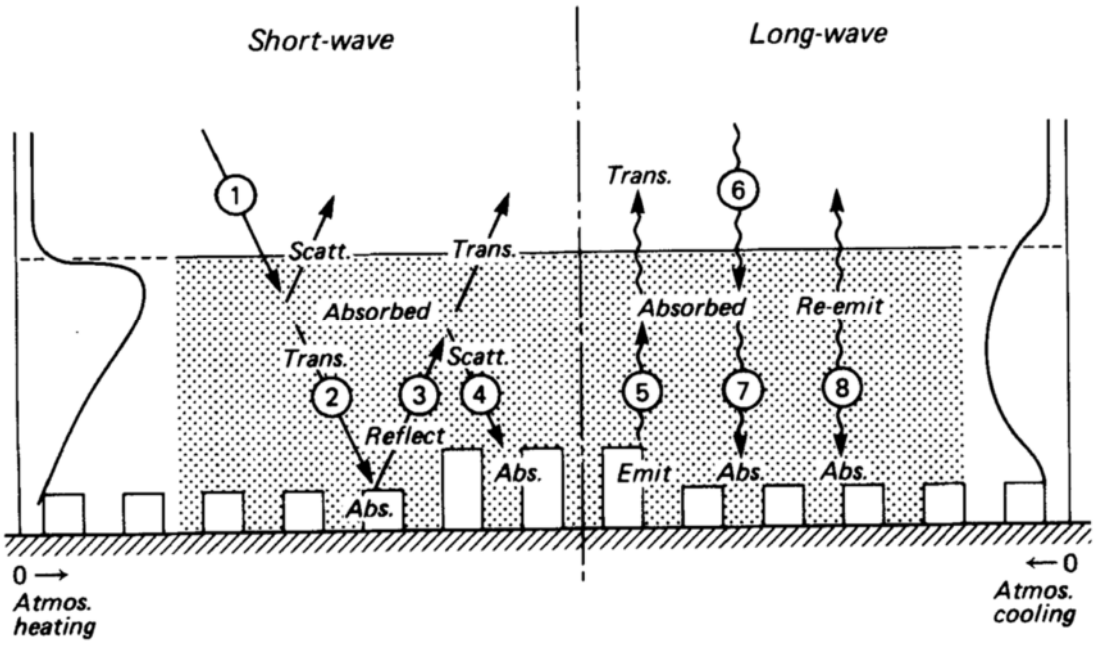

Figure 2. 7: Schematic section- radiative exchange in UBL
Source: (Oke 1982)

The following equation (Oke 1974) may describe the surface radiation balance above :

$$Q^* = K\downarrow - K\uparrow + L\downarrow - L\uparrow \quad (2.4)$$

Where Q^* is net all-wave radiative balance; $K\downarrow$ is the sum of direct short-wave radiation (directly from the sun) and diffuse short-wave radiation (reflected from clouds or pollutants); $K\uparrow$ is reflected short-wave radiation ($K\uparrow = (K\downarrow)\,\alpha$, α is surface albedo; $L\downarrow$ is long-wave radiation emitted to the surface from the atmosphere; $L\uparrow$ is the long-wave emitted to the atmosphere from the surface. Therefore, the equation can be deformed to the following (Erell et al. 2011):

$$Q^* = \left(K_{dir} + K_{dif}\right)(1-\alpha) + L\downarrow - L\uparrow \quad (2.5)$$

where K_{dir} is direct short-wave radiation (directly from the sun); K_{dif} is diffuse short-wave radiation (reflected from clouds or pollutants).

iii) Latent heat flux

Latent heat flux affects the available radiations that cause a rise in air temperature, which is affected by the availability of moisture (Erell et al. 2011). In the near-surface climate, the process of water exchange occurs everywhere. Specifically, water evaporating from the water bodies, from wet soil, and from transpiring vegetation, gains moisture in the atmosphere. Considering that fact that the two effects- evaporation in soil and transpiration in plants- always process simultaneously, the term evapotranspiration is applied to describe the transfer of water from the vegetated surface into the atmosphere (Taha 1997b). When the environment is warm with low relative humidity, the evapotranspiration process can bring moisture into the air and reduces the temperature (Golany 1996), and it creases cool area of 2-8°C lower in air temperature compared to the surroundings (Taha 1997b). Therefore, in the urban built-up area where artificial materials remove the vegetation lowering evapotranspiration rate, and the decreasing latent heat leads to increase in sensible heat releasing into the dry surroundings. Consequently, higher temperatures will be observed in the built-

up area compared to rural area.

iv) Storage heat flux

In the urban microclimate, there are different materials used for street and buildings, and the thermal properties of these materials are often different from those of natural ones. Specifically, the thermal mass of buildings is significantly larger than that of trees of the equivalent volume, and the buildings provide substantial reservoirs of heat storage and release (Oke 1989). Moreover, the thermal conductivity (k), heat capacity ($C = \rho c_p$), and thermal admittance ($\mu = kC^{-1/2}$) of each material used in the urban microclimate determine their ability in energy absorption, storage and emission. As an important component of SEB, the net storage heat flux accounts for significant ama ount of net radiation in daytime (Pearlmutter et al. 2009), and it is difficult to directly measure, or even estimate the storage heat at micro-scale due to the complexity of the physical (optical and thermal) properties of the surfaces (Christen & Vogt 2004). The practical methods to specify the value of storage heat including objective hysteresis model (OHM) (Grimmond & Souch 1994)(Arnfield & Grimmond 1998), and deriving as the residual in the energy balance assuming the closure of overall SEB (Offerle et al. 2006) (Pearlmutter et al. 2009). Anthropogenic heat and advection are often ignored due to obstacles in measurement (Erell et al. 2011).

v) Anthropogenic heat flux

Human activities cause the anthropogenic heat with energy consumptions in traffic (combustion of fuels in vehicles), buildings (operating energy in residential commercial and industrial), and metabolism (heat released from human). It heats the near-surface air temperature (Taha 1997b), Admitting that it has been neglected in the calculation of the other heat flux, however, anthropogenic heat may be significant in certain conditions (Oke 1982). It may be significant compared to the solar energy in summer (Oke 1974), due to higher usage in building services. Early studies (Taha et al. 1992) show that the anthropogenic heat in a large city can increase 2-3℃ in daily average temperature (Taha 1997b). Based on the sources of heat, measurement of

anthropogenic heat is carried out through different approaches. Specifically, with the hourly database of traffic flows through simple observations and estimations in a city, and the standards value of anthropogenic heat for singles vehicle according to statistic data, the anthropogenic heat flux in traffic can be estimated (Masson 2006); for measurement of anthropogenic heat from buildings, the inventory approach- mapping of energy consumption (Pigeon et al. 2007), the micrometeorological approach- estimating anthropogenic heat as the residual in the energy budget (Kato & Yamaguchi 2005), and the modelling approach- integrating the simulated energy results with GIS database according to the building prototypes, can be used for public buildings, and different methods can be applied to the industrial buildings considering the more concentrated sources (Erell et al. 2011); in addition, the metabolism has limited contribution (less than 5 per cent)on total anthropogenic heat flux (Erell et al. 2011).

vi) Wind

Wind is another essential feature of UBL. Due to the friction at the surface where wind filed contacts with the terrain, the mean horizontal wind speed ($\bar{u}$) is sharply decreased (Oke 2002b) (Figure 2.8). Regardless of the significant thermal effects, the magnitude of this fraction is affected by the roughness (z_0) of the surface (Figure 2.8). Due to the fact that the fraction exists everywhere in the real environment, there is roughness in any surface of materials (Table 2.7). The urbanisation, in terms of urban morphology, modifies the roughness of surface, thereby increasing the Z_g up to 518m, comparing to 274m in open flat country and 396m in the sub-urban area (Erell et al. 2011).

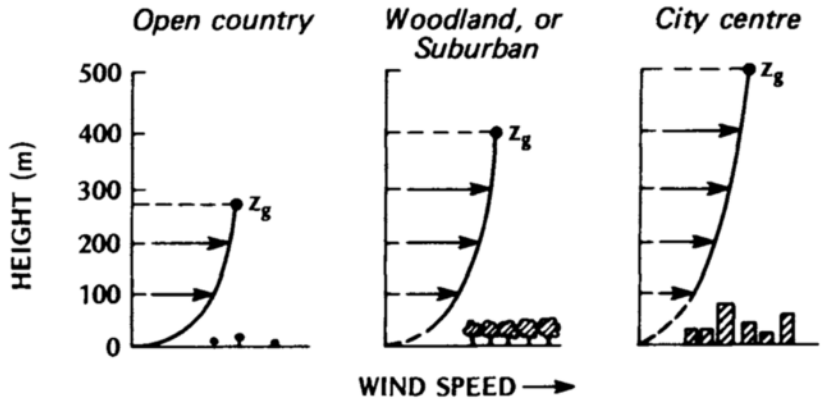

Figure 2. 8: The effect of terrain roughness
Source: (Oke 2002b)

Table 2. 7: Aerodynamic properties of natural surfaces

Surface	Remarks	z_0 Roughness length (m)	d Zero plane displacement* (m)
Water†	Still – open sea	$0{\cdot}1-10{\cdot}0 \times 10^{-5}$	–
Ice	Smooth	$0{\cdot}1 \times 10^{-4}$	–
Snow		$0{\cdot}5-10{\cdot}0 \times 10^{-4}$	–
Sand, desert		0·0003	–
Soils		0·001–0·01	–
Grass†	0·02–0·1 m	0·003–0·01	≤ 0·07
	0·25–1·0 m	0·04–0·10	≤ 0·66
Agricultural crops†		0·04–0·20	≤ 3·0
Orchards†		0·5–1·0	≤ 4·0
Forests†	Deciduous	1·0–6·0	≤ 20·0
	Coniferous	1·0–6·0	≤ 30·0

Source: (Oke 2002b)

vii) Summary

In summary, a variety of energy balance systems exist in the UCL, radiation exchange occurs anywhere in these systems affected by many variables, including moisture availability (Oke 1982). All the contributions by features -including albedo, urban morphology, thermal mass, less vegetated surface, anthropogenic heat, wind, and so on- impact the urban microclimate. Consequently, *significantly more heat is gathered and accumulated in the urban near-surface, and the temperature trends to be raised higher than that in a rural area. This phenomenon is called the 'urban heat island (UHI) effect'*.

2.3.3 Urban heat island effect

i) Definition and introduction

'The urban heat island (UHI) effect, i.e. the characteristic warmth of a settlement compared with its surroundings, it the best-known climatic response to disruptions caused by urban development. If your car has a thermometer, the warmth is relatively easy to observe from the profile of temperatures as you cross a town or city, especially at night and if winds are weak and clouds are sparse.' -- (Oke 2011)

'Heat island- The microclimate, area, or patch of warmer air that forms in and over urbanised areas because of paved or impervious surfaces, reflection from upright

structures, and buildings gathering heat or generating it and then releasing it.' -- (Christensen 2005)

There are many definitions of urban heat island (UHI) (Figure 2.9) in the existing literatures from different perspectives (Commission of the European Communities (CEC) 1990) (Taha 1997b) (Stone & Rodgers 2001) (Wong & Yu 2005) (Q. Chen et al. 2009) (Vardoulakis et al. 2013). It exists as a heat dome of warmer air over the city (Quattrochi et al. 2000). However, all of the definition focuses on the difference in air temperature between the urban area and rural area and emphasise the impact of urbanisation on micro- and mesoscale climates. The urban heat island intensity (UHII) is determined by the difference of temperature between the urban and rural area (Rizwan et al. 2008).

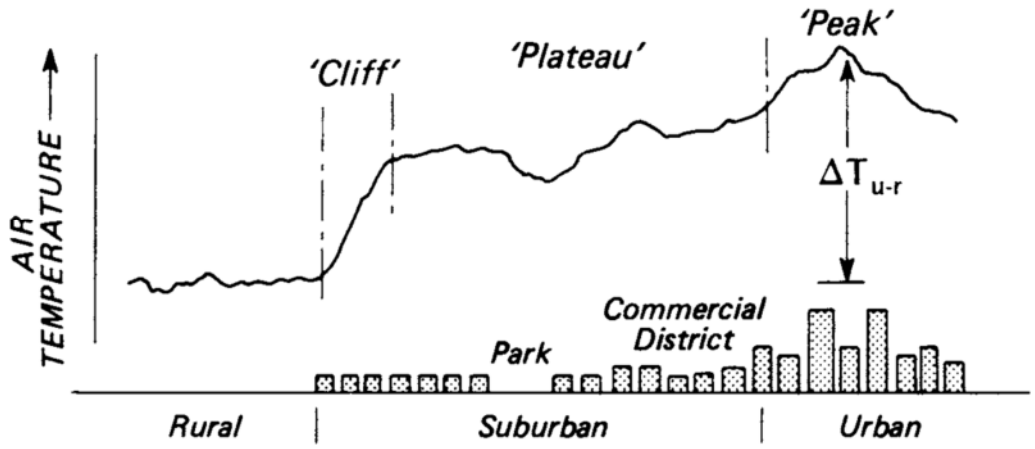

Figure 2. 9: Cross-section of a typical urban heat island
Source: (Oke 2002b)

A meteorologist provided the very first record on higher air temperature in an urban area compared to that in a rural area- Luke Howard- more than a century ago (Howard 1833). During the following 150 years, the early studies on heat island effect were carried out at beginning levels- a simple description of statistical data with empirical evidence for a single sample city (Oke 1982). Since the 1980s, with the establishment of relevant theoretical frameworks due to progress in technologies and the increasing investment on research, the formation processes and the physic-mathematical modellings of UHI effects have been well investigated world-widely (Landsberg 1981)

(Akbari et al. 1990)(Oke 2002b)(Wong & Yu 2005)(Oke 2011)(Santamouris 2013). According to the worldwide research, the existence of UHI effects in the very urban area has been confirmed (Landsberg 1981) (Wong et al. 2011). The magnitude of UHI often reaches its peak value at night, and it is weak or even negative in the urban core during the day (Figure 2.10) (Wong et al. 2011) (Futcher et al. 2013).

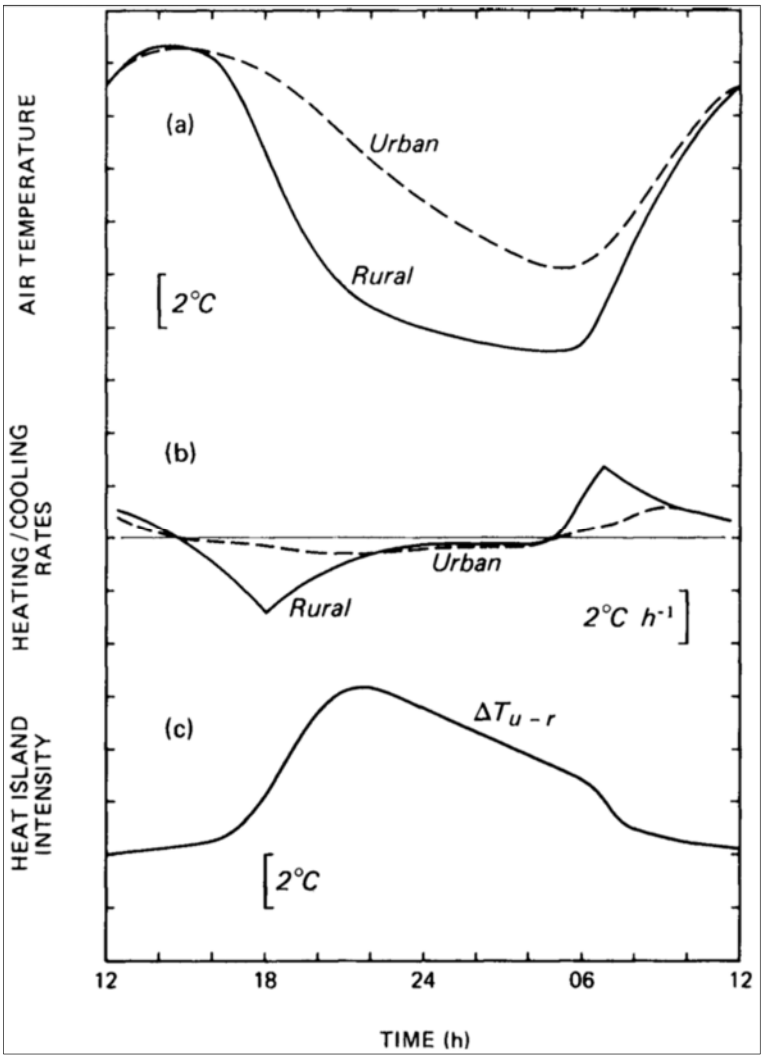

Figure 2. 10: (a) Typical variation in air temperature (b) typical variation in cooling/warming rates and (c) the corresponding heat island intensity
Source: (Oke 2002b)

As discussed in the previous section, the urban atmosphere can be defined into several layers, including UBL and its sub-layer: UCL (again, UCL was regarded as an independent layer from UBL in early studies). Accordingly, there are two types of UHI associated with the layers: UCL heat island and UBL heat island (Roth et al. 1989).

Usually, the UCL heat island is observed by weather stations or automobile. The intensity is most significant at night or after sunset and least around midday following a daily cycle. However, due to the broader spatial distribution, the intensity of the UBL heat island varies vertically- decreasing with height. Therefore, the UBL heat island is considered as extended from the UCL heat island (Roth et al. 1989). Generally speaking, the UCL heat island is more decisive in the urban microclimate, the variation in the upper air can barely directly impact the activities which are limited to the near-surface urban environment.

The traditionally fixed weather station and automobile transects are typically applied for measuring the near-surface air temperature, which is widely implemented in the UHI studies (Voogt & Oke 2003)(Tran et al. 2006). On the other hand, as the renovations in technology, remote sensors equipped in aircraft-borne or satellite have been used for scanning the surface heat island. Through this method, long-time monitoring of conditions of urban land covers has become a reality (Weng et al. 2004).

ii) Effects of UHI on the urban built environment

UHI is widely recognised as a phenomenon of the deterioration in the urban microclimate, especially in summertime in low and mid-latitude regions (Taha 1997b) (Li et al. 2014). It brings a series of adverse effects on the built environment, which can be categorised into three aspects: high urban temperatures, increasing energy demand and environmental degradation (Vardoulakis et al. 2013).

Firstly, a high urban temperature with a lower rural temperature is the most apparent effect of UHI, which was the direct evidence that revealed the existence of this local urban phenomenon (Howard 1833) (Oke 1982) (Lee & Lee 2014). The higher air temperature is considered a result of UHI effects and caused by slow winds, higher heat storage in a dense urban area (Radhi et al. 2013). According to the types and the measurements of UHI studies, both high atmospherical- and surface temperature were recorded world-widely (Table 2.8) (Tomlinson et al. 2012) (Kolokotroni & Giridharan 2008) (Tran et al. 2006)(Kim & Baik 2002) (Goh & Chang 1999) (Giannaros et al. 2013)

(Moreno‐garcia 1994) (Hafner & Kidder 1999) (Kłysik & Fortuniak 1999).

Table 2. 8: High temperature in cities world-widely

Urban Area	Year	Maximum (+)△T-UHI	Type	Author
Birmingham	2012	4.88 ℃	Surface-UHI	(Tomlinson et al. 2012)
London	2008	8.9 ℃	Air-UHI	(Kolokotroni & Giridharan 2008)
Seoul	2001	8.0 ℃	Surface-UHI	(Tran et al. 2006)
Singapore	1999	3.0 ℃	Air-UHI	(Goh & Chang 1999)
Tokyo	2001	12.0 ℃	Surface-UHI	(Tran et al. 2006)
Athens	2013	4.0 ℃	Air-UHI	(Giannaros et al. 2013)
Barcelona	1994	8.0 ℃	Surface-UHI	(Moreno‐garcia 1994)
Altlanda	1997	1.2 ℃	Surface-UHI	(Hafner & Kidder 1999)
Poland	1996	12.0 ℃	Air-UHI	(Kłysik & Fortuniak 1999)
Bangkok	2002	8.0 ℃	Surface-UHI	(Tran et al. 2006)

Source: (see from 'Author')

Secondly, building energy demand is affected by the local meteorological conditions (Yao et al. 2011) (Futcher et al. 2013). As the increase in urban temperature due to UHI effect, energy demand is rapidly rising, especially for heating on hot days in the buildings (Yao et al. 2011). As space conditioning (including both heating and cooling) accounts for a significant proportion in total building energy demand, therefore, UHI has a significant influence on the building energy consumption (Wong et al. 2011) (Du et al. 2014) (Ciscar & Dowling 2014). Moreover, the temperature is the most decisive factor in determining heating degree days (HDDs), and cooling degree days (CDDs) (Ciscar & Dowling 2014), higher urban temperatures increase the CDDS and decrease the HHDs. Consequently, UHI increases the overheating risk in summer but reduce the load for heating. Studies (Yu & Hien 2006) (Wong & Chen 2008) (Li et al. 2014) show that a 1℃ reduction in outdoor air temperature could induce a 5-12.8 per cent saving in building energy consumption in summer. As reported by Ali-toudert (2009) and Futcher et al. (2013), the cooling demands in urban areas with light construction and low density are more sensitive to the UHI due to the absence of over-shading effects by buildings, mainly when the buildings are occupied.

Thirdly, UHI causes the degradation in the urban built environment in two aspects. The first adverse effects are a reduction in ventilation rates in an urban area compared to

that in a rural area due to the increased temperatures (Allegrini et al. 2012) and obstacles of buildings (Lau et al. 2017). Moreover, the decreasing in wind speed exacerbates the pollution problems of harmful gases in photochemistry, including enhancing the ground-level ozone due to CFCs (Cardelino & Chameides 1990) (Oke 1997) (Roth 2002) (Rizwan et al. 2008), and increasing emission of carbon dioxide, sulfur dioxide, and other suspended particulates from power plants (Wong et al. 2011). The second aspect of the degradation in health caused by the UHI effects is the increasing thermal discomfort (Du et al. 2014) and impacting thermal behaviour (Radhi et al. 2013) and health of the people living in urban areas (Allegrini et al. 2012)(Boumans et al. 2014). The increased temperatures (Table 2.9) and wind with decreased speed may increase the heat stress in the summertime, thereby increasing the physiological equivalent temperature (PET) (Matzarakis et al. 1999) (Höppe 1999) (Tan et al. 2010) (Lau et al. 2017). As a consequence of the deterioration in thermal comfort, UHI effects are recorded as a cause of the increased mortality rates (Changnon & Kunkel 1996). In 2003, the summer heat wave led to a death of exceeding 70,000 in Europe, which exemplified possible social impact (Boumans et al. 2014).

However, for the urban area in cold climates (Table 2.10), especially in winter time, the UHI effects have positive impacts in several aspects: Biological activity (plant growth, disease), human bioclimatic (comfort, wind-chill, heat stress), building energy demand (space heating) and cold weather (transport disruption due to ice and snow) (Roth 2002). As reported by Fung et al. (2006), the UHI effect doubled the summer cooling load while just reduced by 30 to 55 per cent of heating load in urban buildings in Athens. On the other hand, UHI effects still have negative impacts as on thermal comfort and on building energy consumption in summer for these cold regions. Therefore, *further investigation of the comprehensive yearly influence of UHI effects on the urban built environment is needed*.

Table 2. 9: Hazards and health outcomes

Hazard	Health outcome
Heat	Respiratory allergies & airway diseases
Severe weather	Cancer
Air pollution	Cardiovascular disease & stroke
Disease vectors	Food-borne diseases & nutrition
Contaminated water	Heat-related morbidity & mortality
Water quantity	Human developmental effects
Food quantity	Mental health & stress-related disorders
Traumatic events	Neurological diseases & disorders
Influx of environmental refugees	Vector-borne & zoonotic diseases
	Water-borne diseases
	Weather-related morbidity & mortality

Source: (Boumans et al. 2014)

Table 2. 10: Impacts of UHI in cold and hot climates

Impact	Cold climate	Hot climate
Socio-economic and health impacts		
Human comfort and mortality	Positive (winter) Negative (summer)	Negative (all seasons)
Energy use	Positive (winter) Negative (summer)	Negative (all seasons)
Air pollution chemistry	Negative	Negative
Air pollution dispersion	Both positive and negative	Both positive and negative
Water use	Negative	Negative
Biological activity	Positive	Probably neutral except disease
Ice and snow	Positive	Not applicable
Meteorological impacts		
UHI circulation, breezes, stability, turbulence, convergence, uplift, mixed layer depth, cloud, precipitation, relative humidity, dewfall, evaporation, fog, visibility, snow, 'contamination' of long-term temperature records		

Source: (Unger 2004)

iii) Factors Causing UHI

As mentioned in previous sections, the primary cause of UHI effects is the modification in both the urban surface and urban atmosphere due to urbanisation. As shown in Table 2.11 and Figure 2.11, existing literatures (Oke 1982) (Arnfield 2003) (Radhi et al. 2013) have concluded several particular causes of UHI in terms of factors of urbanization, which can be summarised into three groups of factors: the temporary effect variables (wind speed, cloud cover, humidity), permanent effect variables (city size, population, green area, urban forms and surface materials), and cyclic effect variables (anthropogenic heat and solar radiations) (Rizwan et al. 2008).

According to the existing research, the reducing UHI intensity is associated with increasing wind speed, increasing cloud cover (Oke 1982) (Ackerman 1985) (Chow & Roth 2006) (DRAHOŠ & Drahoš 2012) (Futcher et al. 2013) (Lau et al. 2017), and

increasing relative humidity (Kim & Baik 2002) (Cui & Shi 2012). Additionally, It increases with city size and population (Oke 1973) (Oke 1982) (Arnfield 2003) (Tran et al. 2006). As shown in Figure2.12, UHI intensity is significantly correlated with city size in terms of urban population, where the population density is a 'catchall' variable for a compact city (Lee & Lee 2014). Furthermore, the most significant values of UHI intensity are recorded during anticyclonic conditions (Unwin 1980) (Oke 1982) and at night (Kim & Baik 2002) (Oke 2002b) (Lee et al. 2012) (Allegrini et al. 2012).

Table 2. 11: Causes of UHI suggested by Oke

Altered energy balance terms leading to positive thermal anomaly	Features of urbanization underlying energy balance changes
A. Canopy layer	
1. Increased absorption of short-wave radiation	Canyon geometry – increased surface area and multiple reflection
2. Increased long-wave radiation from the sky	Air pollution – greater absorption and re-emission
3. Decreased long-wave radiation loss	Canyon geometry – reduction of sky view factor
4. Anthropogenic heat source	Building and traffic heat losses
5. Increased sensible heat storage	Construction materials – increased thermal admittance
6. Decreased evapotranspiration	Construction materials – increased 'water-proofing'
7. Decreased total turbulent heat transport	Canyon geometry – reduction of wind speed
B. Boundary layer	
1. Increased absorption of short-wave radiation	Air pollution – increased aerosol absorption
2. Anthropogenic heat source	Chimney and stack heat losses
3. Increased sensible heat input-entrainment from below	Canopy heat island – increased heat flux from canopy layer and roofs
4. Increased sensible heat input-entrainment from above	Heat island, roughness – increased turbulent entrainment

Source: (Oke 1982)

As reported by Lee et al. (2012) and Vardoulakis et al. (2013), the velocity of local mass has a significant influence on UHI intensity, and high-speed wind can substantially cool the urban area. With constructing buildings and other facilities, the urbanisation increases the surface roughness and slows down the surface winds in urban an area (Cardelino & Chameides 1990) (Allegrini et al. 2012) (Radhi et al. 2013), thereby enhancing the heat stored in the surfaces (Radhi et al. 2013). Moreover, together with less vegetated surfaces, the evaporation process is slowed down in the dense urban areas with narrow and winding streets (Golany 1996). Consequently, one of the passageways of removing heat- evaporation (Taha 1997b) - is less efficient in this dense urban area with low wind speed, low relative humidity, and low cloud cover

rate, the surface radiations and heat storage dominate the heat exchange process (Futcher et al. 2013). Then, the accumulated extra heat results in higher urban temperatures (Oke 1973) (Santamouris 2013).

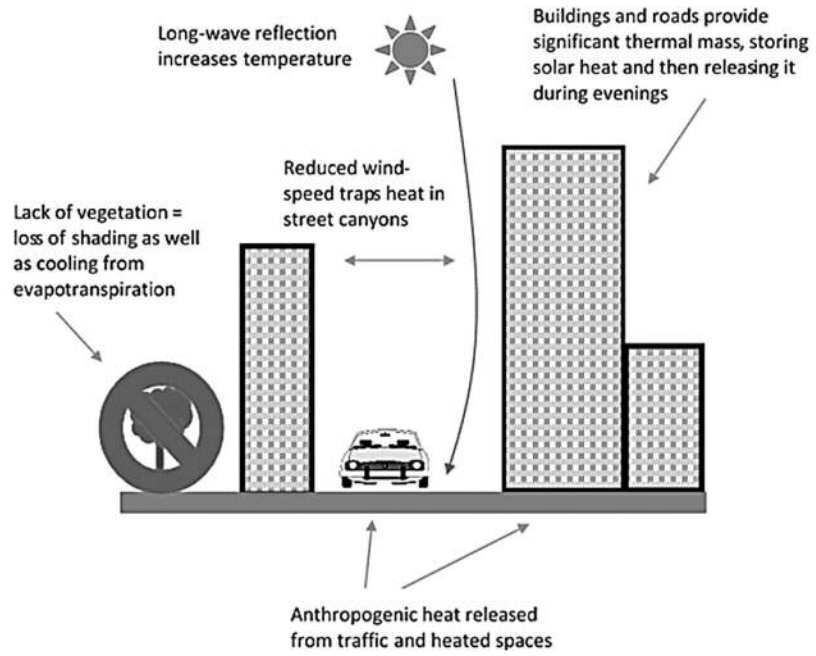

Figure 2. 11: Different sources contributing to the UHI effect
Source: (Wootton-Beard et al. 2016)

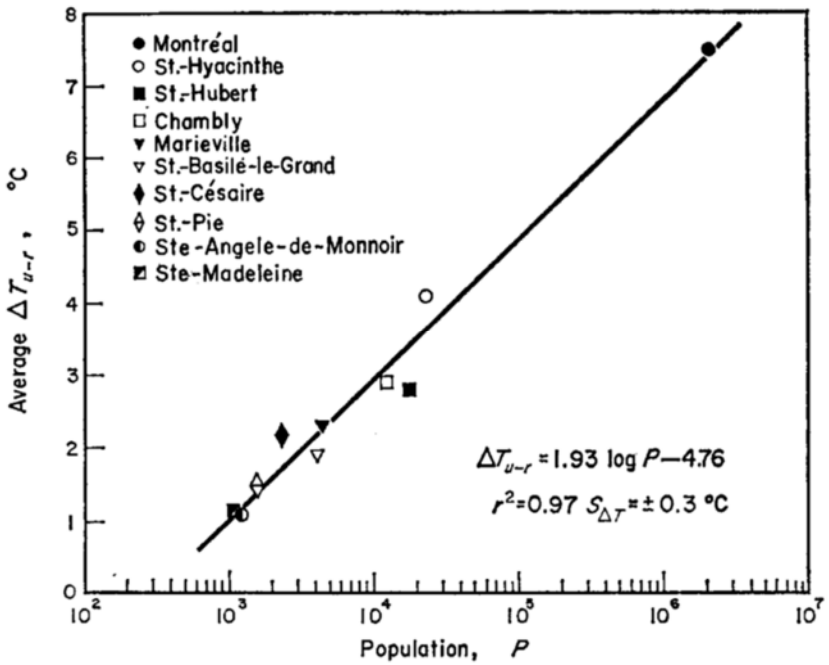

Figure 2. 12: Correlation between the average ΔT_{u-r} (UHI) at 10 places on the St. Lawrence Lowland
Source: (Oke 1973)

Considering the factors mentioned above, as reported by Oke (Oke 1973) , the very early model of UHI associated with meteorological controls was demonstrated by Sundborg (1950):

$$\Delta T_{u-r} = \frac{(a-bN)}{\bar{u}} \tag{2.6}$$

where N is cloud amount, $\bar{u}$ is wind speed, a and b are constants concerned with the city.

Lastly, together with indirect solar heat (ISH), anthropogenic heat plays a vital role in causing urban heat island (UHI) (Taha 1997b) (Oke 1982) (Rizwan et al. 2008)**,** as one of the significant factors of the winter UHI in high latitudes (Oke 1974). Compared with ISH, anthropogenic heat straightforwardly heat urban atmosphere (Rizwan et al. 2008). Generally speaking, extra anthropogenic heat is released due to the intensive heating consumption in cold days (Taha 1997b), traffic and other human activities in the dense urban area(Golany 1996). The anthropogenic heat varies in different areas and the energy structure, which has daily, weekly, and seasonal trends (Chow & Roth 2006) (RIZWAN et al. 2008), and it is negligible in some circumstances (Taha 1997b).

2.3.4 Design Factors and UHI

As introduced in Section 2.3.3, urban form, urban landscape and construction material play initial role in causing UHI effects in forms of altering the thermal properties of urban surfaces (Wong et al. 2011)(Lee & Lee 2014), increasing heat storage capacity and limiting the evapotranspiration (Oke et al., 1991). It plays a crucial role in determining the variation in temperature at micro-level (Wong et al. 2011). The most significant effect of urban form on UHI effect is the obstructing sunlight and daylight (Ratti et al. 2005) and delaying the cooling process in the surface at nights with no wind and cloud (Oke 1981). Moreover, these factors are closely related to the urban planning and design process. Therefore, extra attention should be paid to consider these factors during the early design stages for new urban development projects in terms of mitigating the variation in urban microclimates. In order to investigate the

relationship between urban form and UHI, a series of variables had been applied in quantitative studies.

i) Urban Form

Urban form, including urban geometry, consisting with street patterns, plot-layout patterns and building patterns, determines the thermal properties of urban surface (Lee & Lee 2014), and influences microclimate and outdoor thermal comfort in a complicated way (Shashua-Bar et al. 2010) (Wong et al. 2011) (Yao et al. 2011) (Chen et al. 2012), which is considered as an indirect effect (Ratti et al. 2005).

Urban form plays an initial role in influencing the wind conditions and determines the pattern of population distribution, and these features are two critical factors of UHI intensity, as discussed in previous sections. Building density is the most apparent variable for measuring the concentration of buildings in a city and the density of a city (Erell et al. 2011). Building developments with high density create shelters and decrease wind velocity, therefore higher level of heat is stored in surface contributing higher magnitude to UHI (Radhi et al. 2013). Therefore, stronger UHI effects were recorded in more compact or denser cities (especially at night), which can be identified by the increasing CDDs and decreasing HDDS (Oke 1988) (Ewing & Rong 2008) (Smith & Levermore 2008) (Lee & Lee 2014).

ii) Sky View Factor and Height-Width Ratio

Daytime UHI is dominated by solar radiation (Yang et al. 2011). Moreover, different shadow effects induced by the urban geometry of streets and buildings and layouts (Givoni 1989) (Futcher et al. 2013) are proved to be useful for mitigating UHI effects, which highlights the significance of accessibility of solar radiation in the building and street design (Futcher et al. 2013). Therefore, urban geometry is determinative to radiation exchange in urban rare, thereby contributing to the UHI effect (Erell et al. 2011). In addition, solar access is often represented by the sky view factor (SVF) considering a statistic significance between net radiation flux and SVF (Figure 2.13). Thus SVF is considered as one of the critical indicators of daytime UHI (Roth et al.

1989) (Eliasson 1996) (Yang et al. 2011), and it has been widely implemented to analyse the relationship between UHI intensity and urban geometry (Oke 1981) (Yamashita et al. 1986) (Upmanis & Chen 1999) (Unger 2008) (Chen et al. 2012).

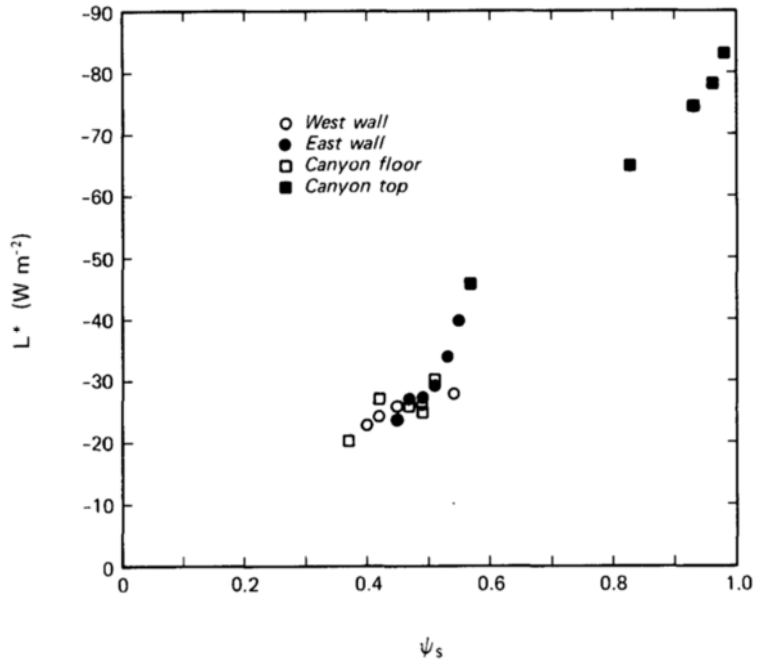

Figure 2. 13: Correlation between net long-wave radiation (L^*) and sky view factor (ψ_s) for a canyon cross-section
Source: (Oke 1982)

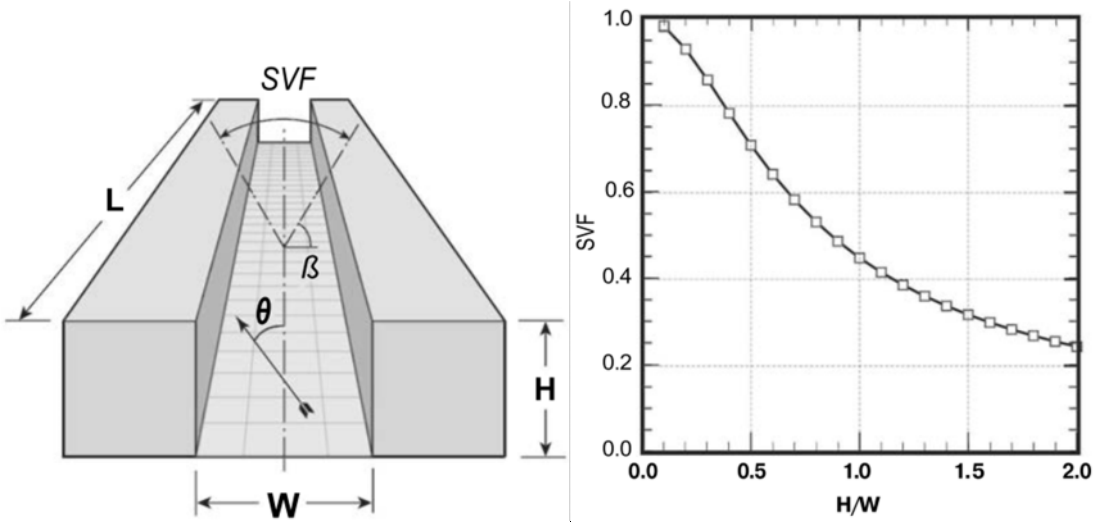

Figure 2. 14: SVF and H/W in an urban canyon (left) and the relationship between SVF and H/W
Source: (Erell et al. 2011)

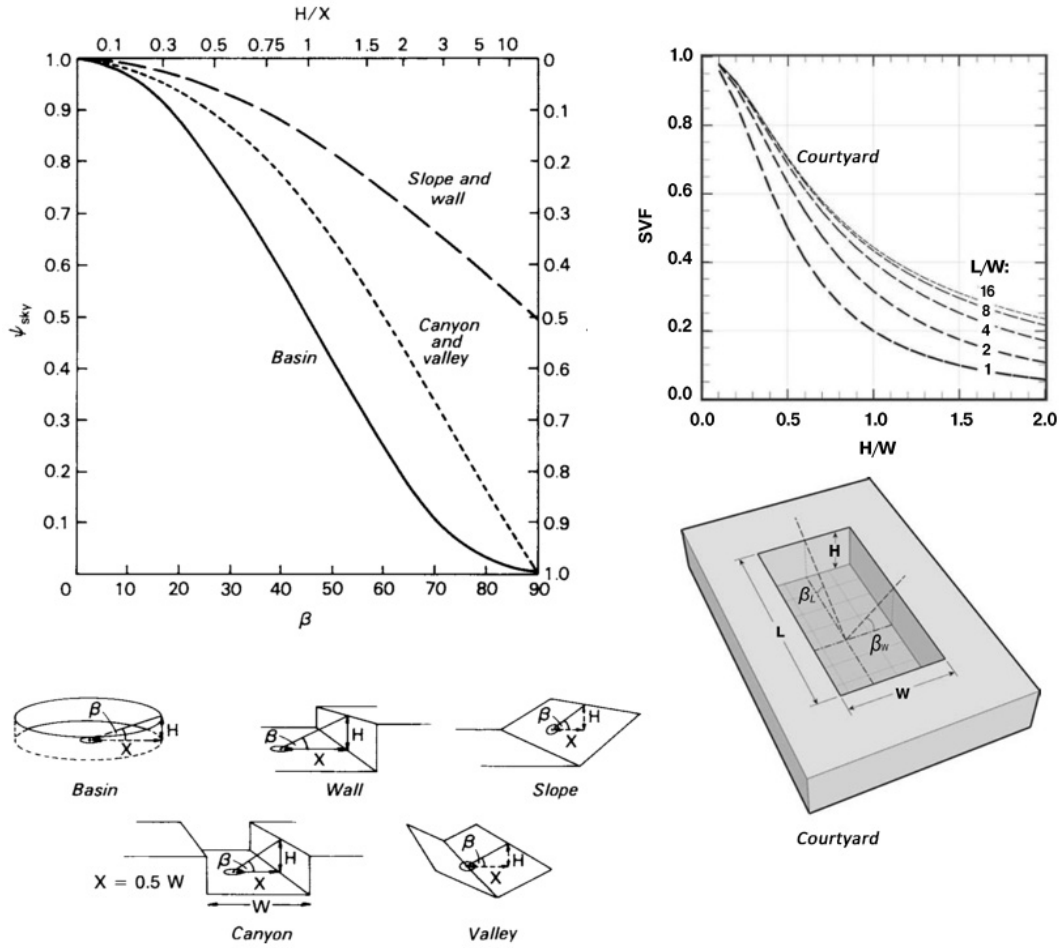

Figure 2. 15: View factors in common geometric arrangements
Source: compiled from (Oke 2002b) (Erell et al. 2011)

Urban canyon is an abstraction of other types of urban form (such as the street, the square, the courtyard, the garden) (Strømann-Andersen & Sattrup 2011). It is defined as '*City street lined with buildings*' in the Dictionary of Landscape Architecture and Construction (Christensen 2005). Urban canyon has been widely applied in urban climatology, in which sky view factor (SVF) and height- width (H/W) ratio (or aspect ratio) are used to describe the spatial geometrical properties (Figure 2.14 left). SVF is closely related to H/W (Figure 2.14 right), especially in simple canyon cases (Oke 1988). In a hot-humid climate, according to the research by Shashua-Bar et al. (2004), warm air environment is observed in wide spacing (low H/W), whereas strong cooling effects tend to occur in a deep canyon (high H/W). In cold area where heating demand dominates, higher H/W ratio is preferred due to effects of wind shelter and higher nighttime UHI (Futcher et al. 2013), and an H/W of 0.6-1.0 is ideal for mid-latitude areas

(Oke 1988). Moreover, SVF is also used to estimate the urban geometry in other cases with no-canyon patterns (Figure 2.15), including basin, wall and slope, valley, and courtyard, etc.

Based on Oke's study (2002b) (Figure 2.14), calculation equations for sky view factor at a point of different geometric arrangements can be presented as follows:

Wall and slope $$\psi_{sky} = (1 + \cos\beta)/2 \quad (2.7)$$

Canyon $$\psi_{sky} = cos\,\beta \quad (2.8)$$

Basin $$\psi_{sky} = cos^2\beta \quad (2.9)$$

Courtyard $$\psi_{sky} \approx cos\beta_W cos\beta_L \quad (2.10)$$

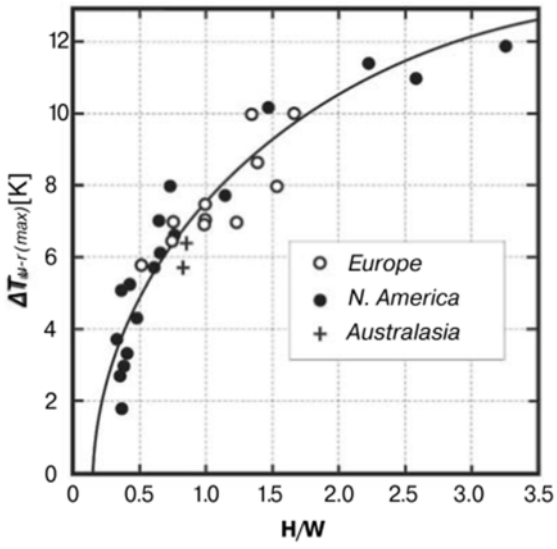

Figure 2. 16: Relation between observed UHI intensity and the H/W ratio in 31 street canyons
Source: (Erell et al. 2011)

On the other hand, the radiation exchange reverses in the surface during the night, when the heat flux exchange influences the air temperature due to the horizontal transport of air volume (Roth et al. 1989). SVF has a weak relationship with air temperature (Eliasson 1996), the relation between SVF and nighttime UHI is considered to be negative (Yang et al. 2011).

However, as shown in Figure 2.16, UHI varies in a different city in the streets with the same H/W ratio. Therefore, it is difficult to accurately predict UHI intensity only based on urban geometry, considering the other uncontrolled influential factors (Chen et al. 2012), including the advection reduces air temperature in microclimate (Erell et al. 2011). Therefore, further study on influences other factors on UHI effect is needed.

iii) Greenery

Urban microclimate is influenced by the greenery (Wong et al. 2011), and shrinkage of greenery is considered as one of the causes of UHI effects (Wong & Yu 2005) (Radhi et al. 2013). Existing literature (Kawashima 1990) (Jonsson 2004) (Potchter et al. 2006) (Yu & Hien 2006) (Akbari 2009) (Hamada & Ohta 2010) (Cohen et al. 2012) reveals that green areas, including massive trees and green parks, can potentially cool down local urban area by 0.5- 5 °C (Figure 2.17). Moreover, this effect is more significant in the suburbs in comparison to that in city centres (Kawashima 1990). Strong cooling effects due to greenery, including trees, grass, forests and parks, were observed at multi-scales (Shashua-Bar & Hoffman 2000) (Onishi et al. 2010), including macro level (Saito et al. 1990) (Kawashima 1990), micro level (Jauregui 1990) (Sonne & Vieira 2000), and mesoscale (Honjo & Takakura 1990) (Avissar 1996).

As reported by Akbari et al. (1990), Rosenfeld et al. (1995), and Chang et al. (2007), the cooling effects are provided by trees though two ways: direct processes- shading effects against solar heat gain into buildings through building envelops, radiant heat gain from the surrounding and indirect, and infiltration due to wind; indirect processes- evapotranspiration.

In micro, as shown in Figure 2.18, in the form of a shading effect, the tree may receive a large amount of radiation through the following process (Oke 1989): 1) absorbing the reflected short-wave radiation from buildings envelopes and the ground; 2) boosting the long-wave radiant energy due to lower leaf temperature compared to all other built surfaces; 3) advection of sensible heat due to lower leaf temperature compared to the air temperature. Moreover, the shadow casting on the surrounding surfaces reduces

the amount of short-wave radiation reflected from them and long-wave radiation emitted by them, thereby mitigating the energy absorption by other urban elements and pedestrians (Erell et al. 2011). Studies (Oke 1989) (Shashua-Bar & Hoffman 2000) show that the majority (80%) of the total cooling effect can be contributed by only tree shading, especially in small areas.

On the other hand, evapotranspiration of vegetation lowers the surrounding temperature by converting the sensible heat of the surrounding environment is converted into latent heat (Chang et al. 2007). This process draws underground-water to the surface soil, then the moisture in the surface soil is increased, thereby raising the water evaporation rate at the ground surface. In addition, evapotranspiration reduces the sensible heat of the hot air in the surrounding area and creates a cooling area, which is called ‘cool oasis’ (Rosenfeld et al. 1995). Therefore, the efficiency of irrigation for vegetation in an urban area can significantly impact the cooling effect of evapotranspiration and UHI variation (Jonsson 2004). Moreover, considering that fact that water balance and wind climate is the fundament for dissipating the heat load, the long-wave emission and sensible heat transfer from the tree will be reduced by the cooling process of transpiration (Oke 1989).

Similar as trees, the vegetative ground cover, including grass (Figure 2.19), can optimise the pedestrian’s thermal comfort in several aspects (Erell et al. 2011): low reflectance of short-wave radiation, evaporative cooling due to a high evaporation efficiency accounting for 70 to 80 per cent of that of a free-water body (lake or pool), and low surface temperature due to highly efficient evapotranspiration.

Furthermore, the density of vegetate area is the critical factor for evapotranspiration (Jonsson 2004), larger green areas can provide a broader range of cooling area (Wong & Yu 2005). Moreover, the density of leaves, stems and branches determines the effective opacity, whose primary function is the effectiveness of shading by a tree canopy (Erell et al. 2011). However, when the direct measurement of the actual solar transmission of trees is often not available in practice, the leaf area index (LAI) is

frequently applied to present (Erell et al. 2011). This indicator is considered with 'plant characteristics such as shape, height, leaf density, and height of the crown and provides a good indicator of the overall "greenness" of a particular area' (Skelhorn et al. 2014).

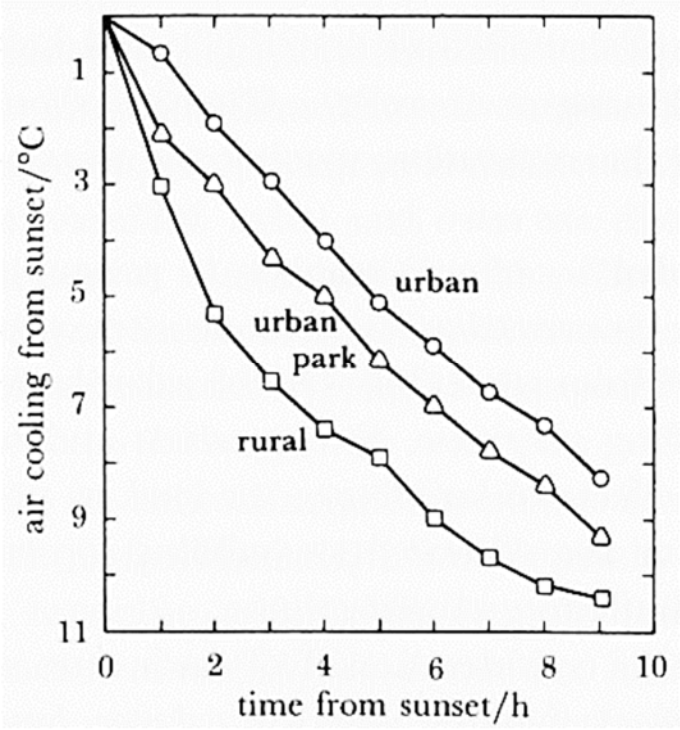

Figure 2. 17: Cooling curve from the urban centre, urban park, and rural area in Vancouver
Source: (Oke 1989)

'*LAI is the one-dimensional vertical leaf area index of the plant from level z to the top of the plant at* z_p *or the ground* $z = 0$' -- (Bruse & Fleer 1998)

Moreover, *LAI* can be calculated from *LAD* (Bruse & Fleer 1998) (Skelhorn et al. 2014):

$$LAI = \int_0^h LAD.\Delta z \qquad (2.11)$$

Where h is the tree height, Δz is the size of the vertical grid, LAI is the leaf area index, LAD is the leaf area density (Morakinyo & Lam 2016).

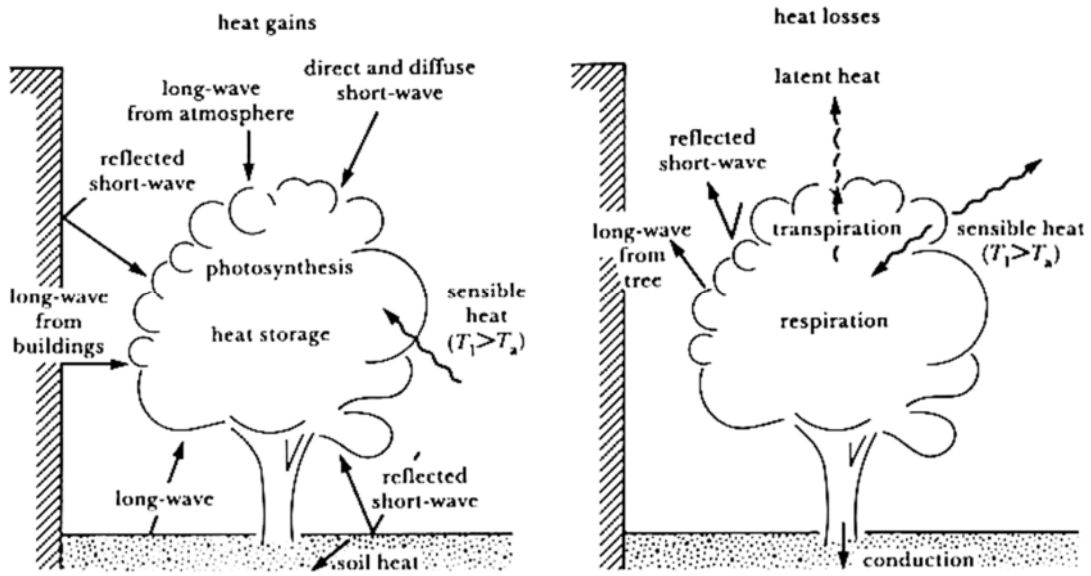

Figure 2. 18: Energy exchange in canyon environment with isolated trees (T_l,T_a, temperatures of leaf and air)
Source: (Oke 1989)

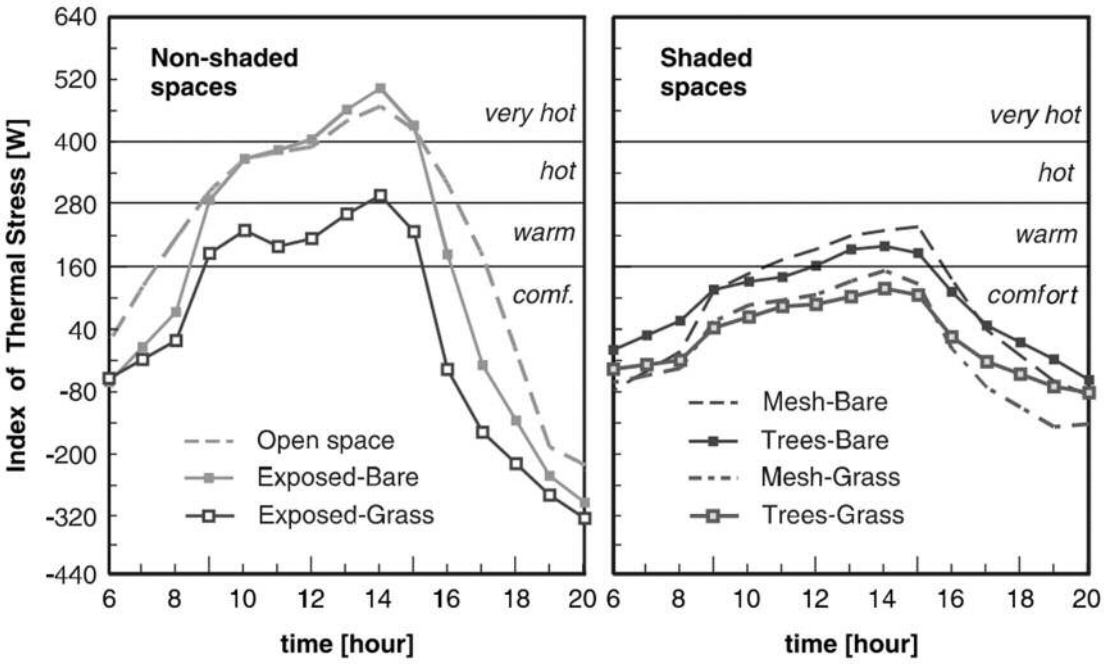

Figure 2. 19: Thermal stress in different ground configuration cases, including surfaces with exposed grass, mesh grass, and grass with trees.
Source: (Shashua-Bar et al. 2011)

At macro/ regional scale, normalised difference vegetation index (NDVI) is calculated using values of red and infra-red bands imagery from Advanced Very High Resolution Radiometer (AVHRR) on NOAA satellites (Ong 2003) (Jonsson 2004) (Onishi et al.

2010), which is a practical indicator frequently used for measuring land surface temperature (LST), and for investigating the UHI effects (Matson et al. 1978) (Brest 1987) (Roth et al. 1989) (Lee 1993) (Lo et al. 1997) (Onishi et al. 2010). Due to the limited resolution of the derived imagines, those studies can only be carried out at the macro-level (Lo et al. 1997).

As reported by Morakinyo & Lam (2016), other descriptive indicators are also used in modelling or quantifying trees: plant area coverage ratio (Shashua-Bar et al. 2010) (Ng et al. 2012) (Coutts et al. 2016), height/crown diameter (Correa et al. 2012), and green plot ratio (GPR) (Ong 2003). All the studies carried out with these indicators confirmed lower temperature was witnessed in highly vegetated areas.

As mentioned above in this section, evaporation process can convert the sensible heat of the surrounding air into latent heat, thereby cooling the surrounding temperature. In an urban area, however, water features wildly exist, which indulging pools, fountains, rivers, and even lakes. Winds coming from these bodies of water are cooler than those from the surrounding area (Golany 1996). Therefore, water bodies are one of the critical factors of the variation in UHI effect (Radhi et al. 2013). Due to its high heat capacity (4.1813 $\mathrm{J{\cdot}g^{-1}{\cdot}K^{-1}}$) and emissivity (0.993 - 0.998), water is observed with the minimal difference in day and night irradiance, and it is often the coolest feature in the day and the warmest at night (Lo et al. 1997).

iv) Albedo Property of Surface

As mentioned in Section 2.3.2, the urban microclimate is influenced by properties of surfaces (Wong et al. 2011). In specific, solar abortion of surface is impacted by its physical features, including material, colour and texture, which cause the difference of surface temperatures and convective thermal exchanges between buildings and streets (Givoni 1989). Moreover, as reported by Oke (1988), absorptance created by particular arrangements of urban geometry can be less than that by a flat plane, which indicates that total albedo in an urban area depends on not only albedo of surface materials, but also geometrical arrangement.

Therefore, albedo is also one of the critical factors of variation in the UHI effect. Existing literature (Weng 2001) (Dousset & Gourmelon 2003) (Zhang et al. 2007) (Onishi et al. 2010) show that artificial surfaces, including road, buildings, business zones and industrial zones, have significant UHI effects in the daytime. There has a significant change in the temperature due to variation in surface albedo (Taha 1997a). As reported by Taha et al. (1988), an increasing the surface albedo by 0.15 can result in a maximum reduction of 4°C in afternoon air temperature in the mid-latitude area. In an extreme case (Taha 1997a), with a 0.3 increase in albedo, a reduction of up to 4.5°C can be achieved in a basin area.

v) Summary of design factors and mitigation strategies of UHI effect

UHI effect can be affected by weather conditions, urban form, and urban surface (the availability of vegetation and water) (Radhi et al. 2013). Corresponding to the design factors that cause UHI, suggestions on mitigating UHI effect can be summarised in several aspects: optimisation of urban geometry, increasing the green and water coverage, using high albedo surface materials. Moreover, the effect of mitigating UHI by every single factor varies in different scenarios and can be impacted by other factors.

Firstly, as suggested by Todhunter (1990) study, urban geometry is a more decisive factor to affect the urban temperature at the microscale, in comparison to surface materials and albedo. Moreover, the impact of surface materials and albedo on the reflectance of radiation are more effective at a mesoscale instead of at a microscale in terms of influence in urban temperature (Andreou 2013).

Then, vegetation is considered one of the most effective strategies for UHI mitigation. Study (Wong et al. 2011) shows that the shading effect of greenery is the governing factor for cooling down urban area, compared to other variables, including building height and urban density. As reported by Chang et al. (2007), vegetation is estimated to mitigate 25% to 50% of increased urban temperature causing by UHI effect, which is considered as the governing factor of mitigating UHI (Wong et al. 2011). Green roof is an effective strategy for mitigation of UHI, which transfers heat in the form of

convection thereby affecting outdoor air temperature (Yaghoobian & Srebric 2015). However, for green roofs, the conductive heat transfer is more effective compared to the convective heat transfer. Therefore, it is more effective to apply green roof for optimising indoor environment and energy demand, rather than affecting outdoor air temperature (Yaghoobian & Srebric 2015). Furthermore, the cooling effect through evapotranspiration by trees are less efficient than that by the cool surfaces (Rosenfeld et al. 1995). In addition, according to the research by Jonsson (2004) and Radhi et al. (2013), during rainier seasons, greater values of cloud and air humidity can decrease the UHI effect. Moreover, these meteorological features, rather than vegetation, are considered as governing factors of UHI variation in tropical cities (Adebayo 1991),

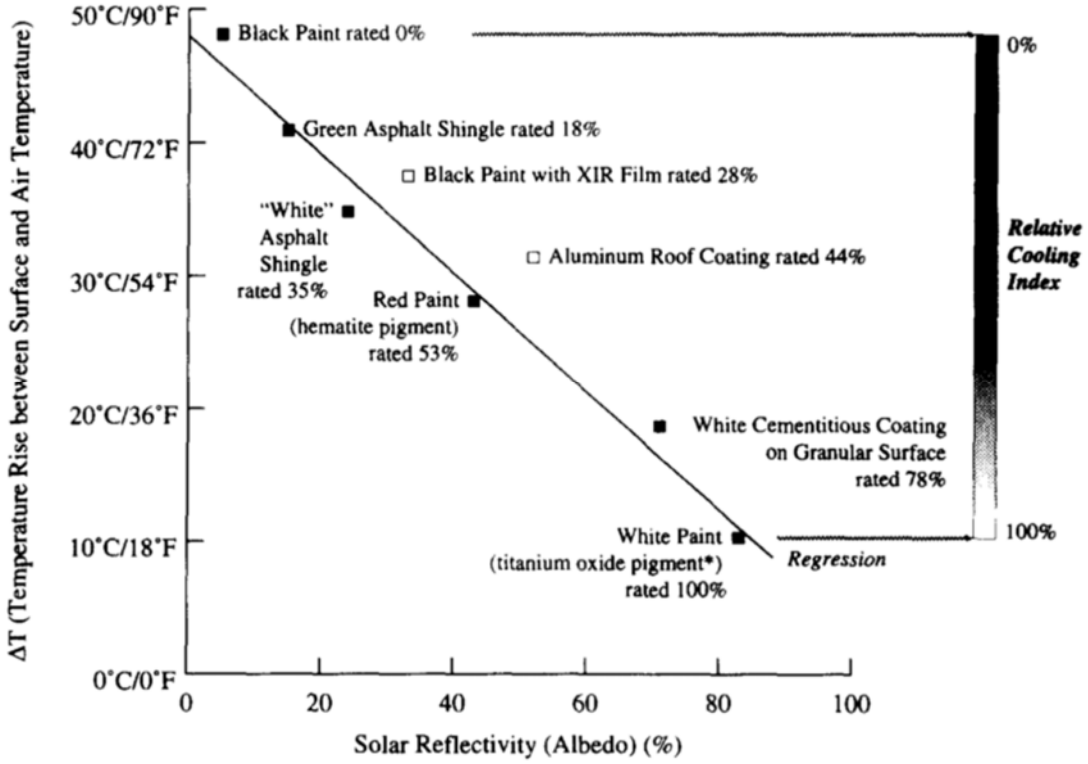

Figure 2. 20: Temperature difference between surface and air vs albedo of building envelops toward the sun

Source: (Rosenfeld et al. 1995)

Albedo plays a significant role in mitigating UHI effects at multi-scales. At a micro-scale of a high-rise outdoor environment, the increasing albedo of the ground and building envelop can result in higher reflected radiation, thereby decreasing the daytime outdoor and indoor thermal comfort and increasing cooling load of the surrounding

buildings (Yang et al. 2011). However, without considering shading factors, altering surface albedo shows no significance in terms of impacting UHI intensity (Yang et al. 2011). Comprehensive strategies integrated with vegetation measures are suggested while implementing the strategy of albedo modification.

To sum up, *by applying the UHI mitigation strategies, positive effects have been achieved in server aspects: the building energy consumption is reduced, outdoor human thermal comfort is improved, and pollutions in both air and noise is mitigated.* Appropriate design of urban geometry with wind tunnels (for example, streets canyons parallel to the wind flows) reduces the shelter effect; wind can easily dissipate the heat stored in among buildings and streets, thereby decreasing atmospheric UHI (Radhi et al. 2013). The cooling effect due to vegetation improve human thermal comfort, by influencing the urban thermal performance, wind environment and the relative humidity, and it can also improve the aesthetic appearance of the city and cause extra 'cold stress' in winter time (Golany 1996) (Cohen et al. 2012). In particular, trees in the streets can absorb dust and reduce noise pollution, which minimises the accessibility of solar radiation, reduces albedo (trees are dark), and shadows the street area (Golany 1996). According to the study by Rosenfeld et al. (1995) (Figure 2.20), a 20 to 40 per cent energy saving can be achieved by increasing the albedo of the exposed exterior surface of a single building (Rosenfeld et al. 1995).

Lastly, although the research is plenty on urban-scale urban heat island, there is still a lack of research which concerns air temperature variation at block scale (Sarkar et al. 2009) (Okeil 2010). As city-block is considered the lower limit scale for a UHI study (Steyn et al. 1981), further studies on UHI at a city-block scale are of significant meanings.

2.4 Urban form and Building energy consumption and the factors

2.4.1 Definitions and classifications

Urban areas consist of buildings and environments, which has unique properties of topography and biophysics (Smith & Levermore 2008). Urban form, is static description of statutes of urban area, which can be defined as: '*to the spatial configuration of urban land use within a metropolitan area*' (Anderson et al. 1996), which includes '*building geometry and layout, the buildings' heights, the thermal properties of building surfaces and the ground*' (Yao et al. 2011). While on the other hand, urban morphology emphases a dynamic process of urban evolution in urban form. There is no clear difference between the two, however, in this study, the 'static' part of urban morphology is all referred to as an urban form.

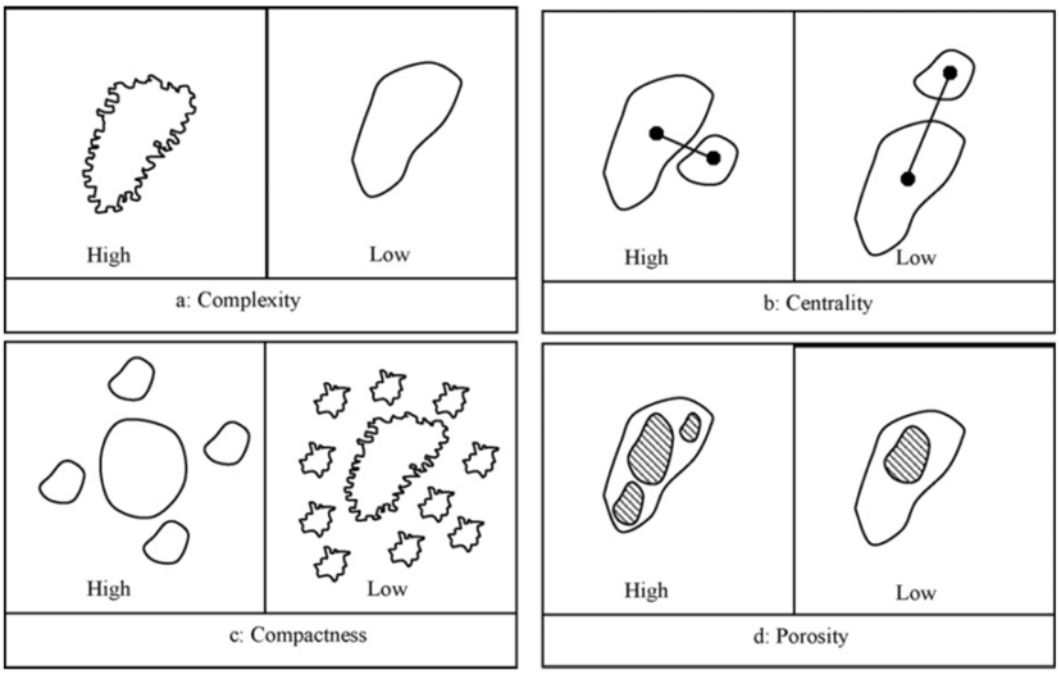

Figure 2. 21: Four spatial metrics of urban form
Source: (Huang et al. 2007)

According to the research by Huang et al. (2007), the dimensions of urban form can be represented by five groups of metrics (Figure 2.21): complexity, centrality, compactness, porosity and density. Complexity metrics are often employed to describe the patches in terms of their shape irregularity and the ruggedness of the boundary.

Centrality measures the distance between the dispersed areas to the city centre, or the distance between the specific urban developments to the central business district (CBD) (Galster et al. 2001). Compactness metrics are used to measure both individual patch shape and the degree of fragmentation of the overall landscape (Li & Yeh 2004). Porosity indicates the proportion of open spaces in the total urban area. Density generally measures the compactness, and it is often represented by population density, which is considered as a catchall functional variable of the compact urban form (Lee & Lee 2014). However, Lowry & Lowry (2014) proposed a new category of metrics to replace the complexity in their study following (Ewing et al. 2002), which is neighbourhood mix. Moreover, this metric addresses land use and heterogeneity in citizens, which encourage diversity of function, building density and population in the urban area.

According to the metrics discussed above, urban form interacts with a variety of parameters in many aspects, including geographic, economy, geometric, topology, astronomy, culture, and society (Adolphe 2001). Therefore, several classifications of urban form can be made with different conceptions in these fields:

Together with considerations of thermal performance, three types of urban form can be categorised: compact forms, dispersed forms, and clustered forms (Golany 1996). The dispersed urban form is often used in low population density areas in the USA, Europe and Asia; The clustered form is suitable for small urban units with close proximity, which can be easily merged with insulation from the outside in either segregated land use (Golany 1996). Compact urban form, which is characterised by '*high density, mixed land use, pedestrian-oriented habitation and energy efficiency*' (Chen et al. 2008) (Chen et al. 2011), is widely suggested in terms of sustainable developments in big cities (Korthals Altes & Tambach 2008) (Tian & Jim 2012) (Wolsink 2016). In particular, it tends to have outstanding performance on energy efficiency by minimising per capita energy use (Resch et al. 2016) and reducing carbon dioxide emissions (Hamin & Gurran 2009) (Liu & Sweeney 2012). In the meanwhile, there is a

debate on whether should implement the concept of the compact city (Breheny 1996) (Burton et al. 2003) (Neuman 2005). However the limited availability of land resources and massive pressure from population promote this concept, but further investigations are still needed to examine its appliance (Chen et al. 2011).

According to the study by Taleghani et al.(2015), three urban forms (singular, linear, and courtyard) have different thermal performance in their microclimate. As reported by Okeil (2010), the linear urban form is often recommended in the form of a row of houses, in order to avoid mutual shadowing and to increase the solar exposure of building facades; The block urban form, however, can adopt the grid street patterns which are mostly practised world-widely, while transportation can be operated in the streets on both directions offering much convince and backyards provide safe and quiet outdoor living spaces.

In addition, other distinguished metrics are introduced in some studies. Torrens & Alberti (2000) proposed indicators for density, scatter, leapfrogging, interspersion, and accessibility. Galster et al. (2001) introduced eight dimensions of urban form: '*density, continuity, concentration, clustering, centrality, nuclearity, mixed uses, and proximity*' (Galster et al. 2001). Ewing et al. (2002) used urban form index according to four factors for US cities: '*residential density, neighbourhood mix, activity strength and accessibility*' (Ewing et al. 2002). Another four metrics, including '*metropolitan size, activity intensity, distribution degree and clustering extent*' (Tsai 2005), were developed at the metropolitan level. Grazi & van den Bergh (2008) implicated indicators- density, fragmentation and accessibility- to access the local spatial planning and policy.

2.4.2 Urban form and effects

'*The amount of energy used depends not only on the climate but also on the layout of the city, the type of transport used and the efficiency with which heat and light are provided in buildings.* ' -- (Erell et al. 2011)

It has been widely recognised that urban form is closely related to sustainability and

climate policy in a city (Jenks 2000) (Gray & Gleeson 2007) (Korthals Altes & Tambach 2008) (Tian & Jim 2012) (Wolsink 2016). As discussed in early sections, urban form plays a significant role in influencing solar access on building façade (Ratti et al. 2005) (Futcher & Mills 2013), creating the urban climate (Futcher & Mills 2013) and determining the variation of temperature in microclimate (Wong et al. 2011). On the other hand, considering the fact that there are two paths between urban form and building energy consumption (Figure 2.22), urban form also has impaction on building energy consumption and GHG emissions, in a direct (providing choices in urban geometry, building sizes and types) and indirect way (impacting UHI effects) (Ratti et al. 2005) (Ewing & Rong 2008) (Strømann-Andersen & Sattrup 2011) (Lee & Lee 2014). Moreover, the travel behaviour, which includes vehicle miles travelled (VMT), mode preference, frequency and travel distance, is significantly influenced by urban form variables, such as density, land use and street design (Forster 2006) (Lee & Lee 2014).

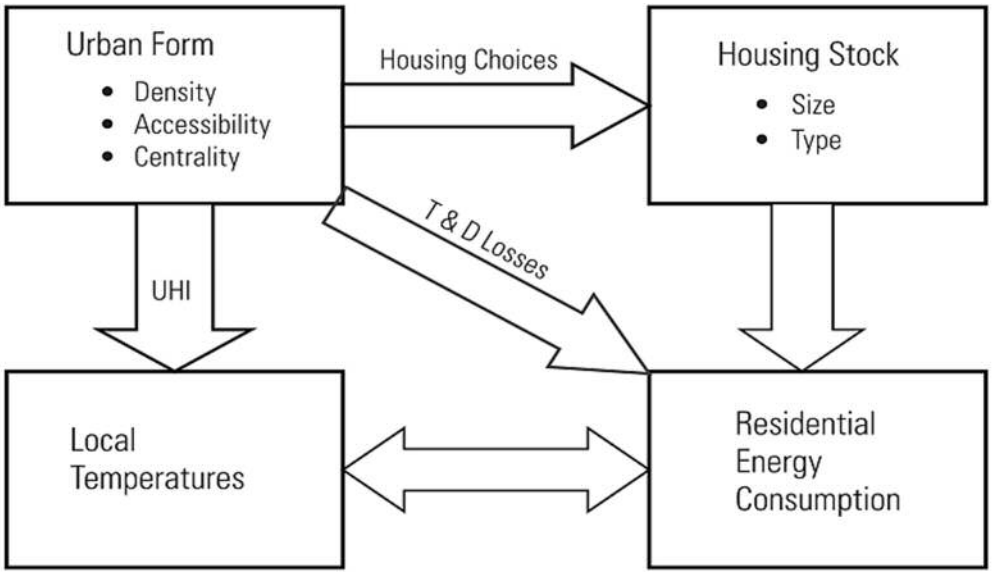

Figure 2. 22: Two paths between urban form and energy consumption in residential buildings

Source: (Ewing & Rong 2008)

As one of the key objectives in plenty of low carbon and eco city development, reduction in building energy consumption is dependent upon several factors (Ratti et al. 2005) (Xu et al. 2012). According to studies by Ratti et al. (2005) and Hamilton et al. (2009), building energy performance is dependent upon urban geometry, building

design, systems efficiency, and occupant behavior, which are controlled by four different actors: '*urban planners and designers, architects, system engineers, and occupants'* (Ratti et al. 2005) (Figure 2.23), respectively. And this situation of 'interdisciplinary' leads to narrow scape for each actor in doing their task. For example, buildings are considered as 'self-defined entities' by building designers, who neglect the effect of urban geometry on energy consumption at an urban scale (Ratti et al. 2005).

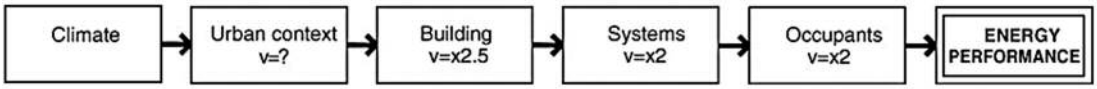

Figure 2. 23: factors of energy consumption in buildings
Source: (Ratti et al. 2005)

In particular, Ratti et al. (2005) reported an effect of 10 per cent of building energy consumption is related to urban form. In some extreme cases, where buildings are well designed in terms of thermal properties, energy performance with a range of thirty per cent in offices and nineteen per cent in residential is affected by urban form (Futcher et al. 2013). At the city scale, urban form factors, including urban density, urban texture, and urban randomness, impact building energy performance to a different extent (Winter 1994) (Compagnon 2004) (Ratti et al. 2005) (Cheng et al. 2006) (Wiedenhofer et al. 2013). As reported by Chen et al. (2011), Ratti et al. (2005) used digital elevation models (DEMs) to investigate the effects of urban texture on building energy consumption. Building design, in terms of building shape, governs building energy consumption, which also affects thermal performance and storage of solar energy (Hachem et al. 2012). Proper design of building fabric and efficient ventilation system can reduce space heating demand (Hamilton et al. 2009). Large courtyards are considered adequate to concentrate solar heat and benefit the sheltering effect preventing cold winds (Ratti et al. 2003) (Taleghani et al. 2015).

However, due to the uncertainty of other unknown factors (Steadman et al. 2014), which is considered as the complexity of the involved processes in an urban

environment (Ratti et al. 2005). Anderson et al. (1996) suggest that urban form is profound but not dominant in terms of influencing building energy consumption. Therefore, the link between urban form and building energy consumption can be neglected (Ratti et al. 2005). The findings by Futcher & Mills (2013) indicate that the energy reduction in a single building due to modification of building form is likely limited and insufficient, compared to the amount of energy saving by operational load management.

2.4.3 Energy balance and building energy consumption

As radiation exchange between surrounding buildings significantly affects the building energy demand (Allegrini et al. 2012), it is necessary to investigate the energy balance of a building, which can be given as following (Figure 2.24) (Oke 2002b):

$$Q^* + Q_F = Q_H + Q_E + Q_G + \Delta Q_S \qquad (2.12)$$

where, Q^* is net all-wave radiation on a building surface, Q_F is the total anthropogenic heat released from indoor, Q_H and Q_E are sensible and latent heat exchange with the outdoor air, Q_G is heat conduction to the underlying ground, ΔQ_S is a net change of energy storage due to building materials and air volume, and Q_M is the anthropogenic heat released from the human body (Oke 2002b).

According to Figure 2.24, heat can be transmitted through several paths: heat conduction through building envelops, ventilation and infiltration, solar penetration through glazing. Sensible heat flow (Q_H) from building surfaces through convection is affected by the wind speed and variance ratio between the building and air temperature, and the wind speed determines the thickness of the laminar boundary layer (Oke 2002b).

In particular, when the temperature between the indoor air and outdoor air is different, heat will be transferred through building components, including walls, roof, ground and glazing (Figure 2.25).

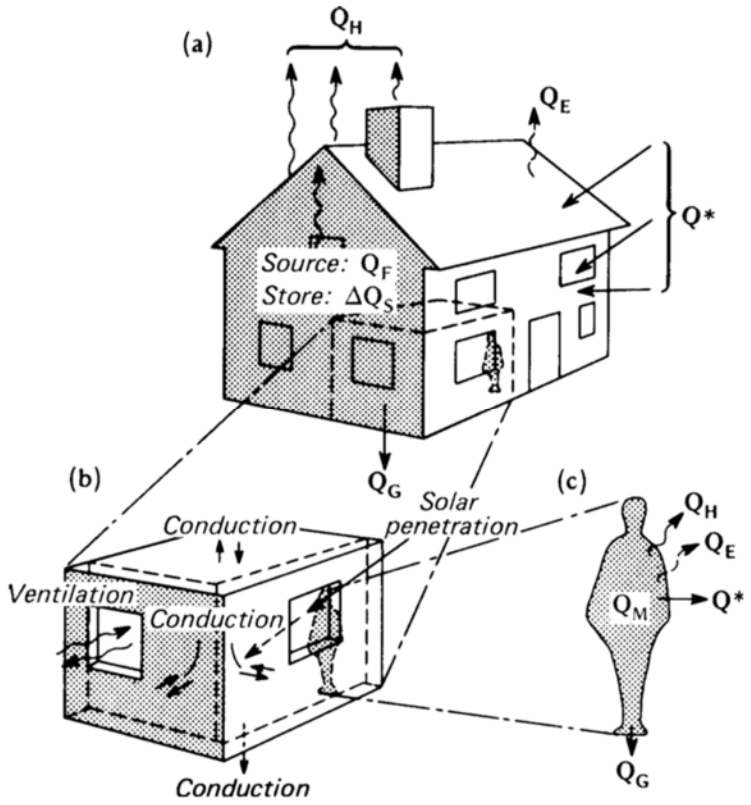

Figure 2. 24: Schematic depiction of the fluxes involved in the energy balance of (a) a complete building volume, (b) a room in a building and (c) a person in a room
Source: (Oke 2002b)

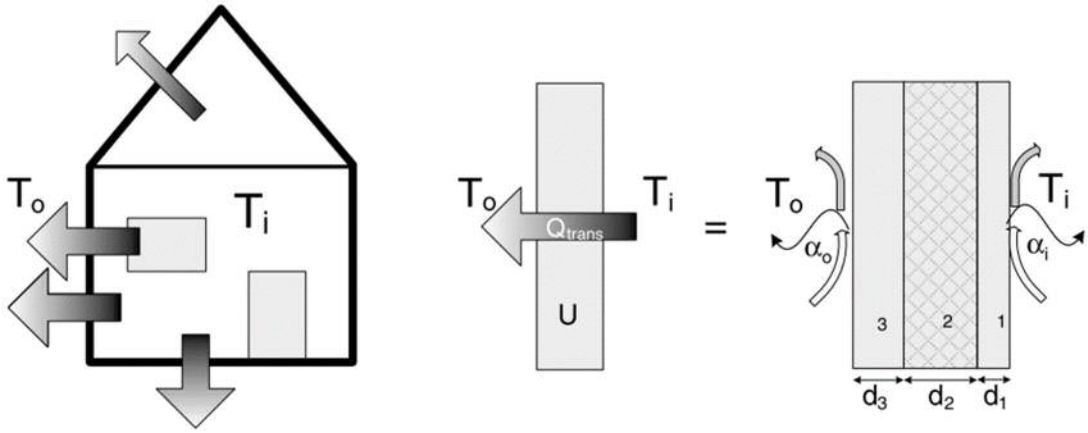

Figure 2. 25: Transmission losses and heat conduction through building envelops ($T_o < T_i$)
Source: (Bueren et al. 2012)

When the indoor air temperature is higher ($T_o < T_i$), the heat loss due to transmission through a wall- area A can be calculated with the following equations (Bueren et al.

2012):

$$Q_{trans} = UA(T_o - T_i)\ [W] \quad (2.13)$$

$$U = \frac{1}{\frac{1}{\alpha_i} + R_c + \frac{1}{\alpha_o}}\ [Wm^{-2}K^{-1}] \quad (2.14)$$

where T_i and T_o are indoor and outdoor air temperature, respectively, U is the overall transmittance, A is the area of the wall, α_i and α_o are the combined heat transfer coefficients of indoor side and outdoor side the laminar boundary layer, respectively, R_c is the thermal resistance of the wall.

According to Equation 2.13, the total energy demand for heating and cooling for maintaining internal comfort in a building is related to outdoor air temperature.

Furthermore, when taking all heat sources inside buildings into consideration, which includes heat released from people, lighting, and other electrical appliances, the total internal heat gains can be calculated by the following equation (Bueren et al. 2012):

$$P_{int} = P_{int,people} + P_{int,lighting} + P_{int,applicances}\ [W] \quad (2.15)$$

2.4.4 Street and building design

The shadowing effect caused by buildings minimise the UHI effect and thereby reducing building cooling demand. Proper design for streets and buildings can be a practical strategy on UHI mitigation and building energy efficiency. The results of a study on building energy performance in central London by Futcher et al. (2013) highlights the importance of solar access, and therefore, the significance of street design. Common indicators of urban form to predict distribution pattern of natural radiation are SVF, H/W ratio and the urban horizon angle (Robinson 2006).

i) Street canyon

As discussed in Section 2.3.4, SVF is often used to measure street geometry, which is also one of the critical variables of the UHI effect (Smith & Levermore 2008). However,

in addition to SVF, the effects of urban geometry should be considered to predict the distribution of irradiation in a street canyon (Robinson 2006). The canyon geometry- shapes of streets and buildings, and layout- provides various shading patterns, which impact with the convective thermal exchange of building-street due to temperature variation in different surfaces of the street canyon (Givoni 1989)(Grosso 1998). On the other hand, street orientation controls '*the amount of light shadowing, radiation, air movement, the intensity of city ventilation, and duration of relative humidity in the air*' (Golany 1996), which is another primary factor of urban form. As a single parameter to describe urban street geometry, H/W ratio has been widely used, which is considered as a governing factor for solar gain on the surface of roads and building walls (Takebayashi & Moriyama 2012). Takebayashi & Moriyama (2012) used the aspect ratio (W/H), another form of H/W ratio to investigate the shading effect by street canyon and the solar access. As reported by Futcher et al. (2013) (Strømann-Andersen & Sattrup 2011), deeper streets canyons decrease the cooling loads. Pearlmutter et al. (2007) addressed the importance of the H/W ratio and the directional orientation of streets in identifying the street canyon energy exchange in various urban geometries. Golany (1996) suggested designing wide, straight and parallel streets which were aligned with the orientation of the prevailing wind for a deeper wind penetration within the city in a hot-humid climate.

ii) Neighbourhood/block

The neighbourhood is a geographic and social unit, which provides the living spaces for people's life (Leung et al. 2010). It demonstrates the basic structure of the city, impacting the local microclimate. In the meanwhile, the effects of modified microclimate on building design should be considered in the guidelines of neighbourhood scale planning (Futcher et al. 2013). The over-shading effect by surrounding neighbourhood can reduce the cooling load in buildings in the summertime. Therefore, a 'neighbourhood' approach is needed when examining building energy management (Futcher & Mills 2013). The parameters of neighbourhood design, including shape, orientation, the density, and the site layout (Hachem et al. 2012),

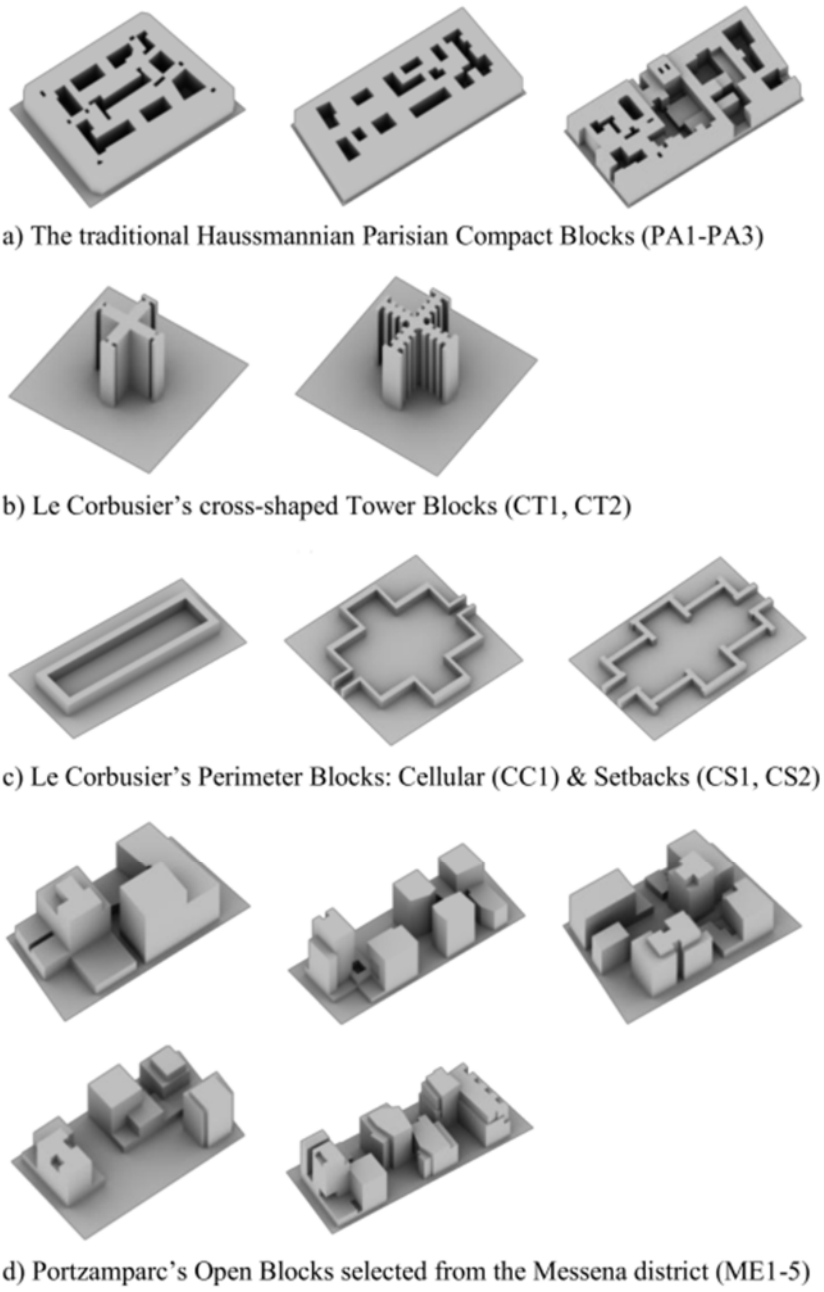

Figure 2. 26: Eleven urban blocks
Source: (Zhang 2013)

As a smaller scale of the neighbourhood, urban street blocks are fundamental units of the urban fabric, which reflect the similar characteristics of buildings, shape the public and semi-public spaces, and significantly impact the live experience (Zhang et al. 2012). Zhang (2013) summarised and categorised eleven forms of the urban block into three groups (the traditional enclosed perimeter block, the free-standing detached buildings, and the open block), and used different urban form indicator to examine the

performance of each block group in terms of the daylighting and openness to the sky. And the results highlighted the outstanding performance of the Open Block.

iii) Surrounding buildings and overshading

Within a neighbourhood of buildings groups, the urban form and fabric modify the urban microclimate, which 'restricts airflow movement below roof level, intercepts solar radiation causing overshadowing and permits long-wave radiation exchanges between building surfaces' (Futcher et al. 2013). The impacts of surrounding buildings can be summarised into two aspects: Radiation exchange and overshading. Between neighbourhood buildings, the radiation exchange has a governing role in energy demand (Allegrini et al. 2012). However, the impact of overshadowing on energy consumption can be substantial (Ratti et al. 2005).

Generally speaking, the shadowing effect causes a reduction in the cooling load and an increase in the heat load (Futcher et al. 2013). Study (Futcher et al. 2013) showed that the effect of shadowing by high H/W ratio is more decisive than the UHI effect in terms of affecting building energy performance. According to the results of the study by Wong et al. (2011), outdoor temperature is lower when increasing the height of the surrounding system, and thereby significantly reducing cooling load by 5 per cent over a large urban area. As reported by Futcher et al. (2013), a shaded building achieved fourteen per cent reduction in cooling demand compared to an unshaded building in Hong Kong. Strømann-Andersen and Sattrup (2011) found the geometry of street canyons have an influence on up to thirty per cent (in office) and nineteen per cent (in residential) of energy performance in low-energy buildings. Studies (Kolokotroni et al. 2006) (Kolokotroni & Giridharan 2008) show that buildings in the city centre of London have an increase in cooling load suffering from high air temperatures, but in the meanwhile, the buildings are recorded a lower cooling load due to higher-level of over-shading by the dense surroundings. On the other hand, as the surrounding built environment, a green park provides lower temperature as a result of multi-effects of cooling (Yu & Hien 2006).

In addition, there is a mutual relationship between on building itself and the surrounding buildings, which refers the mutual shading in the neighbourhood that modifies the thermal environment in building surfaces (Futcher & Mills 2013). The neighbourhoods of building groups provide mutual shading as solar receipts, which can reduce the ground reflectance (Stupka & Kennedy 2010) and shelter wind, thereby improving the performance of a single building (Smith & Levermore 2008) (Futcher et al. 2013).

iv) Function and mix-use

The land use patterns also impact building energy consumption. According to the existing research (Chen et al. 2011), the travel distance will increase due to the fragmented pattern of land used, which is correlated with energy consumption. Futcher et al. (2013) and Xu et al. (2013) found that the regulated load (the fixed consumption due to building fabric and condition systems) is significantly dependent upon the building function (office, residence, or industry). For example, the energy performance in an office, where disposing the internal heat gain is the primary daytime task, is dominated by the cooling load (Futcher & Mills 2013) (Steadman et al. 2014). And their cooling load will increase with the warming trends, for example, in a warm city centre with strong UHI effect. However, if these offices were converted into a residence, the UHI effect will be beneficial by reducing the heat load at night or in the winter time. On the other hand, in the commercial buildings, lighting consumption is massive. Therefore, the total energy consumption will increase if the buildings were located in a dense city centre with strong overshading effects (Liu et al. 2012). In addition, the time issue- operation schedule, which impacts the nature of occupancy, is another factor that should be considered with the urban function (Futcher et al. 2013).

Furthermore, the range and number of land function are related to the size of the land itself: a larger urban patch can easily provide more functions than a smaller one (Chen et al. 2011), which highlights the importance of a compact urban form in terms of its relatively lower energy consumption. In a compact neighbourhood with mixed functions, each land use will be mutually supported and complemented (Beyer 2010), where

residents have good accessibility to the office, retails, and other transit nodes, which provide employees and customers thereby benefiting the local economy and well-being in return (Hamilton et al. 2009). Consequently, high-rise buildings in the form of large building complexes are preferred to serve multiple functions (P. Xu et al. 2013).

v) Building envelop

As discussed in Section 2.5.3, heat flow through building envelop results in variation of indoor thermal performance. Factors of building envelop, including façade materials, exposed surface area, the proportion of glazing will directly impact the building energy consumption (Steadman et al. 2014). Studies (Ferreira et al. 2014) (Steadman et al. 2014) shows that energy consumption for heating and cooling is significantly correlated with the area of the exposed surface of buildings. Therefore, controlling area and the availability of heat transmittance of the building envelope is considered a strategy for optimising the daylighting and ventilation for maintaining indoor thermal comfort (Ratti et al. 2005).

Daylighting and Isolation of building surface are two indicators for building façade performance and are widely investigated. It is assumed that heat gain/loss is homogenous and proportional to the thermal properties and surface area on each face of façade in those studies conducted with only averaged-value indicators (Ratti et al. 2005). Surface to volume ratio has been considered as an interesting morphological indicator in studies of energy use. However, this ratio shows no significant relationship between the total energy consumption in these studies (Ratti et al. 2005) (Steadman et al. 2014). However, wrong conclusions may be made in comparative studies if only the two indicators are considered with, due to lack of concerns on the significant variation of radiation heat gain/loss in each face and floor of a building (Zhang 2013).

Considering these facts mentioned above, total-usable-floor-area-weighted performance indicators are applied in previous studies, which take the building density into consideration and are proved to provide better estimation than the traditional performance indicators (Compagnon 2004). Zhang (2013) used a cumulative-per-

floor- area data in his study, which noted that isolation performance in tower blocks, which absorb most of the built density, is better than that in other typologies (the traditional enclosed perimeter blocks and the open blocks).

2.4.5 Variables of urban form and building energy performance

The urban form has a significant influence on building energy performance, which has been discussed in early sections. When implementing the optimisation strategies of energy performance in planning neighbourhood, parameters need to be specified in order to estimate and evaluate the design results. Therefore, a series of urban form parameters are widely applied and conducted in previous studies. Holden & Norland (2005) used population density and housing patterns (size, age and type) to correlate household energy consumption and transportation. Rode (2014) investigated the effect of urban form parameters- density, ground coverage and building height, which indicate negative correlations of energy demand with these parameters. Torrens and Alberti (2000) measured density, scatter, ecology, and accessibility.

i) Urban density variables

As a characteristic of a compact city, intense use of land and infrastructure (energy supply, water system, roads, building and transportation) reduces the energy consumption per capita thereby benefiting the local economy and well-being in comparison to a dispersed city (Steemers 2003). Ewing & Rong (2008) reported that low-density residents with single-family home were recorded with 54% more heating consumption and 26% more cooling consumption than high-density dwelling units with multi-family housing. Moreover, similar finding (Wilson 2013) shows that energy consumption in areas closed to less developed buildings in wintertime is higher than that around well-developed properties, due to shelter-effect of a denser urban settlement. Therefore, the effect of urban density is highlighted in studies on building energy consumption (Hamilton et al. 2009) (Strømann-Andersen & Sattrup 2011) (Wong et al. 2011) (Hachem et al. 2012) (Zhang 2013) (Wilson 2013) (Liu & Sweeney 2012) (Ferreira et al. 2014) (Lowry & Lowry 2014). Steemers (2003) suggested three

ways to increase density by increasing building depth, building height, and compactness.

There are several variables to describe urban density, such as floor area ratio (FAR), building coverage ratio (BCR), building height, SVF, etc. FAR is a significant variable quantifying the development density, which is 'the ratio of the total floor area of the building to the area of the land on which it is located' (Zhao et al. 2011). Zhang et al. (2012) measured urban density by FAR (or plot ratio) to quantify the usable floor area. As reported by (Oldfield et al. 2008), FAR became a control index of local law in New York to promote deep floor plans. Nowadays, FAR has been world-widely used as a key parameter in local urban planning. BCR is also known as ground coverage ratio, which describes the urban density in two horizontal detentions and is widely used by architects and planners. It can be defined as the ratio of built area to the domain area (Ng et al. 2011). As a natural parameter of buildings, building height is also an important factor in urban planning (Zhao et al. 2011), which is considered as a direct and effective variable to determine urban density (Zhang et al. 2012). As discussed in Section 2.4.3, SVF is widely implemented in studies on urban climate and urban planning, which identifies the urban density by describing the degree of exposure to the sky (Zhang et al. 2012)

ii) Green coverage ratio

The green coverage ratio is defined as '*the ratio of total area of all green spaces to the area of the land*' (Zhao et al. 2011). As discussed in early sections, vegetation plays a significant role in impacting microclimate, thereby influencing building energy performance. Study (Wong et al. 2011) reveals that Green Coverage Ratio (GCR) overrides the other variables in terms of the effect of altering the microclimate condition compared to other variables.

iii) Plot layout

Plot-layout describes the characteristics of the plot of buildings, with which urban blocks can be categorised into three groups: Singular, Linear, Courtyard (Taleghani et

al. 2015), Semi-closed, and Interspersed (Yang et al. 2011). This parameter describes geometry patterns of building in both horizontal and vertical ways, which impacts daylight and solar potential (Grosso 1998).

iv) Summary of the practice of planning parameters

Study (Wong et al. 2011) shows that area with low building density has a lower air temperature. Considering the common preference on taller buildings with less building coverage and more open spaces (Cheng et al. 2006), increasing the building height is becoming a widely-used method for the study of the relationship between building density and environmental performance (Zhang et al. 2012). Moreover, taller surrounding buildings are considered to provide better shading effects reducing SVF thereby reducing outdoor daytime temperature (Wong et al. 2011) (Futcher & Mills 2013). As one comprehensive parameter of urban form combining building height and building coverage ratio, digital elevation model (DEM) is widely implemented in urban planning, especially with geographic information system (GIS) tools (Ratti et al. 2005) (Steadman et al. 2014). When the complete shading is created by the surrounding buildings, increasing height will no longer impact the microclimate in a positive way.

Further measures should be applied, such as increasing the green coverage ratio (Wong et al. 2011). Increasing GCR is considered one of the most effective ways of reducing the outdoor temperature which overrides other design variables (Wong et al. 2011). The combined use of multi-variable, including higher GCR with low building density, is recorded with the lowest outdoor temperature in previous studies (Wong et al. 2011) (Wong et al. 2011).

Arranging plot layout of building blocks with randomness in both horizontal and vertical ways is considered as one of the most recommendations and is encouraged to exploit its daylight and solar potential (Cheng et al. 2006). In specific, scattered layouts area considered as more desirable plot layout in planning building blocks.

In summary, variables of urban form, including building density, building height, and

green coverage ratio, plot layout, show a considerable degree of impact on building energy consumption. However, existing studies were more single-variable focused in the investigation of building energy performance, the literature on the analysis of multi-variables is insufficient. As discussed in early sections in this chapter, urban form variables influence building energy performance in indirection ways by altering outdoor temperature and microclimate, but existing literature on this issue is rare. Therefore, further study on optimising building energy performance by arranging multi design variables is still needed.

2.5 Local research on the evolution of high-rise building and UHI studies in Chengdu

2.5.1 Basic information about the city

As one of the biggest and most prosperous cities in every historical period of China, Chengdu has a long history of human migration and settlement, and it is considered as one of the birthplaces of Chinese civilisation. Due to its fertile lands, as well as the highly developed agriculture and Commerce, Chengdu Pain in history was reputed “the Land of Tianfu (the Heavenly Land of Plenty)” (Li 2007). Chengdu always keeps its high quality urban ecological environment since ancient times, even till recent years, which has plenty rivers and water networks, therefore being named as ‘Garden Water City’ (L. Chen et al. 2009).

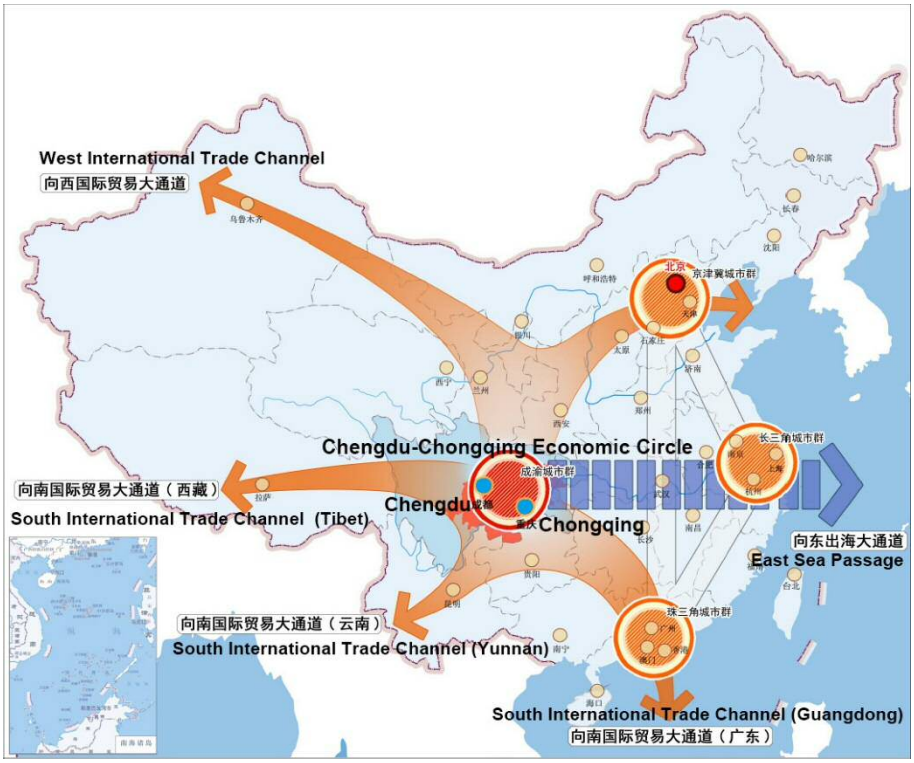

Figure 2. 27: Schematic Diagram of Open Channel of Chengdu-Chongqing Economic Circle

Source: (NDRC & MOHURD 2016)

Chengdu is one of two the cores in the city group of Chengdu-Chongqing Economic Circle (NDRC & MOHURD 2016) (Figure 2.27), which is the fourth economic pole in

China and most developed region in western China. Chengdu is located at the centre of Chengdu Pain and the west margin of the Sichuan Basin within the region of 102°54′E to 104°53′53E and 30°5′N to 33°26′N. The city has 14,600 km^2 city areas, hosting 16 million populations including more than 10 million citizens (Tourism Administration Network of Chengdu 2017). This capital city of Sichuan Provence has been developing rapidly in recent years. Till 2017 (Tourism Administration Network of Chengdu 2017), Chengdu consists of twenty urban districts (Cities of County-level or counties) and two special administration zones (Chengdu Administrative Zone of Tianfu New Area, Chengdu Hi-tech Zone) (Figure 2.28), including 13 districts/zones in the downtown of the city, including five inner-city districts (Wuhou District, Jinjiang District, Qingyang District, Jinniu District and Chenghua District).

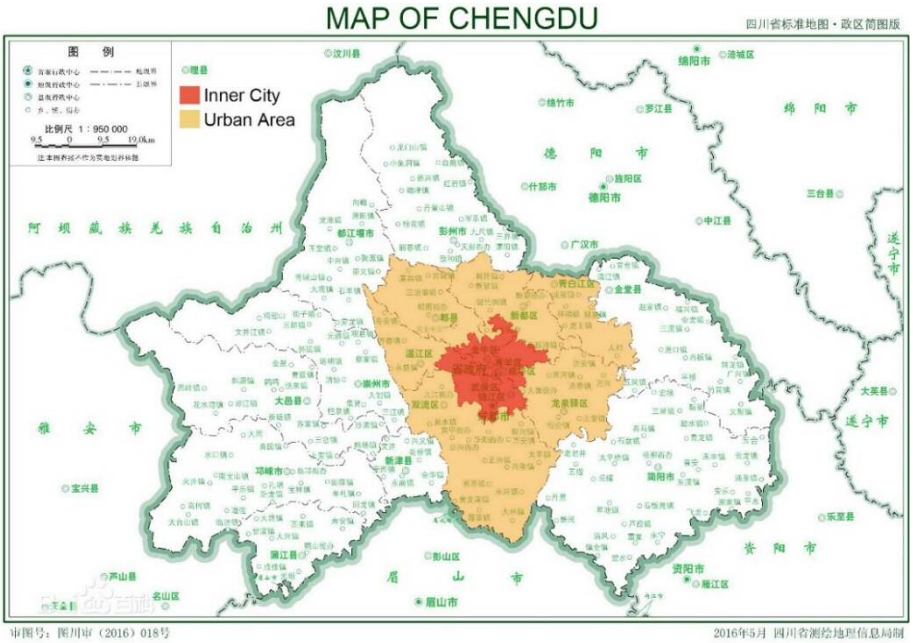

Figure 2. 28: Administrative Map of Chengdu
Source: Compiled from the map on
http://www.scbsm.gov.cn/images/bzdt/szjbzdt/szbzdt4k/cd4/cdzq4k.jpg

Based on the national standard (MOHURD 2017), Chengdu is located in the Hot Summer & Cold Winter Region (Figure 2.29). Together with its metropolitan area, Chengdu has a Subtropical Monsoon Humid Climate with distinct four seasons: warm and comfortable spring and autumn, hot but not extremely hot summer, cold and dry winter with rare ice and snow (Table 2.12). There is quite a lot of rains in summer and

autumn. The annual rainfall is around 1000mm, while the annual average evaporation is 841.1 to 1066.1 millimetres (the monthly evaporation is 115 to 152.1 millimetre in summer) (Anon 2013). The average of wind speed is low (around 1.2m/s) with many cloudy and foggy days all the year. Due to the very humid climate (Xing 2015), the summer is muggy, and winter is gloomy and cold. Since the very beginning of the ancient city of Chengdu, the local climate and geology impacted residents' live and lifestyle, as well as the residential environment (LI & ZENG 2015).

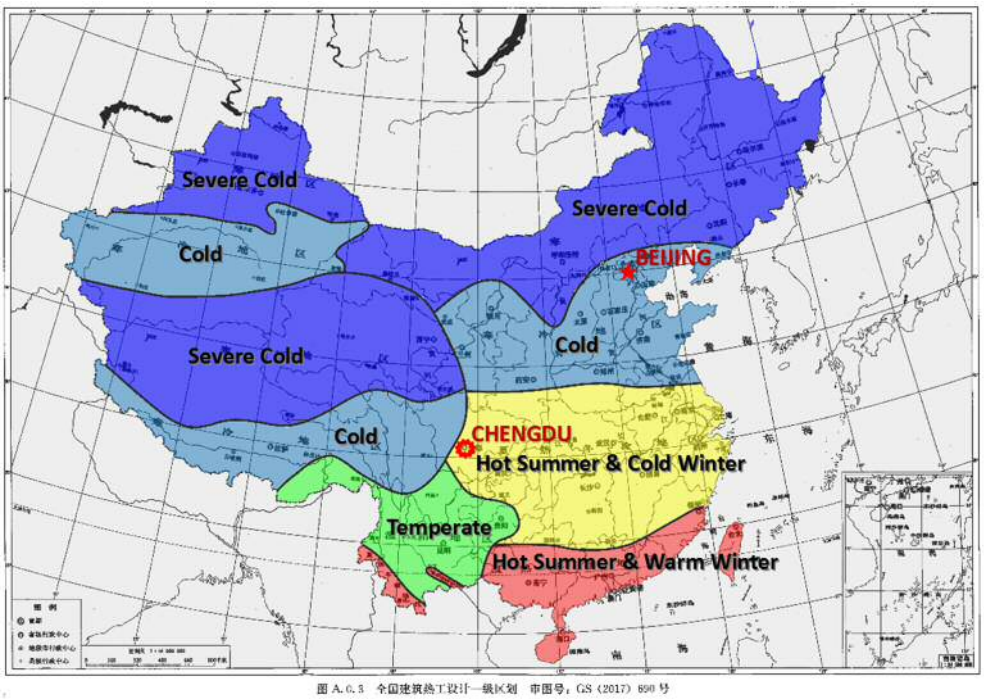

Figure 2. 29: Zonal Map of Thermal Design for Buildings in China
Source: compiled from the Chinese national standard (MOHURD 2017)

Table 2. 12: Annual weather data of Chengdu

Annual Averge	Jan	Feb	Mar	Apr	May	Jun	Jul	Aug	Sep	Oct	Nov	Dec
Daily High Temp.(℃)	10℃	12℃	16℃	22℃	26℃	28℃	30℃	30℃	25℃	21℃	16℃	11℃
Daily Low Temp.(℃)	3℃	5℃	9℃	13℃	17℃	20℃	22℃	22℃	19℃	15℃	10℃	5℃
Average Rianfall(mm)	7	11	20	47	82	110	223	227	115	40	16	6
Average Humidity(%)	79.9	80.6	74.6	69.2	75.0	72.8	81.8	85.2	80.2	82.2	80.0	76.9

Source: (Chengdu Meteorological Bureau (CDMB) 2016)

2.5.2 The 'New' Chengdu

In modern times, just as it was more than 2000 years ago, Chengdu is still one of the

most important cities in China. From the beginning of New China founding in 1949 to the end of the Twentieth Century, Chengdu experienced rapid economic growth. The city contributed a GDP with $82 Billion in 2010, which ranked 12th among all Chinese City, 3rd among all 15 vice-provincial cities, leading the cities in Southwest China (CMBS 2011). While keeping this rapid development trend, Chengdu produced a GDP $163.8 Billion at the 9th place of the ranking in 2014 (CMBS 2015), and $207.3 Billion at the 8th in 2017 (CMBS 2018). At the same time, the city has witnessed a rapid growth in population. The citizens in the urban area increased from 3.36 million in 2000 to 5.35 million in 2010, while the number in 2015 is 6.98 million (Table 4.2). Till 2015, the downtown districts hosted more than 30.39 per cent of the total population in Chengdu with a population density of 8,027 people per square kilometre (CMBS 2016). A significant amount of housing development contributed to the fast urbanisation process of this city in this period, the indicator, Per Capital Residential Floor Area, almost tripled from 11.6 meter square in 2000 to 29.52-meter square, and reached virtually quadrupling data in 2015 (Table 2.13).

To meet the eager needs of rapid urban development, the national government and the municipality of Chengdu launched plenty of ambitious development plans since the beginning of the new Century. Massive investments were invested in mega-scale urban construction and regeneration projects (Figure 2.30) (Figure 2.32). Those actions boosted the city development and modified the urban landscape. As shown in Figure 2.31, the city has witnessed the process of a fast modernization in recent 30+ years. It resulted in an expansion of city area from 152.5 km2 in 1985 to 441.1 km2 in 2000, and it was 597 km2 in 2010, with an 11.5% rate in average annual growth of the urban area (Ren et al. 2014) (PMGCD 2011). Accordingly, the administrative area of downtown had expanded from the original five districts to the current eleven Districts (Figure 2.32) (CMBS 2017). Due to its political and economic impaction, as well as the location advantage, the city has been planned to be the nine national central cities since 2016 (NDRC & MOHURD 2016).

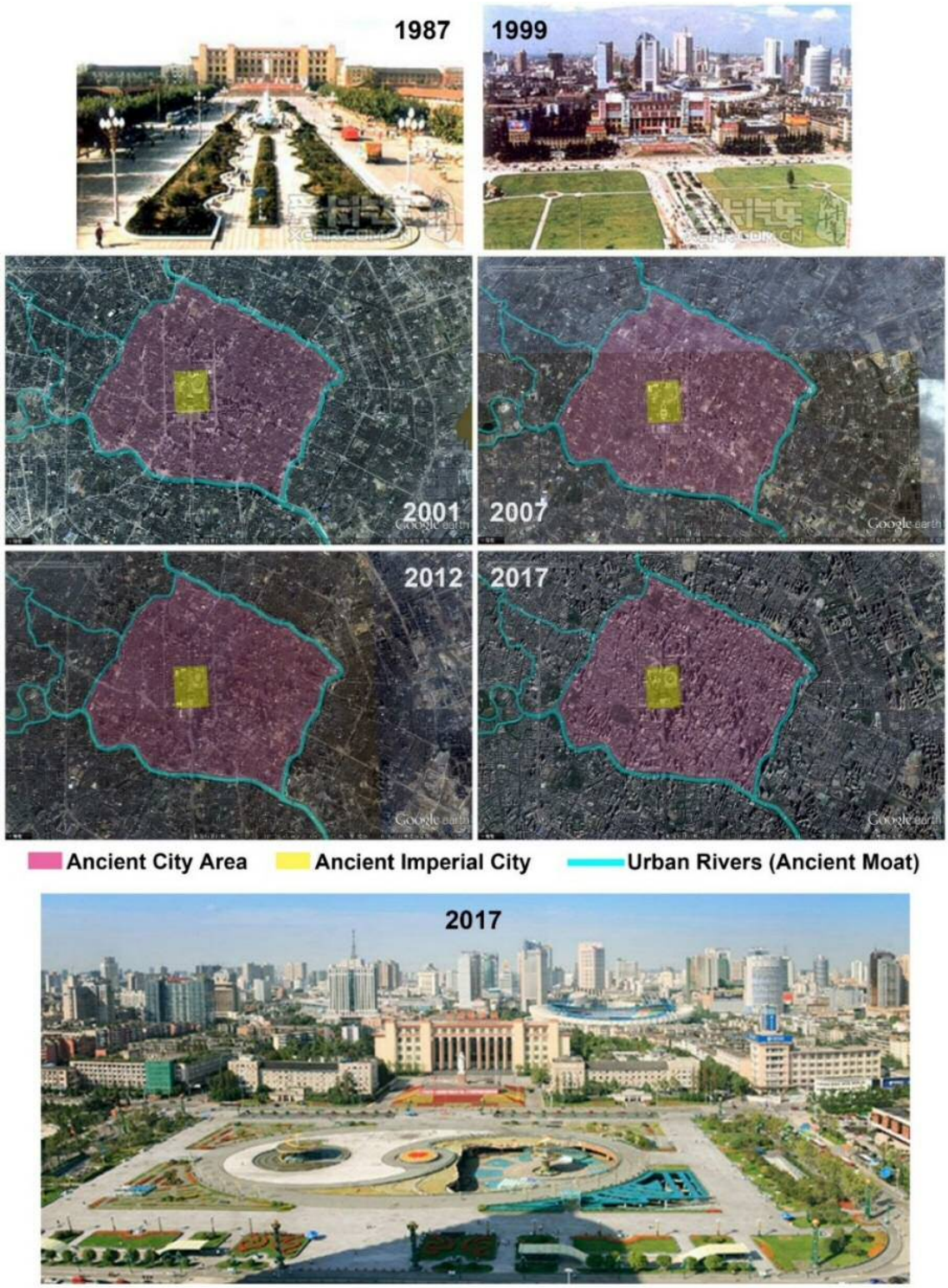

Figure 2. 30: Redevelopment of the urban core with the "Ancient Imperial City" in the city centre of Chengdu.

Source: compiled from the maps on Google Earth, pictures on http://www.xcar.com.cn/bbs/viewthread.php?tid=17986913 (top), https://www.chinadiscovery.com/sichuan/chengdu/tianfu-square.html (down)

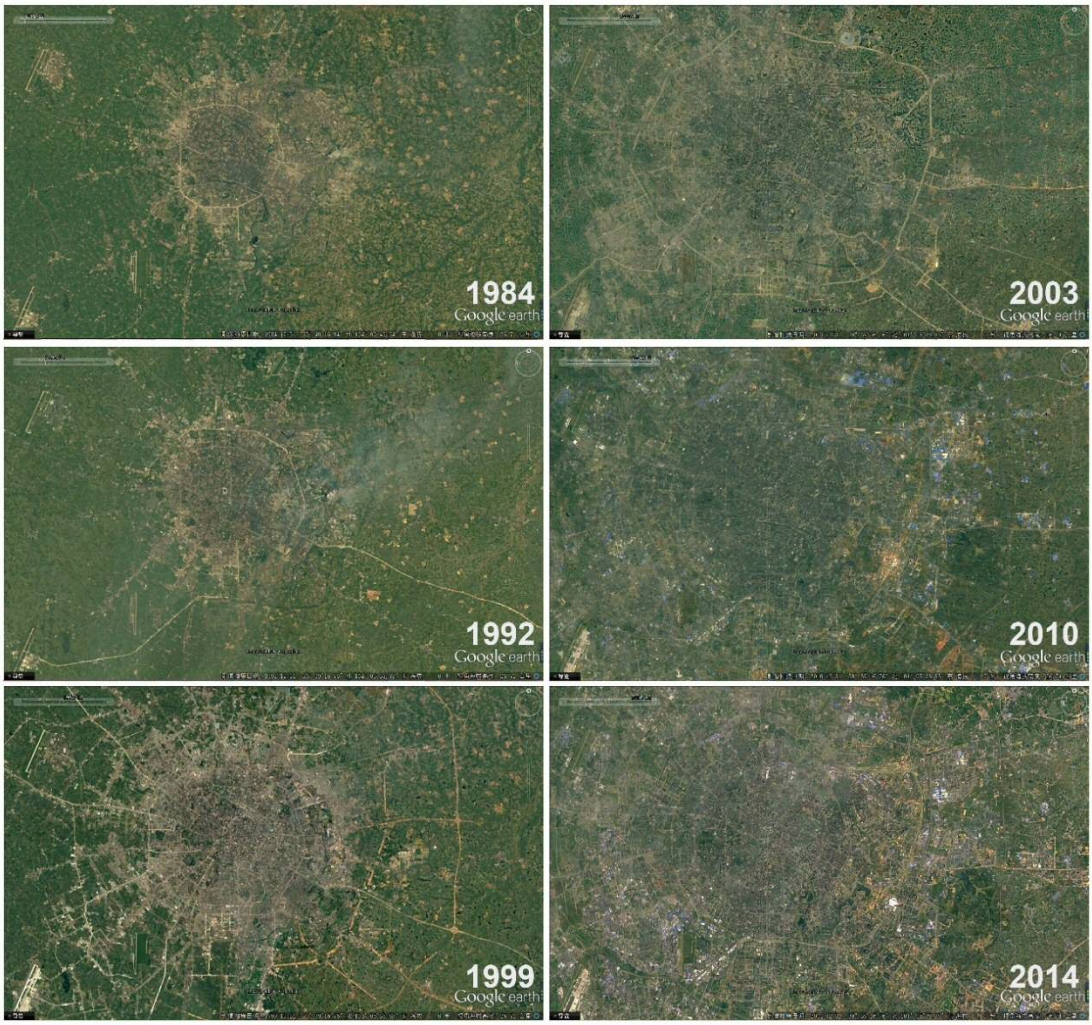

Figure 2. 31: the landscape evolution of the Chengdu urban area

(Source: compiled from the maps on Google Earth)

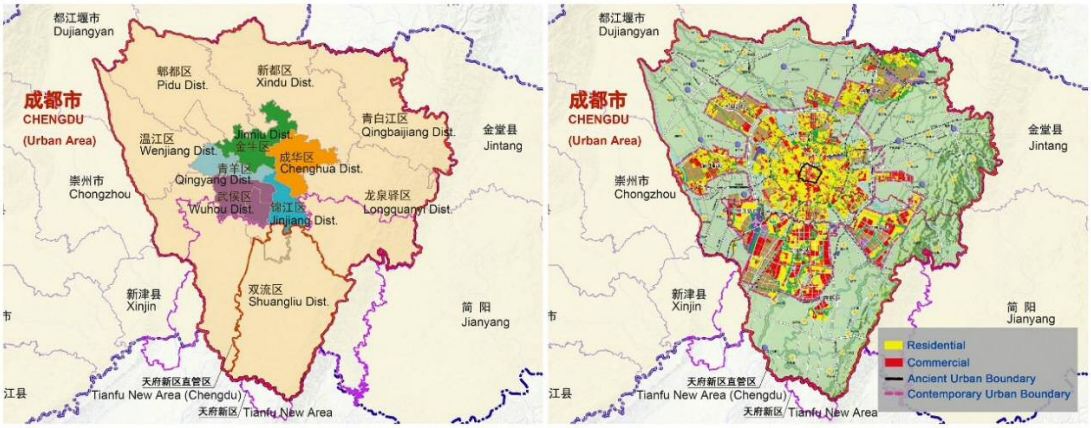

Figure 2. 32: Eleven Districts of Urban Area of Chengdu (left) and the urban structure of Chengdu (right)

(Source: compiled from the maps in "Draft for Chengdu Urban Master Plan (2016 -2035)" (Chengdu Municipal Planning Bureau 2017))

Table 2. 13: Growth trend of urban population and residential floor area.

Year	2000	2005	2006	2007	2008	2009	2010	2015
Population of Urban Area (Million)	3.36	4.73	4.97	5.03	5.10	5.21	5.35	6.98
Per Capita Residential Floor Area (㎡)	11.60	27.67	28.58	27.89	27.82	29.24	29.52	39.44

Source: Annual Data of Chengdu (Chengdu Municipal Bureau of Statistics 2001), and Chengdu Statistical Yearbook (2016) (CMBS 2017)

2.5.3 Energy Structure and potential for renewable energies

Benefitting from its abundant reserves of natural resources, the energy structure of Chengdu has been optimised in recent decades. During period of the Twelfth Five-Year (2011-2015), the consumption proportions of electricity, natural gas, refined oil, and coal products are 37.74%, 15.67%, 30.72%, and 15.87%, respectively; non-fossil fuels took up 26.76% of total consumed energy (Table 2.14) as reported by CMCEIT (2017). Due to its unique geographical conditions, Sichuan Province is the most prominent production base of renewable energy (Lao 2015), whose production and reserves are leading all Chinese provinces in hydropower, natural gas and Shale Gas. In the meanwhile, the whole nation has been playing a role of leader in renewable energy in the world since 2012 (Liu et al. 2013), therefor Sichuan Province is making significant contributions to the world renewable energy. According to Lao's (2015) research, till 2013, the installed capacity of hydropower is 52.66 million KW, which took up 81.60% of the total installed capacity of electricity in Sichuan Province and more than 20% of the total installed capacity of hydropower in China.

Table 2. 14: Table of Energy Development of Chengdu during the 12th Five-Year

Category	Indicator	Unite	2010 Actual	2015 Planning	2015 Actual	Annual Growth	Type
Total Energy Consumption and Structure	Disposable Energy Consumption	million tons of standard coal (ktce)	37.53	55.56	45.56	3.95%	Predicted
	Total Electricity Consumption	billion kW/h	34.13	63	48.64	7.34%	Predicted
	Proportion of Electricity Consumption	%	36.77	46	37.74	[0.97%]	Predicted
	Natural Gas Consumption	billion Cubic metre (bm^3)	4.06	7.20	5.62	5.60%	Predicted
	Proportion of Natural Gas Consumption	%	13.15	16.00	15.67	[2.52%]	Predicted
	Refined Oil Consumption	million ton (kt)	4.49	6.50	5.03	2.30%	Predicted
	Proportion of Refined Oil Consumption	%	17.58	17.00	30.72	[+13.14%]	Predicted
	Coal and other energy consumption	million tons of standard coal (ktce)	9.85	/	7.23	-6.01%	Predicted
	Proportion of Coal and other energy	%	32.50	21.00	15.87	[-16.63%]	Predicted
	Non-fossil Fuels	%	24.2	32	26.76	[+2.56%]	Predicted
Green Development Indictor	Energy consumption per unit of GDP	tons of standard coal/ thousand yuan	6.77	5.7	4.87	[-28.06%]	Predicted

(Source: Chengdu Municipal Commission of Economy and Information Technology (2017))

Consequently, *the dominant sources for the electricity supply in Chengdu are the most 'renewable' and 'low-carbon', which provides an ideal condition for low carbon-eco urban development*. However, considering the outstanding percentage of thermal power and a large proportion of total energy consumption taken by buildings (Su et al. 2010), energy efficiency in the building sector is still of significance regarding reducing CO_2 emission and mitigating UHI effect in Chengdu.

2.5.4 Environment and social aspects

Benefiting from the beautiful nature, rural area of Chengdu with a variety of topography and geomorphology populates large plants and wild animals (Fang et al. 2001), including some rare and endangered animals- the world-widely popular and pursued Giant Panda (Wei et al. 1997). However, like other big cities in China during the rapid urbanization process in the 1990s, the urban ecologic environment in Chengdu lacked concern and protection. Land contamination, air pollution, destruction of vegetation and green area, and other environmental issues perplexed the city decision makers (Zhao et al. 2002) (W. Xu et al. 2007). The general urban development was in an unsustainable model (Luo et al. 2006). Till mids-00s, Chengdu started a series of urban eco-environment moves. Factories with massive emission were moved out from the metropolitan area to suburban regions, while river control and water pollution control significantly improved the urban environment (Fang et al. 2001), renovation planning for land in the inner city with vegetation (He et al. 2014) held the baseline of urban green ratio laying foundation for the future environmental policies.

Accordingly, as the largest city in western China, Chengdu Municipal Government has promulgated announced a series of local policies and action plans: In 2010, Chengdu was permitted to build the national demonstration city of 'renewable energy building' implementation, therefore the renewable energy had been integrated into the overall planning with green building (Liu 2016); The very first pilot projects of low carbon town in Chengdu appeared in 2011, which were the Shouan New Town in Pujiang County as the demonstration area of 'renewable energy buildings', and the implementation of

low carbon & green building technologies in Xinjin County (Liu 2016); Till 2012, six projects in Chengdu had been rewarded the Start Label of Green Building by MOHURD (Liu 2016); Followed the routine made by related national ministries and commissions in 2013, the Action Plan of Green Building in Chengdu was released in 2014 (Chengdu Municipal People's Government 2014). The Plan set clear targets of energy saving strategies on newly constructed buildings, retrofitted existing buildings and implementation of renewable energies, a series of actions would be applied to promote the low-carbon & green urban planning, demonstration projects of low carbon town, and full implementation of green building in all public buildings.

Table 2. 15: CO2 emission in Chengdu 2001~ 2010

YEAR	2001	2002	2003	2004	2005	2006	2007	2008	2009	2010
Total Engery Consumption for GDP	1850.00	1727.00	1825.00	2193.00	2418.00	2640.34	2880.70	3135.91	3400.08	3753.33
CO_2 Emission (10^4tce)	4581.53	4276.92	4519.61	5430.96	5988.18	6538.80	7134.05	7766.08	8420.30	9295.12
CO_2 Growth Rate (10^4t)	3.35%	-6.65%	5.67%	20.16%	10.26%	9.20%	9.10%	8.86%	8.42%	10.39%

Source: (Zhang & Zhang 2013)

However, as shown in Table 2.15, the total carbon dioxide emission kept increasing in the first decade in Chengdu. Due to the adjustment of industrial structure in 2004, which reduced the scale of Secondary Industry- the most significant emission source, the total scale of the Primary Industry and Service Sector was more significant than the Secondary Industry (Zhang & Zhang 2013). Therefore, the growth rate of carbon dioxide emission since 2005 was much lower than in 2004. *Considering the growing trend of carbon dioxide emission in Chengdu, further research and strategies are urgently required*.

2.5.5 Urban morphology and building typology in the urban area of Chengdu

i) General history of typology and urban environment in Chengdu

According to the archaeological documents (Zhang & Tang 2014) (Liu 2016) (Lin 2002), the very first form of buildings appeared in Chengdu were 'Stilted Building' in Shang Dynasty (1600 B.C. to 1046 B.C.) (Figure 2.33). These buildings were developed from ancient nests, which were made of wood, bamboo and thatch. The first floor was built on stilts to avoid humidity from the mud ground. And this form was found in both)(h

residential and imperial public buildings (Zhang & Tang 2014). As the rapid development of society when civilization stepped into feudalistic ages, the foursquare courtyard style building groups with corridors and halls (Figure 2.34) had become the trend in Chengdu in Eastern Han Dynasty (25 A.D. to 220 A.D.). The foursquare courtyard style building groups follow the order: symmetry plan with a foreside hall and backside living rooms, which became the primary form of Dwellings and public buildings in Chengdu and other places in China (Figure 2.35) (Lin 2002). Comparing to the courtyard style building group, the foursquare courtyards in Chengdu have very deep eaves, which form a closed circle corridor leaving a smaller courtyard uncovered (Figure 2.36)(Liu 2016). These design features were designed to protect people in the buildings from the frequent rains and direct sunshine, while the natural ventilation can smoothly flow away from the hot and humid air from inside of buildings (Figure 2.37). Due to being perfectly adapting to the local climate and social requirements, the traditional courtyard style has been inherited to the present.

After the 1980s, the urban spatial form of the city still followed the tradition of urban planning: ‘single centre’, ‘compact’, and ‘two rivers encircled’ (L. Chen et al. 2009). However, as the development strategy was focused on economic, the importance of eco-environment then was being ignored. Together with plenty of green lands and cultivated land, most branches of the urban water network were buried for new construction projects(LI & ZENG 2015)(L. Chen et al. 2009). In the meanwhile, the old foursquare courtyards were replaced with the more modern buildings, most of them were similar matchboxes of parallel slab buildings (Figure 2.38), which lack characteristic and personality during the last period of Twentieth Century (Lin 2002). Even the unsophisticated and elegant foursquare courtyards have always been the ideal style of residence for Chengdu citizens, the irreversible modernisation process makes foursquare courtyards only people’s unforgettable memory of Old Chengdu (Lin 2002). Till today, there are quite a few of traditional foursquare courtyards left in Chengdu; people can only visit them in some public attractions (Figure 2.35). At that time, most of the parallel slab buildings were built up lower than seven storeys in order

to avoid additional investment for the lift system, which is compulsory for building more than six storeys according to the building codes (MOHURD & AQSIQ 2011) (Luo 2005). And the parallel slab buildings were widely built for more than two decades, and many of them still exist nowadays.

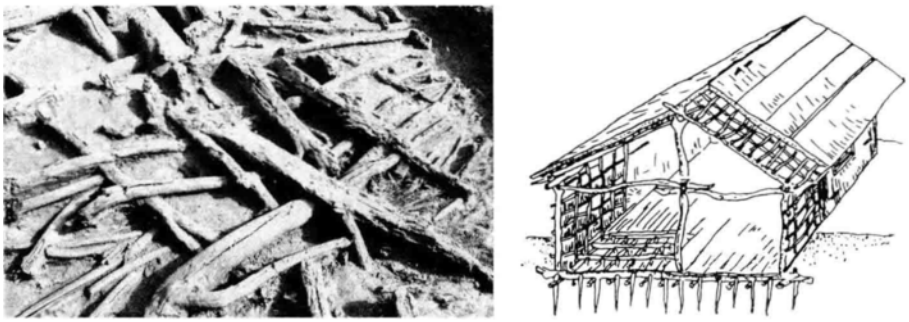

Figure 2. 33: The Twelve Bridge Building Site (left) in Chengdu and the recovery picture (right)
Source: (Zhang & Tang 2014)

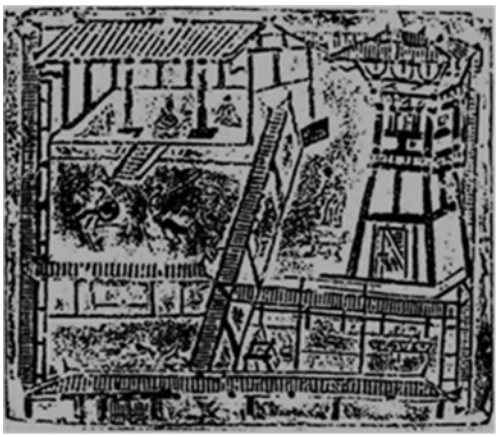

Figure 2. 34: The brick "Courtyard" in Eastern Han Dynasty (25 A.D. ~ 220 A.D.)
Source: (Zhang & Tang 2014)

Figure 2. 35: Layout of Wenshu Monastery
Source: compiled from the picture on https://www.chinadiscovery.com/chengdu-tours/wenshu-monastery.html

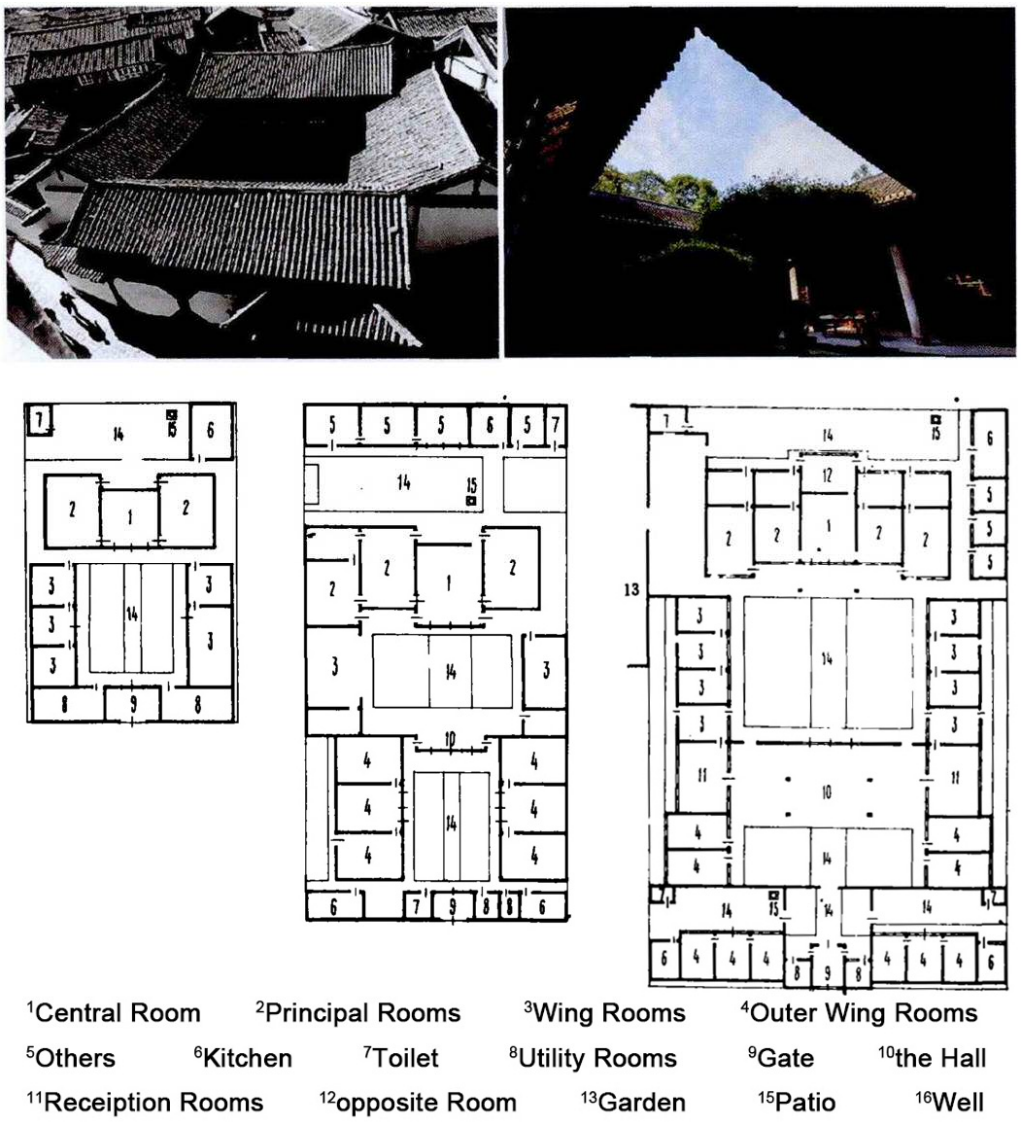

Figure 2. 36: Traditional courtyard and plans in Chengdu

Source: compiled pictures form documents (Liu 2016) (Huang 1981)

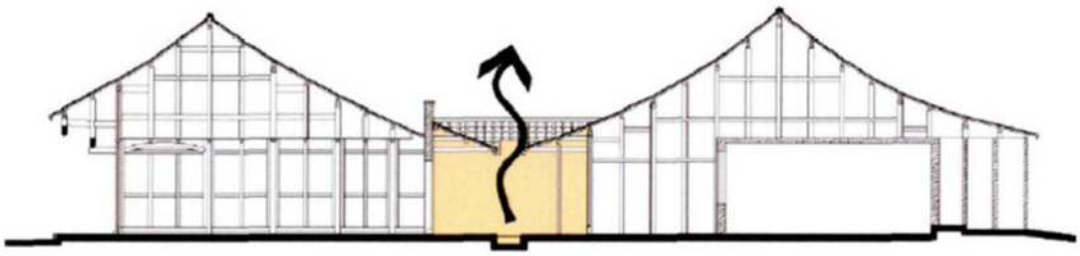

Figure 2. 37: Early passive design strategy in traditional courtyard style building groups in Chengdu.

Source: (Liu 2016)

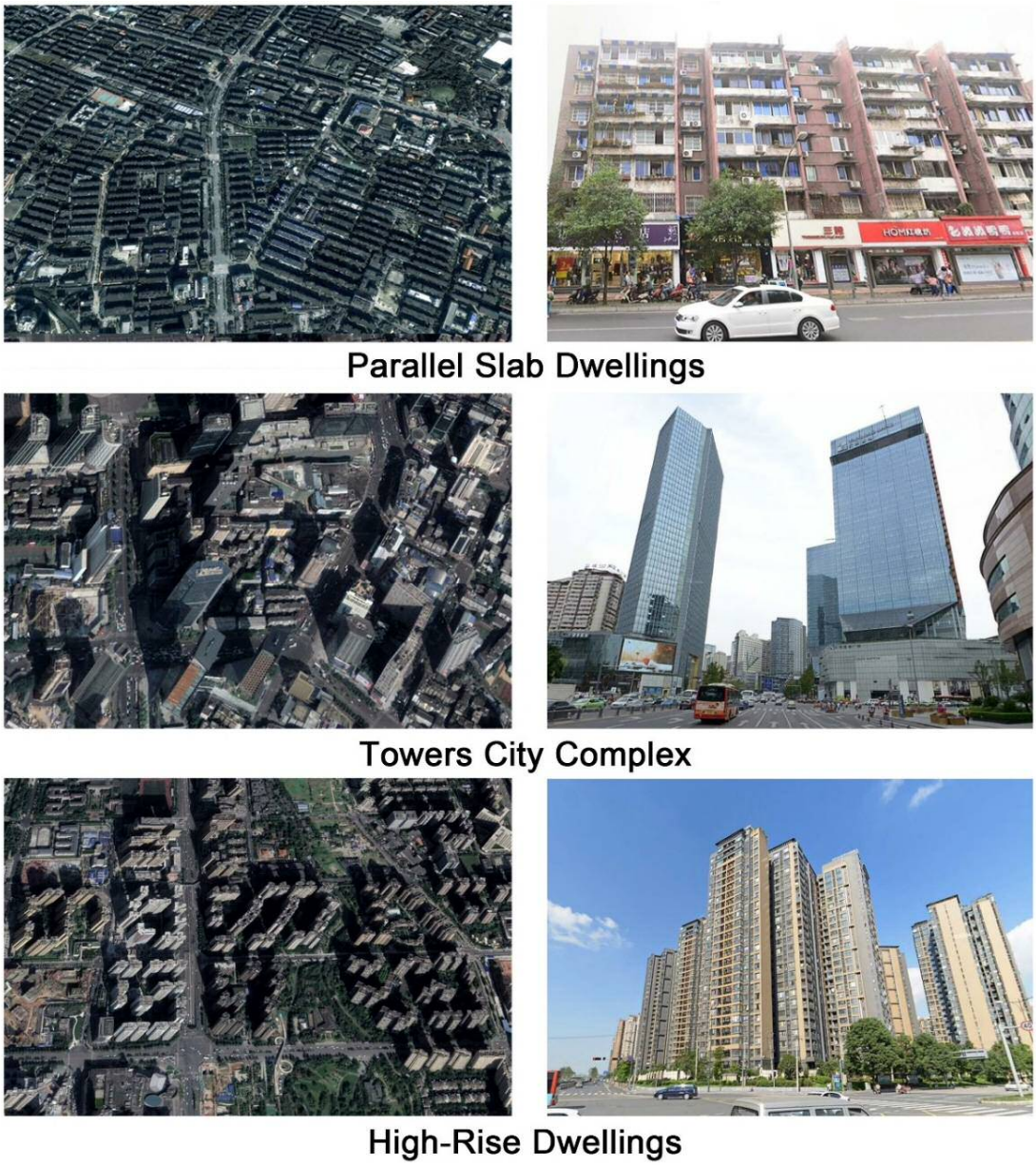

Figure 2. 38: A main urban typology of urban area in Chengdu
Source: compiled from Baidu Map and Google Earth.

2.5.6 High-rise Buildings

'High-rise Buildings: residential building structures with 10 stories and more than ten stories or more than 28 metres, and other civil building structures whose height is greater than 24 metres.'

-- *Technical Specification for Concrete Structure of Tall Buildings* (CAAS 2010)

'The high-rise building is often seen as the rationalisation and symbol of

modernity.' …'In particular, high-rise building is often seen as an icon of a developed (Western) society—especially that of the US which led the world in the construction of the first modern tall building and whose subsequent development became a model for 20th-century urban development.' -- (Yuen et al. 2006)

i) High-rise Commercial Estate in Chengdu: city complex and HOPSCA

The appearance and development of high-rise typology have been impacted by changes in regulatory policies, innovation of technology and materials (Oldfield et al. 2008), and land shortage and massive interest of developers (P. Xu et al. 2013). And those innovations and achievements are always firstly applied in public buildings. Since the first generation high-rising building- the Home Insurance Building in Chicago built in 1885 (Turak 1985), there have been five generations of High-rise public buildings in terms of buildings services and revolutions of façade material (Oldfield et al. 2008). Slender shape with double-skin & triple glazing façade dominates the form of high-rise buildings. The development of high-rise public buildings in China just followed that process in Western cities, and the skyscrapers with multi-functions dominate the form of public buildings in CBDs in most Chinese cities (Wu 2016).

Public buildings (Figure 2.39) in Chengdu also experienced the similar process of 'being taller'. The very first modern high-rise building in Chengdu is the Bell Tower of the former West China University of Medical Science (now West China Medical Center of Sichuan University) built in 1926, which is a thirty metres tall traditional Chinese style brick and wood structure. After new China (People's Republic of China) was founded, a sixty-nine metre- tall landmark of the city centre- Bell Tower and Telecommunications Building was constructed (Kuzi 2017). The tallest modern steel-concrete tower in West China- 116 metre-tall Shudu Tower and 136 metre-tall Bank of China (Sichuan) Tower- were built in 1991 and 1994, respectively, which indicated the achievements of Reform and Open Policy and the beginning of the contemporary movement of super-tall in Chengdu (Chengdu Upwards 2017).

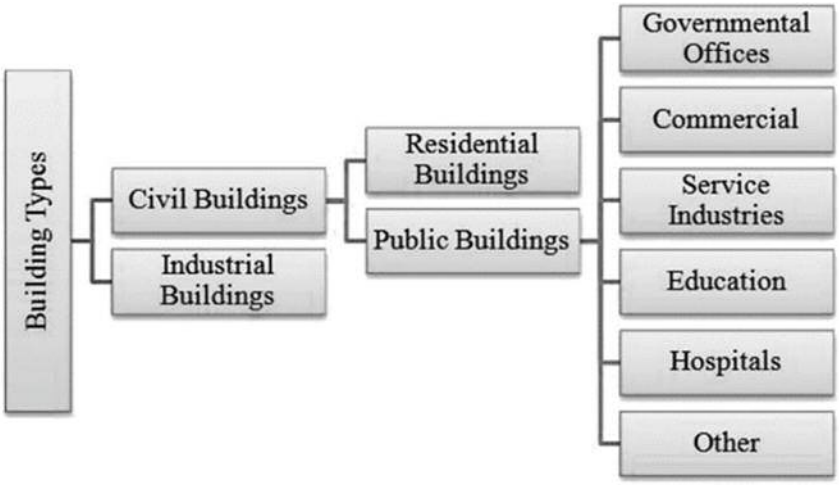

Figure 2. 39: Building types in China.
Source: (Li & Shui 2015)

'City complex should consist of three or more than three kinds of urban functions, such as commerce, office, hotel, convention and exhibition, culture and entertainment, sports, transportation and housing.'… 'Besides the residential, city complex should have an urban function, such as a commercial complex, hotel complex and exhibition complex.'

-- Supplementary Provisions for Planning Management of Large Urban Complex Projects in Downtown Chengdu (CDMPB 2012)

Those high-rise buildings were mostly built as offices, while new buildings after 2000 were designed with multi-functions, and usually in the form of a building group. Commercial, residential and offices were integrated into these real estate projects. Based on Wu's (2012) investigation, more than ninety per cent of new real estate projects- including residential, commercial, and office format- were high-rise or super high-rise buildings in the first decade of New Century. According to the data from Chengdu Commercial Real Estate Alliance (CCREA 2013), there were 122 city complexes in Chengdu till 2013, and the majority of them had above three in terms of floor area ratio (FAR), and some city complex had even higher than six FAR. Further dozens of new city complex projects would be completed during 2013-2015, which leading the number of city complex among the megacities in China. The new urban typology, which consisted of high-rise buildings were widespread and altered the city

skyline. Therefore, that modern urban development led new urban neighbourhood being taken shape in Chengdu (Figure 2.39).

In terms of spatial characteristics, city complex could be a single building, as well as a building group, which specifically can be categorised into four types: independent, combined, stereoscopic circulating, and multi city-block (Zengcui 2010). In Chengdu, except for stereoscopic circulating style, the other three types of city complex have been built.

ii) High-rise Estate Housing

On the other hand, the first high-rise housing appeared lately after World War II, when Le Corbusier gave his aphorism 'a house is a machine for living in' (Jacobs et al. 2007). Due to its problematic living conditions, the optimism of high-rise estate was tempered after the 70s in Western cities (Luo 2005) (Yuen et al. 2006) (Jacobs et al. 2007). However, at that moment, this residential typology was infused into Asia, including Singapore and China, which nowadays is the mainstream of estates in most Chinese cities (Luo 2005).

Since the late 1990s, the circumstances had taken places in both social and economic aspects. In 1998, due to the housing system reform (State Council of the PRC 1998), the old national policy of welfare housing system was terminated, which was replaced by a multilevel housing supply system: commodity dwellings under the market pricing mechanism for general public, affordable dwellings for low-income families, and cheap-renting dwellings for the lowest-income families. However, there were plenty of issues raised in the implementation of the affordable dwellings and cheap-renting dwellings (Xie & Sun 2007) (Xin 2008), the low-income families and the lowest-income families could barely benefit from the new system. Therefore, the scale of both types was extremely restricted, and further actions from the municipal government were required (Xie & Sun 2007). While on the other hand, due to the significant attraction from market interest for decision makers and investors, the commodity house become the only mainstream in practice (Li 2006).

In the specific condition in China, the new market mechanism made people hardly afford a large housing, which was mostly multi-storey or low-rise dwellings, the price of the high-rise dwellings with the smaller living area were much more welcome to them. Moreover, the shortage of multi-storey or low-rise buildings- low capacity- was so apparent that they could barely meet the need of the rapid urbanisation. Together with a series of national policies later in the 2000s, construction of small- and medium-sized apartments was highly encouraged (Yin 2007). Consequently, the parallel slab dwellings were gradually replaced by the high-rise dwellings in the early 2000s, even though people's preference tended to be multi-storey building and low-rise building as their dwelling house in early 2000s (Du 2003).

Figure 2. 40: Plot layout of high-rise housing projects in Chengdu
Source: Google Map

There are several spatial forms fo high-rise building group in Chengdu: high-rise tower, the single building of corridor layout, the combined single building of multi-layout, combined units of the linear layout (Yin 2007). Due to local condition and policies, lands are usually sold at a city-block scale to the developers. Therefore, during the real practice of a real estate project, general planning of a site is arranged with a building group. And the different combination of each form of high-rise buildings results in

several types of plot layout in large-scale real estate projects. As shown in Figure 2.40, at least five types of plot layout can be found in Chengdu. Moreover, in some high-rising housing projects, a minor amount of commercial function (less than 10% of the total floor area) is allowed by local policies in Chengdu, usually at the bottom floors of the high-rise buildings (Yin 2007).

In consequence, till 2010, just within several years, the original constructions in the urban core of the City have been dramatically replaced with modern concrete high-rise buildings and skyscrapers, Therefor, modern urban neighbourhoods have taken shape in Chengdu City. However, issues have been raised in the livability of high-rise buildings.

2.5.7 Local agenda of livability and built environmental performance

As mentioned in the previous sections, Chengdu is located in the area of Sichuan Basin with massive population settled in, the land for urban construction is relatedly intense when compared to other big cities. Therefore, the overall plan arrangement for most buildings in Chengdu is compact (Xing 2015), which leads to narrow space between buildings, over-shading among buildings (Zhao 2010). It is also difficult for buildings to have natural lighting and natural ventilation. Consequently, together with the improper use of water bodies and albedo modification by replacing the natural green area with tiles or even hardened grounds, the irrational urban form aggravates the UHI effects in Chengdu. In summer, there are quite frequent continuous ‘sauna’ (hot and humid) days with above 35°C outdoor temperature; in winter, the outdoor temperature is just above 0°C but with high humidity (Xing 2015). All these factors contribute low livability in summer and winter in Chengdu (Peng 2011). Energy used for increasing the liability in summer and winter takes up one-third of the total buildings energy consumption in Chengdu (Xing 2015). And this issue gets more serious in high-rise buildings.

Accordingly, strategies of optimizing built thermal comfort have been applied in at planning and designing stage. Measures, planning a certain amount of green area, water bodies around buildings (Zhao 2010), and optimising building and master plan

for better ventilation (Wu & Yang 2013) have been suggested. Other strategies such as reducing the area ratio of window to wall, and applying a shading system (Lei & Nanyang 2017)(Yu et al. 2008) were also suggested. Feng (2004) concluded that solar heat gain in summer, insulation in winter and natural ventilation in spring and fall should be considered in design energy-efficiency buildings in Hot-Summer & Cold-Winter Zones. Local research on building energy efficiency shows that improving the building envelop, including exterior walls and windows, could reduce 20.7% and 67.7% energy consumption for cooling and heating, respectively (Gao et al. 2009). However, the only a single measure would be far from enough to create a satisfied thermal comfort in high-rise buildings. Therefore, active services, such as air conditioning and fan, are still a common choice against extreme weathers (Zhao 2010) (Peng 2011). In consequence, energy consumptions for optimising indoor comfort have become a dominant part of a total building energy consumption in this region (Xu et al. 2013), obstructing the 65% Goals of Energy Efficiency (CMCEIT 2017) set by the local authority .

As stated above, existing local research just focused on a single measure and on single buildings, further research on multi-measure strategy in terms of building groups and neighbourhoods is still needed. Moreover, current research and practice only address measures at very late stages of building design as an additional procedure of design strategies. In the meanwhile, early design stages of planning for mitigating microclimate variation and optimising building energy performance have not been focused by local researchers, thereby limiting the potential strategies on optimisation of building energy efficiency and outdoor thermal.

2.5.8 Local research on UHI effect in Chengdu

The relevant studies of urban climate in Chengdu were started relatively late, compared to other big cities in the world. In 1988, Yang (1988) collected historical meteorological data for the period between 1957 and 1987 obtained from fixed weather stations in Chengdu. Moreover, he analysed the hourly temperature data and drew

hourly UHI maps for selected days in August of 1987. Finally, Yang derives equations to calculate the UHI intensity in Chengdu, taking into account of cloudiness, wind speed, temperature and humidity. Lin & Wang (1990) used two sets of data from the NOAA/ AVHRR (National Oceanic and Atmospheric Administration of the USA - NOAA, Advanced Very High-Resolution Radiometer - AVHRR) satellite and concluded the spatial pattern of UHI in Chengdu. Since the beginning of the New Century, as the development of remote sensing, UHI analysis with GIS tools have been widely implemented. Dan & Dan (2001) found the daily change characteristics of UHI in Chengdu with AVHRR data. Chen et al. (2009) analysed the relationship between the distribution of the normalized difference vegetation index (NDVI) and UHI spatial pattern in Chengdu based on the moderate resolution imaging spectroradiometer (MODIS) data and found out that there was an increase of 0.5°C in UHI during 2002 to 2008. Xu et al. (2007) summarised the relationship between the scale of the urban area and the magnitude of UHI in Chengdu by analysing NOAA/AVHRR data. Xia et al. (2007), Dan et al. (2011), and Zhang et al. (2014) used remote sensing data to analyse the impact of urban evolution on UHI in Chengdu. Zhang & Cheng (2016) used MODIS temperature product to conclude the trend of change of UHI from 2009 to 2013. Zhang & Zhou (2013) used a novel automatic extraction method of suburb temperature to calculate rural temperature and summarised the spatiotemporal variation characteristics of the UHI effect in Chengdu during 2005 to 2010.

According to previous studies Table 2.16, the maximum UHI intensity in Chengdu ranged from 6°C to 9°C. In some studies, the factor of the interfere by atmospheric cloud is not considered, resulting in research results with large errors of 3°C to 8°C (Qin et al. 2001) (Li et al. 2007), which can lead to the extreme substantial value results for maximum UHI intensity (Table 2.16). Based on the existing literature of UHI in Chengdu, research intention has been more focused on the urban macro scale, none of them addressed the temperature variation in a micro scale- for example, a city-block scale. Moreover, from a real-estate planning point of view, current research on local UHI ignores the mechanism of impaction of early design measures on microclimate,

fundamental and theoretical data about the relationship between planning variables and UHI at a micro scale is still missing. Therefore, studies of a quantitative research including correlating multiple parameters of urban thermal patterns with on-site UHI values are needed in order to investigate the cause of UHI and the impaction on building energy performance at a city-block scale, which can potentially provide theoretical support and database for the practice of planning and designing a large-scale building group. Finally, a study on mitigation of the UHI effect in the Hot-Summer & Cold-Winter Zones in China is quite rare, relevant theories and technics are neither sufficient to support the evaluation process with different mitigation strategies. Therefore, it is essential to investigate the characteristics of the microclimate in a city block and to explore possible methods and find proper tools to evaluate related optimisation measures in Chengdu.

Table 2. 16: UHI studies in Chengdu

Authors	Method/ Data	UHI Intensity (Max.)
Yang (1988)	Weather satiations/ Statistic data	6°C
Lin & Wang (1990)	Remote sensing/ NOAA/AVHRR	9°C
Dan & Dan (2001)	Remote sensing/ NOAA/AVHRR	9.4°C
Xu et al. (2007)	Remote sensing/ NOAA/AVHRR	7.35°C
Xia et al. (2007)	Remote sensing/ NOAA/AVHRR	9°C
Chen et al. (2009)	Remote sensing/ MODIS	6°C
Dan et al. (2011)	Remote sensing/ NOAA/AVHRR	8°C
Zhang & Cheng (2016)	Remote sensing/ MODIS	16°C
Zhang & Zhou (2013)	Remote sensing/ MODIS	6.4°C

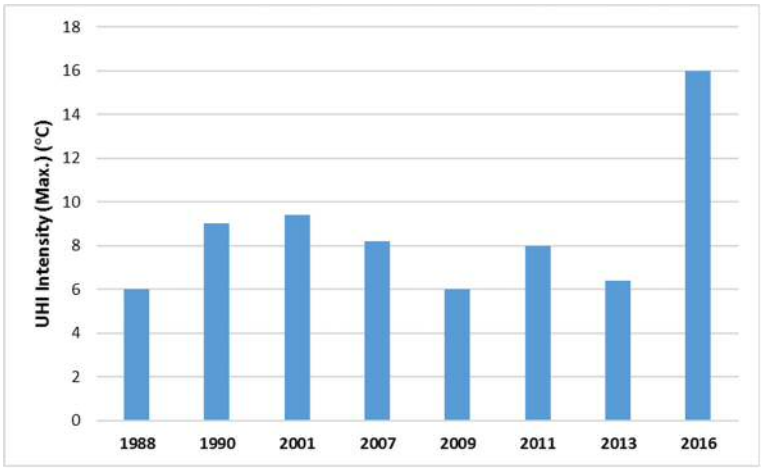

Figure 2. 41 UHII changes according to the time
Source: compiled from Table 2.16

2.6 Summary and conclusion

This Chapter reviewed existing literature on planning high-rise building groups at a city-block scale in four aspects: (i) it presented the background of the low-carbon eco city-global actions toward mitigation of climate change. Furthermore, the definition of low-carbon eco city and the core issues relevant to building industry were clarified; (ii) it then reviewed the theoretical discussion on microclimate and summarized the factors and causes of microclimate; (iii) this chapter also revealed the mechanisms between urban form and building energy performance; (iv) it reviews the evolution of high-rise building estate and studies on built environment in China. Based on the review of existing literature, three research gaps were identified: 1) the lack of research on outdoor temperature and building energy consumption at the city-block level; 2) the absence of research on impact of multi-variable on microclimate and building energy 1.performance; 3) the scarcity of research on design strategies for mitigating building energy demand and optimising outdoor thermal comfort in large-scale building groups in China. According to the empirical studies, the mechanism among microclimate, building energy performance, and urban form was revealed. Finally, relevant parameters of urban form and design features were summarised at a city-block scale: floor area ratio, building coverage ratio, building height, green coverage ratio (including water bodies), plot layout, building function, which were indicators forming guidelines for planning city-block-scale building groups.

In summary, this chapter can dawn the following conclusions:

1. Low-carbon eco-development is proved to a practical response to global climate change, and energy saving and energy efficiency are of vital importance in building industry in regardless global environmental issues with controversies. Among many factors, building energy performance and outdoor thermal performance are two core issues to achieve goals of low-carbon eco-development, especially for the building industry in China.

2. City-block scale provides excellent operability for planners, designers, and stakeholders to practice a common estate development project aiming to achieve goals of low-carbon eco-development. It is also a practical scale for a study of urban heat island phenomenon at a micro scale of urban settlement.

3. UHI mitigation strategies contribute to reducing building energy consumption, improving outdoor thermal comfort, and mitigating pollution in terms of air and noise. Moreover, considering the causes of UHI effect, there are several aspects for mitigation strategies, including optimization of urban geometry, increasing the green and water coverage, and using high albedo surface materials. On the other hand, the question that how to manage those multiple factors in planning a large-scale building group still remains. Moreover, UHI effects raise the temperature and impact on the CDDs and HDDs, thereby increasing the cooling load in summer and decreasing the heating load in winter, another question remains: to what extent the UHI effects affect the building energy consumption during a yearly period?

4. Urban form variables, including building density, building height, and green coverage ratio, plot layout, are shown with considerable impact on building energy consumption in indirect ways by altering outdoor temperature and microclimate. Due to the scarcity of existing research, further study on optimising building energy performance by arranging multi design variables is still needed. Moreover, parameters of urban form and design features at a city-block scale, including floor area ratio, building coverage ratio, building height, green coverage ratio (and water bodies), plot layout ,and building function, were summarized as indicators of guidelines of optimising outdoor thermal performance and building energy performance for planning city-block-scale building groups .

5. Due to the comprehensive implementation of renewable energy, Chengdu shows great potential to achieve low-carbon goals. However, considering that fact that outstanding amount of thermal power and a large proportion of total energy consumption taken by building industry, energy efficiency in the buildings is still of

vital importance in Chengdu. Moreover, large-scale high-rise building groups appear to be the only choice for the real estate developments and dominate the civil construction industry, due to the rapid increase in population and land price.

6. The existing local research on building energy efficiency is focused on improving the thermal performance of building components. In the meanwhile, there is still lacks research and related strategies regarding the impact of microclimate variation. The absence of multi-measure strategy of energy efficiency at early design stages limits the potential strategies for optimisation of building energy efficiency and outdoor thermal in high-rise buildings in Chengdu.

7. Local research on UHI effect still focuses on a macro scale of urban planning. Design measures at early stages of optimising outdoor thermal environment are still missing. Studies of quantitative research including correlating multiple parameters of urban thermal patterns with on-site UHI values are needed in order to investigate the cause of UHI and the impaction on building energy performance at a city-block scale. Relevant theories and technics on mitigation of the UHI effect in the Hot-Summer & Cold-Winter Zones in China are quite rare. Therefore, characteristics of the microclimate in a city block, together with possible methods and proper tools for evaluation of related optimisation measures in Chengdu need to be investigated.

Chapter Three

RESEARCH METHODOLOGY

3.1 Introduction-Research and Research questions

"Research is the process of making claims and then refining or abandoning some of them for other claims more strongly warranted…Research seeks to develop relevant true statements, ones that can serve to explain the situation that is of concern or that describes the causal relationships of interest…" -- (Phillips & Burbules 2000)

In general, research is a systematic and methodical process of enquiry end investigation (Amaratunga et al. 2002). In terms of Built Environment sector, research studies are focusing on exploring strategies and solutions for reduced environmental impact by measuring environmental performance, in particular, the environmental impact of design, construction and management, and buildings(Crawley & Aho 1999). In this research, the impact of design variables of large-scale buildings on the microclimate and building energy performance will be investigated. Crotty (1998) suggested that four questions should be asked when the research is being designed: What epistemology; What theoretical perspective; What methodology; What methods.

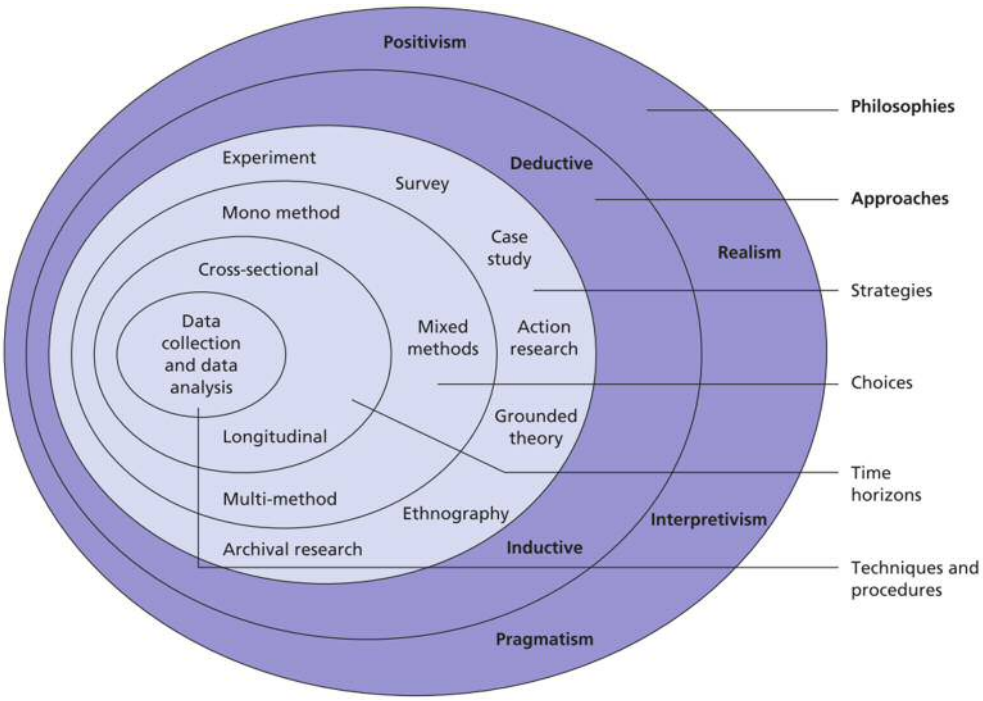

Figure 3. 1: The research 'onion'
Source: (Saunders et al. 2008)

Therefore, in order to achieve the aim of the research topic and making decisions on the methodology for the next procedures, four research questions are raised:

1. *What is the historical background and development process of real estate projects with large-scale high-rise buildings in at the macro context in China, and what are the present situation of energy performance and outdoor thermal comfort?*

2. *How do the design features of the urban configuration of the real estate projects have impacts on microclimate condition?*

3. *What is the diurnal variation of air temperature and other microclimate variables on a summer day and a winter day, accordingly?*

4. *What are the building energy features of the city-block-scale building groups in China, and how do both the design features and microclimate condition of the urban configuration have impacts on building energy performance?*

5. *What is the relationship between the microclimate evaluations and building energy performance, what are best strategies planning in city-block-scale real estate projects in China from the perspectives of both mitigating the variation in microclimate and optimising building energy consumption?*

6. *What are indicators and guidelines for planning city-block-scale building groups?*

In order to answer the six research questions, this chapter establishes a city-block scale building group centred research framework. Afterwards, it applies the research strategy combined with literature review, quantitative observations, and numerical modelling, accordingly. Lastly, it introduces the detailed methods and information on selected target sites.

3.2 Research Framework: an urban form-centred microclimate and building energy performance study

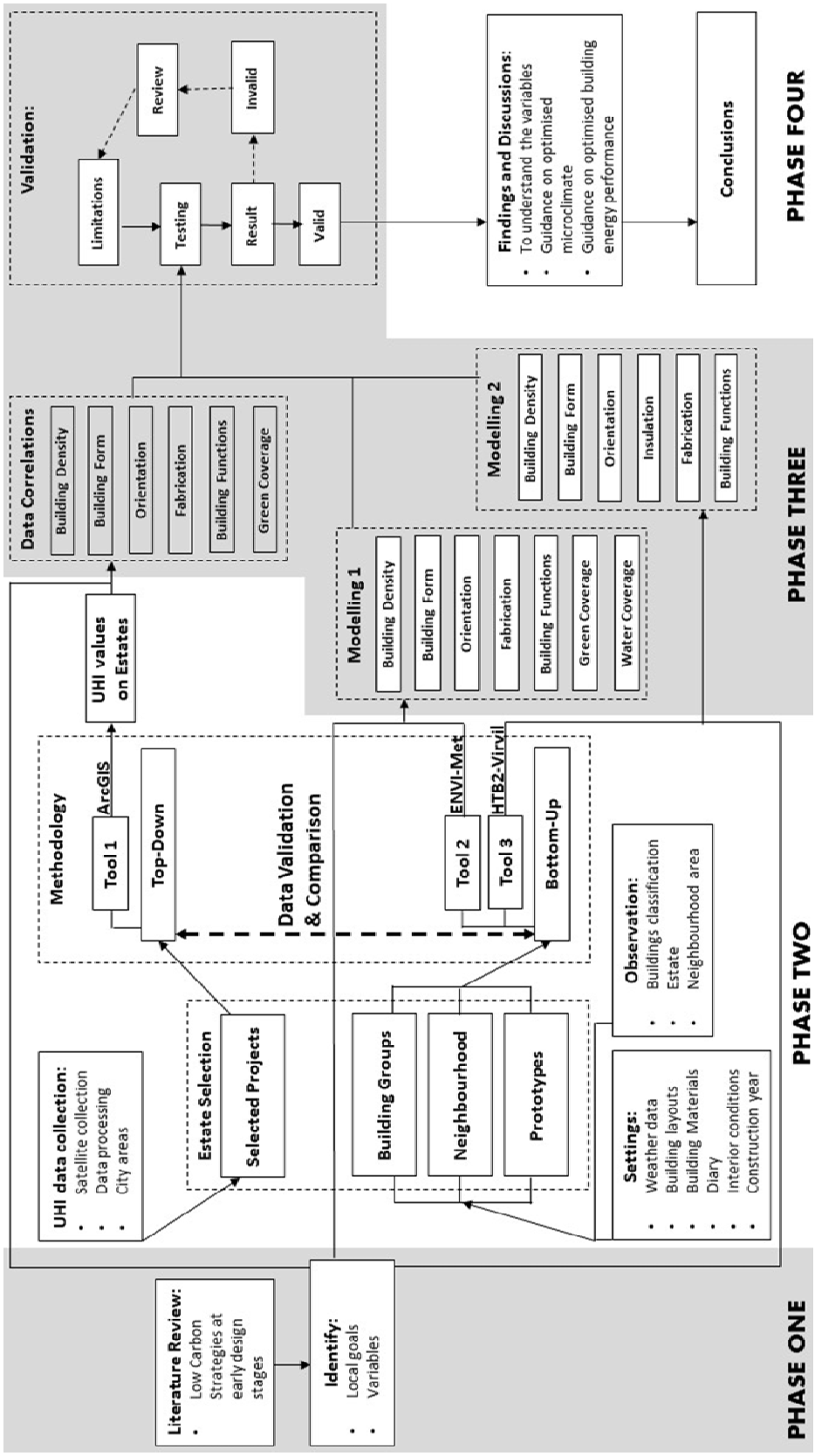

Figure 3. 2: The research framework of this study

In Chapter 2, according to the conclusion of the review on existing literature, a study framework of city-block scale building group should be centred on urban form, and its impaction on microclimate and building energy performance. The research framework is shown in Figure 3.2.

In this study, a mixed method of top-down/bottom up is applied. In Phase Two, the top-down method through observations is used to identify the global pattern of urban microclimate, as well as the intensity of parameters over the entire research subject. On the other hand, in phase three,with the bottom-up method, parameters of microclimate at smaller scales are collected through modelling. The data obtained from the bottom-up method is validated by comparing with data from the top-down method, the accuracy of modelling results is assessed in the mean while. Both quantitative analysis and qualitative analysis are carried out aiming for findings and discussions in Phase Four. Therefore, the basic structure of this research is formed by the following research framework:

Chapter 2 (Literature review) (Phase One):
Research Question One (Macro-context features)
Research Objective One: To understand the development low carbon city in the construction sector and the evolution of the real estate projects with large-scale buildings, and investigate the mechanisms of the impacts of design features of the city-block scale project on microclimate condition and building energy performance.

Chapter 4 (Observation method of Remote sensing satellite imagery) (Phase Two):
Research Question Two (urban form and microclimate issues)
Research Objective Two: To explore the long-term influence of design features of the urban configuration of the real estate projects on microclimate condition.

Chapter 5 (ENVI-Met numerical modelling) (Phase Three):
Research Question Three (urban form and microclimate issues)
Research Objective Three: To understand the diurnal variation of air temperature and

other microclimate variables on typical days, accordingly.

Chapter 6 (HTB2-vrivil plugin numerical modelling) (Phase Three):

Research Question Four (urban form and building energy performance issues)

Research Objective Four: To summarise building energy features of the city-block-scale building groups in China, to explore the influence of both design features of the urban configuration and microclimate on building energy performance.

Chapter 7 (conclusion and discussion) (Phase Four):

Research Question Five (theoretical issues)

Research Objective Five: To summarise the issues of theoretical importance on both microclimate and building energy performance, find out best strategies planning in city-block-scale real estate projects in China from the perspectives of both mitigating the variation in microclimate and optimising building energy consumption

3.3 Research Strategy: a multi-method quantitative study

> *"Research Strategy-General plan of how the researcher will go about answering the research question(s)."* *-- (Saunders et al. 2008)*

Research design turns research questions and objects into research projects, while research questions, the researcher's preference and timeline of schedule are considered (Saunders et al. 2008). Research Strategies should answer research questions and meet research objects (Saunders et al. 2008). Research questions, together with the research topic and are primary drives when choosing the methodology for research (Remenyi et al. 1998)(Bickman & Rog 2009). So in a discussion of philosophy, in particular, identifying unanswered questions, or 'research questions' is the starting point of a research project (Amaratunga et al. 2002). Research questions will be addressed by the research process, and they are the precursor of research objects (Saunders et al. 2008).

Creswell (2002) concludes choices of strategies associated with different data analysis

approaches: quantitative- experiments, survey, correlation studies, etc.; qualitative- Ethnographies, Grounded theory, Case studies, Phenomenological research, Narrative research, etc.; Mix-methods- Sequential procedures, Concurrent procedures, Transformative procedures. Research Strategy indicates the methodology of data collection and data analysis (Ahmed et al. 2016) (Ahmed et al. 2016). There are some types of experiments, including Complex experiments that are identifying the strength of multiple variables (Creswell 2002).

There is no a generally the most superior or inferior label of research strategy, but it is essential to have a strategy that can answer research questions and meet the research objects (Saunders et al. 2008). it should be under the guidance of research questions and research objects, existing knowledge, time schedule of research, availability of other resources, and researcher's philosophical understanding and preference (Saunders et al. 2008) (Gill & Johnson 2010). Research strategy and research methods are intertwined with each other (Knight & Ruddock 2008).

Based on the research framework, a multi-methods quantitative study is conducted for this research. According to the literature review, design variables of urban form have an influence on microclimate and building energy performance at a city-block scale, issues raised in several aspects, therefore, the strategy of multi-method quantitative study is needed to adopt the different research subject from different aspects.

Why 'City-block scale'?

City-block scale provides excellent operability for planners, designers, and stakeholders to practice a common estate development project aiming to achieve goals of low-carbon eco-development. It is also a practical scale for a study of urban heat island phenomenon at a micro scale of urban settlement. City-block scale is an intermediate, or mesoscale, between the macroscale and microscale. And the latter correspond to low carbon urban planning and low carbon buildings, respectively, which have been widely studied in terms of urban developments. Therefore, the city-block scale is a perfect subject for a low-carbon development project in practice, and the

implementation strategies will combine the measures from both macro and micro. In the meanwhile, the research at this scale is a solid supplementary for the general framework of low carbon eco-development in the construction industry (Zang 2013). Specifically, Site Planning and- compact urban structure and breezeway, and Site Ecology- greenery in outdoor spaces are addressed from an urban planning perspective; Building energy efficiency- passive and low energy design, Greenery- a green roof, green wall, and site greening are focused on in a building scope. From stakeholders' (owners and users) point of view, the living community is mostly at a city-block / neighbourhoods scale, and a bottom-up approach of planning a town/ city-identifying and promoting community initiatives with participation of stakeholders as a base or starting point for the urban planning solutions (Alexander et al. 1985) (Xing et al. 2017).

Why "the city of Chengdu"

Chengdu is the biggest and economic prosper city in Western China, and its urbanization level has reached its highest level. Together with Chongqing, Chengdu will be one of the two leading megacities of the "Chengdu-Chongqing Metropolitan Area", which is planning to be one of seven national urban agglomerations by 2020 and an international level urban agglomeration by 2050 (NDRC & MOHURD 2016). Just as other big cities in the world, a number of public issues have been raised due to the enormous pressure from urban built environment: significant urban heat island effect in summer for more than twenty years (Yang 1988) (Dan et al. 2011); extreme energy consumption for cooling in July and August (Zhao 2010) (Peng 2011). The distinct variation in temperature has been caused public health issues: outdoor thermal comfort degree in summer is low (Guo et al. 2008), increasing number of acute illness and death (Ma et al. 2016), low air quality and pollution (Agricultural et al. 2015), etc. . In the meanwhile, Chengdu had witnessed a continues growth in the CO_2 emission in the first decade of the new Century (Zhang & Zhang 2013).

In short, Chengdu is experiencing massive pressure from urbanization, dwindling

energy resources, and threats from the natural environment. Additionally, long-term ignorance of research accounting on the practical environment and weather style has culminated in misleading design strategies. Fortunately, the increase in the popular consciousness of sustainability and the ambitious goals of the provincial government give Chengdu an excellent opportunity to reverse the situation.

iv) Literature review

The literature was carried out in three phases: Firstly, the literature on the general background of low carbon development and its core issues relevant to construction industry was analysed, in order to explore the research gaps. Secondly, potential technical measurements and technical tools were reviewed and analysed. Thirdly, history related research was reviewed. In this phase, fundamental information about the location of the research subject and history of the evolution of urban development within the city of Chengdu.

v) Observation through remote sensor, inspection and survey

This method was applied to collect periodical urban heat island (UHI) data for 103 large-scale development projects through processed MODIS satellite data. The derived UHI maps were adopted into a geographic information system (GIS). By overlaying UHI intensity within the selected site area, temperature variation at microclimate scale was obtained. Moreover, the background of the selected projects was reviewed, including the information of location and development history. Through this method, several prototypes of the target architectures have been summarised, and construction parameters have been collected through investigations and surveys.

vi) Computational microclimate simulation and computational building energy simulation

This method was applied at two stages of this study accordingly. In the first stage, simulation of microclimate for target projects predicted meteorological data, including outdoor air temperature, relative humidity, and wind distribution. The simulation was

created based on the information collected by literature analysis and survey at early stages of this study. In the second stage, the simulation was used to predict the energy performance of building groups of target projects for two different cases. The two cases consisted of a 'control group' and a 'sample group' according to different outdoor temperature conditions. Compared to filed observation, simulation with numerical models overcomes the disadvantages (including high costs and high incident risk), thereby becoming the mainstream of research on urban microclimate (Feng 2015).

3.4 Observation method of Remote sensing satellite imagery

The remote sensing data used in this study is provided by Senior Engineer Shunqian Zhang, from Chengdu plateau Meteorological Institute of China Meteorological Bureau, obtaining and being processed through DVB-S system broadcasts of China National Satellite Meteorological Center and Huayun MODIS satellite remote sensing data receiving and processing system (Zhang & Zhou 2013). For the data collection, the sets of daily average images of the selected ninety-nine days with clear sky during the 2005-2010 period were captured, thereby being chosen for processing. The procedures of collecting and processing were operated under China Meteorological Bureau's Integration & Application Project (national level) of Key Meteorological Technologies- CMAGJ2014M47.

The method of inversion of land surface temperature used for deriving the UHI imagines is the Split-Window Algorithm (Zhang & Zhou 2013), The method of the Split-Window Algorithm has been practised in many studies (Wan, Z. and Dozier 1996) (Tran et al. 2006) , and it has been verified with a high accuracy (Wan, Z., Zhang, Y., Zhang, Q. and Li 2004). Therefore, the UHI intensity calculation process is below:

$$'\Delta T_s = T_s - T_{smin} \qquad (3.1)$$

ΔT_s is the UHI intensity (℃), T_s is the inversed surface temperature at downtown (℃), T_{smin} is the inversed surface temperature at Suburbs (℃).

The inversion of surface temperature at downtown:

$$T_s = A_0 + A_1 T_{31} - A_2 T_{32} \quad (3.2)$$

T_{31} and T_{32} is the brightness temperature of the 32 channel, A_0, A_0, A_0 are defined as follow:

$$A_0 = 66.54067E_2 - 62.23928E_1 \quad (3.3)$$

$$A_1 = 1 + A + 0.43059E_1 \quad (3.4)$$

$$A_2 = A + 0.46585E_2 \quad (3.5)$$

$$A = D_{31}/(D_{32}C_{31} - D_{31}C_{32}) \quad (3.6)$$

$$E_1 = D_{32}(1 - C_{31} - D_{31})/(D_{32}C_{31} - D_{31}C_{32}) \quad (3.7)$$

$$E_2 = D_{31}(1 - C_{32} - D_{32})/(D_{32}C_{31} - D_{31}C_{32}) \quad (3.8)$$

$$C_i = \varepsilon_i \, \tau_i \quad (3.9)$$

$$D_i = (1 - \tau_i)[1 + (1 - \varepsilon_i)\tau_i] \quad (3.10)$$

i refers to the 31st or 32nd band of MODIS, τ is the atmospheric transmittance, ε is the emissivity.' -- (Zhang & Zhou 2013)

In previous studies, the derived mean value of certain selected points was used as T_{smin}, which are mostly subjective selections. While due to the effect of UHI, there is temperature interval of fast change at the urban boundary (Zhang & Zhou 2013), this feature of temperature distribution can be applied to locate the 'real' temperature boundary of the urban area. Therefore, the temperature of rural areas is obtained. In this study, the calculation of surface temperature in suburban areas (T_{smin}) is conducted by using this novel automatic extraction method of suburb temperature:

$$'\Delta T_s \leq \Delta \bar{T}_s + m\delta_{\Delta T_s} \quad (3.11)$$

ΔT_s is the difference of temperature between the current belt and the previous belt (The city core is the first belt, while the external urban zones are the following belts), $\Delta \bar{T}_s$ is the mean value of the difference of temperature between belts, $\delta_{\Delta T_s}$ is the standard deviation of the difference of temperature between belts, m is a constant which usually values 3.'

-- (Zhang & Zhou 2013)

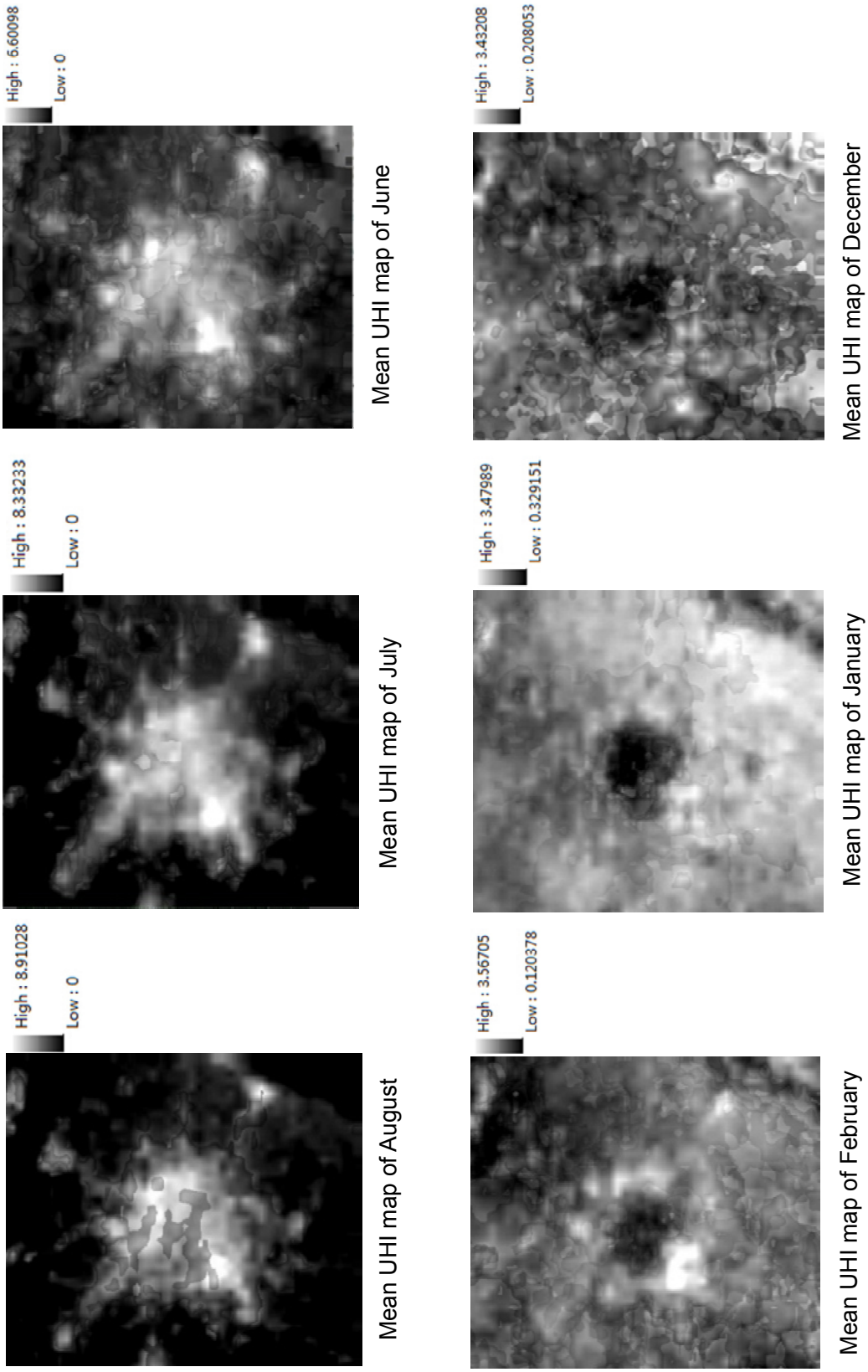

Figure 3. 3: UHI in summer and winter months

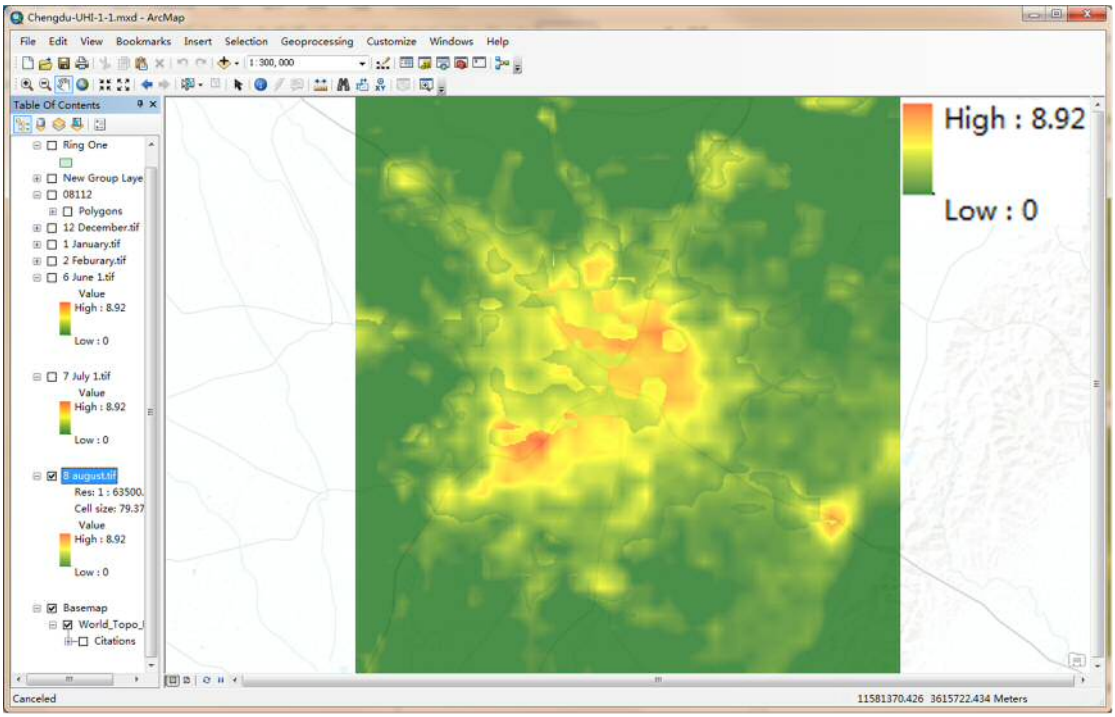

Figure 3. 4: Mapping of UHI in August in ArcGIS

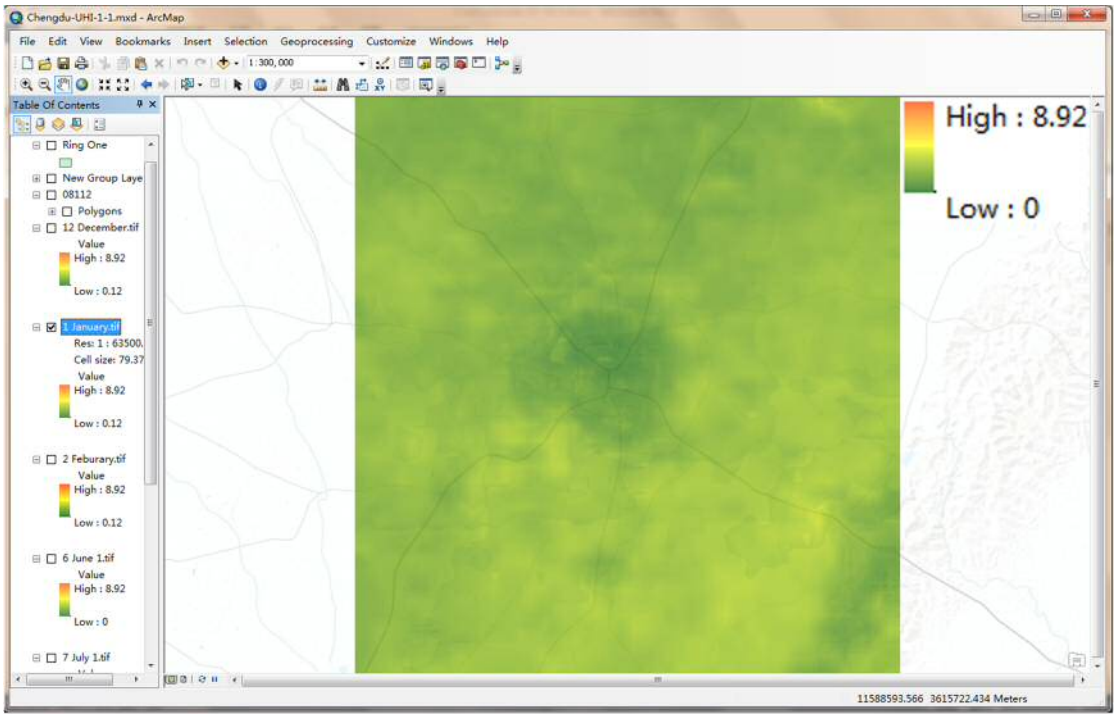

Figure 3. 5: Mapping of UHI in January in ArcGIS

Considering the surface vegetation in Chengdu is evergreen in the four seasons and Vegetation Index in construction area is quite low all the year, the pixels with the Normalised Difference Vegetation Index (NDVI) above 0.2 are defined as the natural ground surface (Zhang & Zhou 2013).

All UHI imagines are processed to 376 × 368-pixel working display, and 139.25 metres × 139.25 metres for each pixel (cell), corresponding to the rectangular area of 52,358 metre ×51,244 metre urban region of Chengdu. Reported by Zhang (2013), satellite imaging has achieved satisfied accuracy after being compared with results obtained from other local researches. Then the raw imagines in typical summer months (June, July, and August) and winter months (December, January, and February) are grouped and recalculated to produce monthly mean imagines for each of six months, accordingly (Figure 3.3). Lastly, the monthly imagines are adopted into the ArcGIS system and integrated with geo-information. Therefore, the spatial distribution of monthly UHI intensity in Chengdu during the 2005-2010 period is obtained. The UHI intensity maps for August and January are shown in Figure 3.4 and Figure 3.5, respectively.

According to these six monthly UHI intensity maps, there were several the intensity centres of UHI in summer, which was located around the inner rings of this urban area, instead of the geometrical centre of this city. Notably, the summer UHI intensity centres were at the north-east corner of the Second Ring (where the commercial and financial sectors are flourishing), and the south-west corner of the Third Ring (where the residential neighbourhoods are intensively distributed). Moreover, there are several 'intensity islands' away from the urban area on the UHI map, which indicated the UHI effect in the satellite towns. In winter months, lower UHI intensity was recorded in the geometrical centre within the First Ring (where most public green-lands and open spaces are widely spread) than the outer rings, therefore, the 'black hole'- pattern of spatial distribution of UHI intensity in the entire urban area was apparent on the winter maps.

3.5 ENVI-Met numerical modelling

In order to simulate the urban microclimate for target projects of those 103 sites, a prognostic and three-dimensional tool, which is named ENVI-Met (Figure 3.6), is selected and introduced in this study. This model includes simple one dimensional model of soil, radiative transfer model and vegetation model (Huttner et al. 2008). It has been evaluated continuously by indecent studies relevant to environmental design and planning process recently (Ambrosini et al. 2014) (Middel et al. 2014) (Salata et al. 2016) (Yang & Lin 2016) (Perini et al. 2017) (Fabbri et al. 2017). Building design and energetic planning are also possible employment for this tool (Ambrosini et al. 2014).

3.5.1 Default setting

In order to initiate ENVI-Met simulation, parameters are required and provided in three files: “Area Input File”, “Configuration File”, and “Database”.

3.5.2 Area Input File

As the beginning category of modelling in ENVI-Met, the input file (*.in) (Figure 3.7) defines the area information, including the scale of the computational domain, size of grid cells, soil properties, building component properties, and parameters about latitude and longitude.

The first section of Area Input File is “File Header”, which aims to define the site for the modelling. An orthogonal Arakawa C-grid is applied in this simulation system (Salata et al. 2016). Considering the scale of the target projects, whose plans are mostly within *450m* x *450m* rectangular while building heights are below *110*m. Therefore, *90* x *90* x *22* grid system with *5m* x *5m* x *5m* cells is defined in the domain. Similar building materials are used in the target project sites, default values are applied in *Wall/Roof Properties*. The Location information is input with the exact latitude and longitude coordinates of each project site accordingly. While for the *Reference Time Zone*, the standard time of China with a reference 120° longitude is input. Lastly, all models for 15 target projects will be created according to building compositions on the satellite

map, so there is no model rotation out of grid north.

Furthermore, in case of errors would possibly occur during calculation process due to boundary effect, the *Nesting Grid* is introduced, 3 lines of extra grids are added surrounding the boundary of the main computational domain. Then, core computational grids with stable lateral boundary conditions is established.

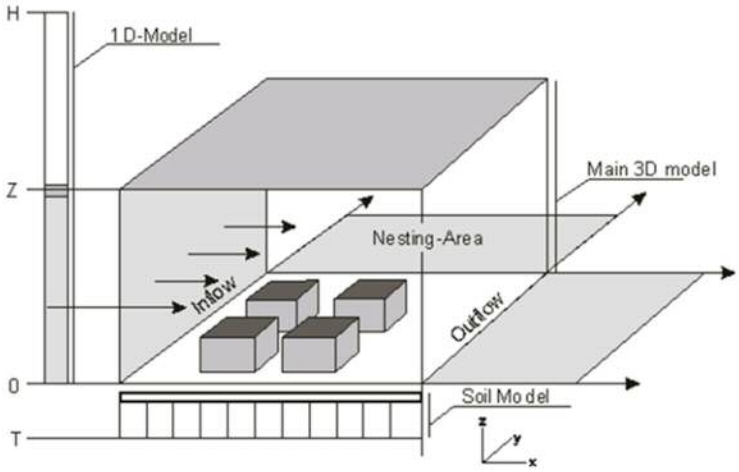

Figure 3. 6: Overview of the model in Envi-Met
Source: (Simon 2016)

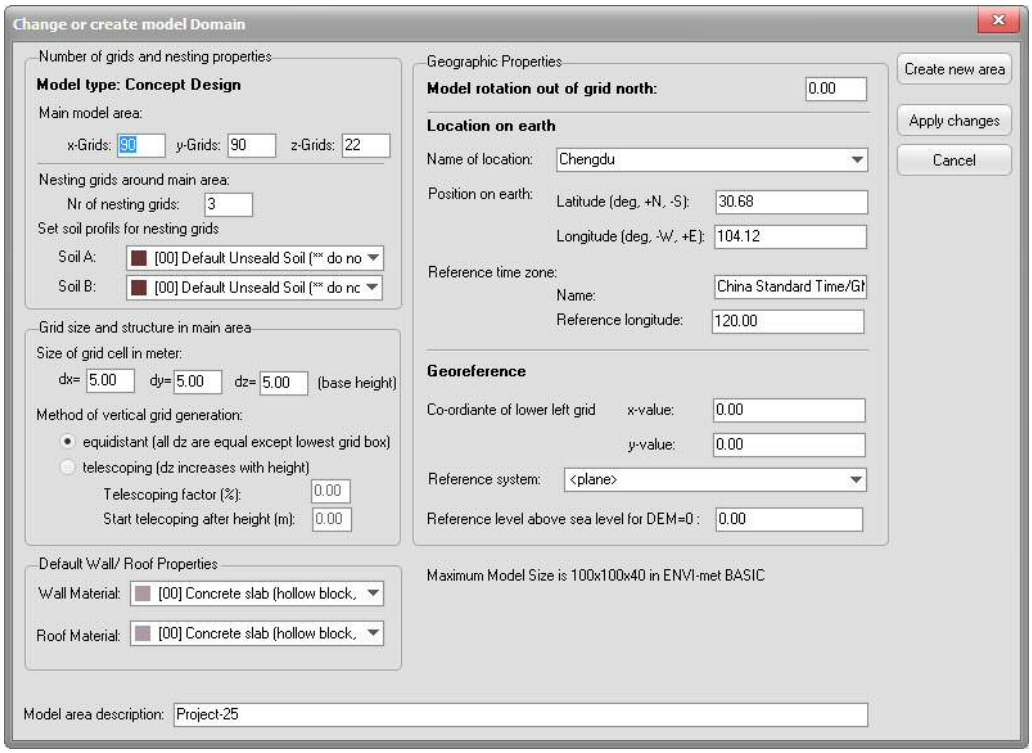

Figure 3. 7: Input file of ENVI-Met

After defining the domain, buildings and plants are ready to construct on the site. Based

on the data of construction information related to the sites collected by investigation and surveys in early chapters, all buildings (including one on the target sites and the surroundings), vegetation (including plants and water bodies), and surface texture (including pavement), and DEM of terrain are reconstructed into 3-Dimensional models in space file (.inx) (*Figure 3.8*).

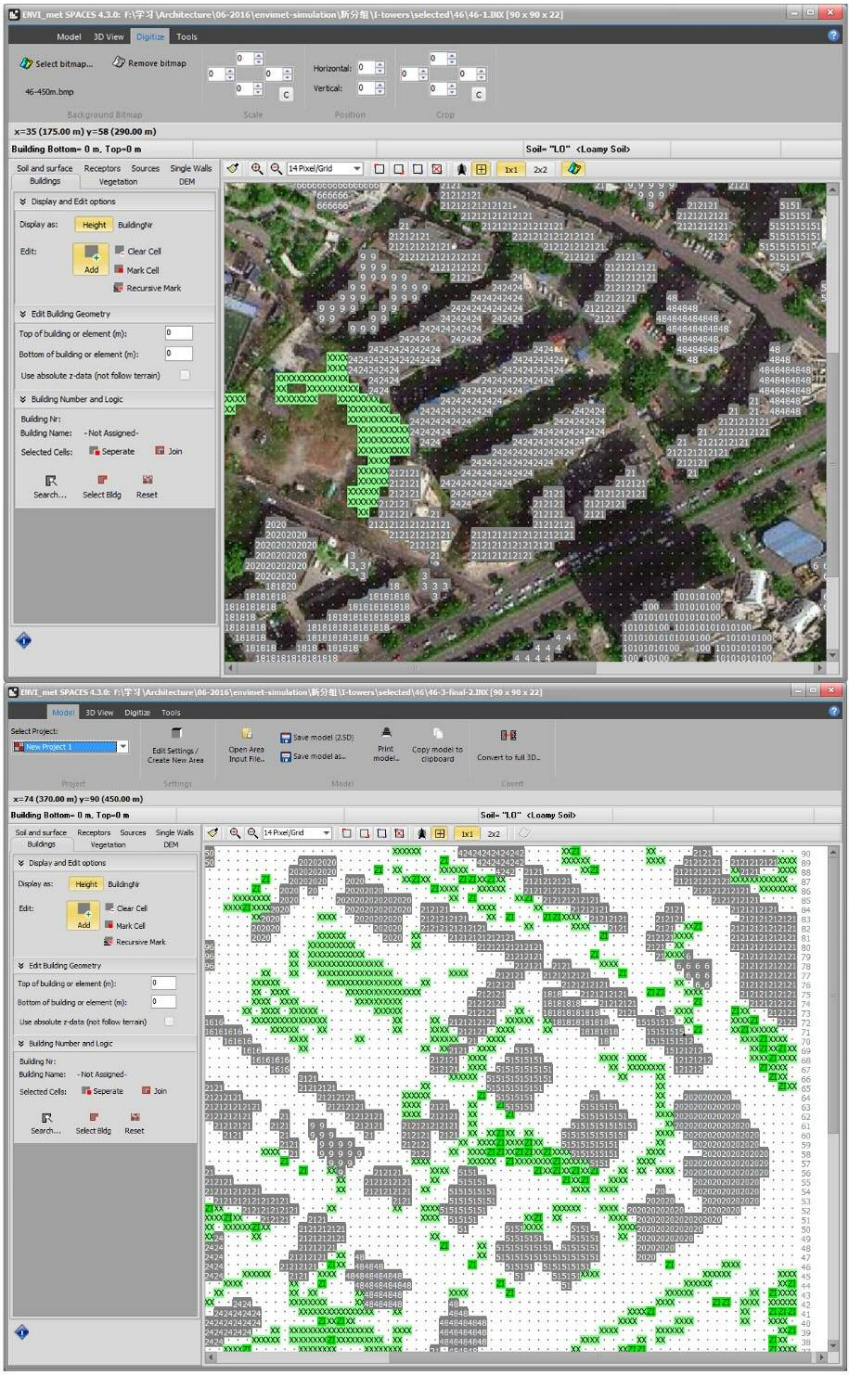

Figure 3. 8: Space File interface of ENVI-Met and modelling.

3.5.3 Configuration File

The configuration file (*.cf) (Figure 3.9) defines the setting for simulation. Parameters, including calculation time schedule, detailed meteorological data, vegetation data, soil data and building data, will be set in this stage (Figure 3.10 and Figure 3.11).

Initialisation time is required in the simulation. Due to the limitation of time in this study, 24 hours simulations of the hottest summer day (August 21, 2005) and the coldest day (January 9, 2005) is initialised in order to obtain the full day data. However, there is an extra one hour as an initial time for simulations. Therefore, the exact initial time is set at 23:00 on August 20, 2005, and 23:00 on January 8, 2005 for a summer day and a winter day, respectively.

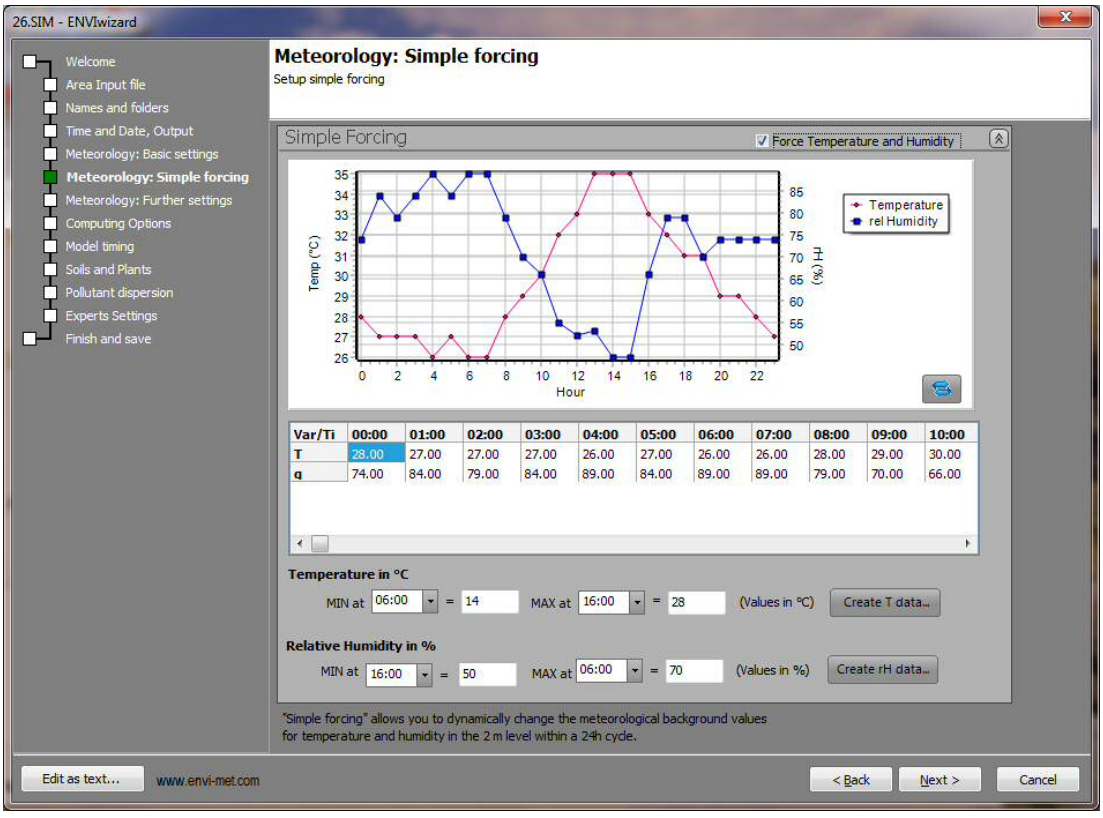

Figure 3. 9: Configuration file of ENVI-Met

```
%---- ENVI-met V4 main configuration file ----------
%---- generated with ProjectWizard ----------
Fileversion                =4.0
JobID                      =Simulation
% Main data ..........
Name for Simulation (Text):          =60-24-run
Area Input File to be used           =05-2017\60\60-final.INX
Filebase name for Output (Text):     =60-24-output
Output Directory:                    =C:\ENVImet4\New Project\24-hour summer-temper revised\60
Start Simulation at Day (DD.MM.YYYY):    =20.08.2005
Start Simulation at Time (HH:MM:SS):     =23:00:00
Total Simulation Time in Hours:      =25
Wind Speed in 10 m ab. Ground [m/s]      =1.3
Wind Direction (0:N..90:E..180:S..270:W..)  =225
Roughness Length z0 at Reference Point [m]  =0.01
Initial Temperature Atmosphere [K]       =302.780
Specific Humidity in 2500 m [g Water/kg air] =7.0
Relative Humidity in 2m [%]          =74
% End main data ..........
[OUTPUTTIMING]_____
Output interval main files (min)         =60.00
Output interval text output files (min)      =30.00
Include Nesting Grids in Output (0:n,1:y)    =0
[TIMING]_____
Update Surface Data each  ? sec          =30.00
Update Wind field each ? sec             =900.00
Update Radiation and Shadows each ? sec    =600.00
Update Plant Data each ? sec             =600.00
```

```
[TIMESTEPS] _____
Sun height for switching dt(0) -> dt(1)    =40.00
Sun height for switching dt(1) -> dt(2)    =50.00
Time step (s) for interval 1 dt(0)         =2.00
Time step (s) for interval 2 dt(1)         =2.00
Time step (s) for interval 3 dt(2)         =1.00
[SIMPLEFORCE] _____
Hour 00h [Temp, rH] = 301.15, 74.00
Hour 01h [Temp, rH] = 300.15, 84.00
Hour 02h [Temp, rH] = 300.15, 79.00
Hour 03h [Temp, rH] = 300.15, 84.00
Hour 04h [Temp, rH] = 299.15, 89.00
Hour 05h [Temp, rH] = 300.15, 84.00
Hour 06h [Temp, rH] = 299.15, 89.00
Hour 07h [Temp, rH] = 299.15, 89.00
Hour 08h [Temp, rH] = 301.15, 79.00
Hour 09h [Temp, rH] = 302.15, 70.00
Hour 10h [Temp, rH] = 303.15, 66.00
Hour 11h [Temp, rH] = 305.15, 55.00
Hour 12h [Temp, rH] = 306.15, 52.00
Hour 13h [Temp, rH] = 308.15, 53.00
Hour 14h [Temp, rH] = 308.15, 47.00
Hour 15h [Temp, rH] = 308.15, 47.00
Hour 16h [Temp, rH] = 306.15, 66.00
Hour 17h [Temp, rH] = 305.15, 79.00
Hour 18h [Temp, rH] = 304.15, 79.00
Hour 19h [Temp, rH] = 304.15, 70.00
Hour 20h [Temp, rH] = 302.15, 74.00
Hour 21h [Temp, rH] = 302.15, 74.00
Hour 22h [Temp, rH] = 301.15, 74.00
Hour 23h [Temp, rH] = 300.15, 74.00
```

Figure 3. 10: Climate and building parameters set in ENVI-Met for August 21, 2005

```
%---- ENVI-met V4 main configuration file ----------
%---- generated with ProjectWizard ----------
Fileversion                =4.0
JobID                      =Simulation
% Main data ..........
Name for Simulation (Text):          =60-WIN-run
Area Input File to be used           =winter\60\60-final.INX
Filebase name for Output (Text):     =60-WIN-output
Output Directory:                    =C:\ENVImet4\New Project 1\winter\60
Start Simulation at Day (DD.MM.YYYY):    =08.01.2005
Start Simulation at Time (HH:MM:SS):     =23:00:00
Total Simulation Time in Hours:      =25
Wind Speed in 10 m ab. Ground [m/s]      =1.21
Wind Direction (0:N..90:E..180:S..270:W..)  =45
Roughness Length z0 at Reference Point [m]  =0.01
Initial Temperature Atmosphere [K]       =279.150
Specific Humidity in 2500 m [g Water/kg air] =7.0
Relative Humidity in 2m [%]          =72
% End main data ..........
[OUTPUTTIMING]_____
Output interval main files (min)         =60.00
Output interval text output files (min)      =30.00
Include Nesting Grids in Output (0:n,1:y)    =0
[TIMING]_____
Update Surface Data each  ? sec          =30.00
Update Wind field each ? sec             =900.00
Update Radiation and Shadows each ? sec    =600.00
Update Plant Data each ? sec             =600.00
```

```
[TIMESTEPS] _____
Sun height for switching dt(0) -> dt(1)    =40.00
Sun height for switching dt(1) -> dt(2)    =50.00
Time step (s) for interval 1 dt(0)         =2.00
Time step (s) for interval 2 dt(1)         =2.00
Time step (s) for interval 3 dt(2)         =1.00
[SIMPLEFORCE] _____
Hour 00h [Temp, rH] = 279.15, 70.00
Hour 01h [Temp, rH] = 279.15, 76.00
Hour 02h [Temp, rH] = 279.15, 76.00
Hour 03h [Temp, rH] = 278.15, 81.00
Hour 04h [Temp, rH] = 277.15, 87.00
Hour 05h [Temp, rH] = 276.15, 87.00
Hour 06h [Temp, rH] = 274.15, 100.00
Hour 07h [Temp, rH] = 274.15, 100.00
Hour 08h [Temp, rH] = 274.15, 93.00
Hour 09h [Temp, rH] = 274.15, 100.00
Hour 10h [Temp, rH] = 277.15, 93.00
Hour 11h [Temp, rH] = 280.15, 71.00
Hour 12h [Temp, rH] = 281.15, 66.00
Hour 13h [Temp, rH] = 282.15, 58.00
Hour 14h [Temp, rH] = 282.15, 58.00
Hour 15h [Temp, rH] = 282.15, 58.00
Hour 16h [Temp, rH] = 282.15, 58.00
Hour 17h [Temp, rH] = 282.15, 58.00
Hour 18h [Temp, rH] = 282.15, 58.00
Hour 19h [Temp, rH] = 281.15, 66.00
Hour 20h [Temp, rH] = 281.15, 66.00
Hour 21h [Temp, rH] = 280.15, 66.00
Hour 22h [Temp, rH] = 280.15, 71.00
Hour 23h [Temp, rH] = 280.15, 71.00
```

Figure 3. 11: Climate and building parameters set in ENVI-Met for January 9, 2005

The hourly temperature and humidity data are collected from the weather station database by the web weather data provider “Weather Underground” (Weather

Underground 2014). In order to get the baseline of urban area temperature, the data of Shuangliu Station at the boundary of the Outer Ring of Chengdu is applied into the configuration file. Therefore, the boundary condition of weather has been set. However, due to the limitation of ENVI-Met, the wind speed and direction can only be initialised as a stable condition during the simulation process. In other words, dynamic wind system is unable to be adopted within the software environment. Therefore, the daily average values of wind speed and direction are used in the primary setting of meteorology. As essential impacts of microclimate, vegetation and soil/road parameters are required in ENVI-Met to define the plant's models and surface texture. In this study, the data on vegetation and surface on the sites obtained in early investigation and surveys is applied with the simulations.

3.6 HTB2-virvil Plug-in numerical modelling

3.6.1 Preparation for modelling and simulation

Existing research on the local energy performance of buildings only uses traditional methods, such as interview, survey, while a direct collection of statistic data from electricity companies in China requires special permissions due to security issues making this direct method hardly working. Moreover, the technical issues, including that available data obtained in those studies only indicates a static and periodical process, raised in those methods. Therefore, computer simulation which is capable of dynamic calculations provides more comprehensive analysis strategies.

As discussed in Chapter 3, HTB2 is the core calculation engine this integrated tool of the energy performance simulation, where three types of default setting will be adjusted. The first setting is the project weather condition, including all of the conventional meteorological data, the second type of configuration is the construction information of buildings, and the third part is the setting for indoor conditions of buildings services.

3.6.2 Weather File settings

For adjusting the default setting, geographic and climatic features of the simulations should be determined. Due to their world-widely acceptance and validation, the weather data provider-the U.S. Department of Energy and the National Centers for Environmental Information of National Oceanic and Atmospheric Administration (NOAA) of U.S, are chosen for this study. The former department introduces the raw data of Chinese Standard Weather Data (CSWD) (China Meteorological Bureau Tsinghua University 2005) which is made into the format of (*epw) weather files, while the later centre provides hourly global data which are derived from the Integrated Surface Data (ISD) obtained from a massive amount of meteorological monitoring stations (NOAA 1998).

In Weather Tool of Ecotect (Marsh 2010), an overview of weather condition in Chengdu has been drawn regarding Sun-path (Figure 3.12), Annual Temperature (Figure 3.13),

Prevailing Winds (Figure 3.14), Cloud Cover (Figure 3.15), Relative Humidity (Figure 3.16). Generally speaking, the average temperature is high in summer months ranging from 21℃ to 30℃, and is low but always above 2℃ in winter months. Solar radiation can access through wide-range directions, which reaches its peak value- 300W/m^2- in August and drops to its bottom-below 100W/m^2 in February. The wind keeps calm all the year, and the prevailing wind direction is not apparent. Winter is cloudy, which is with up to 80% cloud cover ratio. The relative humidity is high all the year round, the average daily value is more than 80% all the year, and it varies ± 10% in a day.

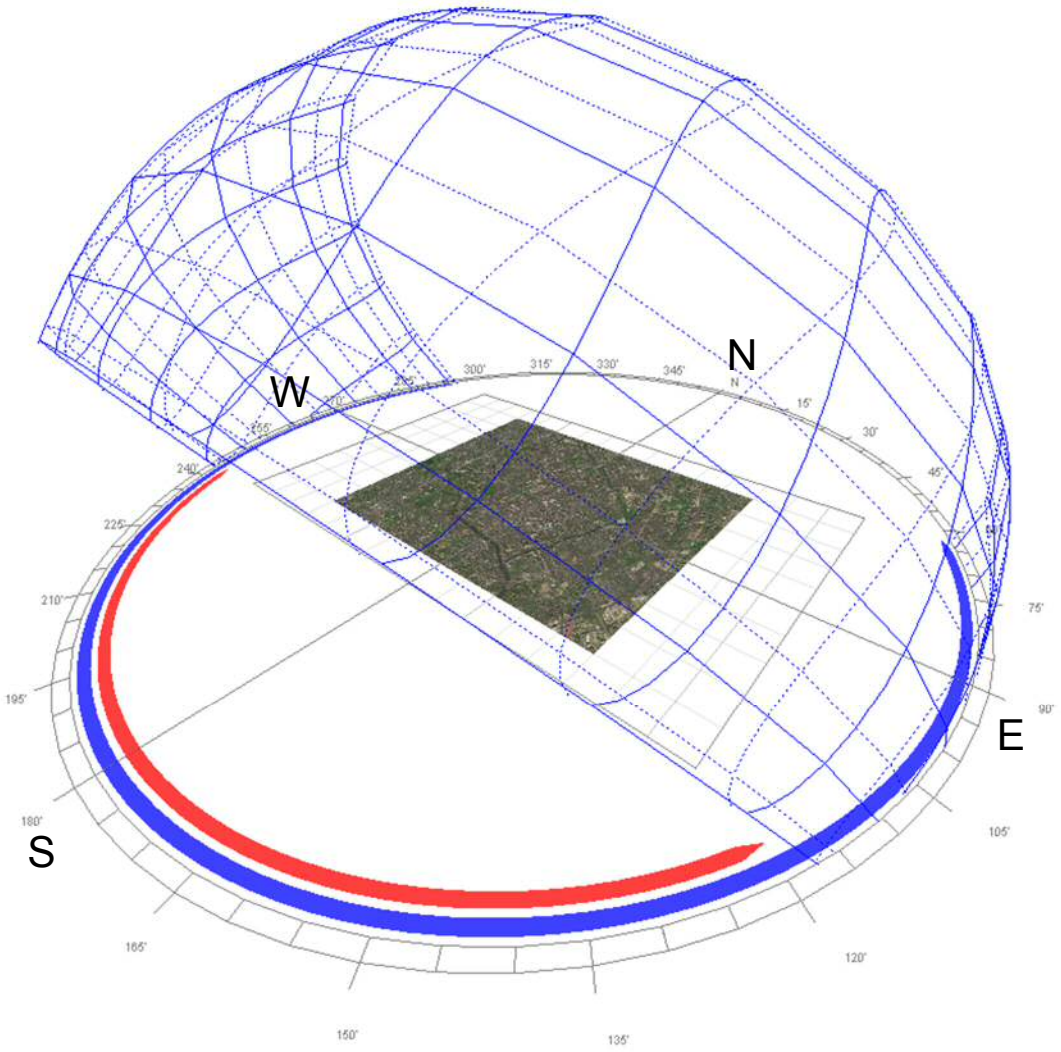

Figure 3. 12: Sun path diagram of Chengdu
Source: Eecotect 2011

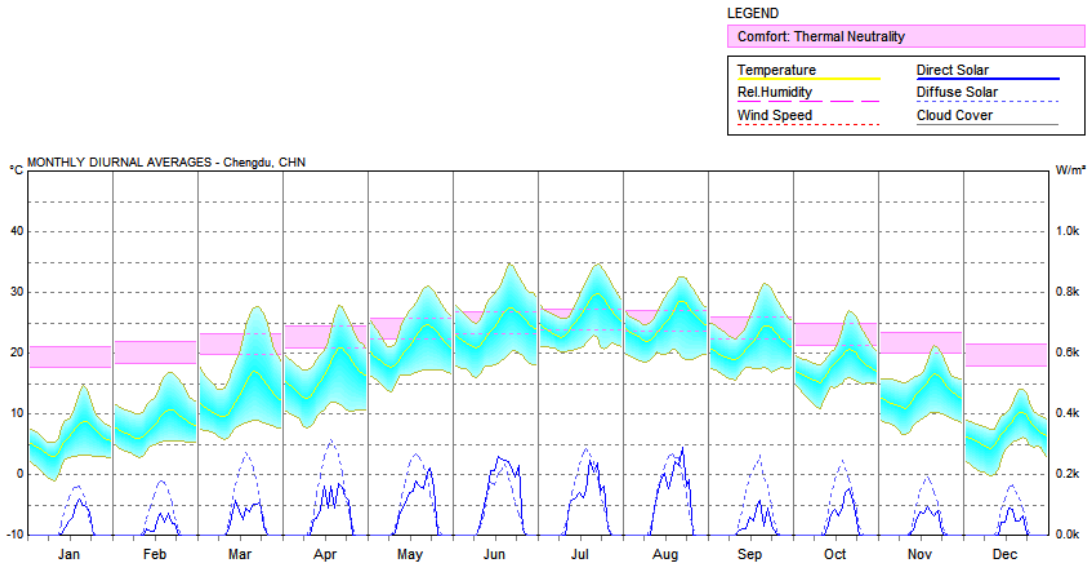

Figure 3. 13: Weather file for Chengdu

Source: Ecotect 2011

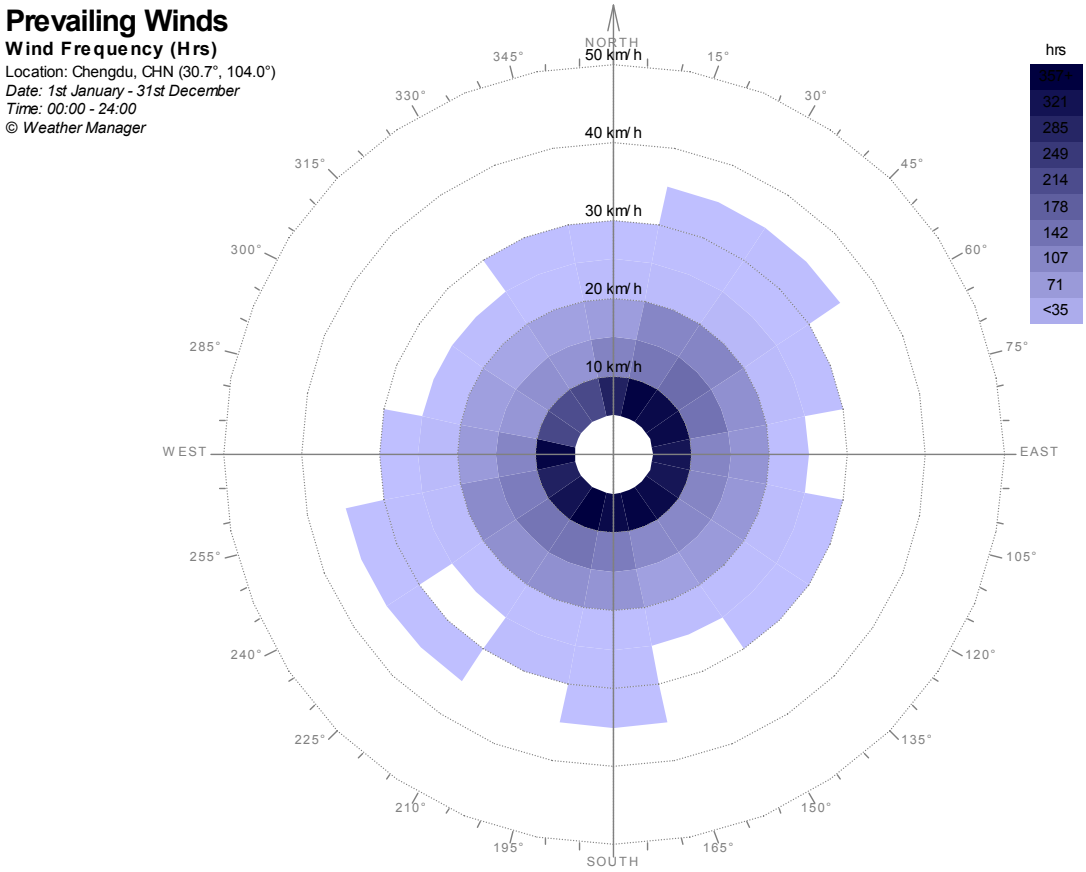

Figure 3. 14: Prevailing winds in Chengdu

Source: Ecotect 2011

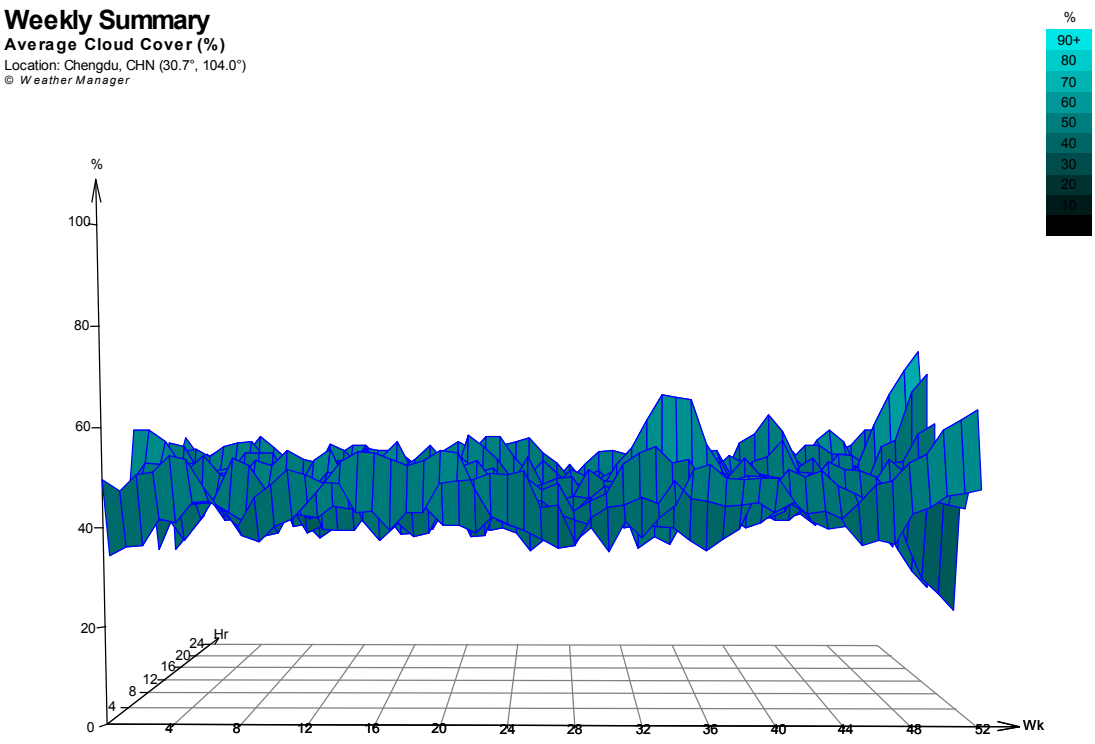

Figure 3. 15: Average Cloud Cover of Chengdu

Source: Ecotect 2011

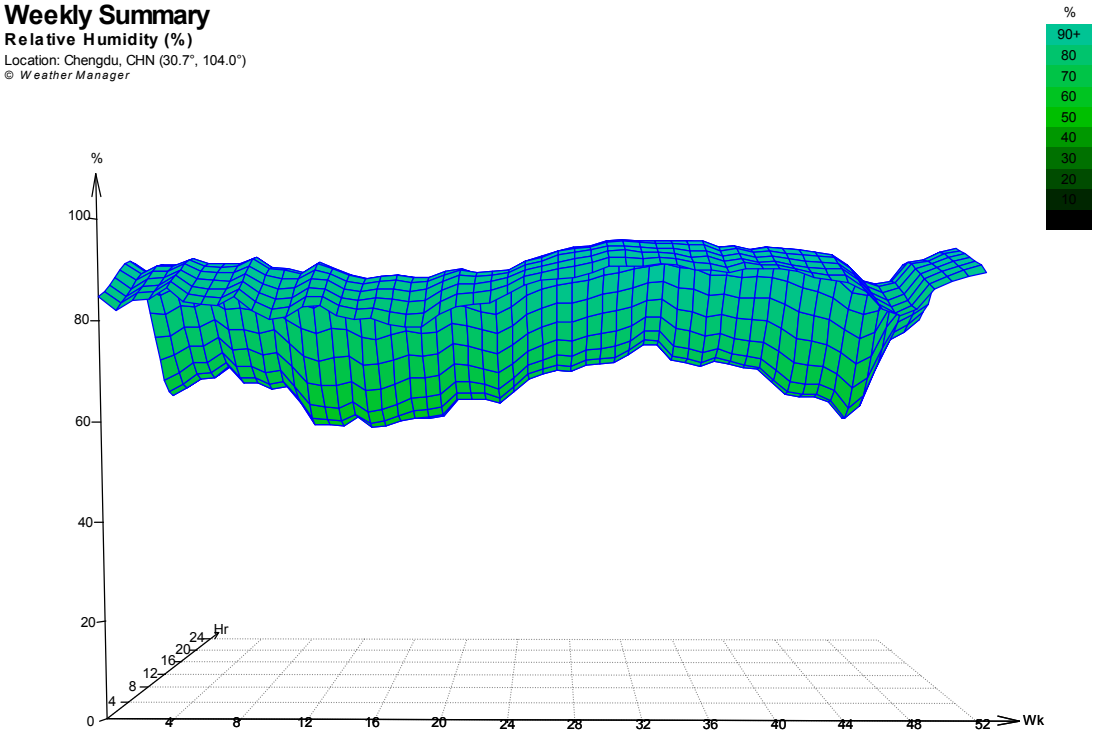

Figure 3. 16: Relative humidity of Chengdu

Source: Ecotect 2011

3.6.3 Configurations of simulation

Compared to other codes and standards, the development of national regulations on building efficiency regarding building materials and constrictions in China has lagged behind the developed countries. The high energy performance of building components was not required until late national standards after the 2010s. In other words, the buildings of target projects sites were designed and constructed using the building materials with relatively lower energy performance. However, the construction details of the thermal performance of the buildings in this study still met the requirements of national and local codes at the time that they were being designed and constructed. Therefore, according to the construction information collected from early survey and investigations on previous building codes (MOHURD & AQSIQ 1993) (MOHURD & AQSIQ 2005)(MOHURD 2010), the materials of building components have been reconstructed and defined in HTB2. Default settings include building types, building components, U-value, Material, the thickness of each applied thickness, and glazing properties, which are shown in *Table 3.1*, *Table 3.2*, *Table 3.3*, and *Table 3.4*.

Table 3. 1: Construction file for Retail

Construction Details of Retail			
Conponent	**U-Value (W/m^{2}K)**	**Material**	**Thickness (mm)**
External Wall (external-internal)	**1.10**	Cement Mortar	8
		Foamed Concrete 730	126
		Cement Mortar	20
Internal Wall	**2.49**	Cement Mortar	20
		Standard Sintering Shale Hollow Brick	150
		Cement Mortar	20
Window (external-internal)	**5.21**	Glass	6
		Cavity	12
		Glass	6
Floor Slab (up-down)	**3.59**	Fine Aggregate Concrete 2300	30
		Reinforced Concrete	100
		Cement Mortar	20
Roof (up-down)	**0.69**	Fine Aggregate Concrete 2300	40
		Cement Mortar	20
		Xps Plate	33
		High Polymer Waterproof Sheet	3
		Cement Mortar	15
		Reinforced Concrete	120
		Cement Mortar	10
Ground (up-down)	**0.84**	Fine Aggregate Concrete 2300	30
		Reinforced Concrete	100
		Earth	1200

Source: U-value is obtained by with calculation tool of HTB2 (Lewis & Alexander 1990), the material is based on survey and building codes (MOHURD & AQSIQ 2005)

Table 3. 2: Construction file for Office

Construction Details of Office			
Conponent	**U-Value (W/m^{2}K)**	**Material**	**Thickness (mm)**
External Wall (external-internal)	**1.10**	Cement Mortar	8
		Foamed Concrete 730	126
		Cement Mortar	20
Internal Wall	**2.49**	Cement Mortar	20
		Standard Sintering Shale Hollow Brick	150
		Cement Mortar	20
Window (external-internal)	**5.22**	Glass	6
		Cavity	10
		Glass	6
Floor Slab (up-down)	**3.59**	Fine Aggregate Concrete 2300	30
		Reinforced Concrete	100
		Cement Mortar	20
Roof (up-down)	**0.69**	Fine Aggregate Concrete 2300	40
		Cement Mortar	20
		Xps Plate	33
		High Polymer Waterproof Sheet	3
		Cement Mortar	15
		Reinforced Concrete	120
		Cement Mortar	10
Ground (up-down)	**0.84**	Fine Aggregate Concrete 2300	30
		Reinforced Concrete	100
		Earth	1200

Source: U-value is obtained by with calculation tool of HTB2 (Lewis & Alexander 1990), the material is based on survey and building codes (MOHURD & AQSIQ 2005)

Table 3. 3: Construction file for Residential

Construction Details of Residential			
Conponent	**U-Value (W/m^{2}K)**	**Material**	**Thickness (mm)**
External Wall (external-internal)	**0.80**	Cement Mortar	8
		Foamed Concrete 730	188
		Cement Mortar	20
Internal Wall	**2.49**	Cement Mortar	20
		Standard Sintering Shale Hollow Brick	150
		Cement Mortar	20
Window (external-internal)	**5.22**	Glass	6
		Cavity	10
		Glass	6
Floor Slab (up-down)	**2.50**	Fine Aggregate Concrete 2300	30
		Inorganic Thermal Preservation Mortar	10
		Reinforced Concrete	100
Roof (up-down)	**0.60**	Fine Aggregate Concrete 2300	40
		Cement Mortar	20
		Xps Plate	32
		High Polymer Waterproof Sheet	3
		Cement Mortar	15
		Argil Fly-Ash Concrete	100
		Cement Mortar	15
		Reinforced Concrete	120
		Cement Mortar	10
Ground (up-down)	**0.66**	Reinforced Concrete	60
		Autoclaved Aerated Concrete Block 626-725	140
		SBS Modified Asphalt Rolling Material	3
		Fine Aggregate Concrete 2300	60
		Earth	600

Source: U-value is obtained by with calculation tool of HTB2 (Lewis & Alexander 1990), the material is based on survey and building codes (MOHURD & AQSIQ 2005)

Table 3. 4: Glazing ratio for civil buildings

Building Type	Orientations of Façade	Glazing Raito
Retail	All	⩽**70%**
Office	All	⩽**60%**
Residential	North	⩽**20%**
	East & West	⩽**30%**
	South	⩽**35%**

Source: (MOHURD & AQSIQ 1993)(MOHURD 2010)(MOHURD & AQSIQ 2015)

For the setting of the internal environment, lighting, services, occupancy, and cooling & heating are defined according to the early surveys on project sites and related design codes(MOHURD 2010)(SCDOHURD 2012)(MOHURD & AQSIQ 2015) (MOHURD 2017). The heat source from lighting, services and occupancy are considered as 'small power' during the calculation process of the simulation.

Table 3. 5: Specifications for parameters of the indoor thermal design

Building Type	Lighting Power Density Value (W/m^2)	Building Area Per Capita (m^2/person)	Electrical Equipment Power Density Value (W/m^2)
Retail	10.0	8	13.0
Office	9.0	10	15.0
Hotel	7.0	25	15.0

Source: (MOHURD & AQSIQ 2015)

Table 3. 6: Internal heat gains for office in the UK

Factor		Heat gains (W/m^2)					
Density(m^2/person)		4	**8**	**10**	12	16	20
Sensible heat gain	People	20	**10**	**8.35**	6.7	5	4
	Equipment	25	**20**	**17.5**	15	12	10
	Lighting	12	**12**	**12**	12	12	12
Latent heat gain		15	**7.5**	**6.25**	5	4	3

Source: CIBSE Guide A: Environmental Design (Butcher 2006)

The internal heat gain can be categories into sensible heat gain (SHG) and latent heat gain (LHG), and the former includes heat from people, equipment and lighting. In the national standard- *Design Standard for Energy Efficiency of Public Buildings* (MOHURD & AQSIQ 2015), 'Lighting Power Density Value (W/m^2)', 'Building Area Per Capita (m^2/Capita)', and 'Electrical Equipment Power Density Value' are specified for all types of public buildings, including retail, office, and hotel (*Table 6.5*). Due to lack of

reference from national standard, the sensible heat gain from people and latent heat gain are referred from a UK design guide- CIBSE Guide A: Environmental Design (Butcher 2006). However, for the sensible heat gain from equipment and lighting, the values based on the Chinese national standard are still applied. Therefore, as regulated in the Chinese national standard (China Ministry of Construction 2005), the reference value for 'Building Area Per Capita' is 8 in a retail and 10 in an office, which refers to 10 W/m^2 sensible heat gained from people and 7.5 W/m^2 latent heat gain for retail, and 8.35 W/m^2 sensible heat gain due to people and 6.25 W/m^2 latent heat gain for office (Table 6.6). Finally, the calculation of total internal heat gain in retails is:

SHG-*people* + SHG-*equipment* + SHG-*lighting* + LHG = Internal heat gain (3-12)

Retail: 10 W/m2 + 13 W/m2 + 10 W/m2 + 7.5 W/m2 = 40.5 W/m^2, (3-13)

Office: 8.35 W/m^2 + 15 W/m^2 + 9 W/m^2 + 6.25 W/m^2 = 38.6 W/m^2, (3-14)

Residential: 4.3 W/m^2 (MOHURD 2010).

Table 3. 7: Settings of Interior condition and diary

		Retail	Office	Residential
Heating/ Cooling	Design Temperature	18℃-25℃	21℃-26℃	18℃-26℃
	Operation Schedule	All the Year 08:00-21:00	Mon-Fri 07:00-18:00	Mon-Fri 00:00-8:00 18:00-24:00; Sat-Sun 00:00-24:00
Incidental Gains	Output Power	38.6 W/m^2	40.5 W/m^2	4.3 W/m^2
	Operation Schedule	All the Year 08:00-21:00	Mon-Fri 07:00-18:00	Mon-Fri 00:00-8:00 18:00-24:00; Sat-Sun 00:00-24:00
Ventilation	Infiltration Rate	0.5, 2.0, 2.0	0.5, 2.0, 2.0	0.5, 1.0, 1.0
	Operation Schedule	All the Year 08:00-21:00	Mon-Fri 07:00-18:00	Mon-Fri 00:00-8:00 18:00-24:00; Sat-Sun 00:00-24:00

Source: (MOHURD 2010) (MOHURD & AQSIQ 2015)

Lastly, the operation schedule is required for "Diary" file (*Table 6.7*), and each indoor features are specified in the regional (MOHURD 2010) and national (MOHURD & AQSIQ 2015) codes. Considering the preparation time and extra working hours, the

operation time for office starts one hour earlier than the standard working starting time at 8:00 and ends one hour after the standard working finishing time at 17:00. Notably, retails in Chengdu are usually closed lately at 21:00, and are operating on weekends.

3.7 Backgrounds of selected research projects

3.7.1 Site selection

Table 3. 8: Basic information of the 103 sites

Project Number	Parcel Code	Project Name	Project Number	Parcel Code	Project Name	Project Number	Parcel Code	Project Name
1	GX94(252/211):2008-029	神仙树馨苑	35	CH19(252/211):2006-069	高地	69	GX12(252/211):2006-011	原筑
2	WH20(252/211):2008-027	双楠锐派	36	ZWH21(252/211):2006-019	合力达泰基南棠	70	JJ17(211):2006-013	东方广场2
3	WH22(252/211):2008-025	逸尚美庭	37	ZCH23(252/211):2006-020	万科金域蓝湾1	71	QY14(252/211):2006-001	天盛壹中心
4	SLG-(2008)-029	和贵久居福	38	ZJJ02(252):2006-015	爱丁郡院	72	GX15(252/211):2006-012	南都领秀
5	JJ50(211):2008-001	明宇金融广场	39	ZWH20(252/211):2006-016	和信派都	73	JN15(252/211):2005-063	万科加州湾
6	PX03(252/211):2008-003	中铁瑞城西郡英华3	40	ZJN07(252/211):2006-017	西西里	74	JN16(252/211):2005-064	蓝光凯丽豪景
7	PX02(252/211):2008-002	中铁瑞城西郡英华2	41	JN31(252/211):2006-055	华宇锦城名都2	75	JJ13(252/211):2005-065	蓝光皇后国际
8	PX01(252/211):2008-001	中铁瑞城西郡英华1	42	JN32(252/211):2006-056	华宇锦城名都1	76	ZCH08(252):2005-015	花样年花郡
9	SLP-(2008)- 007	蜀镇半岛	43	WH17(252/211):2006-057	正黄上岭	77	JN13(252):2005-058	金府世家
10	SLP-(2008)- 008	蜀镇半岛	44	JJ05(211/212/252):2006-051	喜年广场	78	CH09(252):2005-059	东林城市花园
11	JJ49(252/211):2008-005	沙河壹号	45	CH14(252/211):2006-045	蓝光富丽花城	79	CH10(252):2005-060	兴元华盛
12	JN43(211):2007-105	金府国际	46	JN16(252/211):2006-046	西香纪（加洲阳光）	80	ZjnO6(252/211):2005-014	上层建筑
13	GX93(252/211):2008-028	成都合院	47	GX27(252/211):2006-035	融城后街	81	WH09(252/211):2005-047	隐庐巷上生活馆
14	QY39(252):2007-082	天合凯旋天际湾	48	WH14(252/211):2006-037	和谐公寓	82	JJ11(252/211):2005-048	国润天骄
15	QY33(252/211):2007-072	鼓楼国际	49	JN24(252/211):2006-040	正成凌江尚府	83	JJ09(252/211):2005-043	雕墅
16	SLG-(2007)-014	蓝光圣菲TOWN城	50	JJ22(211/212/213):2006-041	EGO潮流广场	84	CH08(252):2005-044	滨河丽景
17	JN37(214):2007-064	金沙国际	51	JJ21(211/252):2006-033	城市理想	85	CH09(252):2005-045	正成沙河明珠
18	WH06(214):2007-065	正成双楠格调	52	JN23(214/252):2006-027	金璐天下	86	ZJJ03(252):2005-09	晶蓝半岛
19	CH27(252/211):2007-046	华宇阳光四季	53	ZJJ07(252/211):2006-013	东城攻略	87	ZjnO5(252/211):2005-011	芙蓉华庭
20	JJ34(252/211):2007-043	蓝光凯丽香江	54	JN17(252/211):2006-030	兴元绿洲	88	CH07(252):2005-040	东方锦都
21	QY31(252/211):2007-032	正成财富领地	55	WH17(252/211):2006-032	廊桥乐章	89	ZjnO4(252):2005-011	凯瑞花都
22	ZJJ09(252/231):2007-003	上锦美地	56	QY17 (211):2006-023	青羊肆	90	CH03(252/211):2005-033	颐和家园
23	GX40(252/211):2007-019	中海翠屏湾	57	JJ16(211/252):2006-024	万达锦华城	91	JN06(252):2005-020	金房水韵天府
24	ZCH12(252/211):2007-007	合能耀之城	58	ZJJ05(252/211):2006-001	上行汇锦	92	WH06(252):2005-021	伊顿社区
25	ZCH17(252/211):2007-008	万科金域蓝湾2	59	JJJ19(252/211):2006-020	弘邦领邸	93	QY02(252):2005-022	蓝光雍锦湾
26	ZCH17(252/211):2007-008	华宇阳光水岸	60	JN19(252/211):2006-017	芙华幸福彼岸	94	JJ03(211):2005-014	东方广场1
27	WH01(252/211):2007-012	海珀香庭	61	CH37(211):2013-194	瑞祥御锦	95	JN05(252):2005-019	三九绿城
28	ZJN09(211/252):2007-001	紫金乐章	62	ZWH05(252/211):2006-009	月光琉城	96	JN03(252):2005-013	中海龙湾半岛
29	ZCH13(252/211/242):2007-002	龙湖三千城	63	ZCH05(252/211):2006-010	浅水半岛	97	ZjnO1(21\25):2005--003	蓝光富丽城
30	ZWH21(252/211):2006-022	花间集	64	CH07(211/252):2012-96	首创A-Ztown爱这城	98	QY01(25/21):2005-008	时代领地
31	QY28(252/211):2007-001	蓝光凯丽美城	65	CH11(252/211):2006-015	蓝光富丽锦城	99	ZjnO3(25):2005-006	金都苑
32	JN34(252/211):2007-004	双城（金仙桥大院）	66	WH07(252/211):2006-016	傲仕门	100	GH01(25):2005--005	枫景雅居
33	JJ28(252/211):2007-005	萧邦	67	QY04(252/211):2006-008	鼓楼世家	101	zjj01(25):2005-001	银唐
34	ZCH11(211):2006-021	天空城	68	JJJ14(211/252):2006-009	正成财富ID	102	GX01(25):2005-004	兴元丽都
						103	Zjj01(21):2005--002	绿野天成

All the 103 selected project sites are shown in Table 3.8. Base on the database of the Chengdu City Planning Bureau, the details of 103 the new-constructing projects were finished before 2010. The 103 projects are finely distributed within the area of 3 rings development of Chengdu city (Figure 3.17), which are chosen as typical buildings projects in the Chengdu city for UHI-urban form correlation in this paper.

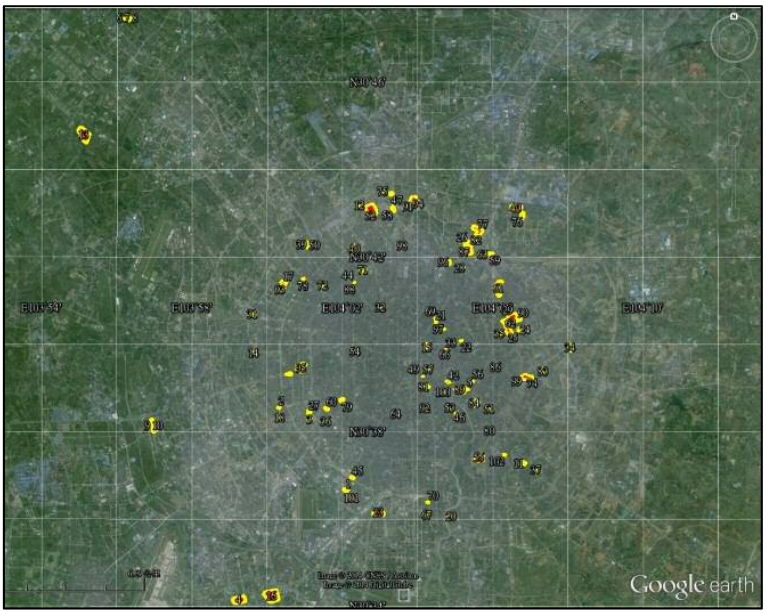

Figure 3. 17: 103 sites in Chengdu City Map

The project features were collected from the open access database of the City Planning Bureau, with the parcel code for the identification of each project. Among the 103 projects, there are 62 commercial-residential mixed, one office-residential mixed, 30 are residential and 10 are single commercial in use. Due to the limitation of construction height in city area for local military restrictions, more than 85% of the target 103 projects are lower than 100 metres, only one project is constructed with 150 plus metres, which is a skyscraper in the very core of central business district (Figure). And the site areas vary from 3000 m² to 355956.44 m² with an average area of 30893.63252 m². More than 50% of the 103 projects are built with 30% building coverage ratio, while the floor area ratio is controlled at or below 5 in 77.7% of all target buildings. The green area covers 25% of the site area in the vast majority of the projects. 43 of the 103 are designed with the enclosed plot, while the other 24 are semi-opened.

Table 3. 9: Identity of selected projects

Project Number	FAR	BRC	GCR	TYPE	Plot Layout	Building Height
1	4	0.24	0.3	Commercial + Residential	IV-Mixed	72
2	2.4	0.3	0.3	Commercial + Residential	II-Linear	30
3	3.01	0.29	0.3	Commercial + Residential	II-Linear	36
4	3.98	0.5	0.4	Commercial + Residential	IV-Mixed	54
5	14.5	0.5	0.3	Commercial	I-Tower	206
6	1.39	0.3	0.38	Residential with 5% Commercial	IV-Mixed	60
7	1.39	0.3	0.385	Residential	IV-Mixed	60
8	1.39	0.3	0.4	Residential	IV-Mixed	63
9	3.3	0.2	0.36	Commercial + Residential	IV-Mixed	54
10	3.3	0.2	0.36	Commercial + Residential	IV-Mixed	57
11	4	0.3	0.35	Commercial + Residential	IV-Mixed	105
12	4.48	0.5	0.25	Commercial	III-Semi-Closed	102
13	2.35	0.25	0.3	Residential	V-Court	51
14	4	0.16	0.25	Commercial + Residential	I-Tower	87
15	9.77	0.3	0.1	Office	I-Tower	139
16	3.75	0.35	0.3	Commercial + Residential	IV-Mixed-Mixed	63
17	2.2	0.4	0.33	Commercial + Residential	V-Court	15
18	4	0.4	0.26	Commercial + Residential	V-Court	39
19	3.14	0.22	0.3	Commercial + Residential	IV-Mixed	51
20	7.85	0.3	0.34	Commercial + Residential	IV-Mixed	126
21	3.02	0.35	0.25	Commercial + Residential	III-Semi-Closed	78
22	7.6	0.3	0.266	Commercial + Residential	III-Semi-Closed	123
23	3	0.3	0.3	Commercial + Residential	IV-Mixed	54
24	4.9	0.3	0.28	Commercial + Residential	III-Semi-Closed	84
25	4.05	0.25	0.3	Commercial + Residential	IV-Mixed	105
26	4.5	0.25	0.25	Residential with 5% Commercial	IV-Mixed	63
27	2.34	0.3	0.25	Commercial + Residential	V-Court	30
28	7.21	0.4	0.23	Commercial + Residential	II-Linear	66
29	5	0.35	0.35	Commercial + Residential	III-Semi-Closed	102
30	3.7	0.3	0.4	Commercial + Residential	III-Semi-Closed	54
31	5	0.3	0.35	Commercial + Residential	IV-Mixed	93
32	4.8	0.3	0.25	Commercial + Residential	I-Tower	87
33	7.04	0.4	0.25	Commercial + Residential	I-Tower	99
34	5.55	0.3	0.45	Residential	IV-Mixed	84
35	4.65	0.35	0.3	Commercial + Residential	III-Semi-Closed	75
36	4	0.35	0.25	Commercial + Residential	II-Linear	45
37	4.05	0.25	0.3	Commercial + Residential	IV-Mixed	105
38	3.5	0.3	0.4	Commercial + Residential	II-Linear	54
39	6.28	0.25	0.3	Commercial + Residential	III-Semi-Closed	96
40	3.61	0.3	0.36	Commercial + Residential	IV-Mixed	102
41	4.66	0.3	0.3	Commercial + Residential	I-Tower	99
42	4.66	0.3	0.3	Commercial + Residential	II-Linear	99
43	4.2	0.3	0.25	Commercial + Residential	IV-Mixed	66
44	12.38	0.4	0.2	HOPSCA (City Complex)	II-Linear	190
45	4.4	0.3	0.25	Commercial + Residential	III-Semi-Closed	54
46	4.2	0.3	0.25	Commercial + Residential	I-Tower	54
47	4	0.3	0.2	Residential	III-Semi-Closed	51
48	2.6	0.3	0.28	Commercial + Residential	II-Linear	48
49	5	0.3	0.3	Residential	I-Tower	66
50	2	0.45	0.28	Commercial	II-Linear	20
51	10	0.76	0.16	HOPSCA (City Complex)	III-Semi-Closed	111
52	3.5	0.4	0.25	Office	V-Court	93
53	5.5	0.35	0.4	Commercial + Residential	II-Linear	102
54	5	0.3	0.25	Residential with 5% Commercial	II-Linear	66
55	4.2	0.3	0.25	Commercial + Residential	II-Linear	60
56	1.5	0.5	0.25	Commercial	I-Tower	16
57	5.45	0.55	0.25	Commercial + Residential	I-Tower	90
58	7	0.3	0.25	Residential	III-Semi-Closed	102
59	8	0.4	0.29	Commercial + Residential	II-Linear	102
60	4.95	0.3	0.25	Residential	III-Semi-Closed	66
61	4.2	0.3	0.25	Commercial + Residential	IV-Mixed	54
62	5	0.35	0.25	Commercial + Residential	IV-Mixed	51
63	4.41	0.3	0.48	Residential	V-Court	54
64	5	0.3	0.4	Commercial + Residential	I-Tower	90
65	5.56	0.3	0.3	Commercial + Residential	II-Linear	66
66	4.2	0.3	0.25	Commercial + Residential	I-Tower	57
67	6.99	0.4	0.25	Residential with 5% Commercial	II-Linear	96
68	10.24	0.45	0.2	Residential + Office	I-Tower	96
69	5.88	0.3	0.26	Residential with 5% Commercial	II-Linear	33
70	5	0.5	0.07	Hotel + Commericial	IV-Mixed	120
71	5.99	0.5	0.25	Commercial + Residential	V-Court	99
72	4.23	0.3	0.25	Commercial + Residential	IV-Mixed	39
73	6.8	0.45	0.25	Commercial + Residential	III-Semi-Closed	96
74	4.2	0.3	0.42	Commercial + Residential	IV-Mixed	99
75	6.95	0.4	0.25	Commercial + Residential	III-Semi-Closed	99
76	3.52	0.3	0.32	Commercial + Residential	V-Court	87
77	3.99	0.3	0.25	Residential with 5% Commercial	V-Court	54
78	3.9	0.3	0.3	Commercial + Residential	III-Semi-Closed	54
79	4.6	0.3	0.3	Commercial + Residential	V-Court	54
80	5	0.45	0.25	Commercial + Residential	III-Semi-Closed	78
81	4.7	0.3	0.25	Residential with 5% Commercial	II-Linear	45
82	4.2	0.3	0.3	Residential	III-Semi-Closed	39
83	7	0.4	0.25	Commercial + Residential	II-Linear	99
84	4	0.3	0.3	Residential with 5% Commercial	III-Semi-Closed	51
85	3.99	0.3	0.3	Residential	III-Semi-Closed	54
86	4.2	0.3	0.46	Commercial + Residential	III-Semi-Closed	78
87	5.58	0.35	0.27	Commercial + Residential	III-Semi-Closed	54
88	3	0.3	0.25	Commercial + Residential	III-Semi-Closed	54
89	3.84	0.3	0.35	Residential with 5% Commercial	III-Semi-Closed	54
90	5.04	0.35	0.25	Commercial + Residential	IV-Mixed	54
91	2.78	0.28	0.3	Commercial + Residential	IV-Mixed	54
92	4.53	0.3	0.33	Residential with 5% Commercial	II-Linear	60
93	1.68	0.3	0.3	Commercial + Residential	II-Linear	12
94	9.21	0.5	0.2	HOPSCA (City Complex)	IV-Mixed	96
95	4.71	0.3	0.3	Residential	IV-Mixed	66
96	3.2	0.3	0.3	Residential with 5% Commercial	III-Semi-Closed	54
97	3.5	0.25	0.35	Commercial + Residential	II-Linear	57
98	4.74	0.3	0.25	Commercial + Residential	IV-Mixed	39
99	3.68	0.28	0.31	Residential with 5% Commercial	IV-Mixed	90
100	2.99	0.33	0.25	Residential	III-Semi-Closed	36
101	5.83	0.25	0.398	Commercial + Residential	V-Court	84
102	2.8	0.3	0.3	Commercial + Residential	III-Semi-Closed	39
103	4.73	0.35	0.3	Commercial + Residential	III-Semi-Closed	54

Source: from author's survey

3.7.2 Variable selection

According to the findings from Chapter 2, variables of building density, green coverage ratio and plot layout, had shown decisive impact on both building energy performance and microclimate variation. In particular, Floor Area Ratio (FAR), Building Coverage Ratio (BCR), Building Height (Height), and Height to Floor Area Ratio (H/A), are key controlling parameters of urban form for planning any construction project in China. Similar as building density variables, variables of Green Coverage Ratio (GCR), Project Type, and Plot Layout are restricted accordingly based on the urban planning and local codes. Therefore, as shown in Table 3.10, eight key controlling variables have been selected and will be applied in the studies of the following chapter.

Table 3. 10: Variable selected

Variables	Abbreviations	Properties
Distance	D	Distance from site to the city centre
Project Type	TYPE	Function of buildings
Plot Layout	PL	Tower, Linear, Semi-closed, Interspersed, and Court
Green Coverage Ratio	GCR	The ratio of green area to total site area
Floor Area Ratio	FAR	The ratio of total building floor area to the total site area
Building Coverage Ratio	BCR	The ratio of building ground floor area to the total site area
Building Height	HEIGHT	Building height
Height to Floor Area Ratio	H/A	The ratio of the building height to the total site area

3.7.3 Construction feature collection.

The project features were collected from the open access database of the City Planning Bureau, with the parcel code for the identification of each project. Among the 103 projects, there are 62 commercial-residential mixed, one office-residential mixed, 30 are residential and 10 are single commercial in use.

Owing to the limitation of construction height in city area for local military restrictions, more than 85% of the target 103 projects are lower than 100 metres, only one project is constructed with 150 plus metres, which is a skyscraper in the very core of central business district (Table 3.9). And the site areas vary from 3000 m² to 355956.44 m² with an average area of 30893.63 m². More than 50% of the 103 projects are built with 30% building coverage ratio, while the floor area ratio is controlled at or below 5 in 77.7% of all target buildings. The green area covers 25% of the site area in the vast

majority of the projects. 43 of the 103 are designed with the enclosed plot, while the other 24 are semi-opened.

3.7.4 Five groups of 15 selected sites from the 103 original sites

Due to the limited time-scale, simulations for all research 103 sites becomes impossible. Therefore, 15 targets city-block projects with the notable difference in building density, building coverage ratio, and building height, are selected and categorised into five groups mainly based on the plot layout form. The five groups are the Tower, Linear, Semi-Closed, Mixed, and Court (Figure 3.18).

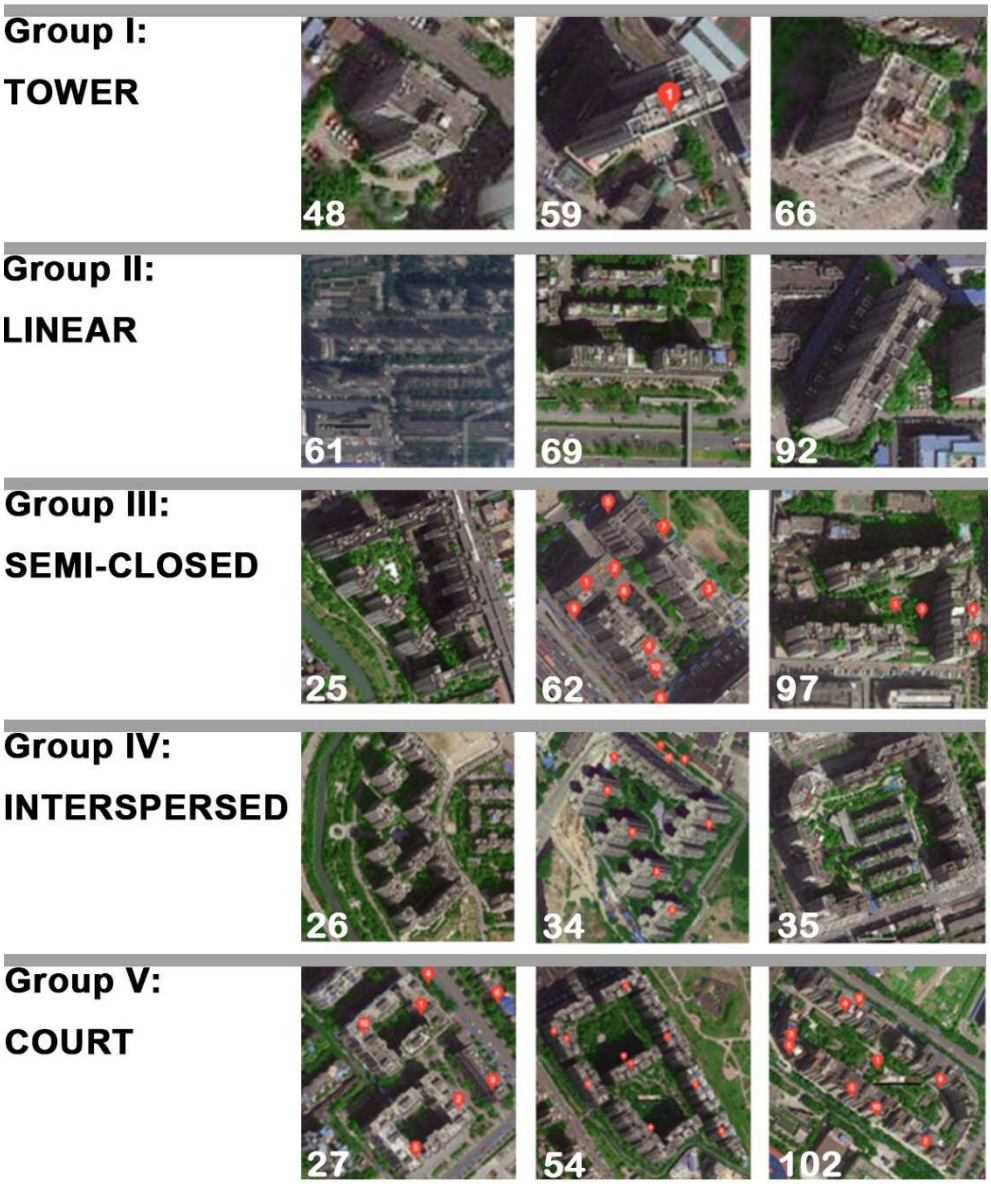

Figure 3. 18: 5 groups of target projects (with original project number) in terms of plot layout.

i) Tower

Figure 3. 19: Target project sites of Tower Group

Three high-rise towers with the function of the residential and small portion of retail are categorised into this Tower Group (Figure 3.19). Site No. 48 is 'Hexie House', a fifteen-floor high-rise building with more than 112 apartments on upper floors and a whole ground floor of retail. Its total area is more than 7,270m^2, while the site area is 2272m^2. No. 59 site is 'Hongbang House', a more than 102m tall high-rise tower with more than 395 apartments and a large area of retail on lower floors, which has high floor area ratio of 8 within 3,045 m^2 site area. No. 66 site is 'Aoshimen House', a more than 57m tall high-rise tower with 163 apartments and a considerable amount of retail area on the lower floors. The site covers 2918$m^{2,}$ land and total floor area is 12256m^2.

ii) Linear

In the linear group, three residential real estate projects are selected (Figure 3.20). Site No. 61 and Site No. 69 are high-rise dwellings integrated with ground floor retail, while Site No.92 is an apartment high-rise building. Site No. 61 is 'Ruixiang Yujin', which has more than 900 apartments with 86,226m^2 on the 20530m^2 large site. No. 69 site is 'Yuanzhu', a residential and retail project with 8325.18 m^2 site area and five-floor area

ratio. And site No. 92 is ‘Yidun Community’, a 60*m*-tall high-rise building that has 360 apartments with more than 4.2-floor area ratio on a 7968.73m^2 site.

Figure 3. 20: Target project sites of Linear Group

iii) Semi-closed

In the Semi-Closed Group, all three estate projects are designed into high-rise apartments with ground-floor retail spaces (Figure 6.21). Site No. 25 is “Wanke Jinlanwan”, a 35-floors+ community with 56295m^2 site area and 5 floor area ratio; Site No.62, “Yueguang Liuyu”, is dwelling community with 668 apartments taking land area of 13,990 m^2 and 5 floor area ratio; Site No.97 is “Language Fulicheng”, covering 30,000 m^2 land area and providing 780 apartments and limited number of retails in a 4-total floor area ratio.

Figure 3. 21: Target project sites of Semi-Closed Group

iv) Interspersed

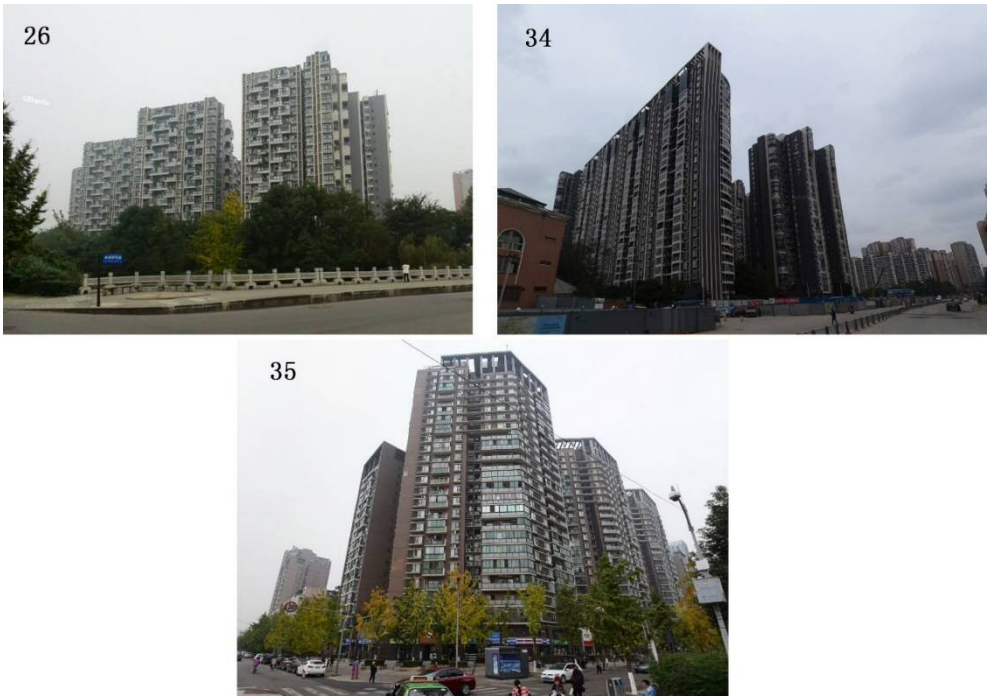

Figure 3. 22: Target project sites of Interspersed Group

In the group of the Interspersed (Figure 3.22), Site No.26 and Site No.34 are dwelling community with high-rise building group; However, Site No.35 is a ‘superblock’ with building group of multi-function, including residential, retail, and office. Site No.26 has

38,000m^2 land and 5 in total floor area ratio, high-rise apartment buildings are in multiform on plan and interspersed with each other; Site No.34 is residential block with more than 84 metres tall high-rise building group, which cover 48,138 m^2 site area with a 5 total floor area; Lastly, Site No.35 is a multi-functional building group, that has verity of forms and layouts. The site takes up around 43,000 m^2 land and is built up with 250,000 m^2 in total floor area.

v) Courtyard

Three project sites with court-form layout are selected for this group. As shown in Figure 3.23, Site No.27 and Site No.102 are two dwelling community with ground floor retail spaces, and Site No. 54 is designed into apartment buildings without any other function. There are more than 600 apartments in site No.27 with a total floor area around 100,000m^2. Site No.54 is a mega dwelling community with more than 4,000 apartments, and its site area is more than 66,800m^2 with a 5-total floor area ratio. In this site, some towers are composed of two big courtyards with large green spaces in the middle.

Figure 3. 23: Target project sites of Tower Group

3.8 Summary

This chapter discussed the mythologies adopted by this study. Firstly, the research questions and research objectives are proposed, which formed the city-block centred research framework is proposed. Based on the research questions, this chapter established the multi-method research strategy. Moreover, this chapter reviewed research methods related to the analysis of urban climate at both the macro and the micro scale. Additionally, it investigated the simulation tools for both microclimate and building energy. Lastly, the background of research subjects, including the targets sites and the city, was introduced.

Results of assessment for all research issues are presented in the following chapters, which are, Chapter 4: Urban Heat Island Effect and Design Variables; Chapter 5: Microclimate and Simulations; and Chapter 6: Building Energy and Simulations.

Chapter Four

URBAN HEAT ISLAND EFFECT AND DESIGN VARIABLES

4.1 Introduction

This chapter aims to answer the second research question:

> *'What are the microclimate features of the city-block-scale building groups in China, and how do the design features of the urban configuration of the real estate projects have impacts on microclimate condition?'*

To answer this research questions, this chapter investigates the impacts of design features on microclimate at a city-block scale. Firstly, the UHI imagines of satellite remote sensing is processed and overlayed on the selected 103 sites and 28 urban zones in ArcGIS- a tool of geographic information system (GIS). Therefore, on-site UHI values and on-zone UHI values are obtained. Secondly, it makes a comparison between the on-site UHI values and on-zone UHI values. Thirdly, this chapter investigates the relationship between each design variables and UHI value for each site, thereby summarising the influence of multi-variable on microclimate at a city-block scale.

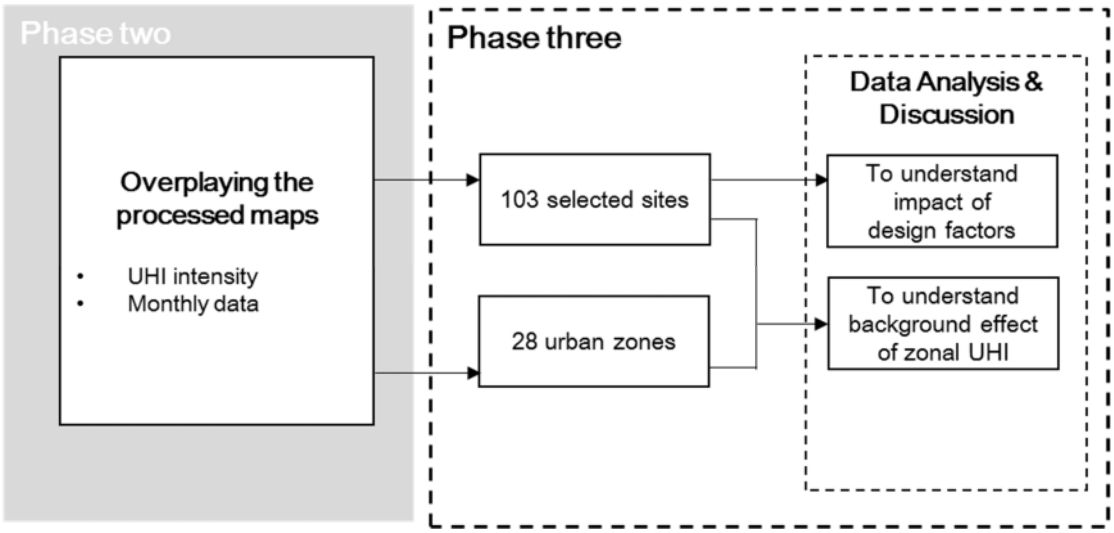

Figure 4. 1: Framework of study on UHI and design variables in phase two and phase three

4.2 Mapping UHI onto 103 projects

4.2.1 UHI on each project, GIS-based (ArcGIS) analysis

In the ArcMap, one of the main tools of Esri's ArcGIS- the Spatial Analysis Tools- is applied. Through which the 103 selected sites are symbolised as shapefile accordingly based on their geo-coordinates (Figure 4.2), and the UHI intensity value within satellite-derived images are input into this tool and are assigned into the different layers (Figure 4.3). A different set of data in the same area on different layers will be measured and overlayed onto the zones and sites shapefile accordingly. After being processed in this Spatial Analysis Tools, the mean value of monthly UHI intensity on every 103 sites is acquired (Figure 4.4).

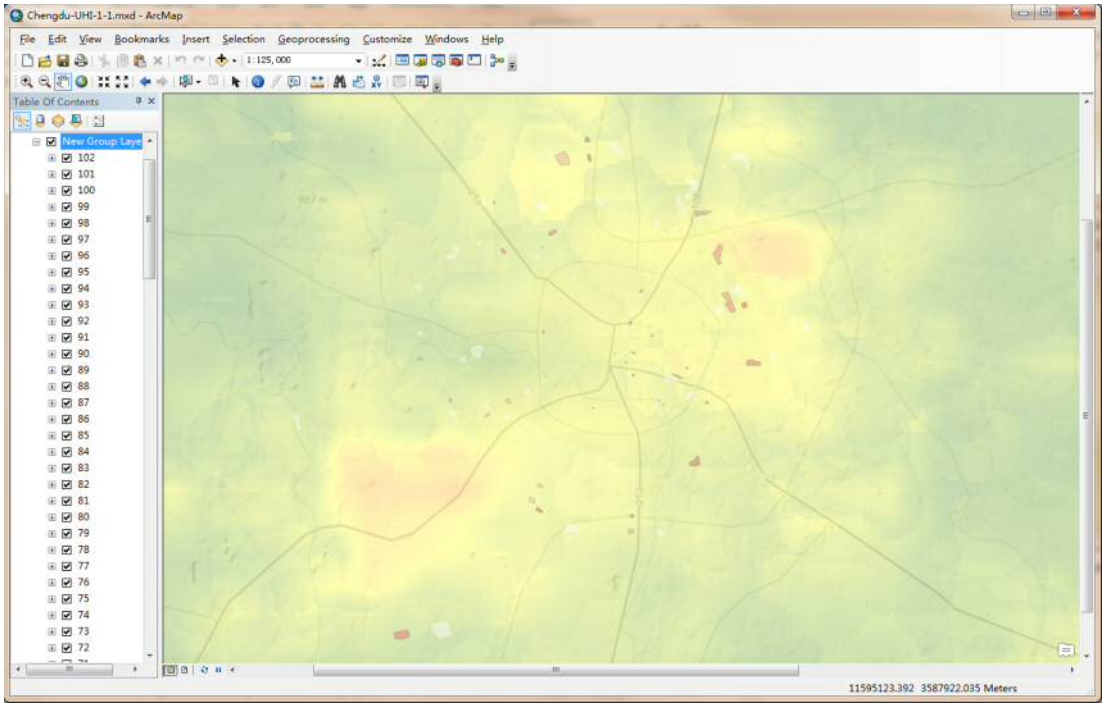

Figure 4. 2: Overlay the UHI intensity layer, the 103 site layer, and base map (terrain) layer.

Table 4.1 shows the UHI intensity of 103 project sites in summer and winter months. The average UHI value of all sites is 4.397°C in August, 4.430°C in July, and 3.684°C in June, respectively (Figure 4.5). The highest UHI value appears in August in most projects, while in some projects the UHI value in July is higher. In December, the average UHI value of all sites is 1.232°C, comparing to 1.312°C in January and

1.320°C in February (Figure 4.6). Moreover, the lowest UHI value is also found in December among the three winter months in most sites.

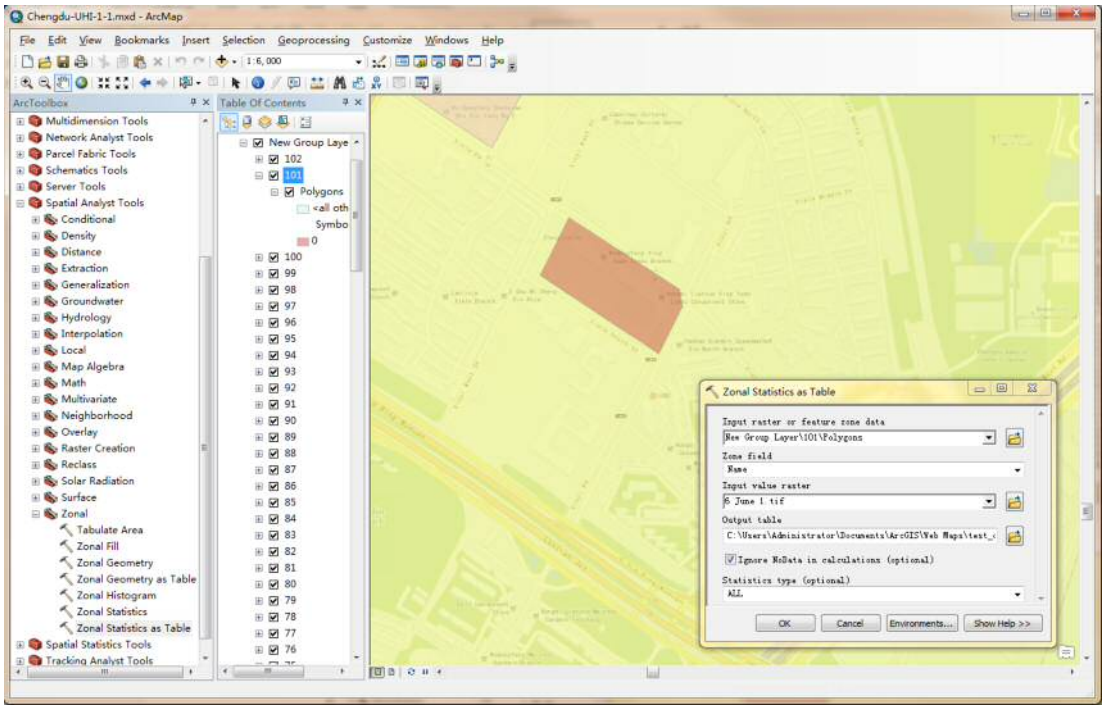

Figure 4. 3: Input data in Spatial Analysis Tools of ArcMap

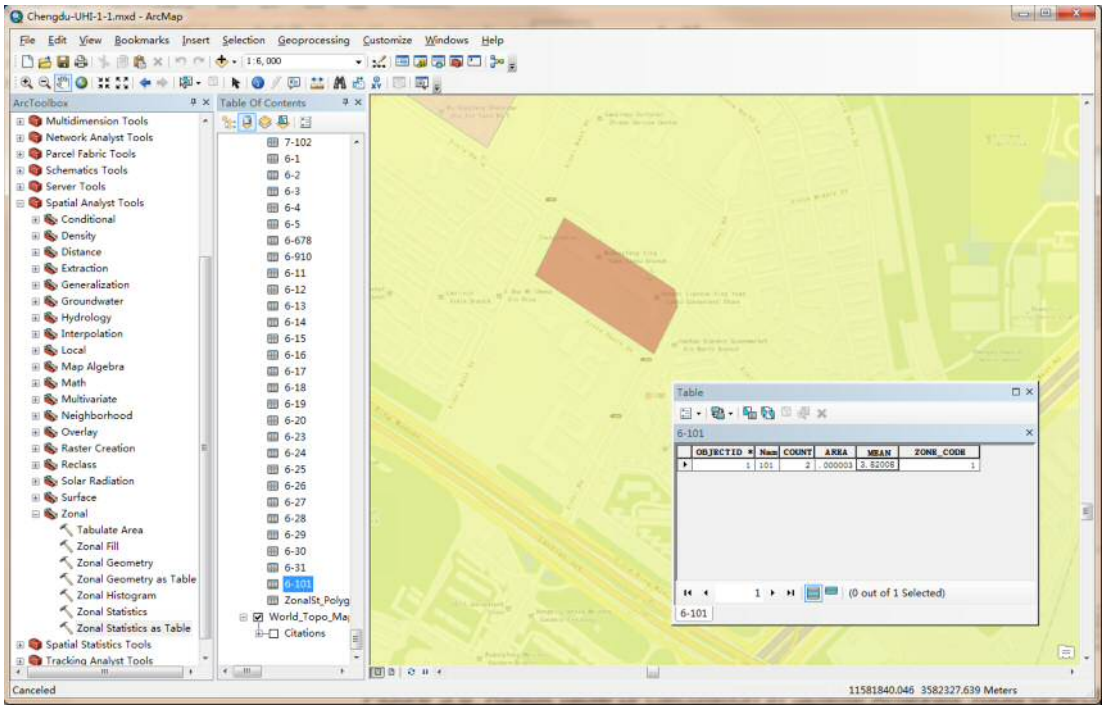

Figure 4. 4: Result table of calculation in Spatial Analysis Tools of ArcMap

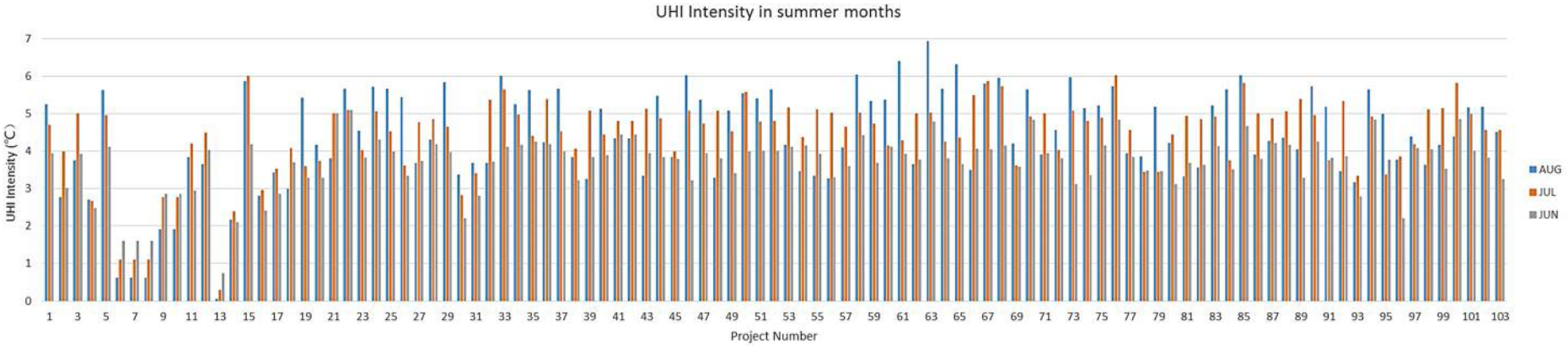

Figure 4. 6: UHII in summer months

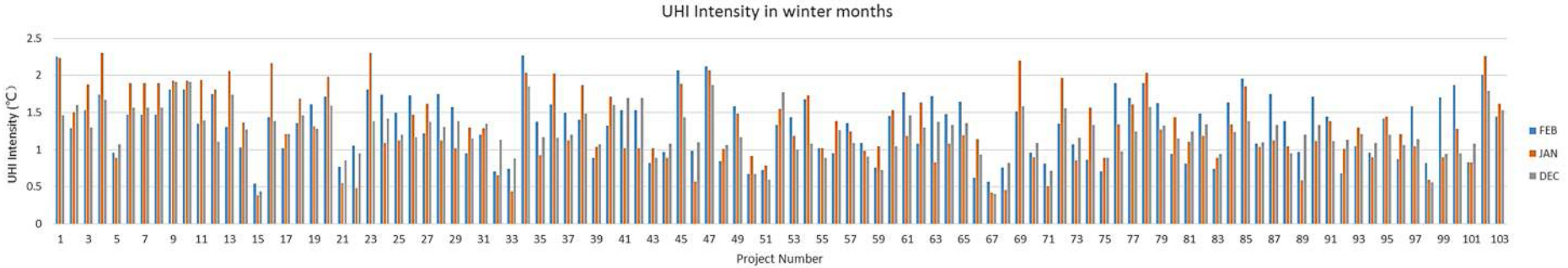

Figure 4. 5: UHII in winter months

Table 4. 1: The mean monthly UHI intensity on every 103 sites obtained in ArcMap

Project Number	August	July	June	Febuary	January	December	Project Number	August	July	June	Febuary	January	December
1	5.257315	4.693781	3.934541	2.25189	2.236471	1.456409	53	4.162	5.16438	4.11997	1.436863	1.179381	1.001901
2	2.77622	3.988384	3.01628	1.290904	1.502785	1.597302	54	3.456729	4.379588	4.153231	1.676574	1.726001	1.075188
3	3.752257	5.001628	3.918335	1.526798	1.872873	1.297796	55	3.3331	5.10834	3.92045	1.014483	1.014517	0.884933
4	2.706738	2.675177	2.486919	1.735304	2.299195	1.672896	56	3.2754	5.029971	3.30662	0.951729	1.378629	1.257229
5	5.623199	4.958261	4.122178	0.953877	0.886677	1.072183	57	4.09534	4.654203	3.594765	1.355166	1.243185	1.08933
6	0.621478	1.097883	1.592762	1.467813	1.897837	1.561727	58	6.0493	5.020571	4.423973	1.089905	0.980018	0.901957
7	0.621478	1.097883	1.592762	1.467813	1.897837	1.561727	59	5.3399	4.7285	3.6911	0.761	1.0402	0.7265
8	0.621478	1.097883	1.592762	1.467813	1.897837	1.561727	60	5.37475	4.147577	4.121126	1.448599	1.528373	1.04502
9	1.918078	2.779302	2.861836	1.809592	1.925098	1.91057	61	6.4092	4.2785	3.93281	1.776601	1.184515	1.460958
10	1.918078	2.779302	2.861836	1.809592	1.925098	1.91057	62	3.644367	5.008445	3.764924	1.078107	1.632193	1.291359
11	3.845387	4.196772	2.947239	1.34976	1.940891	1.386986	63	6.9432	5.024479	4.783307	1.723888	0.826799	1.369974
12	3.649019	4.490853	4.035054	1.743638	1.811446	1.10739	64	5.668344	4.256239	3.808335	1.476196	1.082483	1.329523
13	0.053776	0.29366	0.73872	1.300252	2.059813	1.740701	65	6.318791	4.359386	3.643215	1.646315	1.187568	1.353301
14	2.175275	2.399824	2.101968	1.025135	1.367754	1.271249	66	3.495	5.4926	4.0689	0.6147	1.1421	0.9343
15	5.872726	6.004973	4.175386	0.538105	0.381577	0.437045	67	5.8001	5.876005	4.040682	0.570315	0.415529	0.402129
16	2.804613	2.967063	2.402385	1.436812	2.166309	1.381973	68	5.9517	5.728361	4.150316	0.754324	0.452035	0.819055
17	3.419468	3.52544	2.859905	1.019675	1.205319	1.208952	69	4.19956	3.606773	3.584948	1.513485	2.194024	1.581409
18	3.0012	4.0838	3.6992	1.3524	1.6877	1.4622	70	5.64665	4.916366	4.834974	0.96049	0.895813	1.087624
19	5.418726	3.596203	3.282305	1.603764	1.311137	1.279995	71	3.9024	5.00452	3.938916	0.809665	0.507019	0.717849
20	4.166605	3.727608	3.291817	1.714139	1.980657	1.590559	72	4.5663	4.035825	3.803707	1.350828	1.960372	1.55479
21	3.8097	5.0084	5.009543	0.7693	0.547114	0.8566	73	5.96682	5.071055	3.123388	1.066538	0.852762	1.15672
22	5.6544	5.092012	5.092	1.0491	0.4795	0.9467	74	5.143692	4.802414	3.351773	0.864058	1.560419	1.333985
23	4.545754	4.032218	3.826706	1.803421	2.302302	1.381032	75	5.211725	4.892625	4.139875	0.706936	0.887869	0.887355
24	5.71655	5.054359	4.306984	1.742046	1.084118	1.414913	76	5.725315	6.020825	4.83709	1.896955	1.342884	0.97279
25	5.656375	4.52151	3.985325	1.493189	1.124062	1.201613	77	3.9372	4.552607	3.836368	1.698712	1.603843	1.24554
26	5.439349	3.619559	3.333427	1.729143	1.467324	1.161144	78	3.848133	3.434038	3.474956	1.89745	2.032696	1.575789
27	3.679612	4.775534	3.726655	1.215147	1.614986	1.373076	79	5.187191	3.437965	3.46321	1.624851	1.266079	1.32289
28	4.305784	4.845087	4.174473	1.74877	1.117992	1.301086	80	4.220417	4.434873	3.111036	0.93924	1.436325	1.146275
29	5.841012	4.638812	3.980792	1.57523	1.016367	1.37866	81	3.318625	4.945539	3.678702	0.81165	1.104955	1.242776
30	3.366607	2.821591	2.212042	0.946552	1.291137	1.147465	82	3.56908	4.851651	3.637828	1.489246	1.178665	1.33461
31	3.674957	3.405635	2.808303	1.199728	1.283572	1.344239	83	5.2086	4.9184	4.1371	0.7417	0.8911	0.9361
32	3.689616	5.37359	3.711354	0.706547	0.654117	1.133501	84	5.6509	3.750211	3.5122	1.633025	1.337775	1.238175
33	5.9987	5.6431	4.1179	0.7375	0.4394	0.8771	85	6.03015	5.814543	4.659713	1.957666	1.848823	1.38387
34	5.24805	4.97431	4.168676	2.264929	2.030724	1.85265	86	3.910837	5.014326	3.786287	1.076449	1.036803	1.095297
35	5.634876	4.399827	4.249982	1.373448	0.923475	1.164762	87	4.261772	4.86763	4.221896	1.74965	1.118227	1.331969
36	4.225616	5.394773	4.182057	1.611961	2.024123	1.154002	88	4.350932	5.060874	4.166075	1.384191	1.046677	0.949815
37	5.656375	4.52151	3.985325	1.493189	1.124062	1.201613	89	4.045014	5.391521	3.284774	0.962583	0.584634	1.202669
38	3.834436	4.061261	3.215305	1.40375	1.866612	1.484491	90	5.724285	4.960522	4.25209	1.7139	1.114181	1.333192
39	3.245532	5.080754	3.846163	0.884771	1.039228	1.07358	91	5.186544	3.746584	3.821653	1.447007	1.385387	1.116058
40	5.13514	4.4391	3.893674	1.322289	1.709631	1.599522	92	3.467189	5.329002	3.850028	0.678488	1.008958	1.129921
41	4.336897	4.801563	4.441451	1.526237	1.01332	1.69309	93	3.164618	3.333554	2.79465	1.045323	1.293831	1.208778
42	4.336897	4.801563	4.441451	1.526237	1.01332	1.69309	94	5.64665	4.916366	4.834974	0.96049	0.895813	1.087624
43	3.335965	5.128188	3.938815	0.821437	1.021587	0.891308	95	4.989789	3.371169	3.770708	1.415691	1.443897	1.203959
44	5.471577	4.876922	3.842655	0.961781	0.885443	1.081041	96	3.773527	3.862402	2.206151	0.867409	1.211675	1.064106
45	3.845699	3.990313	3.782816	2.06989	1.885836	1.430684	97	4.387984	4.179514	4.07431	1.584391	1.040869	1.140996
46	6.0204	5.0724	3.2127	0.9817	0.563	1.0985	98	3.638045	5.114045	4.052989	0.820166	0.596205	0.553589
47	5.372238	4.732644	3.942095	2.120212	2.068925	1.872166	99	4.164276	5.152279	3.521046	1.702282	0.899632	0.939899
48	3.2795	5.0724	3.809967	0.843733	1.0097	1.0572	100	4.3934	5.811035	4.852072	1.867932	1.279209	0.951256
49	5.07425	4.528366	3.409952	1.577472	1.482361	1.165526	101	5.157911	4.9838	4.0166	0.827333	0.827333	1.0744
50	5.548807	5.569138	3.985029	0.669314	0.911414	0.668571	102	5.180614	4.561474	3.820081	2.003769	2.256	1.793791
51	5.3967	4.7846	4.0183	0.7221	0.7868	0.5923	103	4.514313	4.556088	3.254407	1.440429	1.615912	1.532077
52	5.6519	4.7994	4.0112	1.3297	1.5475	1.7736							

4.2.2 UHI on zones of the entire urban area

Considering multi-factor impacts on the UHII distribution in the entire city, the segment of UHII maps are needed to be compared with the site UHII in each summer and winter months, which aims to investigate the overlapping between the zone-specific values and site-specific values. In the environment of *ArcGIS*, according to a network of ring-road circles and main radial roads, the city area is divided into 28 zones (Figure 4.7), therefore, the zonal segment maps of UHII in each of 6 months are produced (Figure 4.8).

Just as the single site in the previous section, UHI for each urban zone is processed in *the Spatial Analysis Tools*. Full data for all 28 urban zones are shown in Table 4.2

and Figure 4.8. According to the results, the highest zonal UHII-6.713°C- is observed in August in Zone 17 and the lowest UHII-0.516°C- is recorded in January in Zone 6. Notably, in Zone 5, there is no much difference in UHI of the three summer months and the three winter months, the all the values vary between 1.5°C and 2.0°C. Generally speaking, all the zones within the range of the urban rings have higher UHI in summer than that in winter. However, the UHI keep relatively constant all the year in urban lands far away from the urban rings. Moreover, the urban area located the outer urban ring, such as Zone 4, Zone 21, and Zone 27, has lower UHII in summertime than those within the inner ring, and the zones within the city centre area, including Zone 6- Zone 10, have lowest UHII in wintertime.

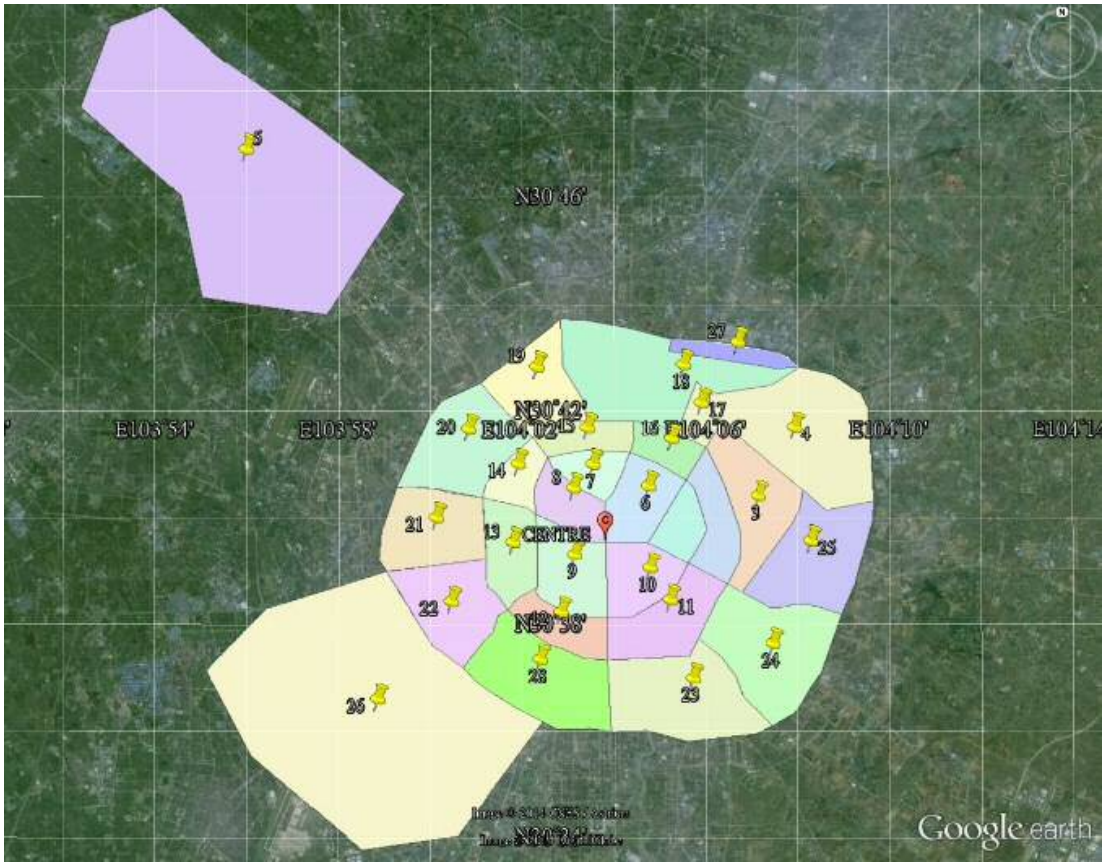

Figure 4. 7: Segment of 28 urban zones

Table 4. 2: The mean monthly UHI intensity on 28 urban zones obtained in ArcMap

Zone	AUG	JUL	JUN	FEB	JAN	DEC
1	5.55341	5.205026	4.352031	1.087809	0.766692	1.185854
2	5.33925	4.985746	4.356925	1.465917	1.050194	1.141702
3	5.97025	5.347357	4.626556	2.010639	1.377176	1.567887
4	3.57965	3.713921	3.767054	1.861237	1.994026	1.679967
5	1.460641	1.877616	1.996638	1.500033	1.876246	1.749101
6	5.361934	5.33399	4.120844	0.796584	0.516298	0.716161
7	5.21496	4.955321	3.853858	0.800518	0.571113	0.970688
8	3.82126	5.3165	3.855696	0.774905	0.659635	0.921684
9	3.58929	4.975744	3.633812	0.830971	1.135352	1.022701
10	4.443037	5.142278	4.045678	0.813762	0.986617	0.981675
11	3.91787	5.154134	3.791466	1.211973	1.248365	1.157507
12	4.460342	5.472078	4.107122	1.081383	1.185633	1.494583
13	3.60771	4.402077	3.032305	0.781727	1.240442	1.131817
14	3.82548	5.360438	3.470711	0.832341	0.749997	1.123209
15	5.653783	4.665157	3.902747	1.06823	0.610732	0.976059
16	5.867913	4.898239	4.4096	1.379669	0.679339	1.210341
17	6.713137	4.634426	4.108377	1.756728	1.061674	1.473614
18	4.731524	3.79176	3.56391	1.571425	1.383467	1.212627
19	4.324341	4.793215	4.11273	1.532524	1.283625	1.37552
20	4.085344	4.048524	2.999368	1.048555	1.268962	1.275132
21	3.281486	3.226117	2.41666	1.024969	1.229934	1.256217
22	3.375577	4.378077	3.594239	1.567106	1.685815	1.530752
23	3.903253	4.101622	3.352824	1.431266	1.716551	1.63356
24	4.088913	4.526496	3.467339	1.786928	2.045012	1.568393
25	4.650552	4.878487	3.793962	2.127735	2.33788	1.609813
26	4.054428	4.493357	3.904975	2.237006	2.34471	1.921191
27	3.696572	3.323082	3.318287	1.781861	1.787179	1.443268
28	4.898335	4.929884	4.146971	1.878594	2.08124	1.71387

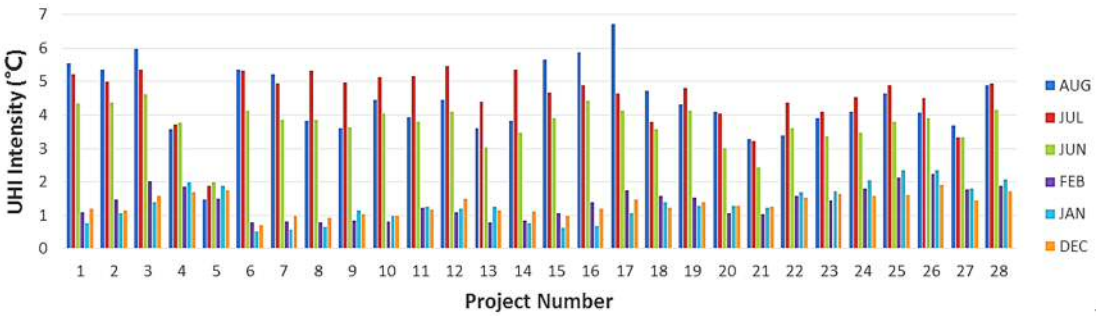

Figure 4. 8: monthly zonal UHII

4.3 Data analysis and discussion

The analysis in this section consists of three parts: the correlation of zonal UHII and UHII at sites, correlation of UHII and each variable of sites, and correlation of UHII and each variable of sites;

4.3.1 Zonal value of UHI VS site value of UHI

The scatter plots (Figure 4.9) shows the zonal mean UHII where each of the 103 projects is located against the UHII at the site in summer months (the left part of Figure 4.9) and in winter months (the right part of Figure 4.9). The correlations are significantly above the 5% level, and the explanatory power R^2 is 0.718 and 0.844, in summer and winter, respectively. The result of the set of correlation indicates that the segment of zonal UHII mapping is homogeneous, and the zonal UHI intensity is illustrated with the background effect on each selected sites at a statistic scale. Higher zonal UHI intensity is recorded with higher average UHI intensity at selected sites within the zone. However, as shown in Figure 4.9, there are still vast variations of UHI intensity between sites in the same zone. This indicates that the background effects form zonal UHI is not decisive enough to accurately determine a site-specific UHI intensity in a city-block scale study. Thus, it is still needed further investigations on the other relevant parameters, including the variation in the design variables of each site, and differences in the surrounding environment and infrastructure.

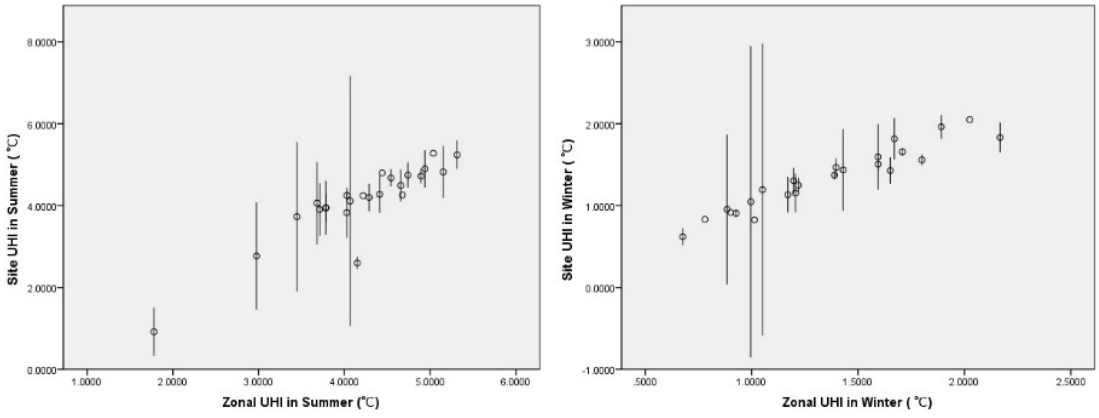

Figure 4. 9: Zonal value of UHI VS site value of UHI in summer (L) and winter (R)

4.3.2 Distance from city centre vs UHI

Generally speaking, the city centre is the most prosperous area of the entire city, with the most frequent human activities, higher UHI intensity is usually recorded in the city centre. However, in many cases, there is no sufficient evidence for to what extent this parameter- Distance away from the city centre- can impact the UHI intensity on a specific site in the city.

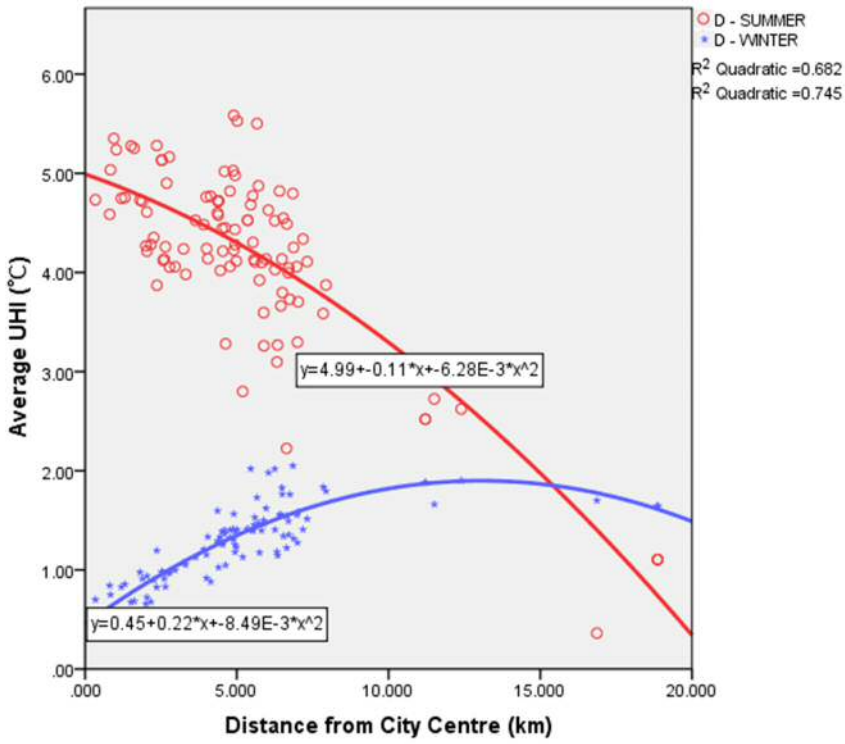

Figure 4. 10: Regression of Distance from the city centre and UHI on 103 sites

As shown in Figure 4.10, which is the scatter plots and quadratic-fit estimation of Distance away from the city centre to the project site against UHII-summer and UHII-winter. It numerically describes the patterns- 'hot' inner Rings in summer and the 'black hole' in the city centre in winter- in Figure 3.3 and Figure 3.4, respectively. Moreover, it shows a significant correlation between the distance from the site to the city centre and UHII both in summer and winter, which have more than 5% significance. The R^2 values are 0.682 in summer (0.512 in June, 0.743 in July, 0.406 in August), and 0.745 in winter (0.426 in December, 0.459 in January, and 0.243 in February), respectively.

Generally speaking, the longer distance away from the site to the city centre, the more

decrease the UHI intensity in summer. For example, a project that is 10km away from the city centre is suffered around 2°C lower UHII comparing to that in the city centre in the summer months. In winter months, however, most of the projects with peak value (around 2°C) of UHII are located at the area around 6 km away from the city centre, and UHII in projects in area 6-20 km to the centre slightly decreases by less than 1°C. However, surprisingly, for the sites within 13 km range from the city centre in winter, the UHII falls to the lowest value (around 0.5°C at the city centre) as the distance to the city centre is getting closer. While in the 1980s, the city centre was the recorded the highest UHI intensity of the entire city (Yang 1988).

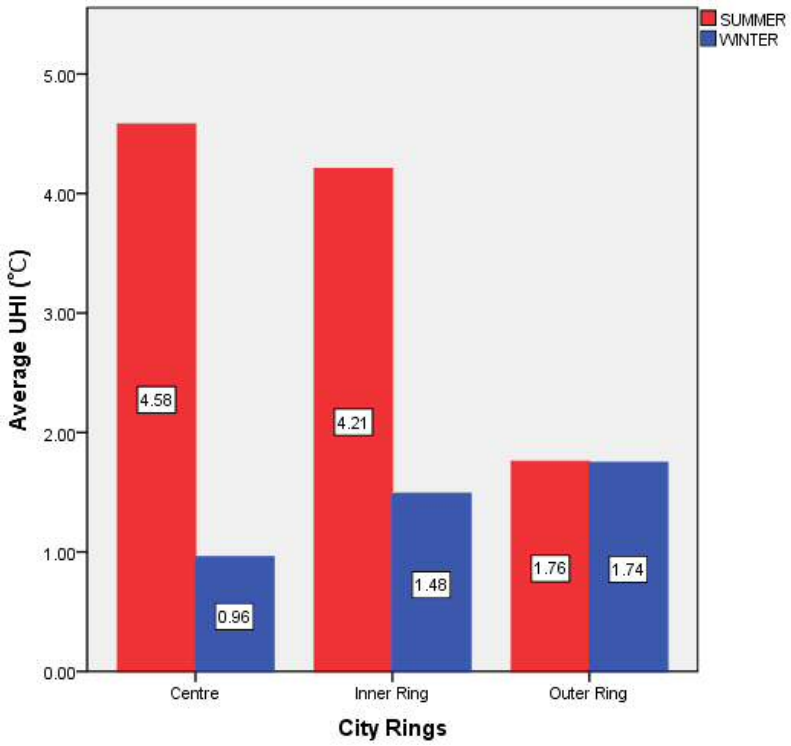

Figure 4. 11: Average UHI intensity of city rings of the road network in Chengdu

Moreover, when the 103 sites are grouped regarding their location on the city rings, average UHI of each city ring can be obtained (Figure 4.11). This intuitively presents the pattern of UHI distribution across the city in summer and winter. Which is that city centre experience the highest UHI in summer and lowest UHI in winter, and UHI-summer and UHI-winter over the out ring area are recorded constantly at the same level.

Dan's (2011) study shows a similar result that the UHI intensity peaks appeared around the boundary of the city centre, where urban density was the highest in Chengdu. On the other hand, for the 'black hole' pattern of the distribution of UHI in winter in the city centre, this is possibly the consequence of urban regenerations since the late 1990s. This movement removed heavy industrial from the city centre thereby leaving plenty of open spaces with greening (Yang 2000)(Q. Chen et al. 2009). However, high-rise buildings including skyscrapers were built along the boundary of the centre and the inner ring, which block the low-angle winter sunlight and do over-shading on these open spaces of the city centre. Moreover, the dense fog on winter days, together with the particles in the atmosphere (Qiao et al. 2013), further reduces the incoming of solar radiation. Consequently, most solar shortwave radiations could not reach this and it would hardly be stored there. The similar phenomenon of the 'black hole', which is also called 'urban cool island', was also recorded in other cities (Qiao et al. 2013). In short, the pattern of spatial distribution of UHI in both summer and winter in Chengdu indicates the necessity for further studies on other variables of the sites, including green spaces coverage, urban density, building layout, and on-site meteorological parameters.

4.3.3 Plot Layout vs UHI

According to the plot plan, the projects are categorised into five groups: Tower, Linear, Semi-closed, Interspersed, and Court. The result of the mean value of UHII in each type of projects is shown in Figure 4.12. In general, sites with less openings in terms of plot layout (Interspersed and Court) are recorded lower UHII in summer and higher UHII in winter, while the 'fully open' projects (tower) suffer the UHI nearly 0.9°C higher in summer and 0.7°C lower in winter than the projects in more closed plot layout (Mixed and Courts). Comparing to other four types of plot layout, the Tower layout suffers highest UHII (4.611°C) in summer and lowest UHII (0.865°C) in winter. On the contrary, the Interspersed Group, which has multi openings on the plan, inner courtyards, and Interspersed buildings, is recorded the lowest UHII in summer and highest UHII in winter. It reveals the most appropriate form of plot layout for city blocks in Chengdu in

terms of plot layout form of building group with minimum the thermal impacts of building group on outdoor spaces. Moreover, the majority of the building groups with the first three plot layout (Tower, Linear, and Semi-closed) is located within areas of 5km away from the city centre, and the Interspersed Group is more frequently planned in outer urban areas. Therefore, the location of the buildings has a significant impact on plot layout, which indicates the possible influence of background effect provided by the surrounding area on on-site UHI.

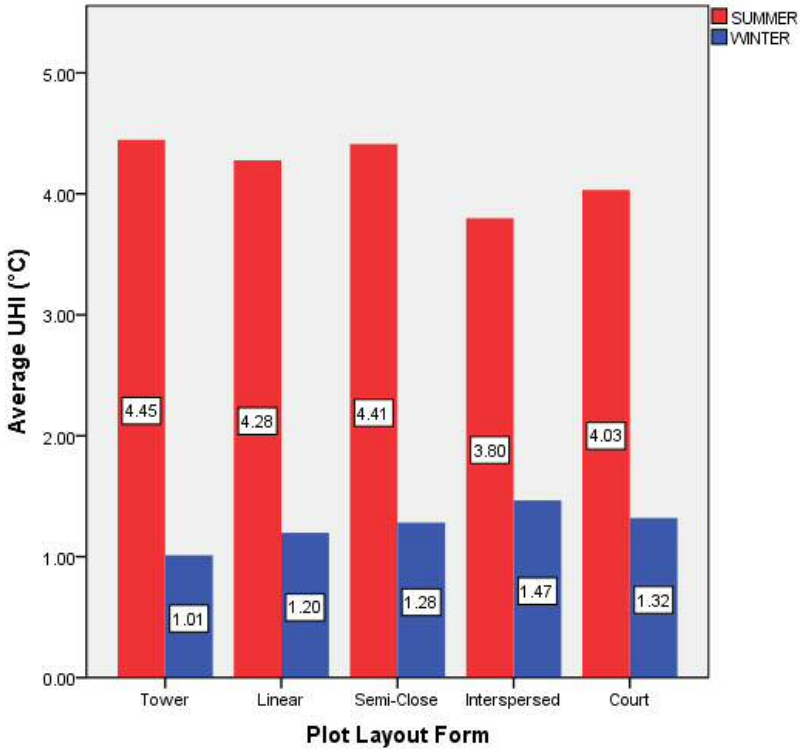

Figure 4. 12: Plot layout VS UHI

The interspersed form is often design more homogeneously in terms of buildings height, buildings within the group provide over-shading to each other, while this form allows as much as possible openings on the layout of the site and let the breeze take away a considerable amount of heat stored within site due to high-angle sunlight in the summertime. In the meanwhile, the inner courtyards within the interspersed sites provide much larger greening, sometimes even with water bodies, which dramatically mitigate the UHI effect on site. In winter time, when wind speed drops to below 1m/s, interspersed group benefits its wide-spread and highly free building settlement to receive and store as much as solar radiations, which leads to the highest UHI intensity

comparing to other layout forms. However, towers massively receive the solar radiations and store them within the buildings without any over-shading in summer, significant solar heat results in the highest UHI intensity in towers. Moreover, the compact layout avoids towers receive more solar radiation comparing to other layout forms with much larger site area.

4.3.4 Function vs UHI

As mentioned in early Chapters, civil buildings are categorised into residential buildings and public buildings. While in the current construction market, some residential are integrated within traditional public buildings, which blurs the boundary between residential buildings and public buildings. Therefore, aiming for a comprehensive perspective, residential buildings and public buildings are being studied together, and all 103 the projects are assorted into eight groups based on their designed functions: *Residential*, *Residential with 5% Commercial*, *Commercial*, *Commercial + Residential*, *Office*, *Office + Residence Hotel + Commercial*, and *HOPSCA*. The most common forms of dwelling in Chengdu are solo residential and residential with limited commercial (small retails below 5% of total building area), while other five types of buildings are more public-oriented, including shopping malls, office, hotels, and the mix of them.

As shown in Figure 4.13, the projects of solo residential are observed the lowest UHII (3.87°C) in summer while their UHII (1.53°C) in winter is the highest among all project types. On the other hand, comparing to residential, average UHII of the public building types is higher in summer and lower in winter. Among which the project type- *Office*- is recorded the highest value (5.35°C) in summer and lowest (0.45°C) in winter. Introducing other types of use will alter the on-site UHII pattern: the integration of 5% portion commercial raises UHII-summer and lowers the UHII-winter in residential building projects; comparing to the solo commercial, the mix of commercial and residential projects tend to have lower values in summer and higher values in winter; the *HOPSCA* and *Office+ Residence Hotel+ Commercial* sites have more average

portion of each function, which decreases the UHII in both summer and winter when comparing to solo office sites. Generally speaking, office project sites suffer highest UHII-summer and lowest UHII-winter among the three types of solo functions (other two are residential and commercial). Moreover, the location of projects has impacts on building types: *HOPSCA* and *Office + Residence Hotel + Commercial* are located within city core area of less than 3km away from the city centre; *residential* is frequently built in regions more than 6km away from urban core; lastly, the majority of *commercial* and *offices* stands within the middle areas between 3km and 6km.

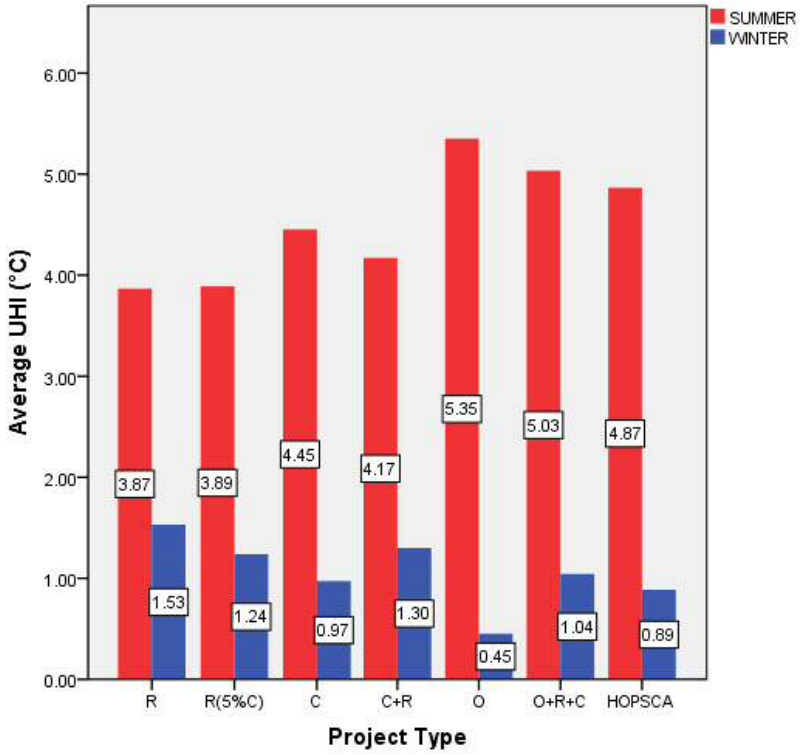

Figure 4. 13: Project Type VS average UHI

In existing studies (Su et al. 2010) (Li 2012) (P. Xu et al. 2013) (He 2015) on building energy consumption in Chengdu, the energy consumption per unit area in commercial buildings with big shopping malls ranks the top of the list of all types of public buildings; then hotels rank the second highest, which is followed by offices; and residential has the lowest parameter of energy consumption. However, the density for sites of commercial and hotel in this research is relatively low, while office sites are significantly denser. Therefore, when the nature of the energy consumption in others' studies is

reflected on the on-site UHI values, the official sites, which follows commercial and hotel in the energy consumption per unit area, have the highest UHI-summer among all types of project function, as shown in Figure 4.13 in this section. Moreover, projects with office function are mainly high-rise towers. The “disadvantageous” layout form enhances the UHI effect on office sites in winter, while reduces the solar heat stored in winter thereby resulting in low UHI-winter. Lastly, the data indicates that the multi-factor effects are impacting the UHI distribution on each site, and further study on more design variables are still needed.

4.3.5 Performances of design variables on site and point basis

The independent design variables involved in this study are, floor area ratio (FAR), building coverage ratio (BCR), green coverage ratio (GCR), building height (HEIGHT), and height-to-floor area ratio (H/A=building height/site area). Whereas the FAR, BCR and GCR are site-specific design variables to describe the density level of projects, Height and HFA are point-specific variables to indicate the vertical height level of the project. The dependent variables are three summer months (August, July and June) and three winter months (February, January and December).

The results of bivariate regression using calculated UHII data of 103 project are shown in Table 4.3. In scattering plots and correlations of FAR, BCR, GCR, HEIGHT and HFA with UHI, FAR, BCR, HEIGH and HFA show a positive relationship with UHI-summer and negative relationship with UHI-winter; while for GCR, it is negatively related to UHI in summer months and positively related to UHII in winter months. In the linear correlations, the independent variables appear to be significantly (more than 5%) related to UHI intensity in most months.

Table 4. 3: The sign of the R^2 values for correlations between design variables and UHI

(±)	FAR	BCR	GCR	HEIGHT	H/A
Summer	(+)	(+)	(−)	(+)	(+)
Winter	(−)	(−)	(+)	(−)	(−)

i) Floor Area Ratio

As shown in scatter plots and correlation figure (Figure 4.14), individual site data- FAR- is positively related to summer UHII, while negatively related to winter UHII. FAR is shown with significant linear correlation with both summer UHII and winter UHII, with more than 10% R^2 values in summer (R^2=0.193) and winter months (R^2=0.165), while all of the monthly R^2 values (0.139 in June, 0.123 in July, 0.197 in August, 0.161 in January, 0.098 in February, and 0.129 in December) meet 5% of significance level. As project with larger FAR tend to suffer higher UHII in summer months and benefit lower UHII in winter, every one decease in value of FAR at site will reduce 0.20°C in summer UHII, and will benefit 0.07°C higher UHII in winter months, thereby reducing both cooling demand in summer and the heating demand in winter . According to Figure 4.14, in general, the distribution of FAR values is relatively uneven: more than two-thirds of the points fall within the range of 1- 8, which is restricted by the local statues for urban planning in the urban area of Chengdu.

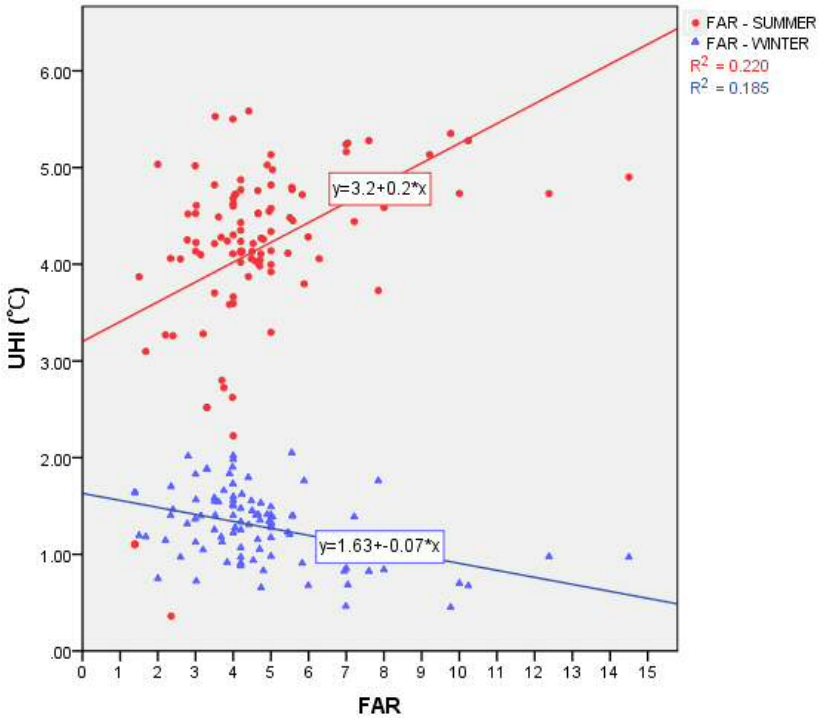

Figure 4. 14: Scatter plots and correlations of FAR with UHII

ii) Building Coverage Ratio

Shown as Figure 4.15, BCR of an individual site is revealed with the relatively weak relationship in correlations with UHI in both summer and winter compared to FAR. Moreover, there are considerable variations in UHI at individual sites with certain BCR level. In order to obtain the general tendency of the independent variable, rather than the individual site data, average values of UHI in summer and winter are used in another correlation, which is shown in Figure 4.16.

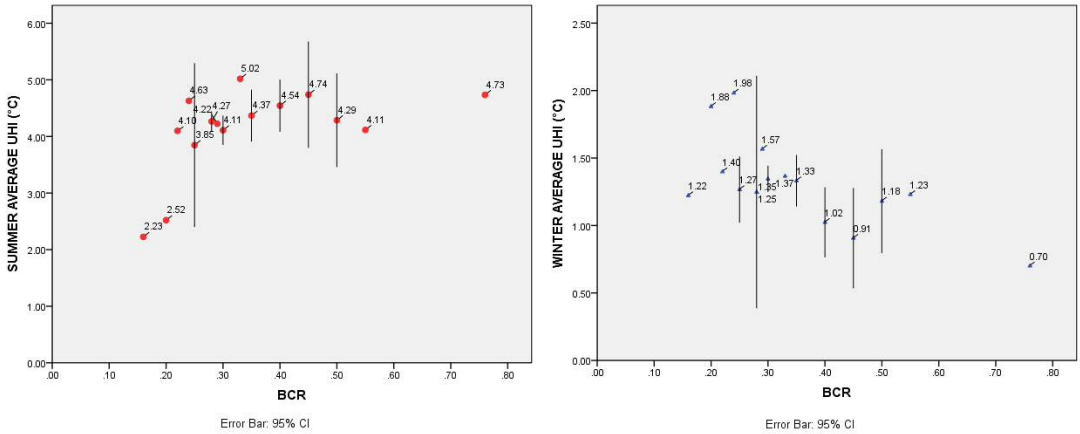

Figure 4. 15: Scatter plots and correlations of BCR with UHII in summer (left) and winter (right)

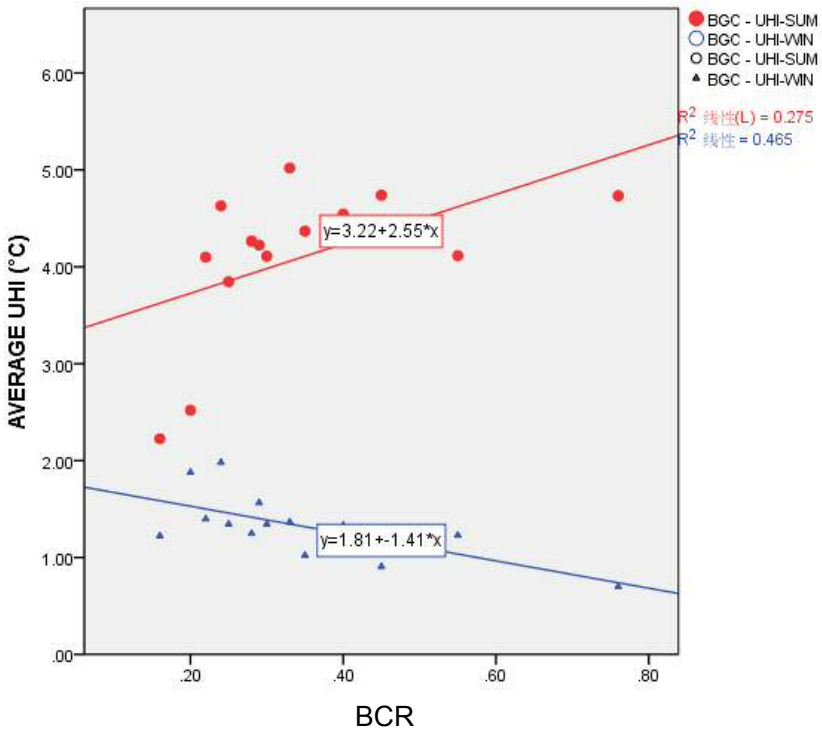

Figure 4. 16: Scatter plots and correlations of BCR with average UHI

The linear correlations with BCR with average UHI-summer and average UHI-winter are more than 5% of significance, and R^2 value is 0.275 for summer, and 0.465 for winter, respectively. In general, the denser plot in plan rises UHI in summer months and lower UHI in winter months at the project site. Specifically, it is estimated that every 0.1 (10%) increase in the value of BCR will increase 0.255°C in UHI-summer. While in contrast, every 0.1 decreases in the value of BCR will increase 0.141°C in UHI-winter. The distribution of BCR values is also restricted by local planning policies with certain levels, most projects were designed with the BCR 30%, 35% or 40%.

iii) Greening Coverage Ratio

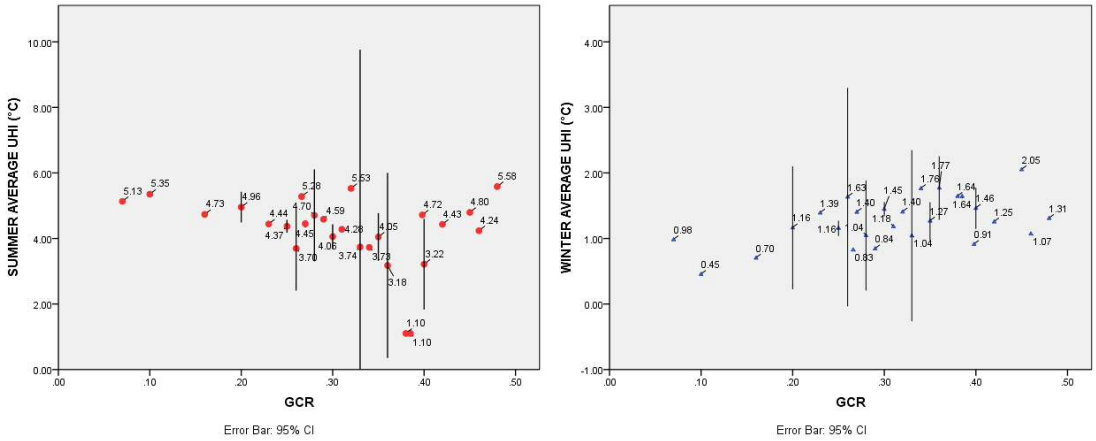

Figure 4. 17: Scatter plots and correlations of GCR with UHI in summer (left) and winter (right)

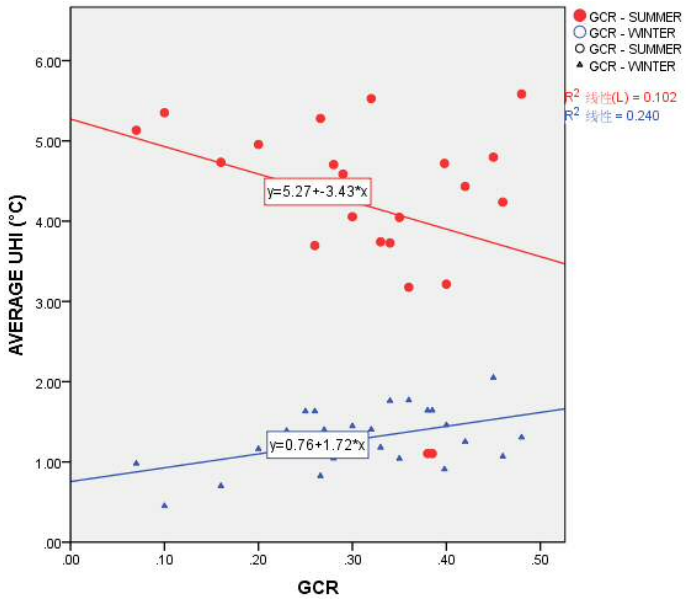

Figure 4. 18: Scatter plots and correlations of GCR with average UHI

Similar to correlations of BCR, there are significant variations in UHI-summer and UHI-winter between individual sites with some specific same values of GCR (Figure 4.17. The uneven distribution (25% and 30% for most projects restricted by local planning policies) may negatively influence the results for individual site data. Therefore, the average data for a site with the same GCR is used.

According to Figure 4.18, all R^2 values of GCR in summer and winter meet 5% significant level, while the R^2 value for correlation in summer (0.102) is lower than that in winter (0.240). Generally speaking, increasing GCR is an effective way to mitigate UHII in summer months and acquire warmer outdoor temperature: every 0.1 increase in the value of BCR will reduce 0.343°C in UHI-summer and increase 0.172 UHI-winter in Chengdu city.

iv) Building Height and Height to Site Area

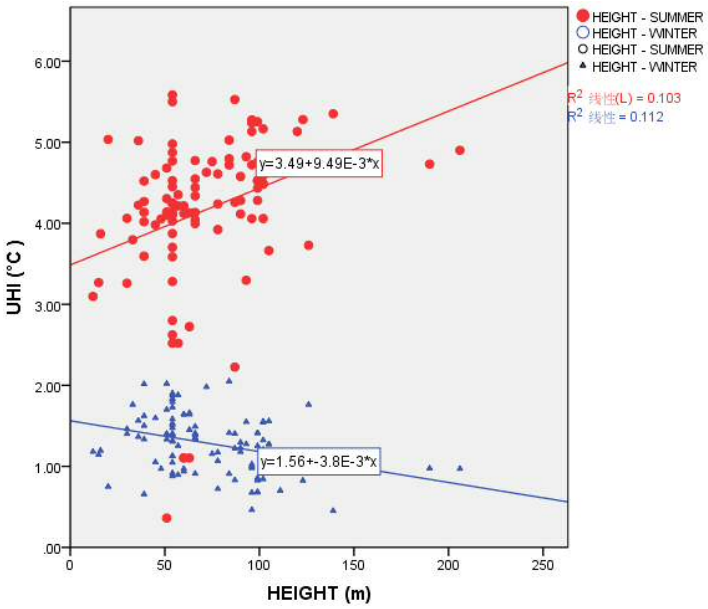

Figure 4. 19: Correlation of building height with UHI

In this study, two relevant variables of building height are analysed. As shown in Figure 4.19 and Figure 4.20, all the height parameters are shown with a positive relationship to UHI-summer and negative relationship to UHI-winter. Comparing to HEIGHT, H/A is shown more significant correlation with UHII in both summer and winter. In scatter plots and correlation of UHII-summer and Height, R^2 value reaches 0.103 in summer (0.067

in June, and 0.051 in July, 0.121 in August), and 0.112 in winter. The R^2 value in all months is observed at a more than 5% significant level. On the other hand, H/A is shown with the most significant correlation with winter-UHII (with R^2 value 0.171 in January, 0.270 in February and 0.182 in December). As linear-fit estimated in Figure 4.19, every increase in building height by 50 meters in average building height of project will result in 0.475°C higher UHII in summer and 0.19°C lower UHII in winter in Chengdu; While if only taking H/A in consideration (Figure 4.20), every 10 increase in will increase will suffer 0.5°C higher UHII in summer and 0.3°C lower UHII.

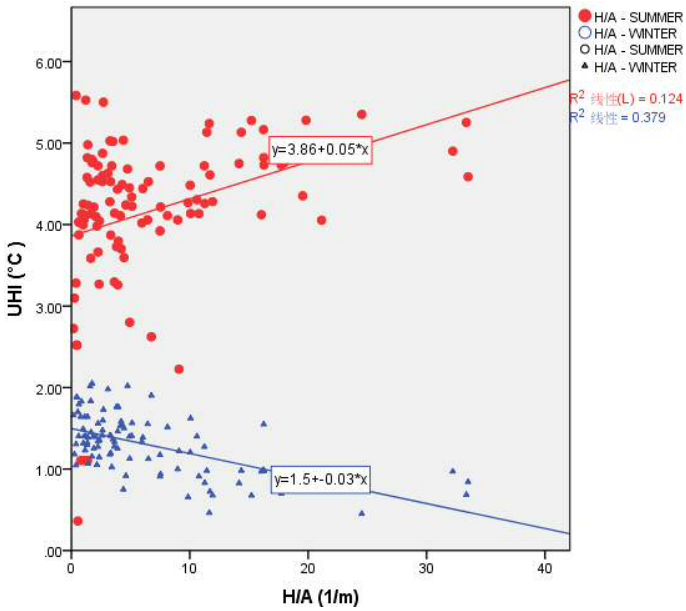

Figure 4. 20: Correlation of H/A with UHI

v) Summary

All the correlations of parameters with both UHI-summer and UHI-winter are higher than 5% of the significant level. Besides all the variables, the background effect-zonal UHII is shown to be one of the significant factors (not decisive enough) of UHII variation at site-level.

On the other hand, the parameter-density away from city centre shows a strong correlation with UHII in terms of the quadratic curve. However, none of every single variable can independently determine the on-site UHII, which is due to the multi-factor effect that all variables are contributing to the UHI formation at the same time in the

dense urban areas (Feng et al., 2011). Increasing GCR and openness in plot layout (less enclosure in plot layout on site) are effective to mitigate UHII in summer months and benefit higher winter UHII. In the correlation of the other variables, however, increasing the value of variables rises UHII in summer and reduces the UHII in winter, which is negative to the optimisation of building energy performance. Residential is shown with lower UHII in summer, while lowest UHII in winter in observed in public projects, especially in office projects. Furthermore, increasing the portion of office function in a project tends to raise UHI in summer and lower UHI in winter. Lastly, H/A is shown with higher significance in correlations with UHII in summer and winter months, which indicates H/A is a more practical variable to describe the building height in a UHI analysis.

Moreover, as indicated in Table 4.4, all R^2 value of the correlation reach the 5% significance level, among which the lowest 0.102 appears in the case of GCR with UHI-summer. Moreover, the table indicates the significance of each design variable. Considering the average UHI values are used in the correlation with BCR and GCR, the most decisive variable for UHI in summer and winter are FAR and H/A, respectively.

Table 4. 4: R^2 values (linear) of correlation between the design variables and UHI

R^2 Value	FAR	BCR	GCR	HEIGHT	H/A
Summer	0.220	0.275	0.102	0.103	0.124
Winter	0.185	0.465	0.240	0.112	0.379

4.3.6 Multiple regression analysis

All the independent variables analysed in multiple regression analysis are listed in Table 4.5 and Table 4.6, for summer months and winter months, respectively. The two categorical variables, including site-specific variable (Distance) and design-specific variables, are forced into all the models in order to check the background effect. For plot layout values, Towers, linear, semi-closed, interspersed, and the court is assigned with 1, 2, 3, 4, and 5, respectively. The objective is to build more parsimonious models that exclude irrelevant independent variables, and to reduce the impacts from inter-

correlation among independent variables on the partial regression coefficients.

Table 4. 5: Regression results of the 5 summer UHI models entering Distance, Floor Area Ratio, Building Coverage Ratio, Green Coverage Ratio, Height-to-Area Ratio and Plot Layout

summer

Variables	Model-1	Model-2	Model-3	Model-4	Model-5
	Coefficients	Coefficients	Coefficients	Coefficients	Coefficients
D	-0.242308867	-0.230186353	-0.23137822	-0.230094601	-0.230808874
FAR	-	0.054927649	0.059601447	0.059050827	0.063547716
BCR	0.134503611	-	-0.216292248	-0.274405454	-0.26350719
GCR	-0.456942153	-0.223512643	-	-0.298284486	-0.298145006
H/A	-0.021670633	-0.005737317	-0.004414853	-	-0.002930771
PL	0.154049641	0.166992498	0.164172228	0.169731081	0.162941019
Intercept	5.169765767	4.766576162	4.76401303	4.844278042	4.86071038
R2	0.702373172	0.712759021	0.712850271	0.71318624	0.71338151
Adjusted R2	0.687031582	0.697952785	0.698048739	0.698402026	0.695467854
F static	45.78229589	48.13910967	48.16057222	48.23971162	39.82333504
Number of cases	103	103	103	103	103

Table 4. 6: Regression results of the 5 winter UHI models entering Distance, Floor Area Ratio, Building Coverage Ratio, Green Coverage Ratio, Height-to-Area Ratio and Plot Layout

winter

Variables	Model-1	Model-2	Model-3	Model-4	Model-5
	Coefficients	Coefficients	Coefficients	Coefficients	Coefficients
D	0.050918044	0.048381364	0.048267655	0.053061107	0.049190328
FAR	-	-0.020589987	-0.015671116	-0.009523768	0.014845715
BCR	-0.50648613	-	-0.427313257	-0.446647291	-0.387587553
GCR	0.183081205	0.253570952	-	0.146603556	0.147359427
H/A	-0.048844187	-0.055122755	-0.053336215	-	-0.015882399
PL	0.046981024	0.042736241	0.04507824	0.069852868	0.033056253
Intercept	1.076842374	1.019034507	1.202722443	0.974735037	1.063784959
R2	0.567412187	0.565634416	0.571773232	0.550407963	0.589076534
Adjusted R2	0.545113846	0.543244437	0.549699687	0.527233116	0.563393818
F static	25.4463859	25.26283866	25.9030998	23.75023045	22.93669097
Number of cases	103	103	103	103	103

According to the result of multiple regression analysis, a reliable UHI calculation equation is produced:

$$UHIsummer = 4.860 - 0.231D + 0.059FAR - 0.271BCR - 0.299\,GCR - 0.005H/A + 0.168PL$$

R^2 = 0.713 (summer model-5);

$$UHIwinter = 1.064 + 0.049D + 0.015FAR - 0.388BCR + 0.147\,GCR - 0.016H/A + 0.033PL$$

R^2 = 0.589 (winter model-5).

i) UHI-summer

As shown in Table 4.5, the explanatory powers (R^2) of regression for the yielded models range from 0.7023 to 0.7132. Models of with FAR entered have higher R^2 value than the model without this variable. UHI-summer differences induced by the background effect as indicated by the coefficients of Distance is in general agreement with the descriptive statistics. The background effect has dominated the summer UHI, as the model including only the site-specific variable (Distance) explains more than 90% of the UHI-day variation (with an R^2 value of 0.659). Moreover, FAR has the second largest weight in terms of influence on UHI intensity among all the variables. In the summertime, when the solar angle is higher than that in other seasons, the obstruction effect of direct solar gain due to building height is not significant. And the compact urban form with higher level of anthropogenic heat emitted and with higher potential of heat storage due to buildings and materials tends to suffer higher UHI intensity.

ii) UHI-winter

As shown in Table 4.6, the generated models have R^2 values ranging from 0.550 to 0.572. Models with H/A entered have higher R^2 value than the model without H/A entered. The background effect is under a dominant impact on the winter UHI. The site-specific variable (Distance) can explain more than 80% of UHI-winter variations (R^2=0.468), while adding other design variables into the models can only increase R^2 by 0.083 to 0.121. Comparing to other variables of building density and green coverage, H/A shows the most significant influence on UHI intensity, which corroborates the discussion in early chapters of this study- obstruction of lower solar-angle sunshine due to building structure results in lower level of solar gain and storage. Therefore, UHI in the city centre surrounded by tall buildings is less significant.

4.4 Summary

The following research object has been achieved in this chapter:

> *To summarise the microclimate features of the city-block-scale building groups in China, to explore the influence of design features of the urban configuration of the real estate projects on microclimate condition;*

The heat island effect and its characteristics in a humid subtropical monsoon large city of South-western China have been investigated by using remote sensing technology and a surface temperature inversion method of the the Window-Splitting Algorithm. The urban area in Chengdu has been recorded with the urban microclimate change due to dense urban settlement and lack of greening. A more than 6°C temperature difference between the urban area and rural area were recorded. The observation results are very close to the data from existing studies (Yang 1988) (Dan et al. 2011) (Zhang & Zhou 2013). Moreover, in this chapter, it is proved that design variables of city-block projects, including building density, building plot layout, green coverage ratio, and water coverage, have impacts on the microclimate. Moreover, areas, which are shaded by high-rise buildings with relative high green coverage ratio and water coverage in a short distance, have a lower atmospheric temperature in Chengdu.

4.4.1 Background effect by zonal UHI effects

By comparing with the on-site UHI values, the zonal UHI intensity is shown with background effect on each selected site at a statistic scale. The zonal UHI intensity for each zone is positively related to the average value of all sites within the zone area. However, due to the massive variation of UHI intensity among sites within the same zone, zonal UHI is proved to be not enough to determine a site-specific UHI intensity at a city-block scale.

4.4.2 Distribution patterns of UHI in Chengdu

According to these six monthly intensity maps, several intensity centres of UHI-summer can be identified, which were located around the inner rings of this urban area.

In specific, north-east corner of the Second Ring, south-west corner of the Third Ring is UHI intensity centre in summer. In winter month, lower UHI intensity was recorded in the centre of the First Ring.

Study results in this chapter show a significant correlation between the distance (D) from the site to the city centre and UHI intensity in summer and winter. The longer distance away from the site to the city centre, the more decrease in the UHI intensity in summer. However, in winter, UHI intensity peaks at the area around 13km away from the city centre. Moreover, within the 13km range, the UHI intensity falls when the site is approaching the city centre, which proves 'black hole' in winter UHI map of Chengdu. This phenomenon is called the urban cool island, which can be results of the over-shading effect of the dense and tall buildings and winter foggy weather.

The highest measured site-mean UHI reached 6.94°C in summer (on site No.63) and 2.26°C in winter (on site No.34). Note that the strongest UHI in Chengdu occurs in August, due to humid, calm and clear weather conditions. It can be concluded that the site 63 presented the highest monthly mean UHI intensity across the five years. This is due to the area's low height to floor area ratio (H/A) (2nd lowest) and high green area coverage (GCR) (2nd highest) (Table 3.10), which means the least solar obstruction by building construction and most solar heat transferred into project site. On site 34, the highest winter UHI intensity was recorded, where the Green Coverage Ratio is third highest among the 103 sites.

4.4.3 Design specific factors: Floor area ratio (FAR), Building coverage ratio (BCR), Green coverage ratio (GCR) and Height to floor area ratio (H/A)

Floor area ratio is shown with significant relation to both summer months and winter months. According to the correlations, a reduction of one in FAR on site will have 0.20°C lower UHI intensity in summer, and 0.07°C higher winter-UHI intensity.

Due to the enormous variation in UHI intensity among the sites with the same building coverage ratio, an average value is used for the site with the same BCR. The results

show that denser plot in plan tends to have the higher summer-UHI intensity and lower values in winter. In specific, every 10% increase in BCR will increase UHI intensity by 0.26°C in summer, and have a reduction of 0.14°C in winter UHI intensity.

After being derived with the average values for the sites with the same green coverage ratio, GCR shows a strong relationship with UHI intensity. Every 10% increase in BCR will lead to a reduction of 0.34°C in summer-UHI intensity and an increase of 0.17°C in UHI intensity in winter.

Lastly, both building height and height to area ratio show a strong relationship with UHI in two seasons. Increasing the value of two variables will both have higher summer-UHI and lower winter-UHI. On the local-macro scale, increasing Height and H/A values of the ground or building facade in a high-rise built environment can exacerbate thermal discomfort due to the high amount of reflected radiation, and this reflected solar heat may cause indoor glare and increase cooling energy use. For a given density, a careful mix of buildings of various heights helps to improve local ventilation as compared to a homogeneous height setting (Ng et al. 2005).

4.4.4 Design-specific variable: Plot layout (PL)

Four types of building layouts are covered in this study (Table 3.9 and Figure 3.17). Among them, the interspersed type is the most widely accepted one which has lowest average UHI intensity (3.80°C) comparing to tower type with the highest average UHI intensity (4.45°C). This is due to denser building construction obstruct more direct solar radiation in humid weather, therefore the over-shading effect between each other reducing the direct solar gain into the project site. In winter, the situation is interspersed type projects were recorded highest UHI intensity (1.47°C), the tower type sites have lowest average UHI intensity (1.01°C) comparing to the highest UHI intensity in interspersed type average value (1.47°C). Due to cloudy weather in winter in Chengdu City, the direct solar heat gain is low in any sites, so the anthropogenic heat dominates the UHI effect. Therefore, obstruction effect by building construction is significant preventing the anthropogenic heat escaping into the external environment.

4.4.5 Design-specific variable: Project type (Type)

Based on the groups of different building functions, average UHI intensity are derived. Sites with the only residential building have the lowest UHI intensity in summer and highest UHI in winter. On the other hand, office-only sites were recorded with the highest value in summer and lowest UHI intensity in winter. In this study, the office buildings are mainly towers, which enhance the patterns of UHI in summer and winter.

4.4.6 Summary of the Top-Down process

The derived MODIS data of land surface temperature has been widely implemented investigating the UHI effect (Tran et al. 2006)(Pongracz et al. 2006)(Cheval & Dumitrescu 2009)(Tomlinson et al. 2012)(Yao et al. 2017). The traditional methods of measuring the near-surface temperature include using sets of weather stations in both urban and rural land, and transects of air temperature. In comparison to those, the surface temperature is easier to observed through MODIS in the studies of UHI (Tomlinson et al. 2012), which can provide substantial images in a relatively short time. Moreover, in this case, due to the high resolutions of the images, the on-site surface temperature at an even city-block scale and building scale data becomes available. Therefore, the derived LST images not only reflects the general pattern of UHI over the entire city at a macro scale, but also precisely describes the UHI values of blocks, streets, and buildings, at a micro scale. *This Top-Down process carried out in this study is a practical approach to investigate the long-term urban temperature at different scales.* However, the access that high-resolution satellite imagines is usually under very restricted regulations for state secretary reasons, collaborates and consults for cross-discipline and cross-department are highly recommended.

Chapter Five

MICROCLIMATE AND SIMULATIONS

5.1 Introduction

Main goal of this chapter is to answer the third research question:

'What is the diurnal variation of air temperature and other microclimate variables on a summer day and a winter day, accordingly?'

In order to answer this research question, this chapter focuses on analysing and predicting hourly microclimate performance at city-block scale. Firstly, the hourly data, including air temperature and other microclimate variables, obtained through simulation tools is presented. Secondly, this chapter investigates the relationship between the simulated results and design variables. Moreover, it compares the simulated air temperatures with the calculated temperatures which are derived from data obtained in Chapter Five, thereby validating the accuracy of the simulations.

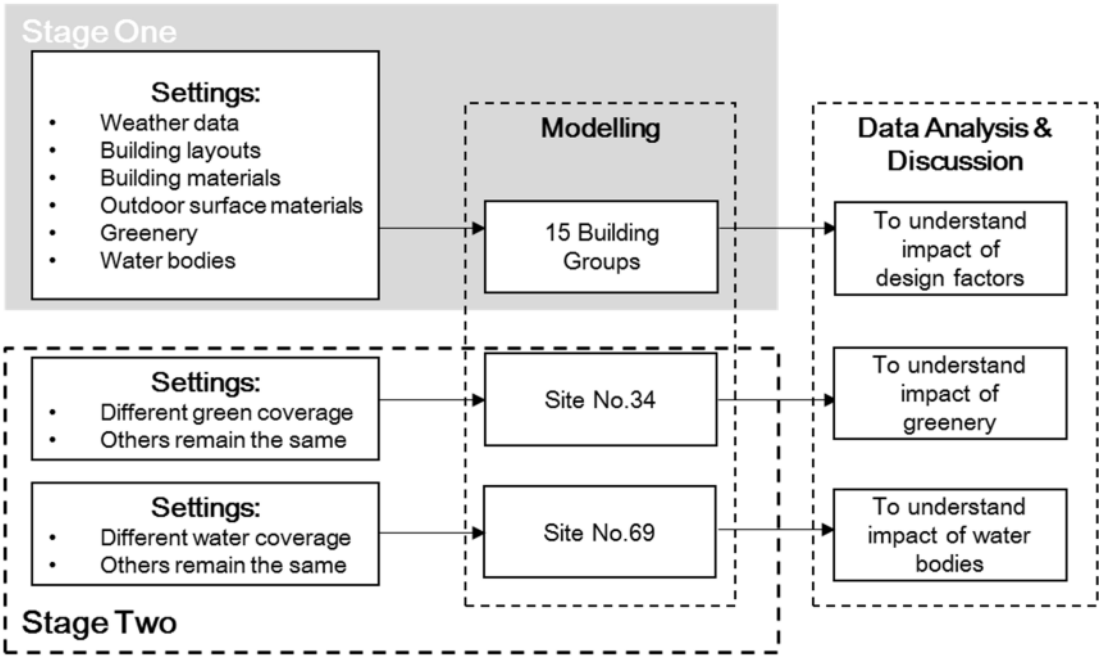

Figure 5. 1: Framework of two-stage microclimate modelling in phase three

5.2 Simulation data analysis for selected 15 project sites

5.2.1 Introduction

According to Chapter 3 (Section 3.7.5), five project sites- Tower, Linear, Semi-closed, Interspersed, and Court- are grouped. The settings of buildings and outdoor environment on the project sites are reconstructed according to the satellite maps (Figure 3.18), and information gathered from the survey (Table 3.9). By the embedded 3D View function in ENVI-Met, the completed reconstruction of target projects is illustrated in the overview (Figure 5.2).

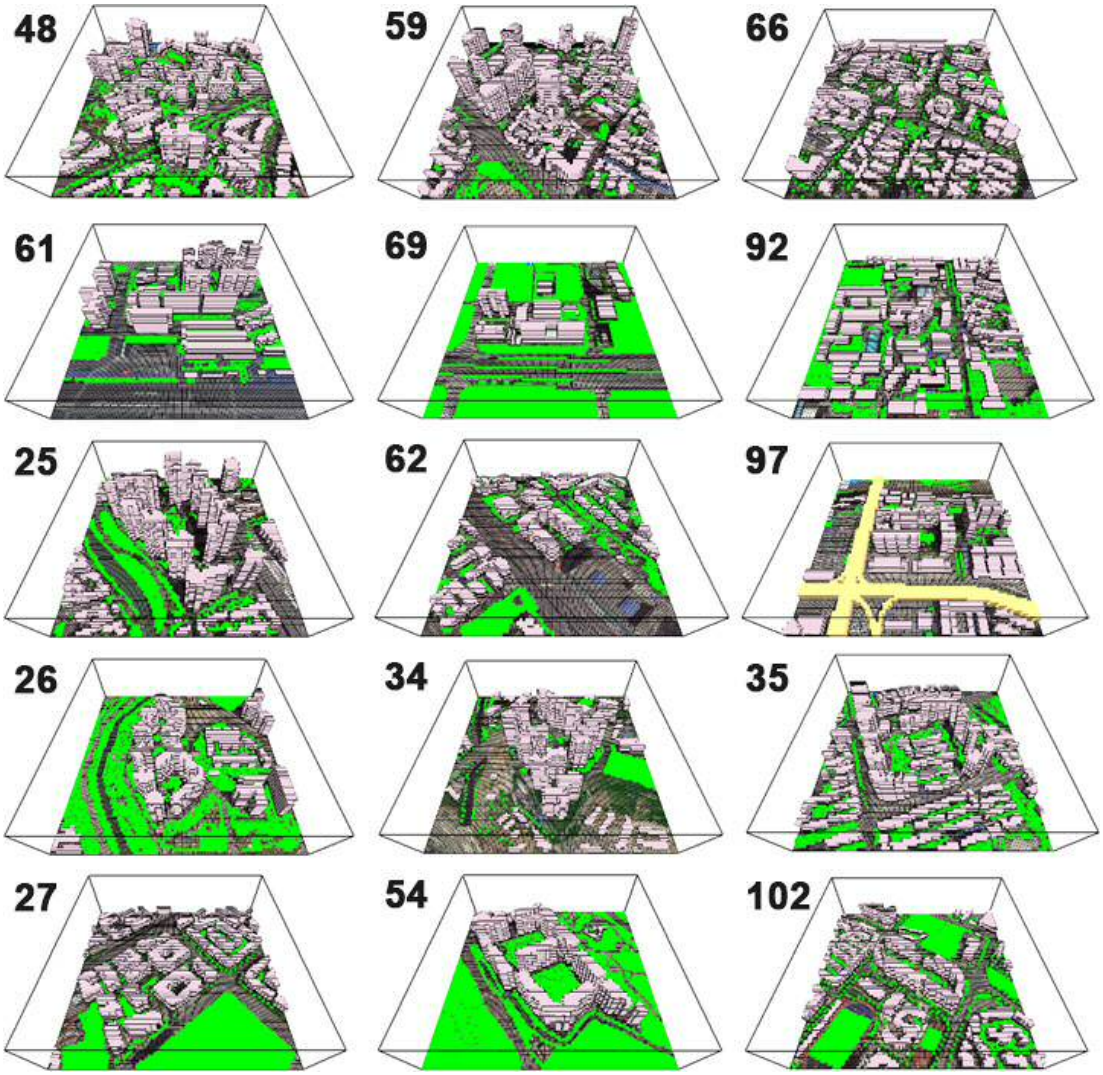

Figure 5. 2: 3D view of 15 target projects (with original project number) in ENVI-Met

The most significant parameters of microclimate- atmospheric temperature, relative humidity and wind velocity- were calculated and are shown in the following sections

for the five groups of projects sites which were previously described. The results were obtained from a 24-hour simulation process for each of the selected fifteen sites. In order to avoid affecting by errors due to boundary conditions caused by model, extra five row of grids have been added into the core grids, and the sites are located in the centre of each model.

Based on the site groups, digital map of sites will be shown at first, which is followed by the 2D area input space file of ENVI-Met. Then, the results of the simulations will be presented according to the meteorological parameters (atmospheric temperature, relative humidity, and wind speed), respectively. Detailed data descriptions and the relevant discussion are therefore carried out afterword.

5.2.2 Microclimate for five groups in the summertime

In order to have more accurate microclimate conditions around the selected 15 target sites, several points closed to main buildings (marked with circles) were selected for each site according to the plot layout. In this section, one site was chosen from each group as the example of each group for data analysis.

i) Group one- Tower

For the simulation at 15:00 on 21st August 2005 on-site No.59, the atmospheric temperature is shown in Figure 5.4. It can be seen from Figure 5.3 that the site is surrounding with massive buildings, especially with tall building groups on the west of the site. Due to the solar angle at 15:00, the southern area has higher atmospheric temperature compared to the northern area in the entire simulation model. Moreover, there is a street crossing by the west side of site No.59, which impacts the temperature on site. The west point has an atmospheric temperature of 33.67°C, which is higher than the other three points of site No.59. Since the west point is in an open space- a wide street with massive solar accessibility, there is more solar exposure than other points, resulting in higher air temperature. On the other hand, the north point is shaded by the skyscraper, and less solar gain results in relatively lower air temperature. Therefore, both building height and plot layout have impacts on the air temperature in

the surrounding open spaces.

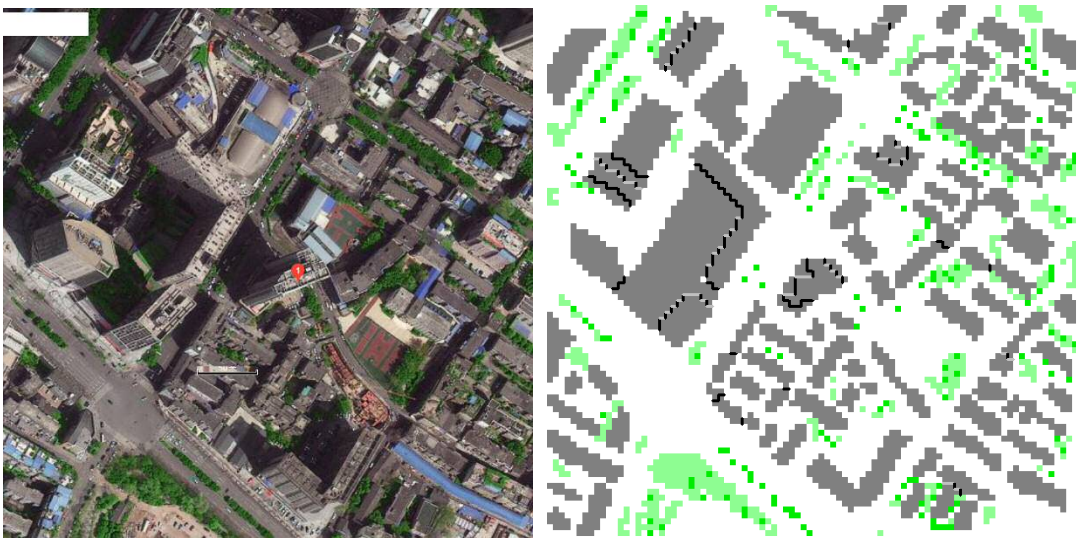

Figure 5. 3: Satellite map (left) and ENVI-Met model plan (right) on Site No.59

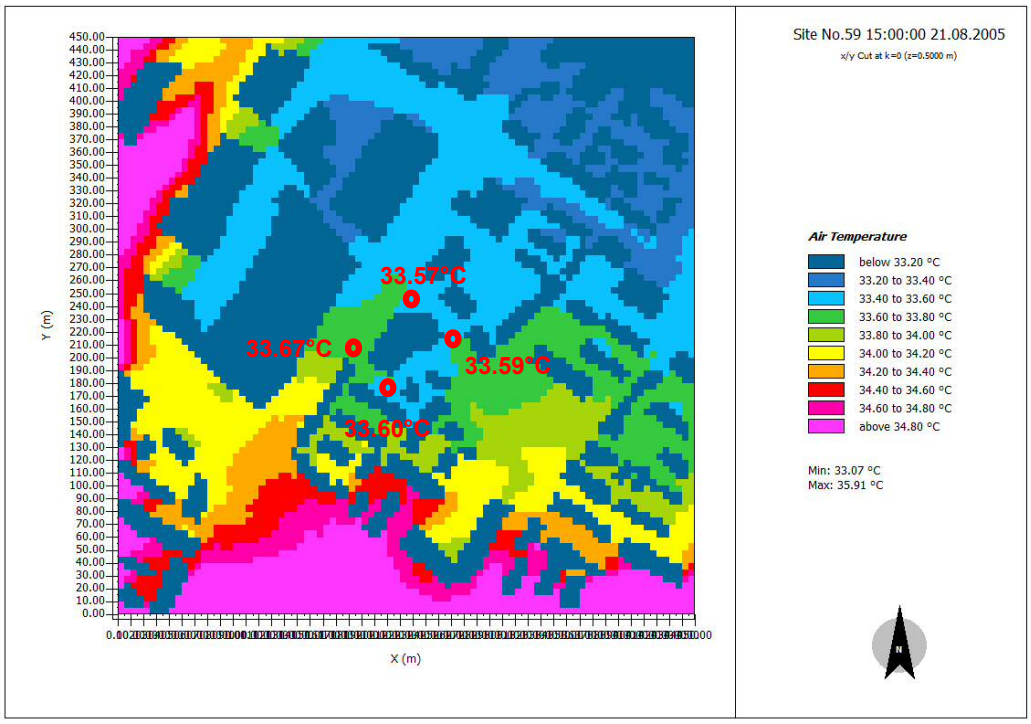

Figure 5. 4: Simulation result of atmospheric temperature on site No.59 at 15:00

According to the results of relative humidity (Figure 5.5), there is a trend that relative humidity is compensating the temperature. In specific, the hotter areas have lower relative humidity, and the colder areas have higher relative humidity. On the other hand, areas with more vegetation coverage (Figure 5.3) have more than a 2% increase in relative humidity, which is most obvious in the southern area with large open spaces. In a comparison of the four points, the south point is in a narrow area with the highest

relative humidity; even it has higher air temperature than the east point and the north point. Plot layout has a more significant influence on the relative humidity. It is easier to gather humidity in areas with a more compact and narrower layout.

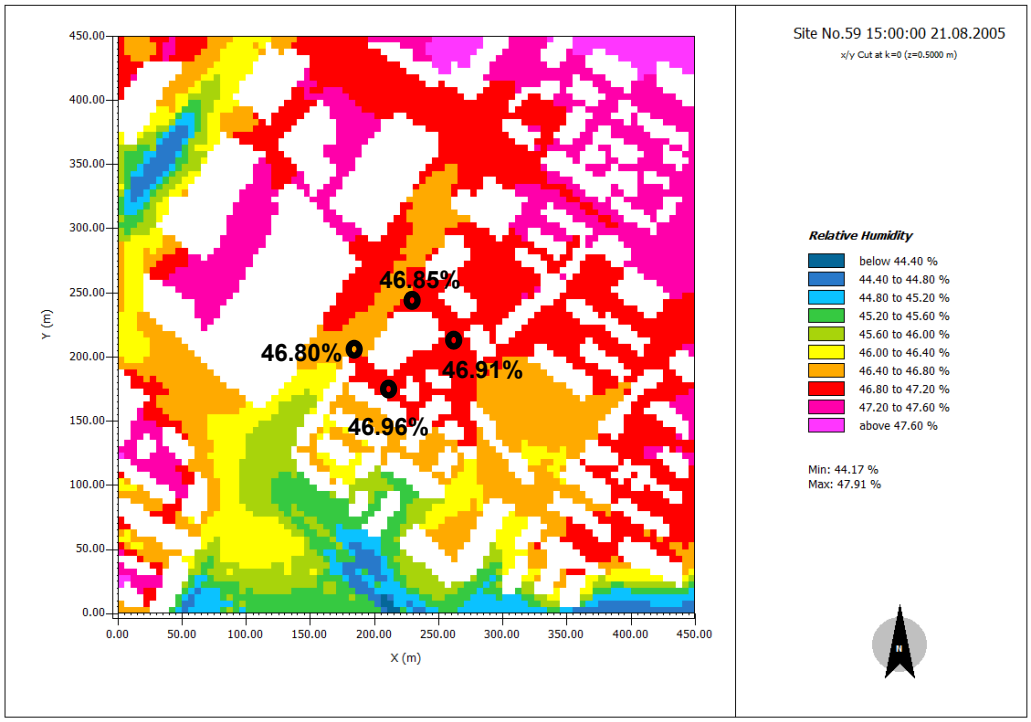

Figure 5. 5: Simulation result of relative humidity on site No.59 at 15:00

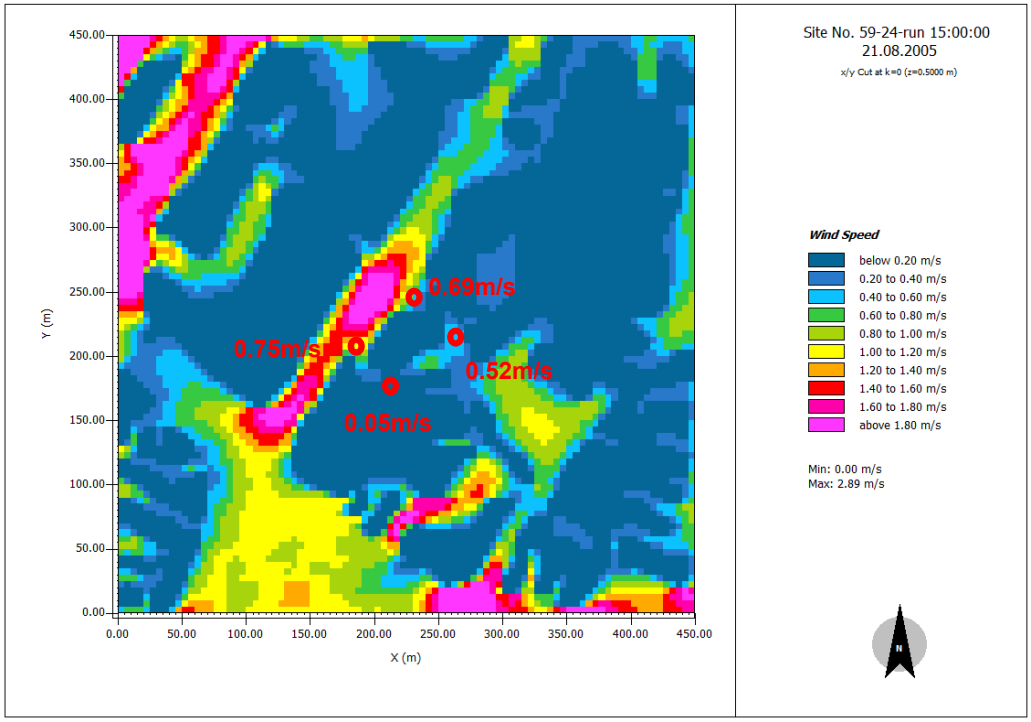

Figure 5. 6: Simulation result of wind speed on site No.59 at 15:00

The wind speed of site No.59 at 15:00 on 21st August 2005 is shown in Figure 5.6, in which it can be seen that the wind distribution is generally impacted by the urban settlement. In open spaces, the wind speed is as high as more than 1.8m/s, especially in big streets where a wind tunnel is naturally formed. On the other hand, the narrow spaces with plenty of obstacle to wind are breezeless. Therefore the south point has the calmest wind condition, while the other three points in wider streets is recorded above 0.5m/s wind. However, in comparison to the temperature distributions (Figure 5.4), the strongest wind with more than 1.8m/s cannot cool down enough the area. Comparing to the surroundings, it is still hot but with the relatively strong wind in some areas in this case.

ii) Group two- Linear

Figure 5. 7: Satellite map (left) (picture after 2010) and ENVI-Met model plan (right) on Site No.61

Site No.61 is a high-rise building group with a linear plot layout. Back in 2005, there were high-rise surroundings on its north-east side and west side, the building on the south side was not built yet (Figure 5.7). As shown in Figure 5.8, the atmospheric temperature at 15:00 varies at different points of site No.61. In the large southern open area, where there are wide streets and railways, the temperature is up to 36.03°C. The west and south points of site No.61, which are located in the wide street and open space, have higher than the atmospheric temperature the other points. Between the

two points within site, the point with higher green coverage is recorded lower atmospheric temperature than the other one with less vegetation, which is 33.79°C and °C and 34.04°C, respectively. The point on the north side with over-shading effect by the buildings on the site has an atmospheric temperature of 33.64°, which is lower than that at the point on the east side of the site. And the latter is open to sunlight.

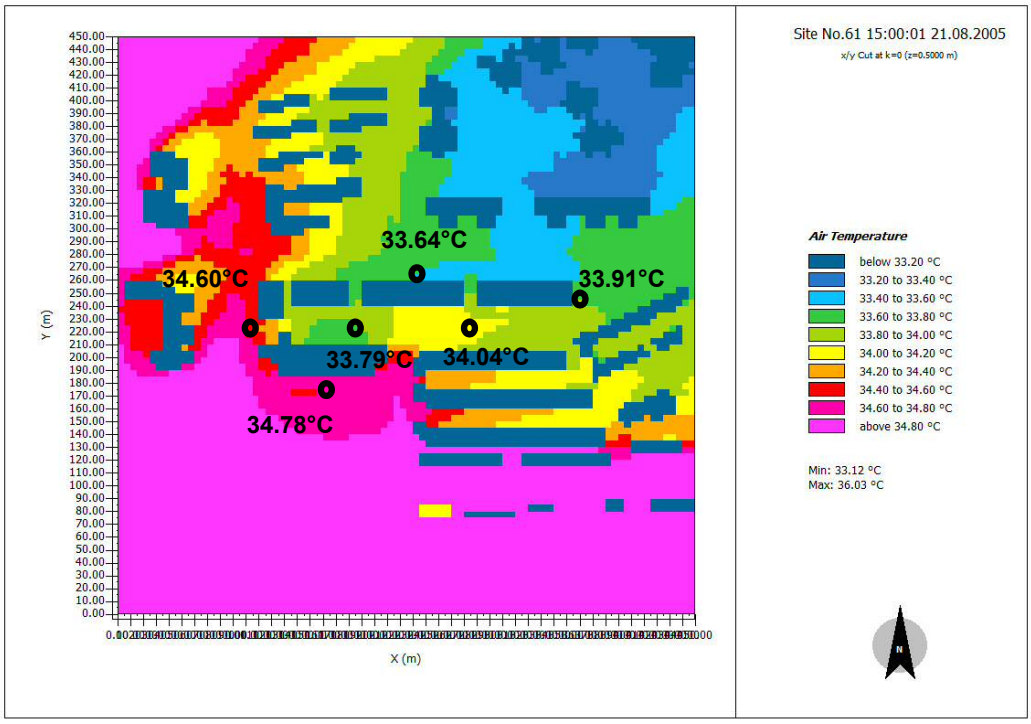

Figure 5. 8: Simulation result of atmospheric temperature on site No.61 at 15:00

On the other hand, the relative humidity (Figure 5.9) has compensating trend of atmospheric temperature on the site, as well. The north point, which is shaded by site buildings with the lowest atmospheric temperature, is recorded with the highest relative humidity among all selected points. Moreover, the hotter points on the west and south side are drier. In comparison to the two centre points, the greener one has 0.6% higher humidity than another point.

Figure 5.10 shows the wind speed map of site No.59. In general, the areas with open spaces have higher air movement than obstacle areas. Three points (two centre points and the north points) are sheltered by high-rise buildings have less than 1m/s wind speed, however, the rest points have higher wind accessibility are recorded stronger wind of more than 1.3m/s.

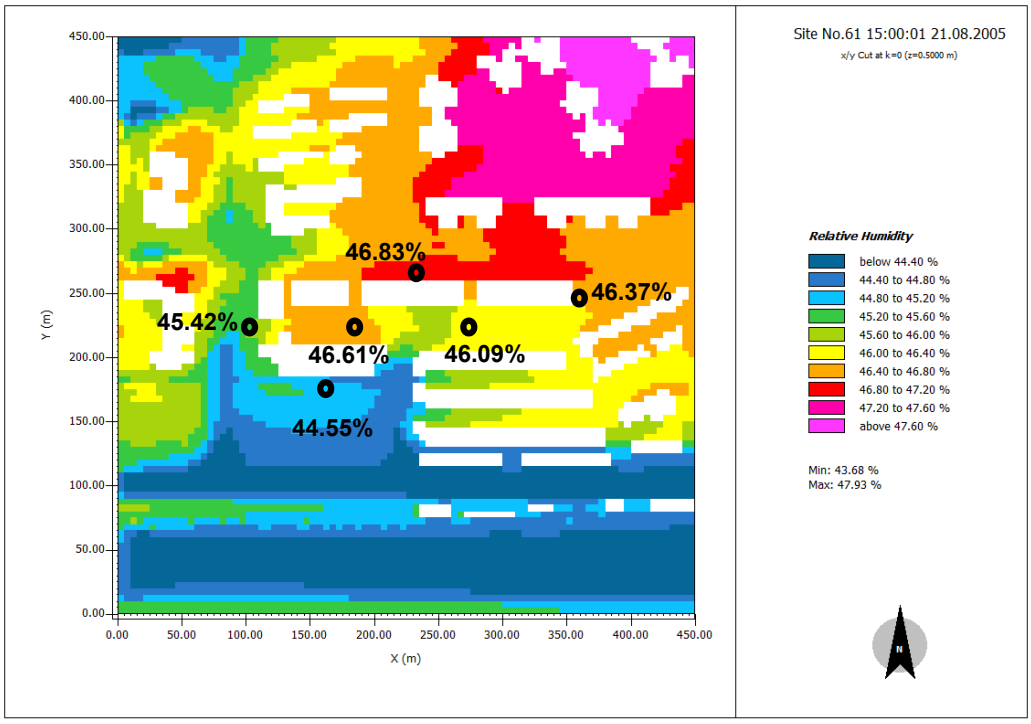

Figure 5. 9: Simulation result of relative humidity on site No.61 at 15:00

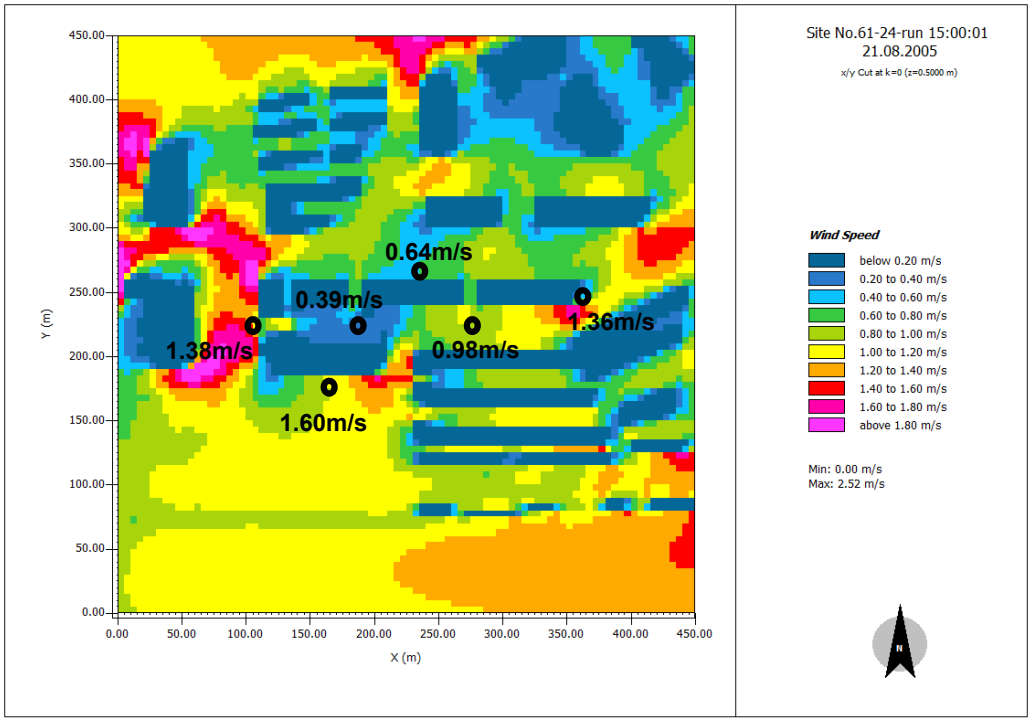

Figure 5. 10: Simulation result of wind speed on site No.61 at 15:00

iii) Group three- Semi-Closed

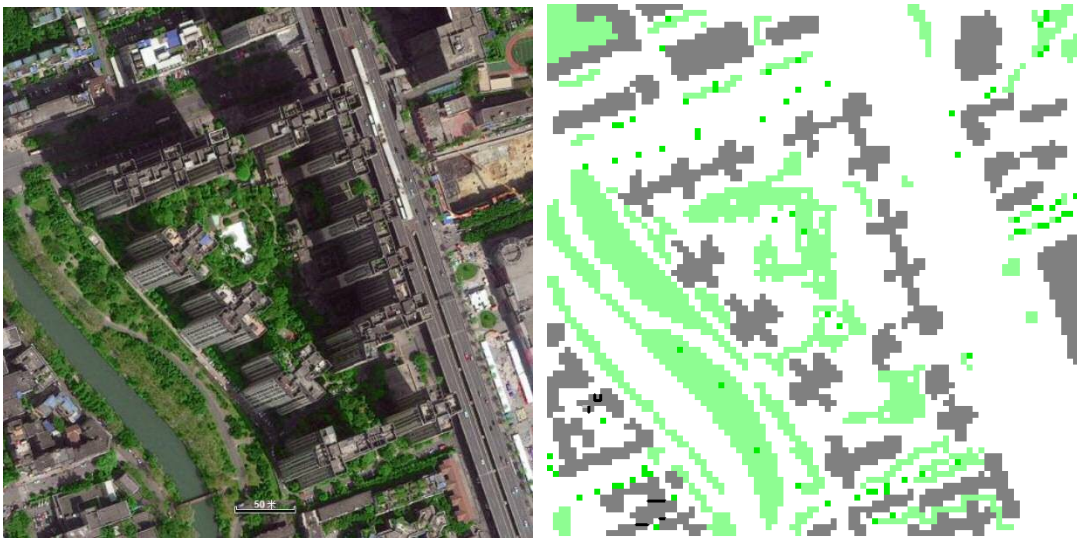

Figure 5. 11: Satellite map (left) and ENVI-Met model plan (right) on Site No.25

On-site No.25, the high-rise buildings compose a semi-closed court (Figure 5.11). There is considerable green coverage within and surrounding the court, and a river crosses by its west side. As shown in Figure 5.12, the atmospheric temperature of the majority of the selected points is around 33.70°C. The centre point in the middle of the court with the large green area is shown with more than 0.3°C reduction in atmospheric temperature. The south point is located on the road exposed to the sun, which is hotter than the other points.

According to the relative humidity map of the site No.25 (Figure 5.13), the large green areas in the court and on the south-west side of the site are recorded more than 1% higher relative humidity, while the hottest point on the south side is driest among all selected points.

The wind speed map of site No.25 is shown in Figure 5.14. The points located in open spaces have stronger winds compared to the sheltered points. In specific, wind speed at the points closed to the corner of high-rise buildings (the south, the east, the north, and the south-west points) are more than 1.5m/s. The west point is located in a wind tunnel, which has the strongest wind with a speed of 3.14m/s.

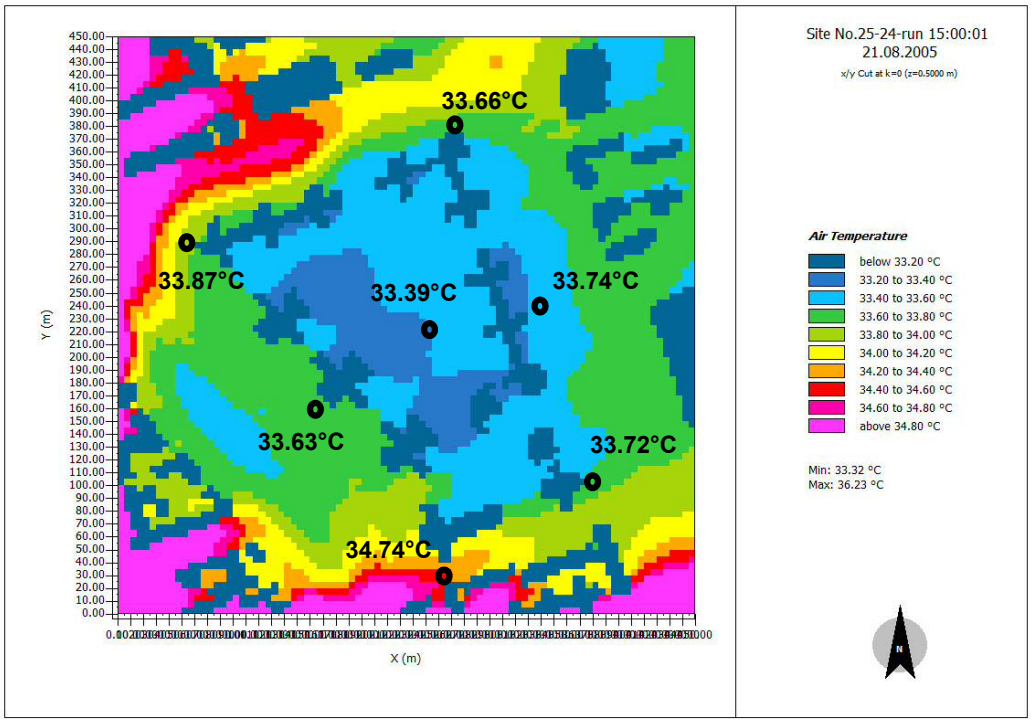

Figure 5. 12: Simulation result of atmospheric temperature on site No.25 at 15:00

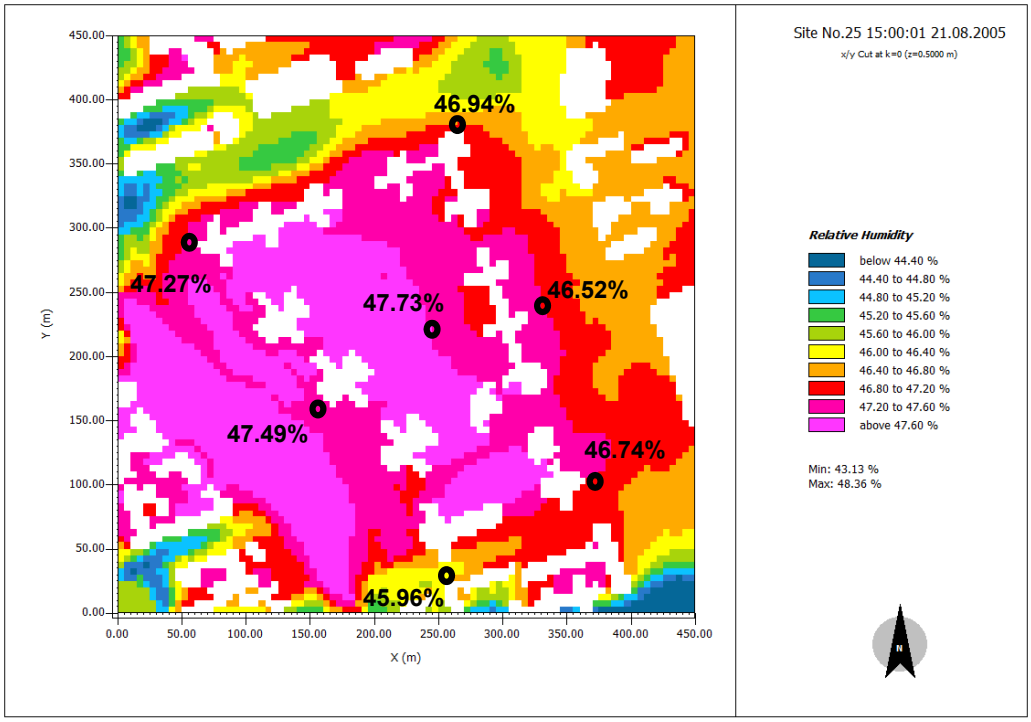

Figure 5. 13: Simulation result of relative humidity on site No.25 at 15:00

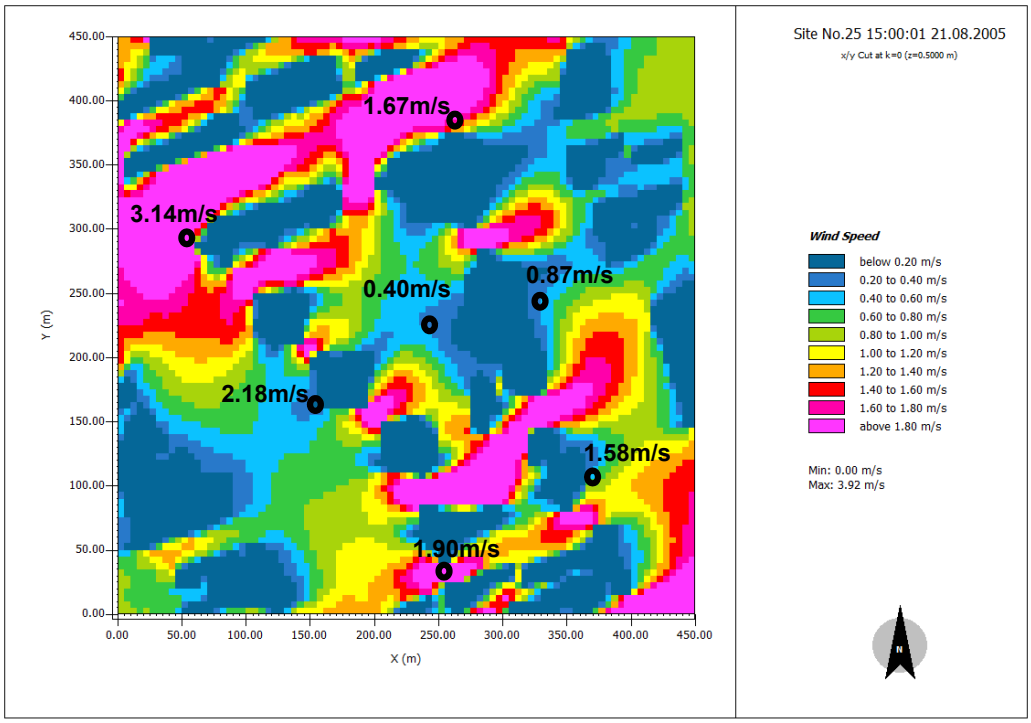

Figure 5. 14: Simulation result of wind speed on site No.25 at 15:00

iv) Group four- Interspersed

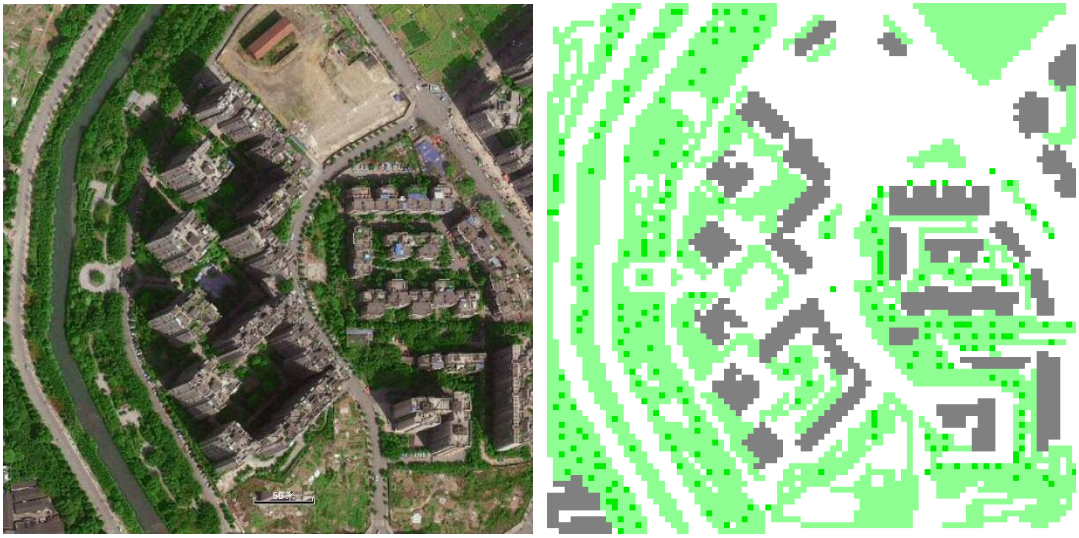

Figure 5. 15: Satellite map (left) and ENVI-Met model plan (right) on Site No.26

On-site No.26, the high-rise buildings are planned in an interspersed form (Figure 5.15). The site is well vegetated and there is a small river across by on the west side. The atmospheric temperature map is shown in Figure 5.16, the atmospheric temperature at the points exposed to the afternoon sun is higher than 34.10°C. The well-shaded and well-vegetated points (the centre and the north-east point) have the lowest

atmospheric temperature. As shown in figure 5.16, the greening areas around the west and south side of the site, especially ones closed to the river, effectively cool down the temperature with a magnitude of more than 0.40°C at 15:00.

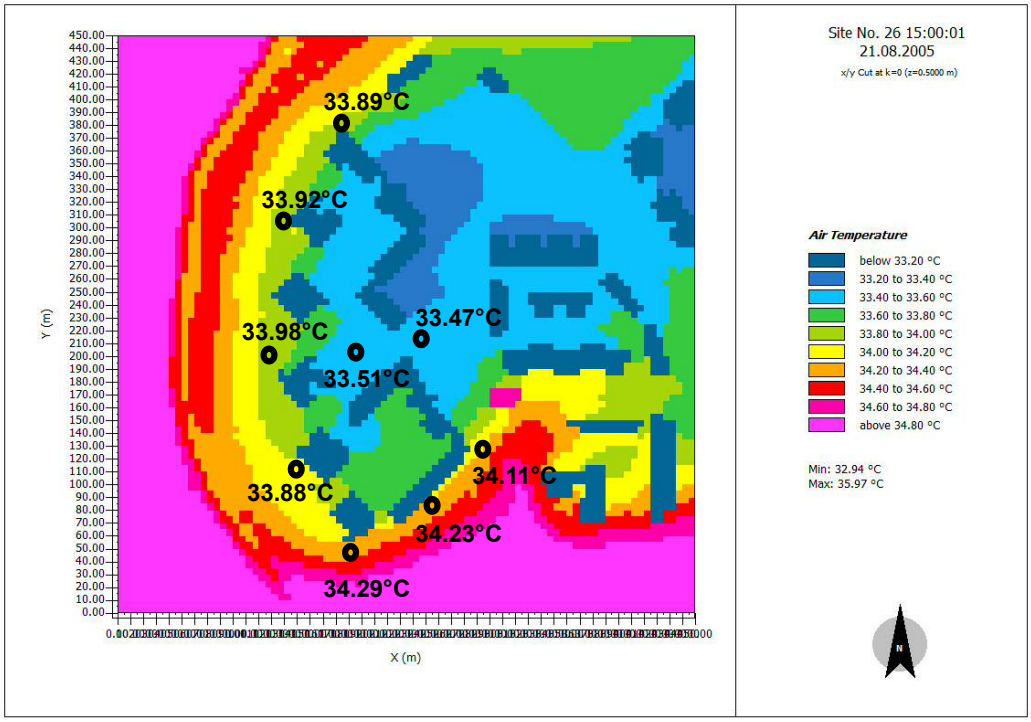

Figure 5. 16: Simulation result of atmospheric temperature on site No.26 at 15:00

The compensating trend of temperature on site No.26 can be seen in the relative humidity map (Figure 5.17). The hottest points (the south, the south-east, and the east points) are driest. On the other hand, the coolest points in the middle of the site have the highest relative humidity, which is more than 1% higher compared to the values at the hottest points.

According to the wind speed map of site No.26 (Figure 5.18), the wind is strong (with a speed of more than 1.19m/s) at the points which are located at the openings and shape corners on the plan of the building group. The points of the leeward or sheltered (the south-east and the north-west points) have calm winds with a speed of less than 0.38m/s.

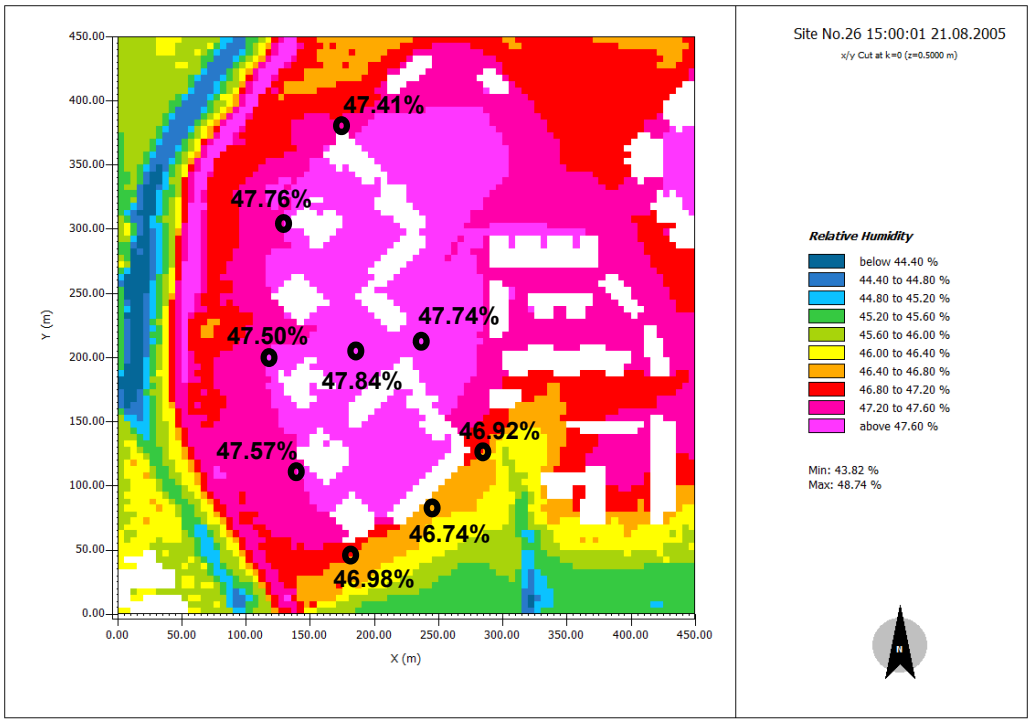

Figure 5. 17: Simulation result of relative humidity on site No.26 at 15:00

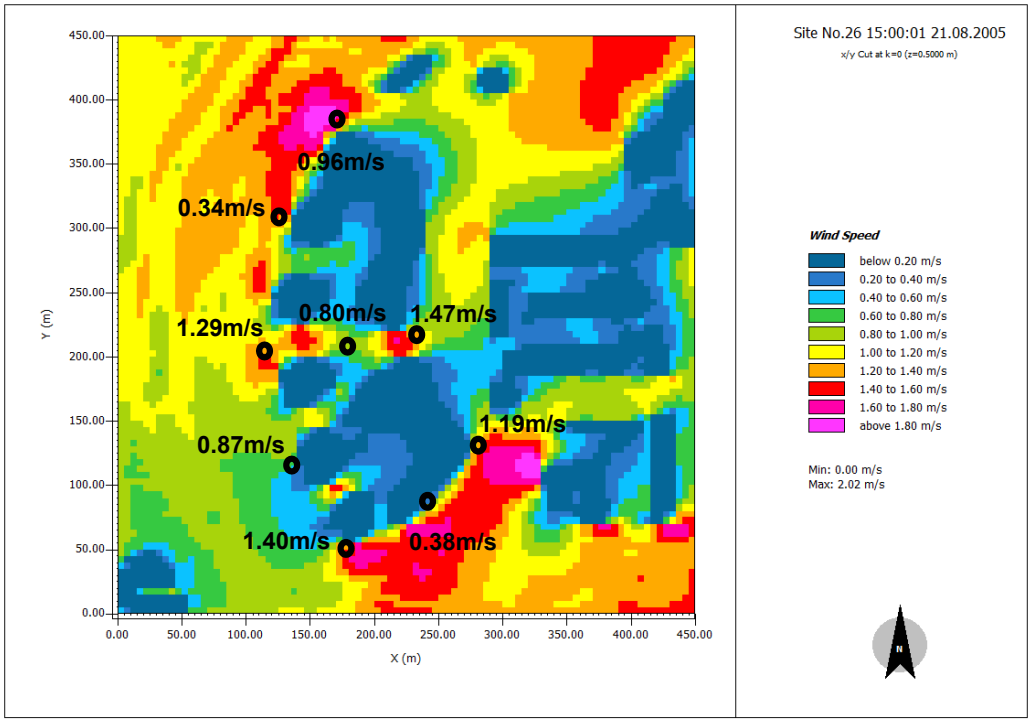

Figure 5. 18: Simulation result of wind speed on site No.26 at 15:00

v) Group five- Court

Figure 5. 19: Satellite map (left) and ENVI-Met model plan (right) on Site No.27

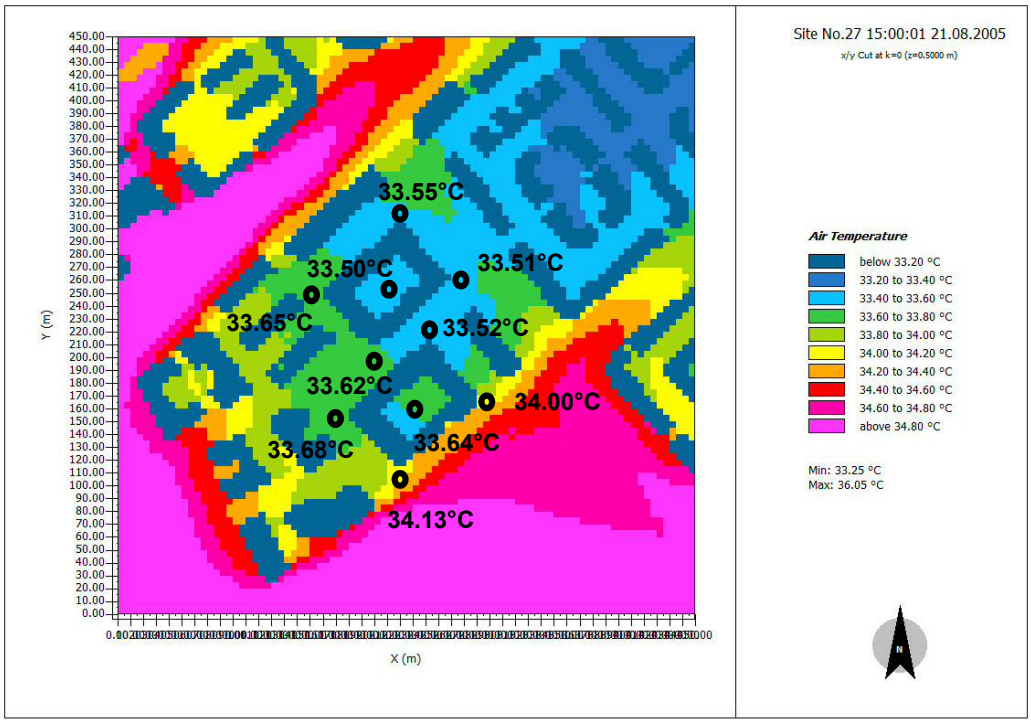

Figure 5. 20: Simulation result of atmospheric temperature on site No.27 at 15:00

On-site No.26, two courts are composed of high-rise buildings (Figure 5.19). The atmospheric temperature of site No.27 is shown in Figure 5.20, most of the selected points are well-shaded by high-rise buildings with an atmospheric temperature of around 33.50°C. The points exposed to the sun (the east and the south points of southern court) are more than 0.50°C hotter than the other points.

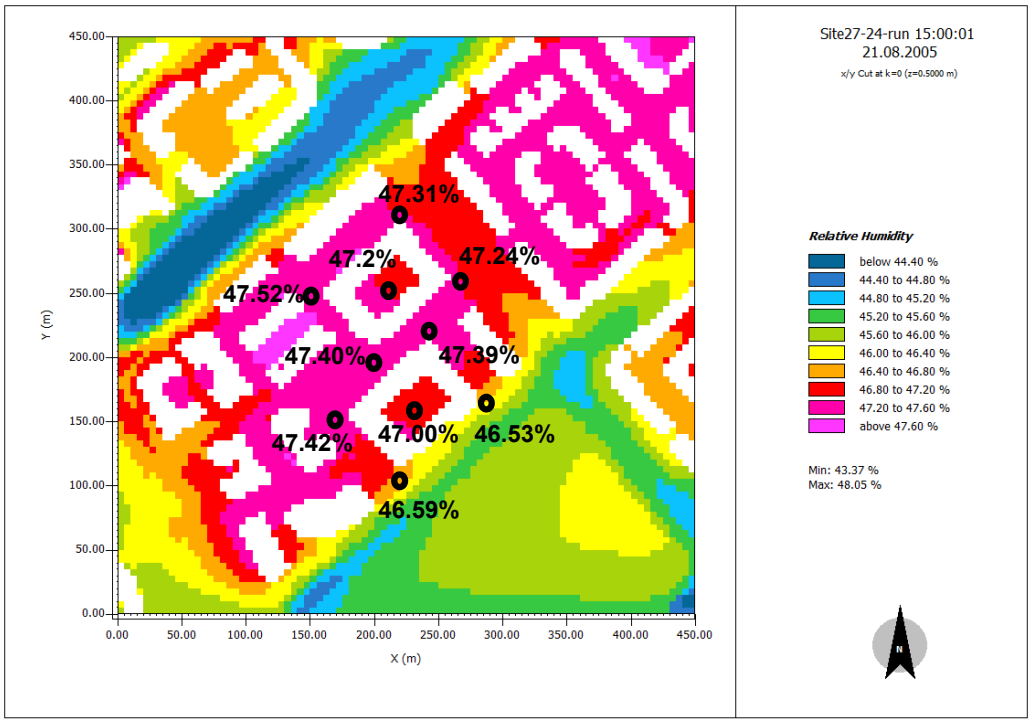

Figure 5. 21: Simulation result of relative humidity on site No.27 at 15:00

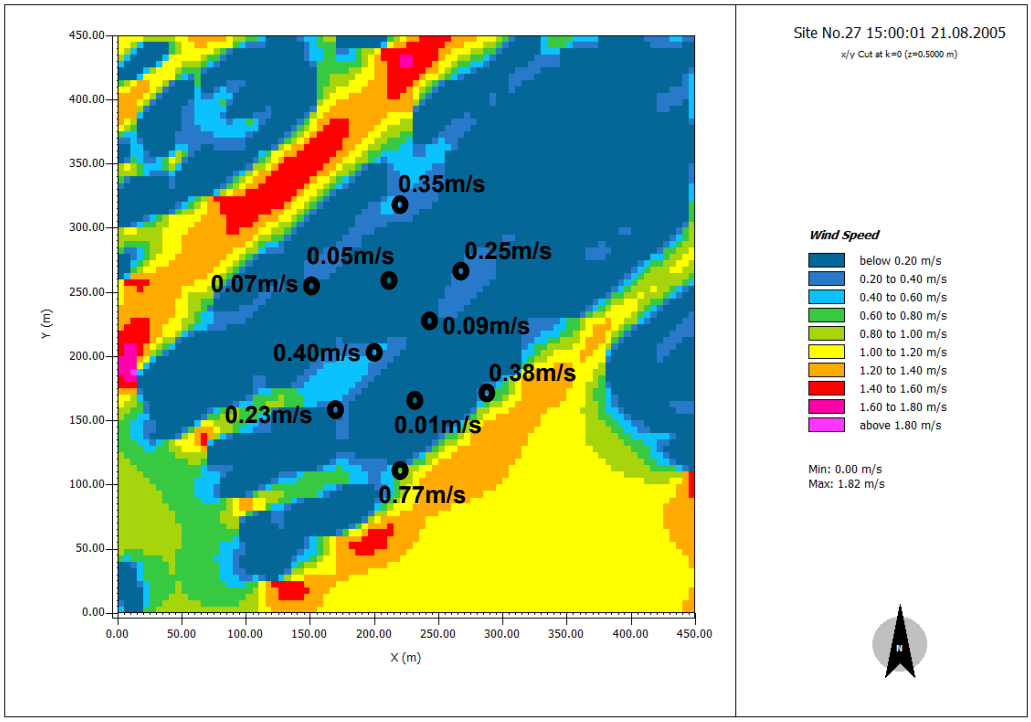

Figure 5. 22: Simulation result of wind speed on site No.27 at 15:00

The compensating trend of relative humidity to temperature still exists on site No.27 (Figure 5.21). However, the points outside of court with higher greening coverage are damper than the centre points within the two courts, and the vegetation contributes a

0.3% increase in relative humidity.

As most of the selected points are well sheltered by buildings, the wind speed is below 0.38m/s around the site (Figure 5.22). At the two centre points, which are totally sheltered, the wind is calm. Only the south point of the south court is recorded with a relatively stronger wind with a speed of 0.77m/s.

5.2.3 Atmospheric temperature of all fifteen project sites

i) Summer

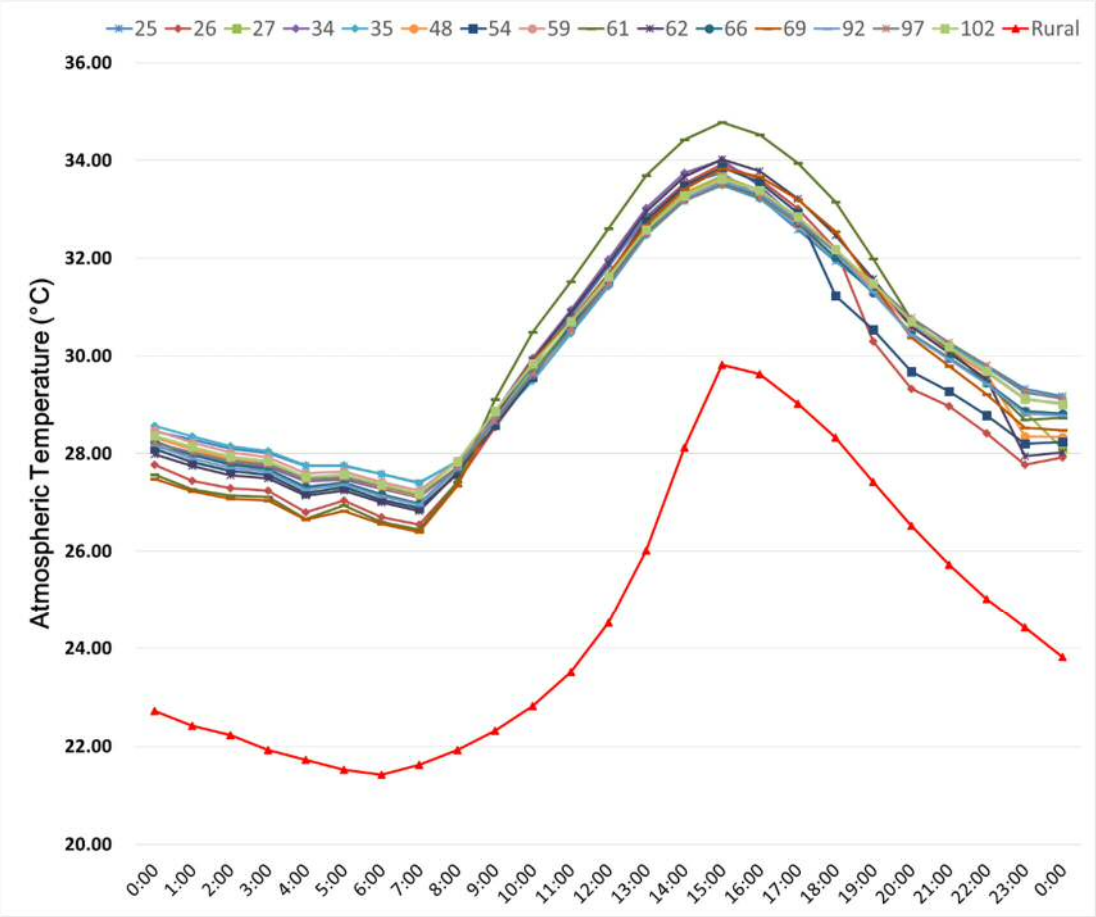

Figure 5. 23: Simulated on-site atmospheric temperature VS rural atmospheric temperature on 21st August 2005 (marked with original site number)

Table 5. 1: Simulated summer atmospheric temperature

Time	25	26	27	34	35	48	54	59	61	62	66	69	92	97	102	Rural
0:00	28.46	27.77	28.09	28.15	28.57	28.33	28.10	28.47	27.57	27.99	28.26	27.48	28.17	28.21	28.37	22.72
1:00	28.28	27.44	27.84	27.97	28.35	28.09	27.82	28.23	27.26	27.74	27.98	27.23	27.90	28.02	28.14	22.42
2:00	28.10	27.29	27.64	27.80	28.15	27.88	27.64	28.02	27.14	27.56	27.78	27.08	27.71	27.84	27.94	22.22
3:00	28.02	27.24	27.56	27.73	28.05	27.80	27.57	27.92	27.11	27.49	27.68	27.04	27.63	27.77	27.85	21.92
4:00	27.75	26.80	27.21	27.43	27.76	27.47	27.19	27.59	26.67	27.14	27.32	26.64	27.27	27.49	27.52	21.72
5:00	27.74	27.04	27.29	27.47	27.76	27.52	27.31	27.63	26.94	27.24	27.40	26.83	27.37	27.51	27.56	21.52
6:00	27.58	26.70	27.06	27.28	27.58	27.31	27.06	27.42	26.59	27.00	27.16	26.55	27.13	27.34	27.36	21.42
7:00	27.40	26.54	26.87	27.10	27.40	27.13	26.88	27.24	26.44	26.83	26.98	26.39	26.94	27.16	27.17	21.62
8:00	27.84	27.42	27.62	27.72	27.85	27.73	27.58	27.85	27.42	27.61	27.70	27.34	27.70	27.71	27.83	21.92
9:00	28.76	28.55	28.71	28.84	28.65	28.67	28.58	28.74	29.12	28.79	28.70	28.83	28.75	28.67	28.88	22.32
10:00	29.80	29.58	29.71	29.96	29.49	29.57	29.56	29.62	30.49	29.90	29.64	29.90	29.62	29.64	29.84	22.82
11:00	30.81	30.65	30.63	30.94	30.46	30.55	30.62	30.59	31.52	30.90	30.58	30.73	30.53	30.54	30.70	23.52
12:00	31.82	31.65	31.59	31.97	31.42	31.52	31.63	31.56	32.61	31.89	31.50	31.68	31.44	31.49	31.62	24.52
13:00	32.84	32.79	32.63	33.02	32.46	32.59	32.76	32.59	33.70	32.94	32.53	32.69	32.49	32.49	32.59	26.02
14:00	33.53	33.53	33.34	33.74	33.17	33.30	33.48	33.28	34.42	33.66	33.21	33.41	33.20	33.18	33.27	28.12
15:00	33.74	33.92	33.68	34.01	33.49	33.64	33.86	33.59	34.78	34.02	33.55	33.83	33.56	33.50	33.62	29.82
16:00	33.24	33.61	33.39	33.48	33.21	33.37	33.55	33.29	34.53	33.78	33.27	33.66	33.32	33.24	33.39	29.62
17:00	32.58	33.01	32.83	32.78	32.65	32.81	32.93	32.68	33.94	33.21	32.72	33.20	32.79	32.74	32.84	29.02
18:00	31.94	32.19	32.13	32.14	31.96	32.13	31.23	32.00	33.16	32.46	32.02	32.54	32.11	32.14	32.18	28.32
19:00	31.35	30.29	31.35	31.47	31.36	31.42	30.54	31.38	31.98	31.57	31.29	31.46	31.30	31.50	31.49	27.42
20:00	30.68	29.33	30.46	30.67	30.66	30.61	29.68	30.60	30.74	30.60	30.44	30.37	30.42	30.78	30.70	26.52
21:00	30.21	28.97	29.96	30.16	30.20	30.11	29.28	30.13	30.13	30.06	29.96	29.79	29.93	30.27	30.18	25.72
22:00	29.81	28.42	29.45	29.69	29.77	29.63	28.78	29.66	29.45	29.52	29.46	29.21	29.42	29.81	29.70	25.02
23:00	29.32	27.77	28.85	29.12	29.25	28.35	28.20	29.11	28.70	27.95	28.86	28.53	28.82	29.27	29.12	24.42
0:00	29.17	27.93	28.10	29.01	29.13	28.34	28.23	29.03	28.73	28.02	28.82	28.48	28.78	29.12	29.01	23.82

The simulated atmospheric temperature on 21st August 2005 for the selected 15 target sites shown in Table 5.1 and illustrated in Figure 5.23 with rural temperature from the weather station. According to the results, the atmospheric temperature curves on the selected 15 sites share a similar trend. The temperature starts around 28.00°C at 0:00, then it gradually reduces to below 28°C at 7:00; after this decrease period, outdoor temperature increase massively with a steep slope and it peaks at 15:00 with a magnitude of around 34°C; since then, it starts a cooling process ending with an above 28°C at midnight.

Comparing to the rural atmospheric temperature, the simulated atmospheric temperatures on the selected 15 sites are around 5.5°C to 1.5°C higher during the whole day, which show UHI effects on each site accordingly. In specific, the UHI value of the sites in the early morning (0:00 to 9:00) range from 3.0°C to 5.0°C; during the mid-day (11:00 to 13:00), UHI reaches an above 5°C peak value on most sites; during the afternoon time (14:00 to 18:00), the magnitudes of UHI on the 15 sites reduces to their bottom values around 17:00; during the evening period, UHI values gradually rise up to 3.6°C on the 15 sites.

Base on the simulation results, UHI intensity reaches its peak value and bottom value , in the morning and in the afternoon, respectively. Moreover, the evening UHI is higher than the afternoon UHI. In general, the simulation UHI follows a similar trend of daily variation as summarised in the existing literature which was discussed in Chapter Two.

ii) Winter

On the other hand, Table 5.2 and Figure 5.24 illustrate the simulated atmospheric temperature on 9th January 2005 for the selected 15 target sites and rural temperature from the weather station. According to the results, the difference of atmospheric temperature among the selected 15 sites varies within 1°C. Moreover, the temperature curves of the 15 sites drop to their daily bottom values during 8:00 to 9:00 with the magnitudes of around 4°C, and rapidly rise since 10:00 until their peak values during

15:00 hour ranging from 8°C to 9°C. Afterwards, the atmospheric temperature gradually reduces and reach the magnitude of around 7°C at midnight.

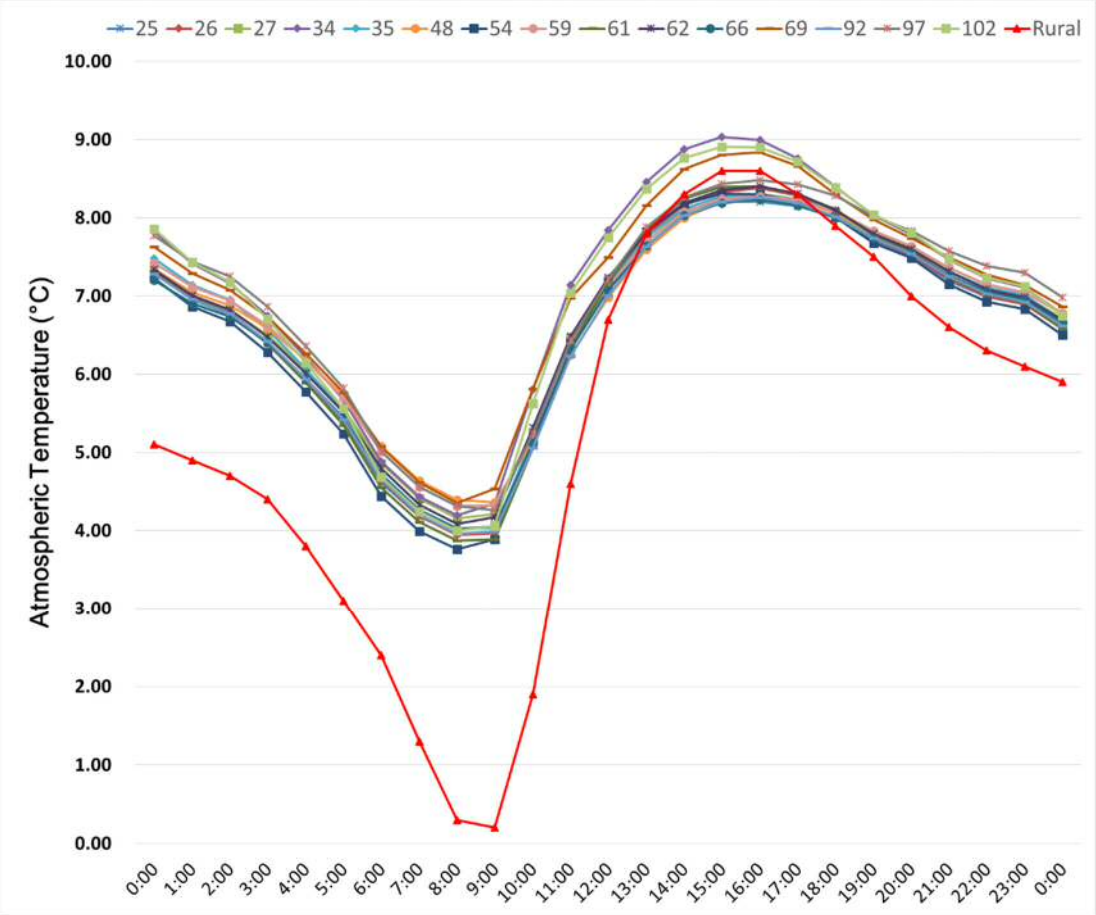

Figure 5. 24: Simulated on-site atmospheric temperature VS rural atmospheric temperature on 9th January, 2005 (marked with original site number)

The rural atmospheric temperature on 9th January 2005 was lower than the simulated on-site temperature in most hours. However, during the early hours in the afternoon, rural area were shown with higher atmospheric temperature than most of the targets sites, which means negative UHI intensity during this period. This effect is called urban cool island (Chow & Roth 2006) (Middel et al. 2014), which has been indented in Chengdu with the satellite observations as discussed in Chapter Four. According to Figure 5.23, the maximum hourly UHI intensity (around 4°C) occurs in the morning during 9:00 hour on most sites. Moreover, the average UHI of all the 15 sites in the morning and in the evening is around 2.5°C and below 1°C, respectively.

Table 5. 2: Simulated winter atmospheric temperature

Time	25	26	27	34	35	48	54	59	61	62	66	69	92	97	102	Rural
0:00	7.30	7.34	7.30	7.83	7.48	7.34	7.23	7.42	7.32	7.34	7.20	7.63	7.28	7.77	7.86	5.10
1:00	6.95	6.98	7.00	7.42	7.14	7.05	6.86	7.12	6.97	7.01	6.90	7.29	6.96	7.44	7.43	4.90
2:00	6.77	6.79	6.82	7.16	6.95	6.88	6.67	6.94	6.78	6.82	6.74	7.08	6.78	7.25	7.18	4.70
3:00	6.39	6.42	6.50	6.74	6.57	6.59	6.28	6.62	6.39	6.48	6.41	6.73	6.42	6.86	6.71	4.40
4:00	5.90	5.93	6.05	6.22	6.06	6.17	5.77	6.18	5.89	6.01	5.94	6.26	5.94	6.36	6.15	3.80
5:00	5.39	5.41	5.56	5.67	5.52	5.72	5.24	5.70	5.35	5.51	5.44	5.77	5.42	5.82	5.56	3.10
6:00	4.62	4.64	4.86	4.89	4.72	5.08	4.44	5.01	4.55	4.79	4.71	5.07	4.66	5.02	4.69	2.40
7:00	4.18	4.19	4.41	4.44	4.27	4.64	3.99	4.56	4.11	4.33	4.26	4.61	4.20	4.56	4.24	1.30
8:00	3.96	3.94	4.16	4.19	4.03	4.39	3.76	4.31	3.87	4.08	4.02	4.35	3.96	4.32	4.00	0.30
9:00	3.97	3.96	4.21	4.34	4.03	4.36	3.89	4.32	3.89	4.17	4.05	4.54	3.99	4.26	4.06	0.20
10:00	5.08	5.16	5.26	5.81	5.20	5.15	5.15	5.24	5.06	5.32	5.11	5.81	5.06	5.24	5.63	1.90
11:00	6.36	6.40	6.46	7.14	6.39	6.25	6.41	6.39	6.34	6.49	6.32	6.98	6.23	6.43	7.04	4.60
12:00	7.19	7.16	7.13	7.84	7.13	6.98	7.18	7.12	7.17	7.23	7.07	7.50	7.01	7.21	7.75	6.70
13:00	7.77	7.79	7.70	8.46	7.76	7.60	7.83	7.70	7.84	7.82	7.65	8.16	7.63	7.88	8.37	7.80
14:00	8.09	8.16	8.07	8.87	8.12	8.00	8.18	8.08	8.24	8.19	8.03	8.62	8.03	8.26	8.76	8.30
15:00	8.21	8.33	8.25	9.03	8.28	8.20	8.31	8.24	8.39	8.36	8.19	8.81	8.20	8.44	8.91	8.60
16:00	8.20	8.38	8.31	8.99	8.30	8.28	8.30	8.28	8.40	8.40	8.24	8.83	8.26	8.48	8.90	8.60
17:00	8.15	8.28	8.23	8.76	8.23	8.23	8.20	8.22	8.30	8.30	8.16	8.66	8.19	8.43	8.72	8.30
18:00	8.02	8.05	8.05	8.39	8.09	8.07	8.01	8.09	8.11	8.09	8.00	8.30	8.02	8.29	8.39	7.90
19:00	7.70	7.73	7.77	8.03	7.80	7.81	7.68	7.83	7.78	7.80	7.74	7.98	7.74	8.02	8.04	7.50
20:00	7.51	7.53	7.58	7.79	7.62	7.61	7.48	7.64	7.58	7.60	7.55	7.74	7.54	7.83	7.81	7.00
21:00	7.19	7.22	7.31	7.46	7.31	7.36	7.15	7.36	7.24	7.31	7.27	7.49	7.25	7.57	7.47	6.60
22:00	6.99	6.99	7.10	7.23	7.11	7.15	6.93	7.15	7.02	7.09	7.06	7.27	7.03	7.39	7.24	6.30
23:00	6.90	6.89	7.00	7.10	7.01	7.04	6.83	7.05	6.92	6.98	6.96	7.14	6.93	7.29	7.12	6.10
0:00	6.58	6.58	6.71	6.77	6.68	6.78	6.50	6.77	6.58	6.69	6.66	6.86	6.62	6.98	6.75	5.90

5.3 Results comparison and validation

5.3.1 Introduction

In order to validate the accuracy of the simulations, the calculated air temperature from satellite image is introduced based on the information obtained from the long-period remote sensing, which has been discussed in Chapter 4. In consideration of the main focus of urban built environment has been addressed on urban temperatures- either the air temperature and the surface temperature, the simulated air temperature from ENVI-met modelling were applied to compare with the previously calculated data. As mentioned in Chapter 3, according to the actual constructional and geographical information, 15 selected project sites 15 models with a spatial resolution of 450m x 450m x 110m had been created. During the simulation, the average value is used for wind speed. It is calculated from the historical data collected in a weather station in the urban area of Chengdu on 23rd August 2005 and 9th January 2005, which was 1.3 m/s and 1.21m/s, respectively.

For the calculated air temperature from satellite image: based on the average season daily UHI values for each site obtained from Chapter 4, the site temperature T_a is derived:

$$T_a = T_{rural} + \Delta T_{site\ average} \quad (5.1)$$

Also, an assumption, which the UHI values keep constant all day, is introduced in the calculation process. For the simulated air temperature from ENVI-met modelling, a site average data is used accordingly, which is an average value of several characteristic points on the plan of each target sites.

5.3.2 Validation of summer models: Simulated and Calculated Comparisons

Figure 5.25 shows the simulated air temperature T_a in summer at metre height of 0.5m obtained from ENVI-Met simulations, which are compared against calculated T_a from satellite image at each of the fifteen sites in Chengdu. According to the simulated results from ENVI-Met for each site, well trends of T_s are presented by ENVI-Met

which showing two distinctively constricting periods. It can be noted that the simulated results T_s from EVNI-Met in the morning and at noon at most sites were higher than calculated results converted from data of weather station, which shows the overestimated cases. According to Figure 5.24, the average error during this period is up to 3°C (less than 2°C during period between the period between 0:00 and 11:00). This is due to the absence of the vertical long-wave flux divergence, which results in a 2-4 °C difference between the simulated and measured temperature (Bruse et al. 2002) (Taleghani et al. 2015).

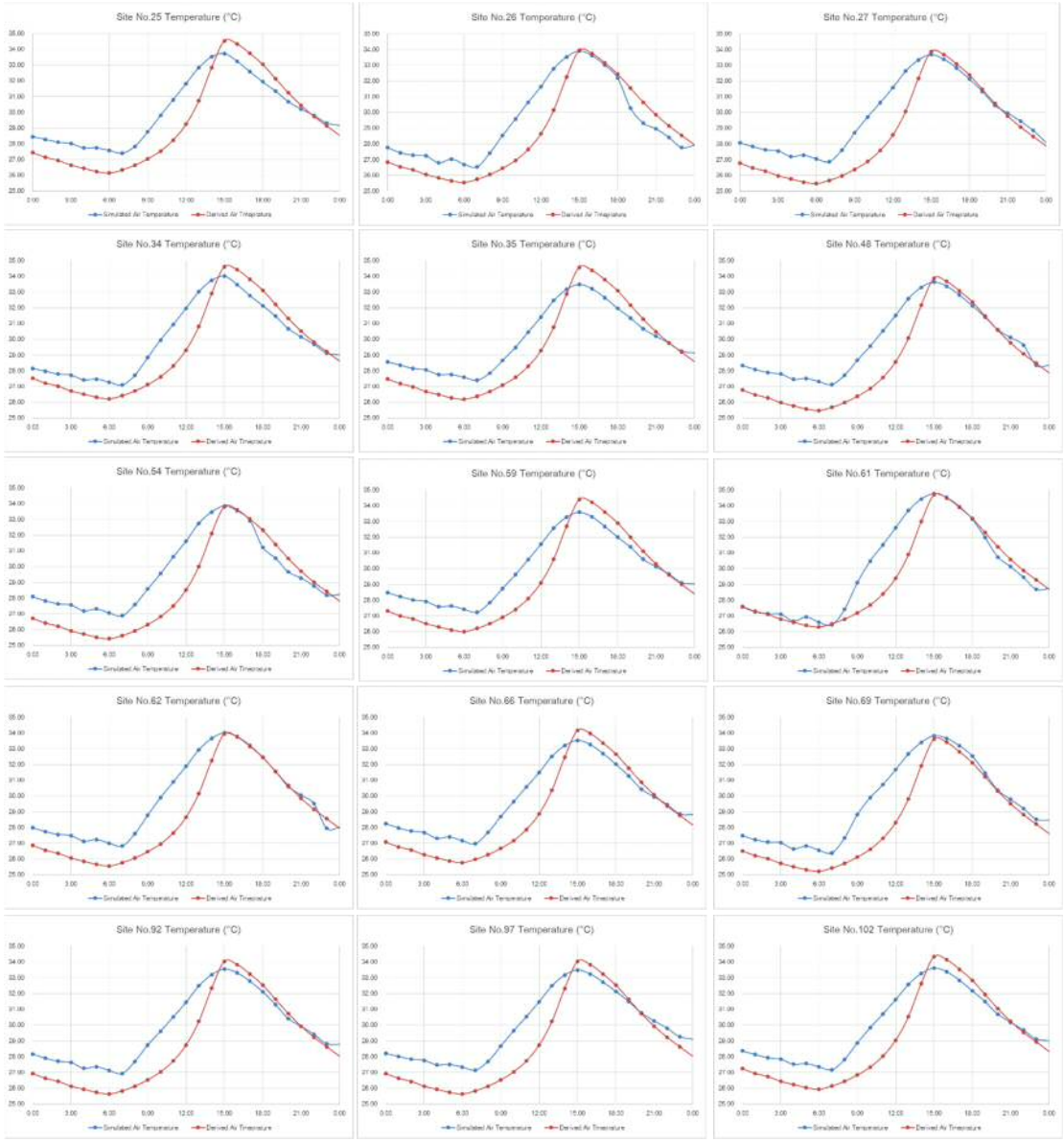

Figure 5. 25: Comparison between the air temperature from ENVI-Met (Blue) and from satellite image (red) for 15 sites (with original site number) in summer

On the other hand, in the period between 15:00 to 18:00, the simulated temperature from ENVI-Met are matched with the calculated temperature from satellite image with minor differences (less than 0.10°C) in many cases (Site 26, Site 27, Site 47, Site 54, Site 61, and Site 62). In the meanwhile, the simulated results were underestimated in the rest cases, which are up to 1.00°C lower than the calculated data. And these underestimations end at 23:00 in most cases, followed by the early morning overestimations.

As indicated in Table 5.3, the average error during the simulation period of twenty-four hours was found to be around 1.00°C. The trend of the air temperature curve from ENVI-Met was similar with the ones from satellite image (Figure 5.25), and the correlation coefficient, R^2, between the two types of temperatures, ranged from 0.788 to 0.897 (Figure 5.26). Therefore, T_a through two different methods- the ENVI-Met simulation and calculations derived from data obtained from satellite image- are well correlated, which indirectly presents the reliability and accuracy of ENVI-Met simulations in terms of summer-time atmospheric temperatures in Chengdu.

Table 5. 3: Correlation coefficient and average error for correlations between air temperatures from ENVI-Met and from satellite image of each site (with original site number) in summer

Site No.	Correlation coefficient (R^2)	Average Error (°C)
25	0.858	0.73
26	0.788	0.74
27	0.862	1.12
34	0.849	0.61
35	0.897	0.61
48	0.870	1.20
54	0.797	1.02
59	0.880	0.76
61	0.830	0.59
62	0.842	1.11
66	0.871	0.86
69	0.856	1.26
92	0.876	0.97
97	0.895	1.11
102	0.879	0.85

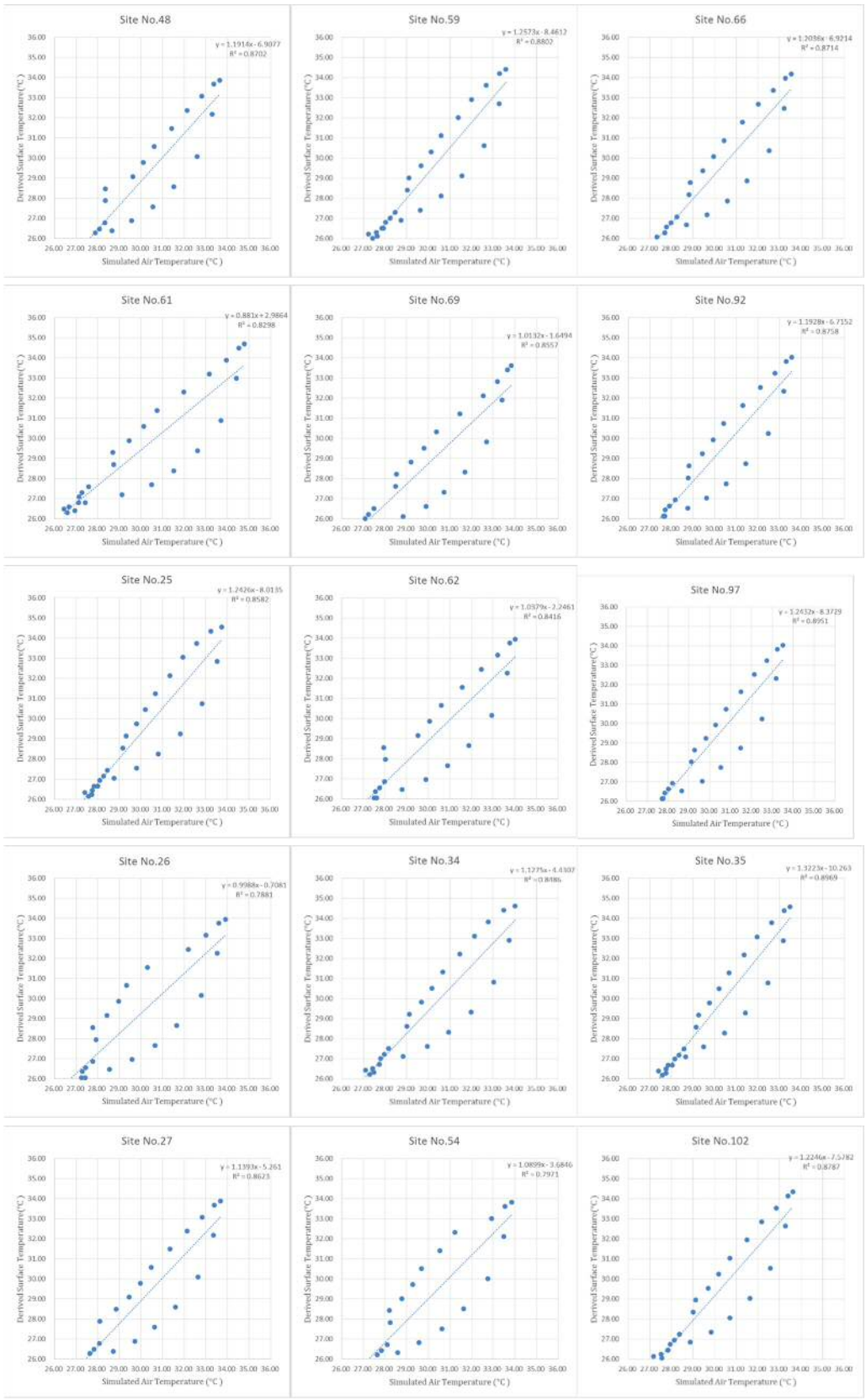

Figure 5. 26: Correlations between the air temperatures from ENVI-Met and from satellite image for 15 sites (with original site number) in summer

5.3.3 Validation of winter models: Simulated and Calculated Comparisons

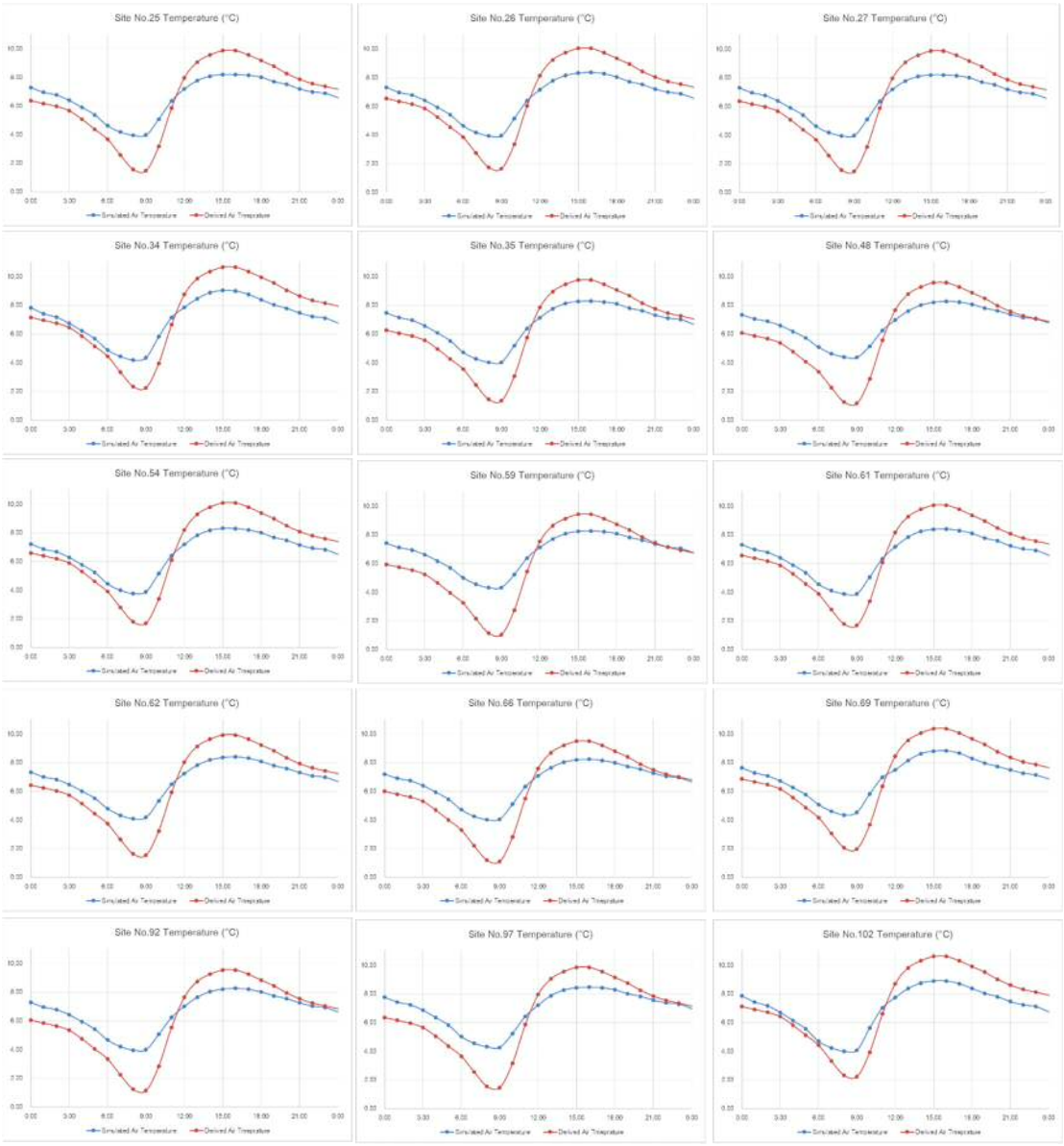

Figure 5. 27: Comparison between the air temperatures from ENVI-Met (blue) and from satellite image (red) for 15 sites (with original site number) in winter

Figure 5.27 illustrates the atmospheric temperature T_a simulated by ENVI-Met, which is plotted against calculated T_a at 15 targets sites in winter in Chengdu. According to the results of comparisons, the variations in simulated results are less than the calculated ones, with two distinctive contracting periods presented, which is similar as the comparisons in summer. In the period of the entire morning (from 0:00 to 11:00), the simulated values of T_a is overestimated. The difference between the two sources of temperatures range from 0.40°C to 3.00°C (less than 1.00°C in the early morning,

and 2.00°C to 3.00°C during the period between 7:00 to 10:00) in most cases. Afterword, the calculated T_a are higher than the simulated values since noon till mid-night, and the difference range from 0.02°C to 1.80°C. And these difference mentioned in the winter cases still indicates the absence of vertical long-wave flux in ENVI-Met models (Bruse et al. 2002) (Taleghani et al. 2015).

Table 5.4 shows the average error between the simulated and calculated values, which ranges from 0.02°C to 0.64°C. It shows a significant correlation between the two groups of values, which achieved above 0.93 of the correlation coefficient (R^2) in any case of correlations (Figure 5.28). Thus, the simulated T_a from ENVI-Met and the calculated T_a from satellite image in winter time are strongly correlated, thereby validating the accuracy of simulation values obtained from ENVI-Met simulations.

Table 5. 4: Correlation coefficient and average error for correlations between the air temperatures from ENVI-Met and from satellite image of each site (with original site number) in winter

Site No.	Correlation coefficient (R^2)	Average Error (℃)
25	0.958	0.05
26	0.957	-0.09
27	0.958	0.02
34	0.934	-0.28
35	0.946	0.27
48	0.957	0.49
54	0.957	-0.21
59	0.955	0.64
61	0.960	-0.12
62	0.961	0.10
66	0.964	0.44
69	0.949	-0.04
92	0.957	0.38
97	0.937	0.39
102	0.935	-0.32

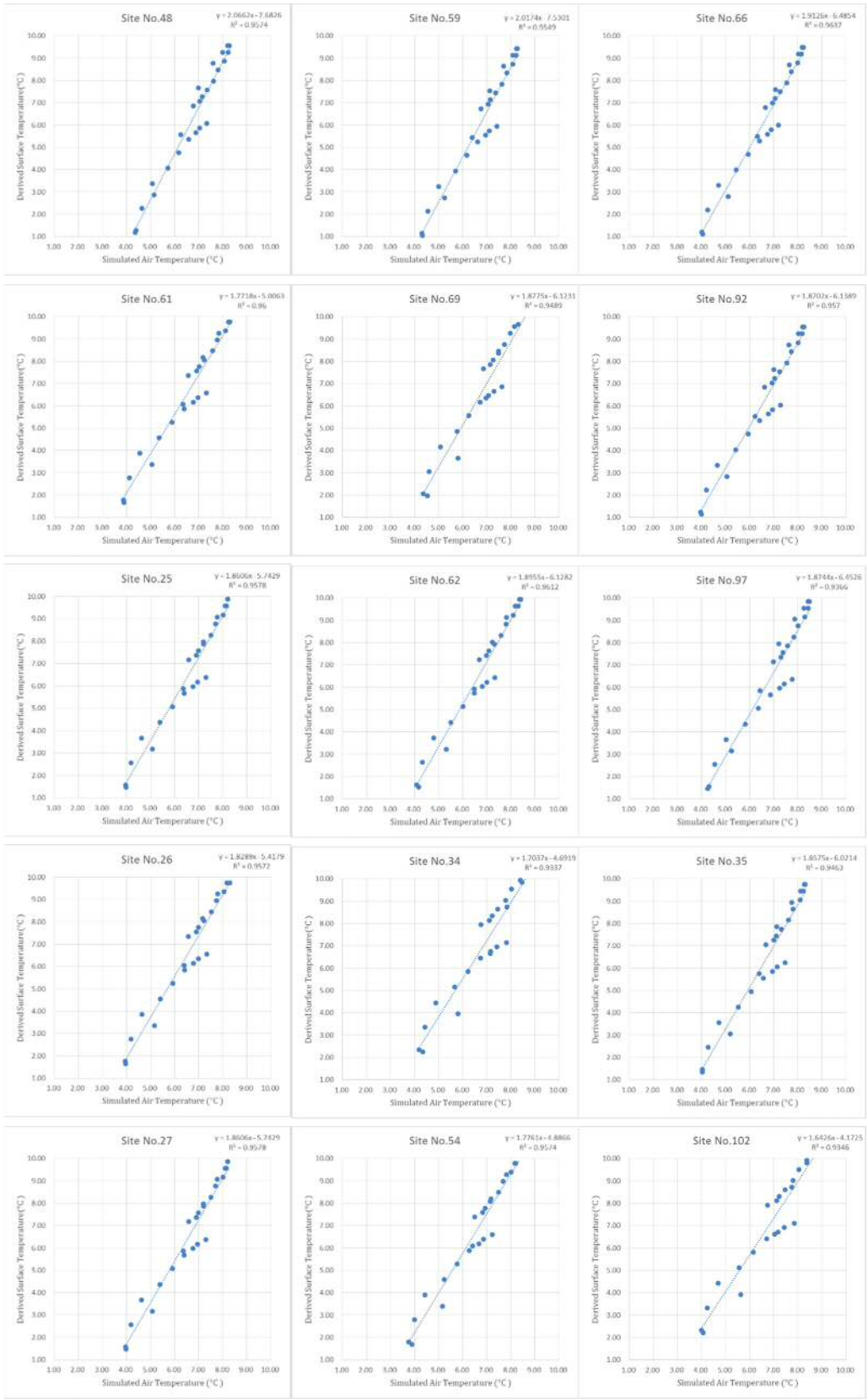

Figure 5. 28: Correlations between the air temperatures from ENVI-Met and from satellite image for 15 sites (with original site number) in winter

5.4 Discussion

5.4.1 Simulated UHI and building plot layout

The simulated UHI values are derived based on the simulated atmospheric temperature on selected 15 sites and the diurnal weather data in the rural area, which are illustrated in Figure 5.29. Comparing to the data from Figure 5.15-'Plot Layout VS UHI', simulated UHI show similar trends with plot layout form of each site. In specific, groups of Tower and Linear have higher summer UHI and lowest winter UHI, on the other hand, groups of Interspersed and Court are shown with the lowest summer UHI and higher winter UHI. Though the maximum average value of summer UHI occurs in a semi-closed group, which is different from the case in chapter 3. The difference between simulated data and observation data ranges from 0.35° to 0.96°C and from 0.05°C to 0.41°C, for summer UHI and winter UHI, respectively, which corresponds the analysis results of accuracy and validation in the previous section. At the same time, the difference indicates the potential for improving the modelling process and simulation tools.

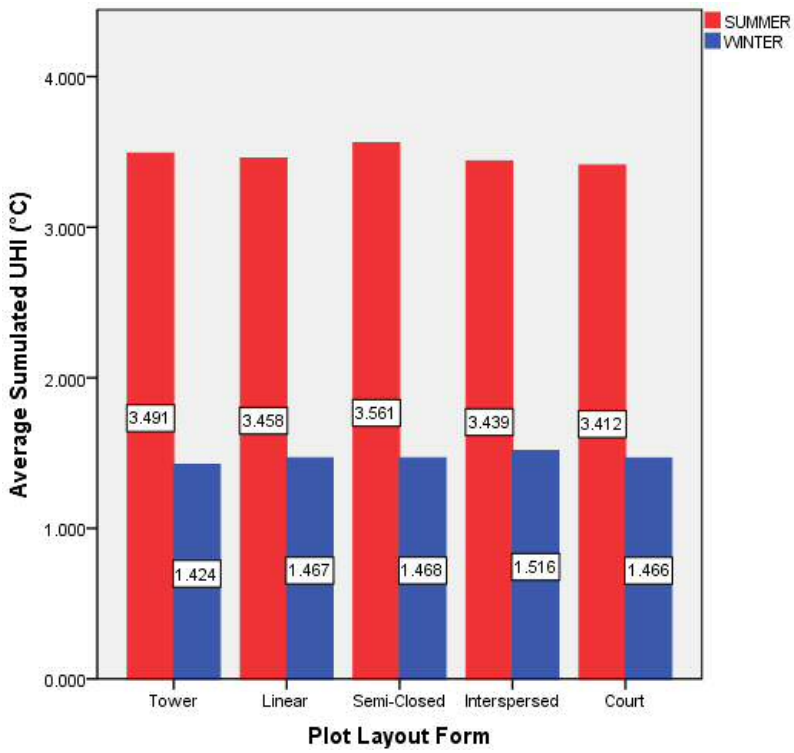

Figure 5. 29: Plot layout VS simulated UHI

5.4.2 Simulated UHI and building density

As one of the main design parameters in a building group, the building density is considered as one of the key factors of atmospheric temperature. According to Figure 5.30 based on the simulation results, the building density factor, especially building height, is shown significant correlation with simulated summer UHI, with more than 5% (13.9%) significance. On the other hand, the correlation between simulated summer UHI and the other two building density variables, FAR and BCR, fails to show more than 5% significance. Generally speaking, the comparison between simulated summer UHI and building height still indicates a denser project site tends to have higher UHI in the summertime.

Comparing to the correlation between building height and satellite data-derived summer UHI (Figure 4.19) with an R^2 value of 0.103, building height and simulated summer UHI (Figure 5.30) are also shown with significant relationship (with an R^2 value of 0.139). Based on the simulation results, every 100 meters rising in building height will lead to 0.28°C increase in atmosphere UHI in the summertime. Comparing to the satellite observation-derived data with a magnitude of 0.95°C, the simulation results show similar trends regarding the temperature variation due to building height.

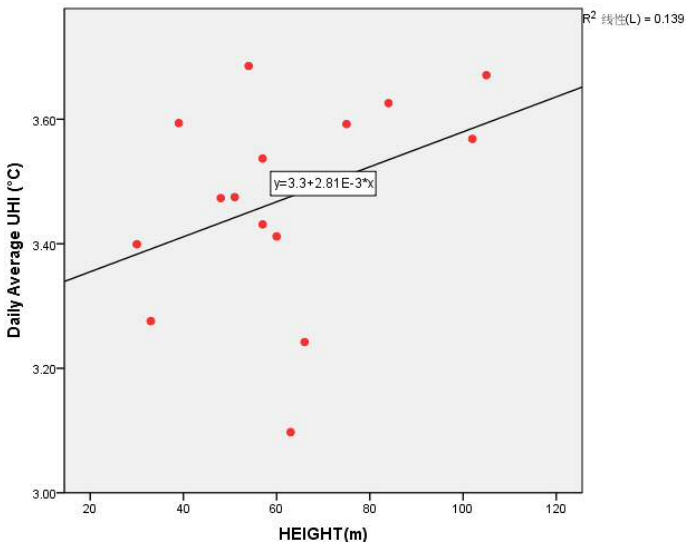

Figure 5. 30: Correlations between simulated summer UHI and building height

Lastly, however, unlike the satellite observation data in Chapter 4, the simulated winter

UHI show a weak relationship (less than 5% significance) with building density variables, which is possibly due to low sample size and imperfection of modelling process.

5.4.3 Simulated UHI and green coverage ratio

The simulation results of winter UHI shows a strong relationship with green coverage ratio. As shown in Figure 5.31, the correlation between GCR and simulated winter UHI is of more than 5% significance with an R^2 value of 0.327. Moreover, the linear equation between the two parameters is closed to that in Figure 4.18 for GCR and satellite observation data-derived UHI. Every 10 per cent rising in green coverage ratio will lead 0.17°C increase in winter atmospheric temperature in both cases.

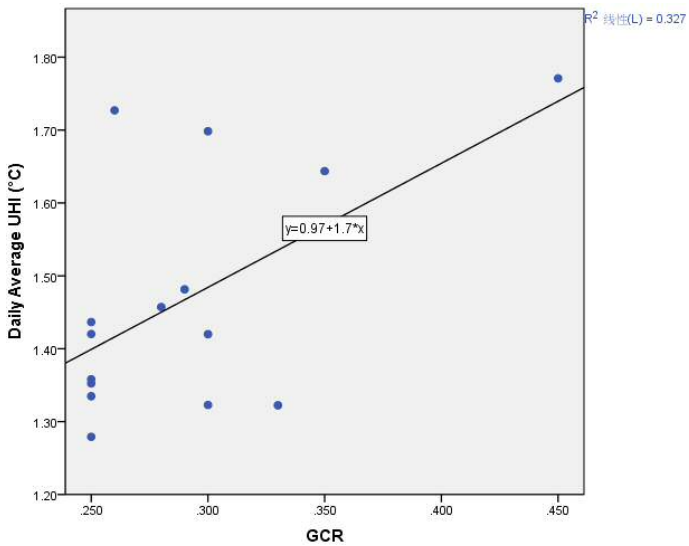

Figure 5. 31: Correlations between simulated winter UHI and green coverage ratio

However, the simulated UHI fails to show a strong relationship with GCR (with an R^2 value of less than 5%). In order to investigate the vegetation on summer atmospheric temperature, further simulations with improved models are needed, which will be discussed in the following section.

5.4.4 Simulation of vegetation cooling effect

The green coverage ratio is one of the common design parameters in designing the outdoor spaces, while the vegetation is one of the key factors in determining the microclimate. In order to analyse the impact of vegetation on the atmospheric temperature in this study, a set of models with different green coverage ratio are made. In order to avoid the effect of other different design features which vary in each site, models with 0%, 10%, 20%, 30%, 40%, and 50% GCR are defined in the same model (for Site No.34) in Envi-Met platform (Figure 5.32), and in the meanwhile, other variables of design features are kept constant. In this scenario, the predicted results only reveal the pattern of the individual impact of vegetations. Moreover, considering the fact that cooling effect varies in different types of vegetation, in this section, grassland is only considered in the simulation in regarding simplifying the samples.

The temperature reduction for five types of green coverage ratio on an hourly basis is shown in Figure 5.33. According to the figure, the temperature reduction effect of greening starts around 10:00 and is gradually enhanced afterwards; at 15:00, the reduction effect reaches the peak value in each type of green coverage ratio; afterwards, the effect gradually decreases in the late afternoon and the evening. Furthermore, the difference gap between each case of green coverage ratio can be witnessed during period 12:00 to 18:00.

At 15:00- the peak hour, the maximum reduction in the case of 50 per cent green coverage ratio is shown the highest in comparison to other cases, which is 0.32°C difference regarding the outside atmospheric temperature. Which is followed by the case of 40 per cent green coverage ratio with a maximum reduction of 0.26°C, and the value is 0.20°C, 0.13°C, and 0.06°C in case-30%, case-20% and case-10%, respectively. Within the middle-day hours- between 12:00 and 15:00, the cooling effect of greening reaches a maximum when the solar angle is at its peak value while the relative humidity drops to the bottom (Figure 3.9).

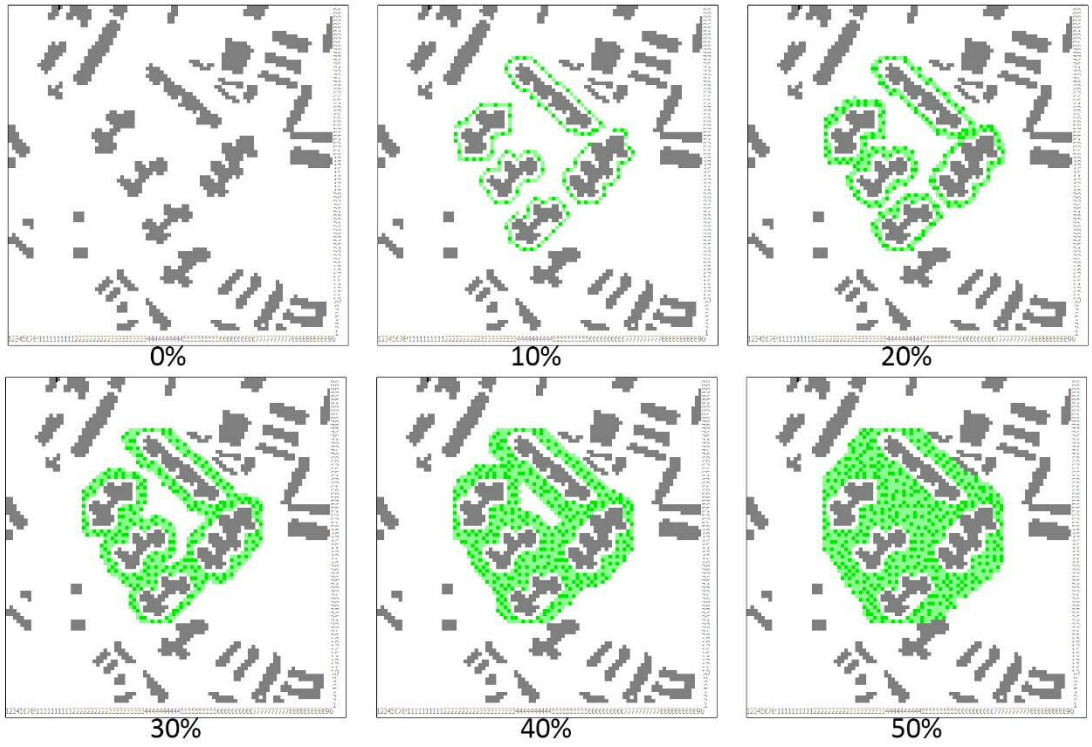

Figure 5. 32: Simulation models with different GCR on-site No.34

Because the main contributor of cooling effect in grassland in this study is evapotranspiration, which is closely related to both the air relative humidity and sunlight intensity, the middle-day hours with high solar radiation and low relative humidity promote the cooling effect of greening in summer times. Thus, the atmospheric temperature in a greener site is lower in comparison to a no-green site, which reaches its peak around 15:00 in a daily cycle. On the other hand, in the other hours (early morning and night) in a summer day, when the solar radiation is low, and the relative humidity is high, the evapotranspiration process is restricted, and the cooling rate becomes low.

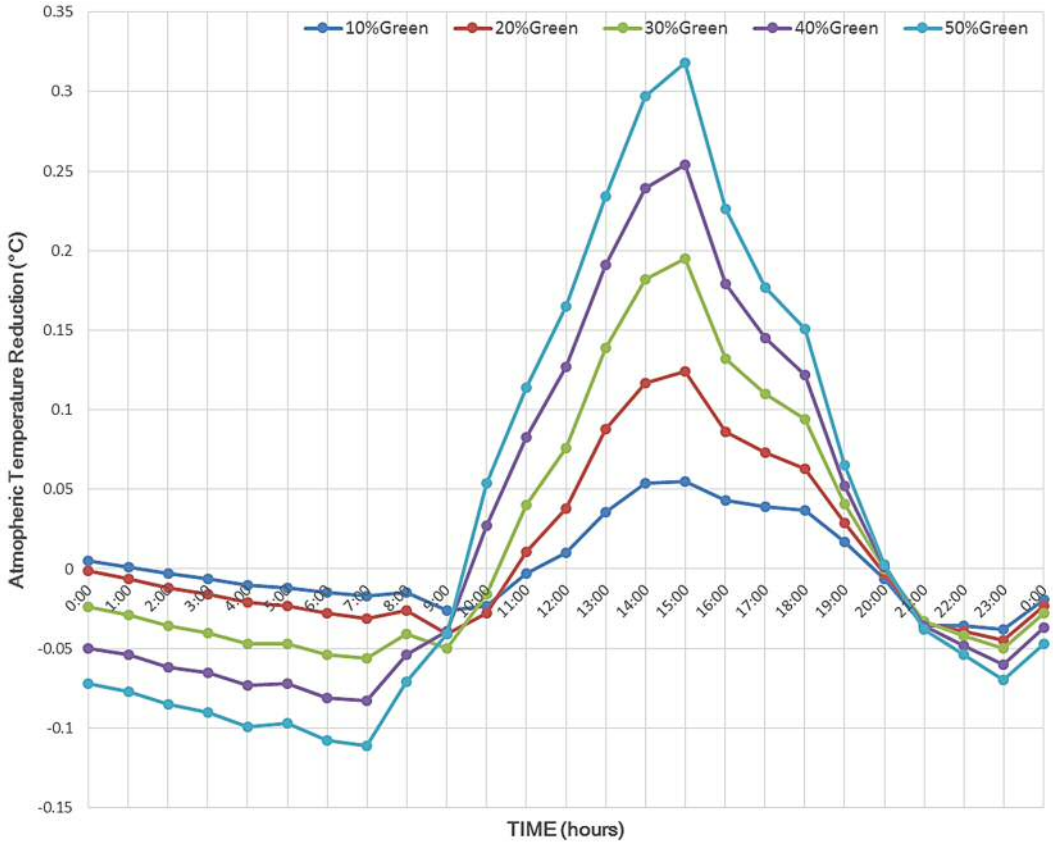

Figure 5. 33: Hourly temperature reductions for different green coverage ratios

Table 5. 5: Average temperature reduction for different GCR in different periods

Green Coverage Ratio	Average Atomspherica Temperature Reduction (°C)	
	Full Day	12:00-18:00
10%	0.00	0.04
20%	0.01	0.08
30%	0.02	0.13
40%	0.02	0.18
50%	0.03	0.22

During the period 12:00 to 18:00 (Table 5.5), model with 50% grassland coverage achieved the highest average atmospheric temperature reduction (0.22°C), which is followed by 40%, 30%, 20%, 10% GCR models with an average magnitude of 0.18°C, 0.13°C, 0.08°C and 0.04°C, respectively. According to the regression (Figure 5.34), average temperature reduction is shown in a linear pattern with GCR (only with grassland), higher temperature reduction corresponds to higher grass coverage values. The regression is shown with more than 0.05 significance (R^2 value of 0.9998), which confirms the atmospheric temperature variation due to a greening coverage variation on a site of a large-scale building group.

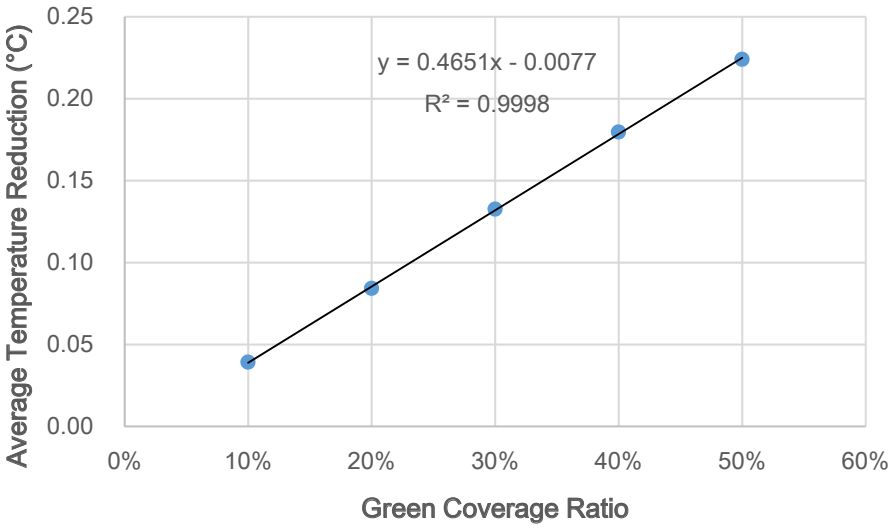

Figure 5. 34: Correlation between average temperature reductions (12:00-18:00) for different green coverage ratios

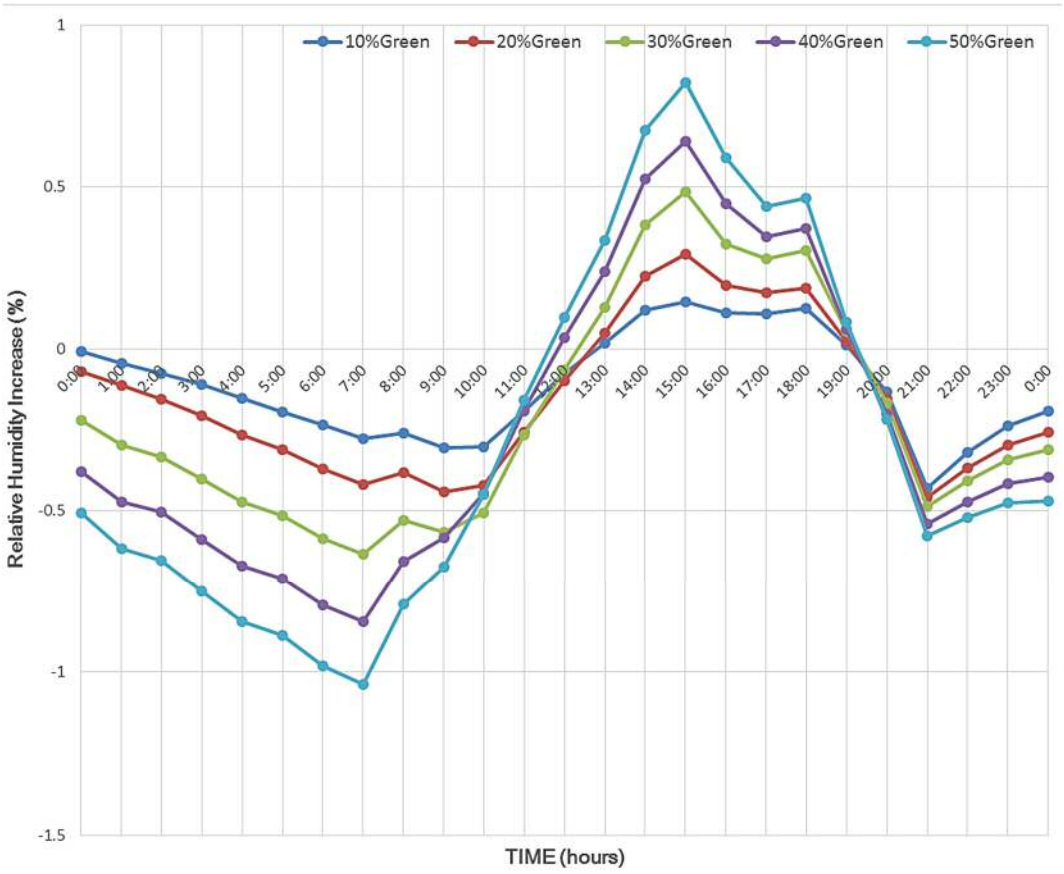

Figure 5. 35: Hourly relative humidity increase for different green coverage ratios

As discussed in previous chapters, microclimate can be impacted by altering surface albedo and relative humidity. Therefore, vegetation (grassland in this case) can influence the atmospheric temperature through these two ways. Figure 5.35 shows the

relative humidity variation due caused by different coverage of grassland. During the period between 12:00 to 18:00, the relative humidity increases up to 1%, when the atmospheric temperature is reduced (Figure 5.34). Moreover, this increase in relative humidity indicates the evapotranspiration process by grassland is cooling the outdoor environment.

It is undeniable that, tall trees can provide the extra cooling effect through shading effect, in comparison to grasses. Therefore, the simplified simulation with solo grassland for greening aims to analysis the baseline of cooling effect by vegetation. It can be estimated that more realistic models with considerable numbers of tall trees will achieve better cooling performance than this simplified case.

5.4.5 Simulation of water body cooling effect

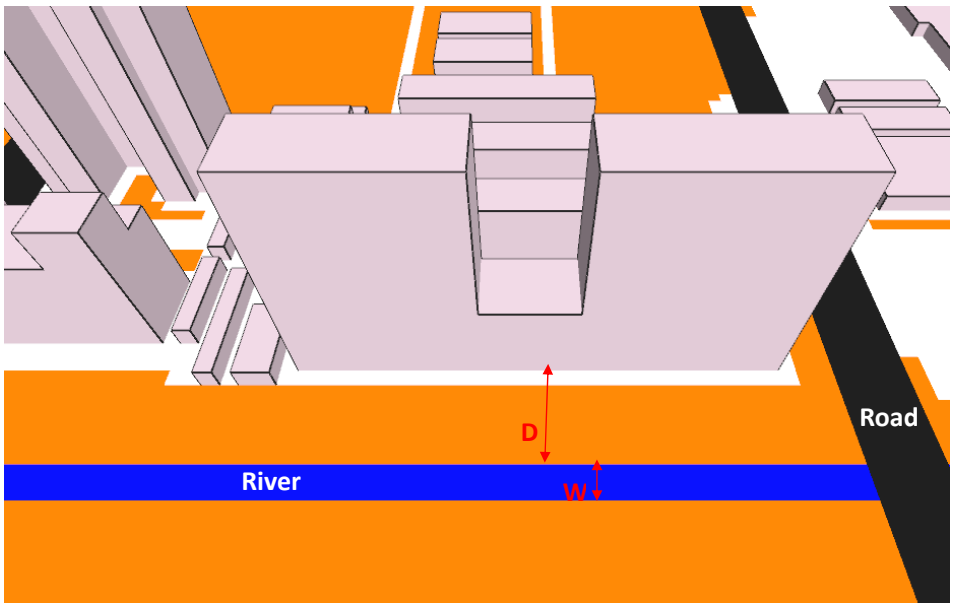

Figure 5. 36: Modelling water body in ENVI-Met on site No.69

Water bodies, including water ponds, pools, fountains, and rivers, are usually planned in city-block projects, which are initial factors of microclimate as discussed in the early chapter. In this section, small rivers are defined in models of site No.69 as further discussion of the impact of water bodies on the microclimate, especially on atmospheric temperature and relative humidity. As shown in Figure 5.36, the rivers are modelled in front the main high-rise buildings of linear group, and two variables-

Distance from the river to building, and Width of the river, are considered and analysed in each testing group. On the other hand, except for the rivers, other elements in each model are kept constant.

Table 5. 6: Temperature reduction at 2.5m away from each façade of the main building on site No.69 during 15:00 hour for different settlements of the river (unite: °C)

	D5-5	D10-5	D20-5	D30-5	D5-10	D10-10	D20-10	D30-10
E	0.051	0.040	0.027	0.021	0.092	0.072	0.051	0.039
N	0.010	0.010	0.009	0.009	0.020	0.019	0.018	0.017
S	0.061	0.041	0.026	0.020	0.103	0.073	0.048	0.037
W	0.032	0.028	0.024	0.020	0.061	0.054	0.045	0.038

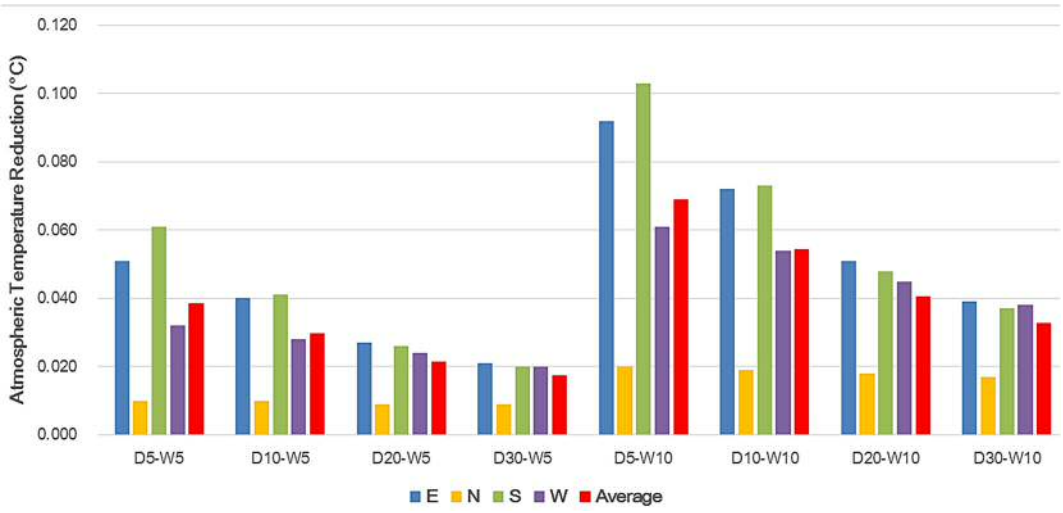

Figure 5. 37: Atmospheric temperature reduction for the different green coverage ratios

Table 5.37 shows the conditions of atmospheric temperature reduction in response to a different distance of building-river and the width of the river. The simulation results indicate that the cooling effect becomes weaker as distance to river increase. In specific, when the distance between building and river is within 5 metres, a 5-metre wide river can reduce outdoor temperature by 0.06°C, white a 10-metre wide one can achieve 0.1°C temperature reduction. As shown in Figure 5.36., the slope of temperature reduction by the river will approach zero when the distance between the building and river is larger than 20 metres. However, even the river is located 30 metres away from the building, it can still reduce more than 0.02°C (by 5-metre wide river) and

0.04°C (by 10-metre wide river) atmospheric temperature at spots in front the building façades (East, South, and West) which is closed to river. These series of simulations provide qualitative analysis for a study on the cooling effect of water bodies in city-block projects.

Moreover, based on the simulation results (Table 5.7) of relative humidity at selected points in front of each façade of the main building, there is only minor variation (less than 0.12% in all conditions) in relative humidity due to the impact of setting up of the river within site. Moreover, these results indicate the evaporation effects play a minor role in cooling the environment. In other words, air is cooled down directly by the relatively cold water bodies when winds are breezed through the river area, and these results correspond the findings on the cooling mechanism of water bodies in an urban area (Golany 1996)(Lo et al. 1997).

Table 5. 7: Relative humidity increase at 2.5m away from each façade of the main building on site No.69 during 15:00 hour for different settlements of the river (unite: %)

	D5-5	D10-5	D20-5	D30-5	D5-10	D10-10	D20-10	D30-10
E	-0.037	-0.020	-0.008	-0.006	-0.058	-0.033	-0.015	-0.011
N	0.002	0.001	-0.001	-0.002	0.003	0.001	-0.002	-0.004
S	0.029	0.019	0.008	0.002	0.048	0.032	0.013	0.003
W	0.028	0.016	0.003	-0.001	0.044	0.023	0.004	-0.003

Due to simplifications in the modelling stage, the simulations may hardly reflect all situations of practical complicity, including large fountains and lakes. However, the discussion of the simulation results provides suggestions on common design features of the city-block landscape, such as small water ponds/pools/rivers, and ravine stream.

5.5 Summary

The following research object has been achieved in this chapter:

To understand the diurnal variation of air temperature and other microclimate variables on a summer day and a winter day, accordingly;

The urban area in Chengdu has been recorded with the urban microclimate change due to dense urban settlement and lack of greening. The studies on UHI effects in Chengdu and their the distribution patterns at an urban scale are found to be a long time-span observation by collecting remote sensing data (Yang 1988) (Dan et al. 2011) (Zhang & Zhou 2013). A more than 6°C temperature difference between the urban area and rural area. Moreover, in this chapter, it also proves that the design variables of city-block projects, including building density, building plot layout, green coverage ratio, and water coverage, have impacts on the microclimate. Moreover, areas, shaded by high-rise buildings, with relative high green coverage ratio and water coverage in a short distance, have a lower atmospheric temperature in Chengdu. By comparing the calculated data derived from remote sensing images, the simulated results of all 15 selected sites are shown with considerable accuracy, thereby confirming the reliability of the research products in this chapter.

5.5.1 Urban settlement and microclimate in the summertime

Based on prediction through ENVI-Met model, it has been provided that open spaces with massive solar exposure have higher air temperatures in summer daytime in Chengdu. Moreover, the shading effect of tall buildings can effectively reduce the air temperature in summertime in Chengdu. In the meanwhile, air temperature and relative humidity are found with a relationship of compensating each other in Chengdu. The hotter areas are drier, and the relative humidity is high where the air temperature is low.

On the other hand, the urban settlement is the key to determine the pattern of wind distribution in Chengdu. In open spaces without obstacles, wind can flow through these spaces at a relatively high speed. It gets stronger where the pattern of the path is

suddenly changed, especially at the opening of the tall building group and street with building rows on both sides. In this study, the wind speed can be high in these open space. However, local wind with relatively low speed, which ranges from 1.0m/s to 3.5m/s, plays a minor role in determining the local air temperature at a microclimate scale.

According to the results of simulations, green areas are recorded with lower air temperature, which can increase the relative humidity locally with a magnitude around 1%. However, further investigations on the impact of green area on altering air temperature and relative humidity are still needed.

5.5.2 Building plot layout, density, green coverage ratio and on-site average UHI

Through the prediction of ENVI-Met, city-block scale sites in forms of the interspersed and the court are recorded with lower UHI in summer, and higher UHI in winter. On the other hand, building groups with interspersed and court plot layout are proved to have lower summer UHI and higher winter UHI, which had been verified in Chapter 4 through analysis of remote sensing observation.

In the summertime, building height is highly related to UHI intensity, compared to another design variable. Though tall buildings can provide shading effect to reduce the air temperature at the points closed to them, the over-all on-site UHI intensity is proved to be raised with the increase in building height.

In winter time, building density variables have a weak relationship with UHI. However, GCR is shown a strong relationship with UHI. Sites with high GCR tend to be warmer, which reveals a similar finding from the study in chapter 4 through remote sensing observation.

5.5.3 Vegetation, water bodies and temperature reduction in the summertime

Inspired by the findings above, further study on modification of surface elements, including vegetation and water bodies is made in this chapter. It is proved that it is

possible to cool the microclimate of city-block sites by generally increasing in green coverage ratio with the only grassland. It confirms that this modification provides up to an hourly temperature reduction of 0.32°C. Moreover, this cooling process is also proved to increase the over-all relative humidity in the daytime. On the other hand, it is found that the cooling effect of water bodies settled within city-block sites reduces up to 0.1°C air temperature within the range of 5 metres from the water body in the daytime, a larger water coverage can offer the greater effect of on-site cooling.

It is recommended that a combination of grass, tall trees and water bodies can offer an additional solution for an optimised on-site cooling strategies thereby encouraging multiple cooling mechanisms, including evapotranspiration, shading, and direct heat exchange.

Finally, it can be summarised that urban settlement, including planning of plot layout of building group, and building height and density, plays a significant role in determining urban microclimate at city-block scale. Moreover, planning outdoor features by adding sufficient coverage of multiple types of vegetation and water elements offers outstanding improvement for urban microclimate in Chengdu, which can be an additional solution of mitigating on-site UHI effect. Lastly, in regarding the comparison with data from the satellite image, the results of modelling are proved to be accurate, thereby confirming the reliability of ENVI-Met in this study.

Chapter Six

BUILDING ENERGY AND SIMULATIONS

6.1 Introduction

In this chapter, the fourth research question will be answered, which is:

> *'What are the building energy features of the city-block-scale building groups in China, and how do both the design features and microclimate condition of the urban configuration have impacts on building energy performance?'*

In order to answer the research question, this chapter aims to simulate energy demand and derive the energy supply in two stages of simulations (Figure 6.1): in the first stage of the simulation process, prototypes will be set up to investigate the building energy performance and energy use; in the second stage, the outdoor environment varied in terms of UHI values, and this is adopted by adjusting the weather data for the second simulation. Through the two stages of simulation, the impact of variation of outdoor microclimate on building energy performance will be investigated and analysed. Moreover, the influence of design factors on building energy performance will be discussed. Specifically, technical tools will be applied to simulate prototypes of 15 real estate project sites applying HTB2 and Virvil Plug-in, which are integrated with Google SketchUp.

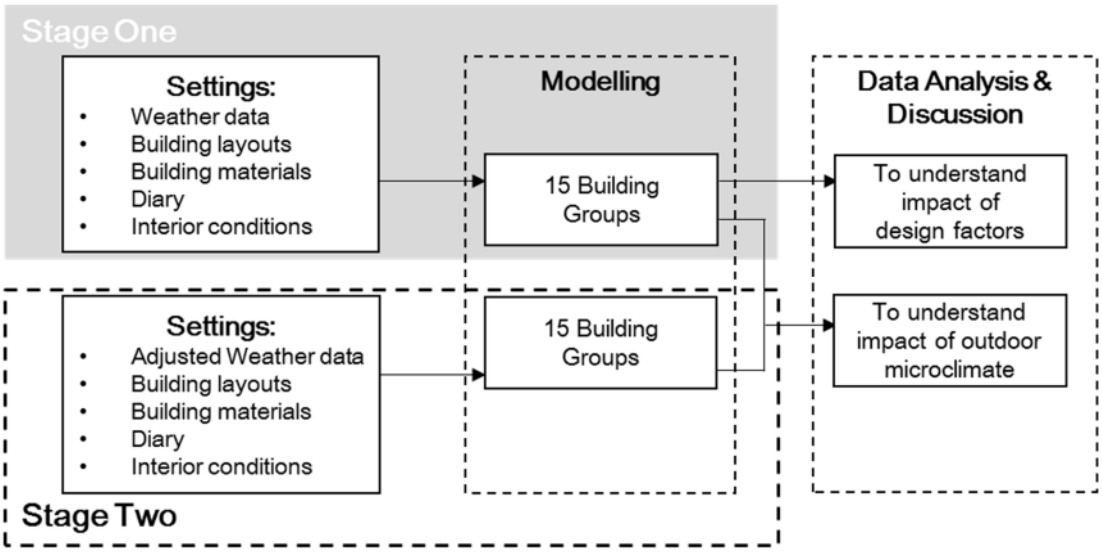

Figure 6. 1: Framework of two stages of modelling in phase three

6.2 Energy Simulation with HTB2-Virvil Plugin for selected 15 project sites

6.2.1 Introduction of modelling

As the 15 target project sites are defined into different categories according to the plot layout in Chapter 3 (Section 3.7.2), there are five group of project sites: Tower, Linear, Semi-closed, Interspersed, and Court. The settings of buildings on the project sites are reconstructed in the form of overall volume stretched from the building layout of satellite maps. The buildings rebuilt for the simulations are marked in different colours, and the surrounding buildings are defined as background group in light purple (Figure 6.2). Lastly, the configuration of construction details and indoor environmental conditions are defined according to the parameter specified in the previous section.

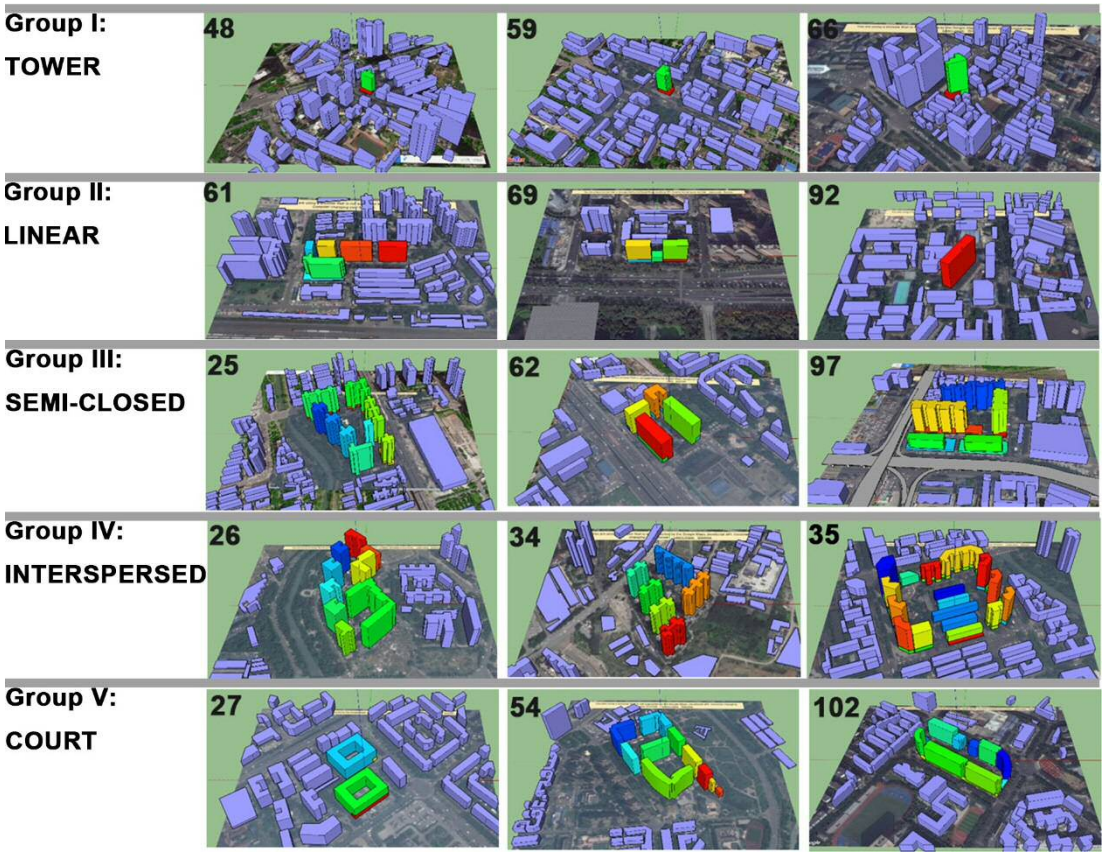

Figure 6. 2: 3D view of 15 target projects in HTB2-SketchUp Virvil Plug-in (with original project number, colours stand for different building/space ID at each site)

For each prototype in the following sections, the imagines of modelling of the target sites in SketchUp (Google 2014) will be presented in the beginning, including the pictures of facades emphasised by HTB2 Virvil Plug-in tool (WSA 2015) according to the building types and glazing ratio: Residential in green, retail in red, office in orange, roof in blue, 70% glazing-ratio façade in yellow, 30% glazing-ratio façade in light teal, 20% glazing-ratio façade in dark teal. Moreover, the detailed result of the simulations will be illustrated, which reveals the heat gain from different sources and energy demand for heating and cooling for each month. Lastly, data analysis and the relevant discussion will be carried out.

6.2.2 Tower

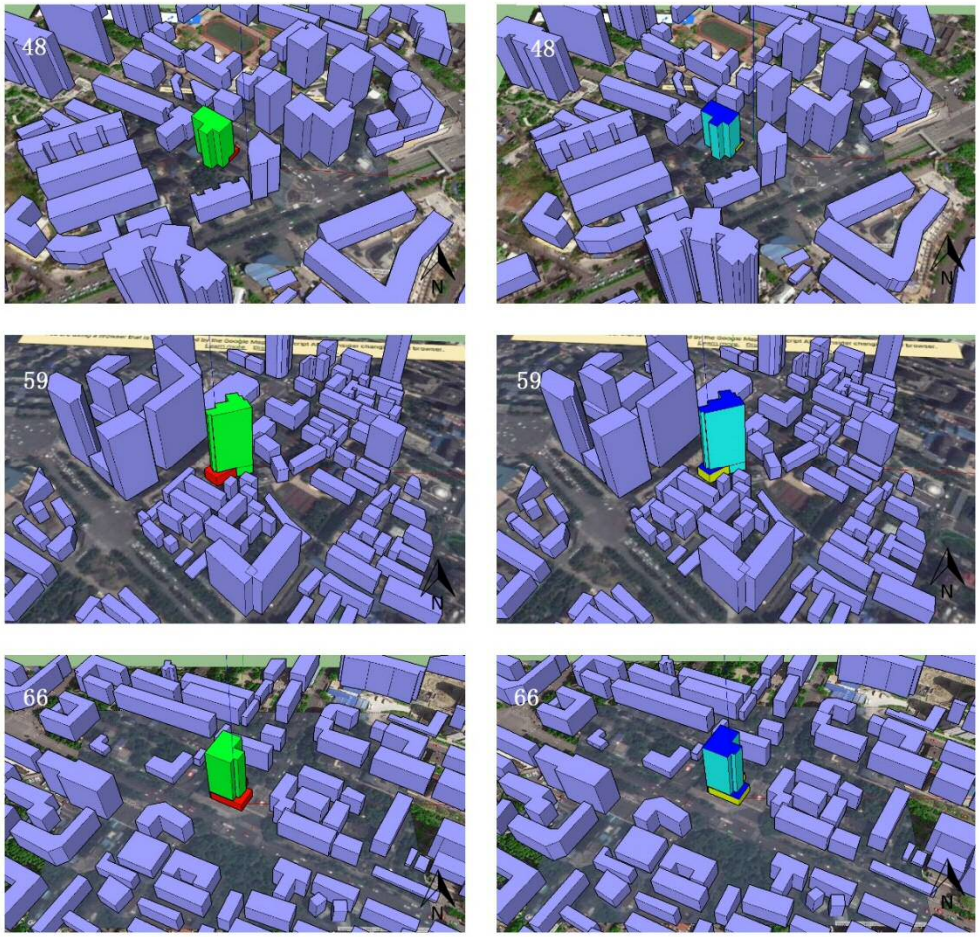

Figure 6. 3: Models of Tower Group reconstructed in SketchUp with Virvil Plug-in

The overview of the simulation result of upper floors residential of Project Site No.48 regarding energy gains is shown in Figure 6.4. There are two heat sources; incident

gain keeps steady around 2kWh/m^2 monthly all the year. Solar gain is much lower, which is around 0.4kWh/m^2 in each winter month and fluctuates around 1kWh/m^2 in each summer month. On the other hand, the fabric gain and ventilation gain stay negative, which means building itself releases the heat through ventilation and radiance by building envelope into outdoor spaces in all 12 months. And the heat loss through ventilation and fabric are high in winter, and it drops to the minimum below 0.2kWh/m^2 in July. The need for heating in winter months is as high as nearly 12kWh/m^2 in January. In summer months, the requirement for cooling is much lower and peaks at around 3kWh/m^2 in July. Lastly, there is a one month gap between heating and cooling starting from mid-September to mid-October. Generally speaking, the possible energy efficiency strategy is reducing the incident gain and solar gain in summer and mitigating heat loss due to ventilation gain and fabric gain in winter.

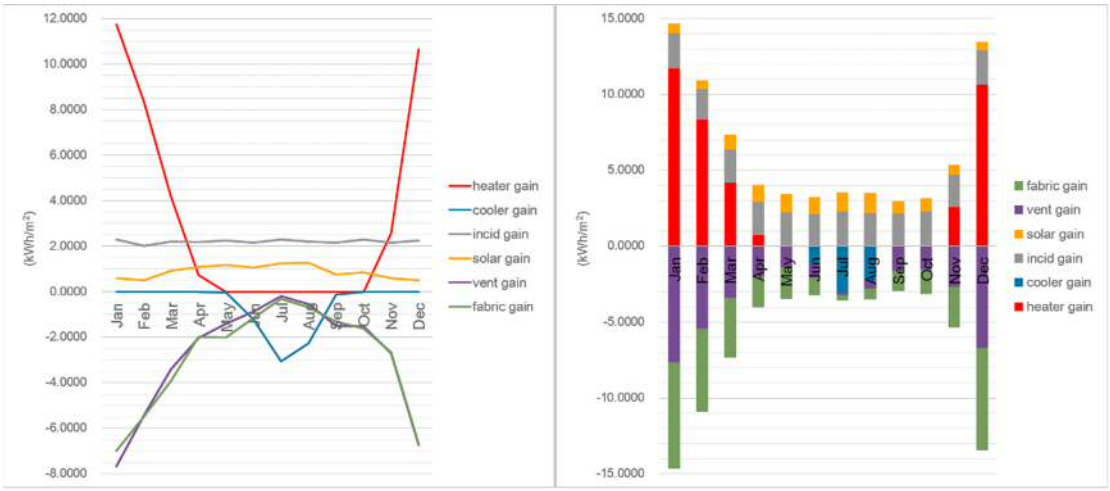

Figure 6. 4: Gain (left) and proportion (right) of monthly gain from different heat sources for residential upper floors of Site No.48

On the other hand, due to the limited total area, different gains from heat sources in the ground floor retail are much lower than the upper floor residential (Figure 6.5). The monthly solar gain is as low as 1kWh/m^2 in winter and 3kWh/m^2 in summer, while the incident gain still leads all the heat sources at a constant level around 16kWh/m^2 monthly all the year. Moreover, ventilation gain in June, July and August brings in as much as 2kWh/m^2 heat in a month, while it takes away much more heat in winter months. Lastly, the fabric gain keeps removing heat from building into fabric all the year,

fluctuating from minimum 12kWh/m^2 to maximum 23kWh/m^2 monthly. Therefore, reducing the energy loss through ventilation and fabric provides opportunities to mitigation heating demand, while lowering incident gain and increase ventilation loss is a potential energy saving strategy for summer months.

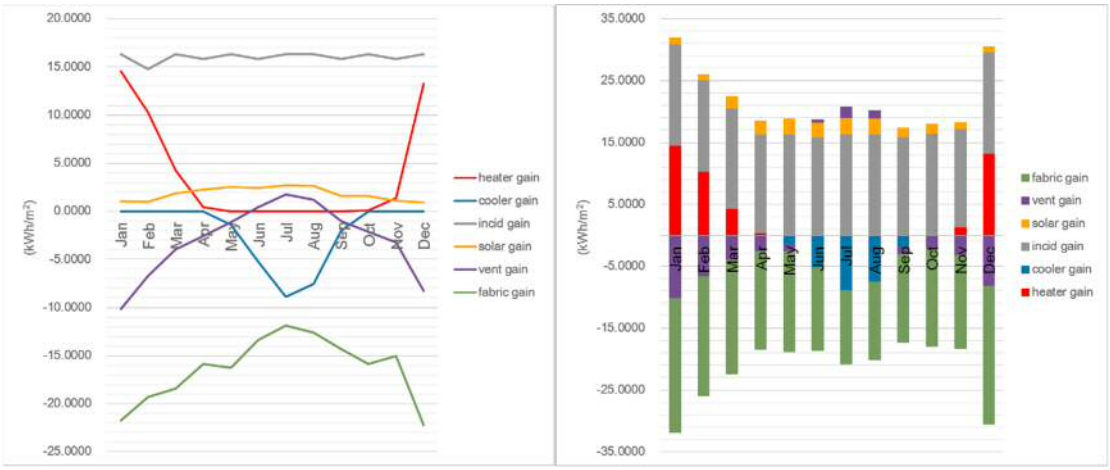

Figure 6. 5: Gain (left) proportion (right) of monthly gain from different heat sources for ground floor retail of Site No.48

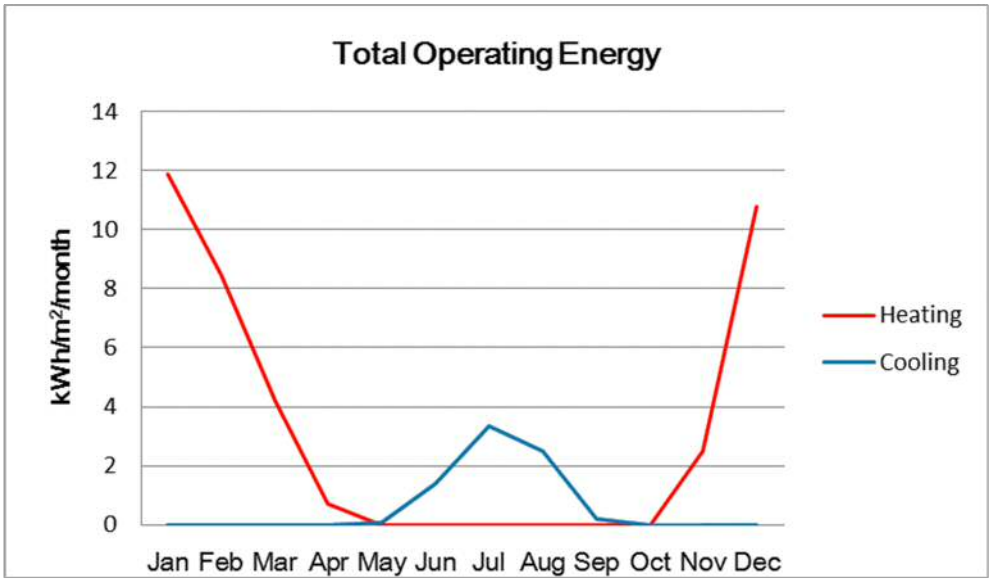

Figure 6. 6: The total operating energy for heating & cooling in site No.35

As a unity, project site No. 48, heating demand in winter is much higher than the peak value of cooling demand in summer (Figure 6.6). Specifically, the heating demand in January is nearly 12kWh/m^2/month. It drops to zero from May until October, when the cooling demand starts increasing and reaches the peak value of 3.5kWh/m^2/month in July.

6.3.3 Linear

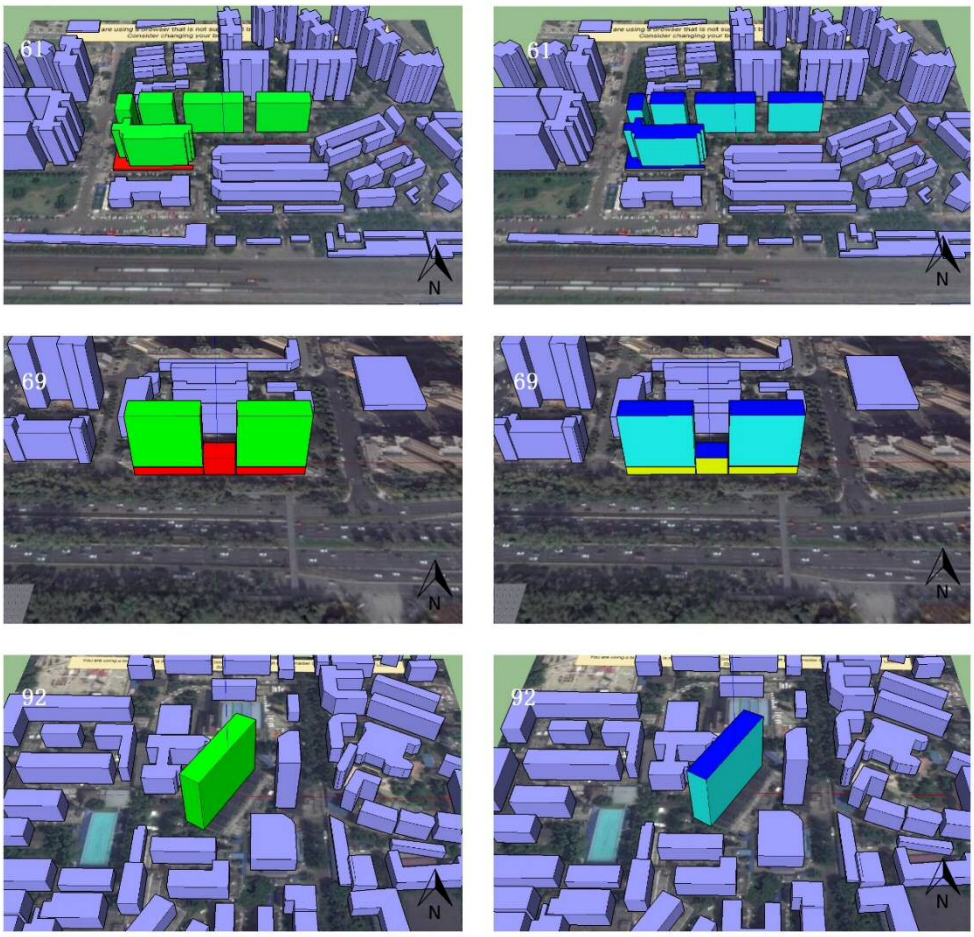

Figure 6. 7: Models of Linear Group reconstructed in SketchUp with Virvil Plug-in

The simulation results of retail building No.2 and residential building No.3 of Site No. 69 are shown in Figure 6.8 and Figure 6.9, respectively. In retail building No.2 (Figure 6.8), incidental gain keeps steady above 15kWh/m^2 every month, while the solar gain is around 1kWh/m^2 in winter months and increased to 2kWh/m^2 in other seasons. Moreover, ventilation gain contributes 0.5kWh/m^2 monthly in July and August, while in other months it helps building to release heat into outdoor spaces. Fabric gain could benefit mitigating the vast amount of cooling demand in most months of the year, except for January. In this case, there was no need for heating all the year round.

Gains by different heat sources to residential building No.3 are shown in Figure 6.16. Comparing to retail building No.2, the incidental gain keeps at the same level while the solar gain in residential is about ten times higher and ventilation gain stays negative all the year round. Consequently, massive heating demand is needed in proximately

half a year from mid-October to mid-May next year. On the other hand, cooling demand occurs in three summer months, which peaks at the same level as retail building No.2 in July.

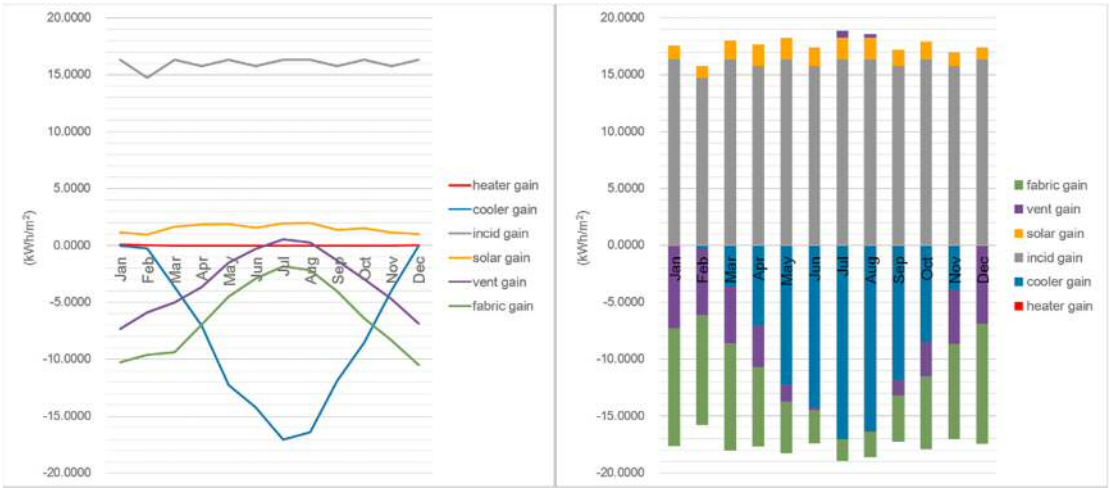

Figure 6. 8: Gain (left) and proportion of monthly gain (right) from different heat sources for retail building No.2 of Site No.69

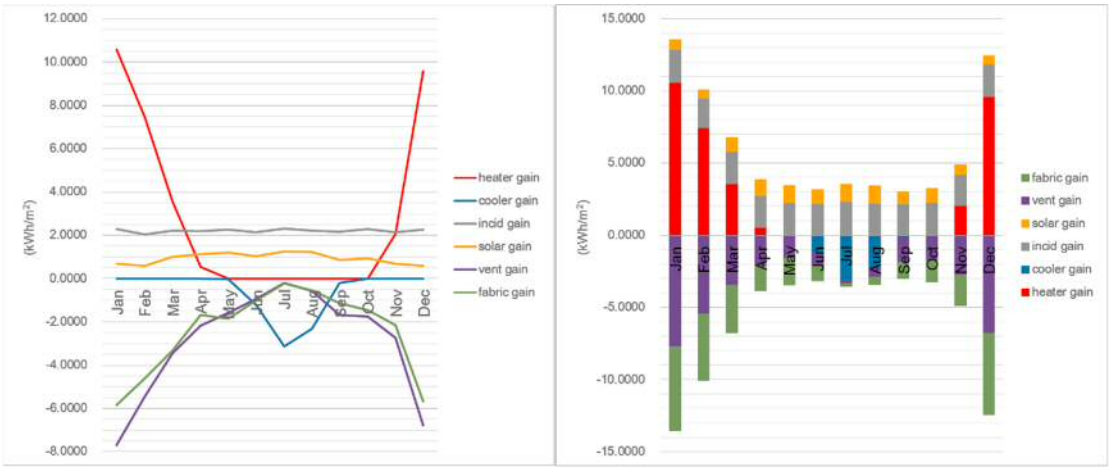

Figure 6. 9: Gain (left) and proportion of monthly gain (right) from different heat sources for residential building No.3 of Site No.69.

When taking all buildings of site No.69 into consideration, there is clear cooling period starting from February to December and heating period in winter and midseason months (Figure 6.10). The highest heating demand- 8.3kWh/m^2/month appears in January, and cooling demand rises to 5.5kWh/m^2/month in July.

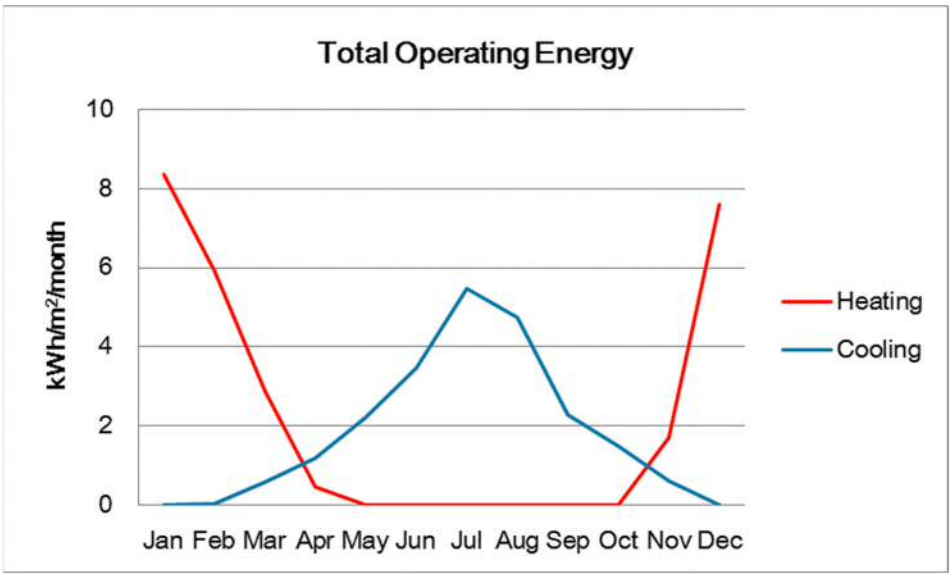

Figure 6. 10: The total operating energy for heating & cooling in site No.69

6.3.4 Semi-closed

Site No. 62 is shown as an example for data analysis for this group. According to Figure 6.12, in retail space No.2, the gains due to incidental and solar are lower than the loss by ventilation and fabric in winter times, which leads 6kWh/m^2 heating demand in both December and January. Incidental gain stays the constant 16.3kWh/m^2 monthly during the period between April and October, which contributes the cooling demand up to 15kWh/m^2 in July, together with 3.8kWh/m^2 heat from solar and 1.3kWh/m^2 gain due to ventilation. In winter times, the heating demand is as low as one- third of the peak value of cooling demand. Avoiding the heat loss due to ventilation and fabric could save energy for heating in winter.

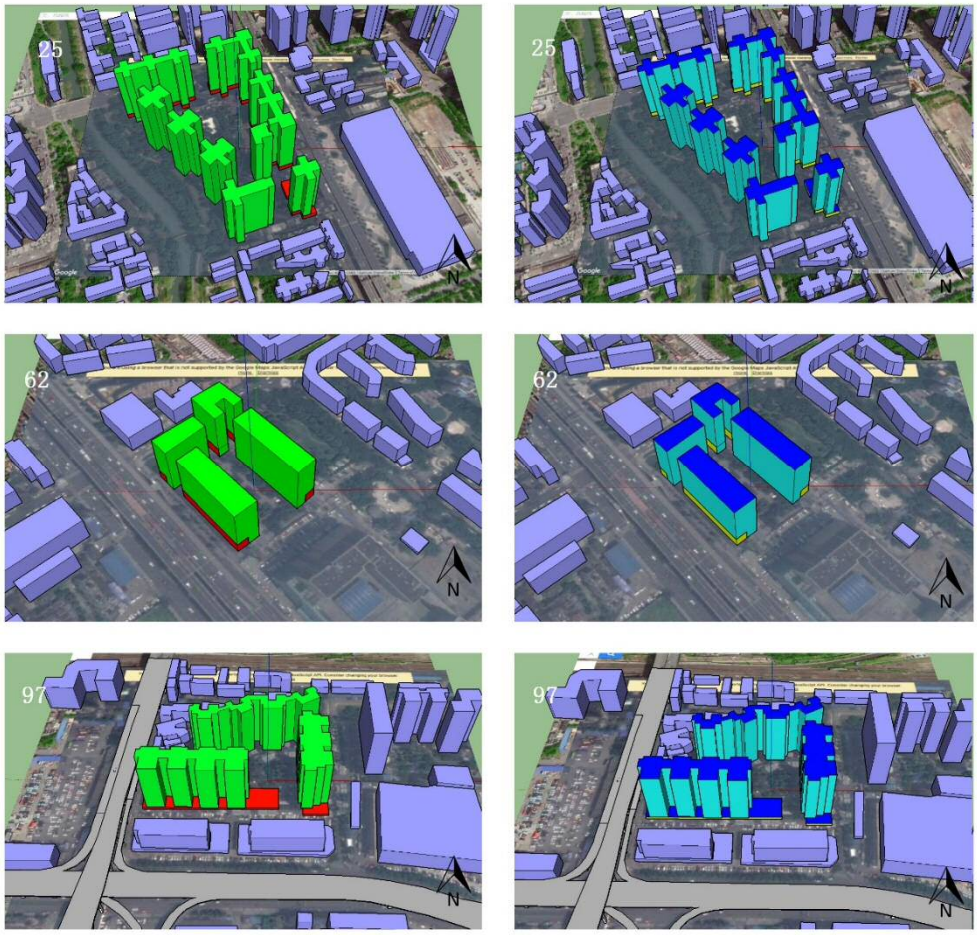

Figure 6. 11: Models of Linear Group reconstructed in SketchUp with Virvil Plug-in

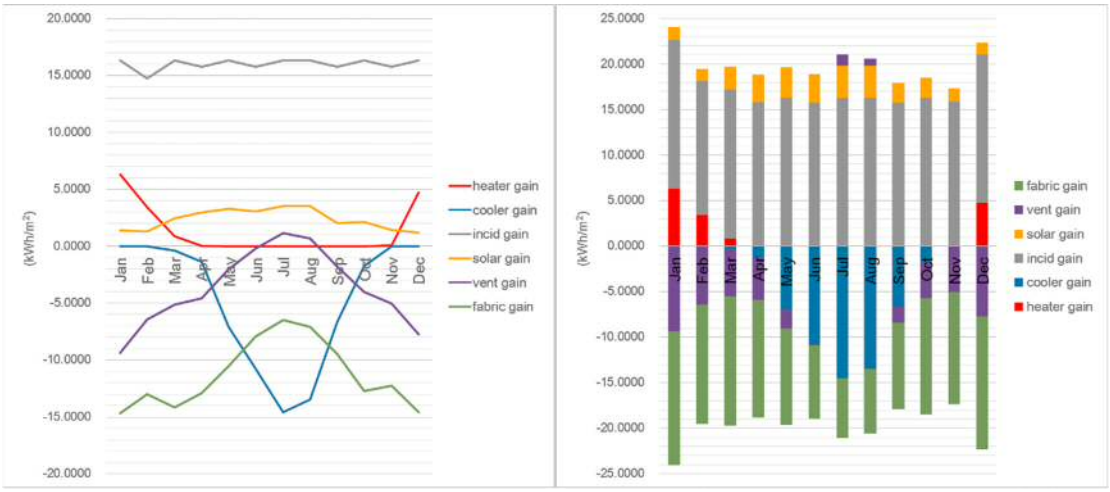

Figure 6. 12: Gain (left) proportion (right) of monthly gain from different heat sources for retail space No.2 of Site No.62

For the No. 5 spaces of residential upper floors (Figure 6.13), the incidental gain and solar gain stay constant in each month, while the intensity of the former is more than ten times higher than that of the later. In the meanwhile, ventilation gain and fabric gain

keep negative in the whole year indicating that heat is lost from buildings into outdoor spaces through both ways. Therefore, increasing the heat loss through ventilation and fabric while reducing the incidental gain and solar gain could be possible mitigation strategy for reducing cooling demand in the three summer months; reducing the heat loss due to ventilation and fabric is potentially reducing the heating demand in winter and mid-seasons.

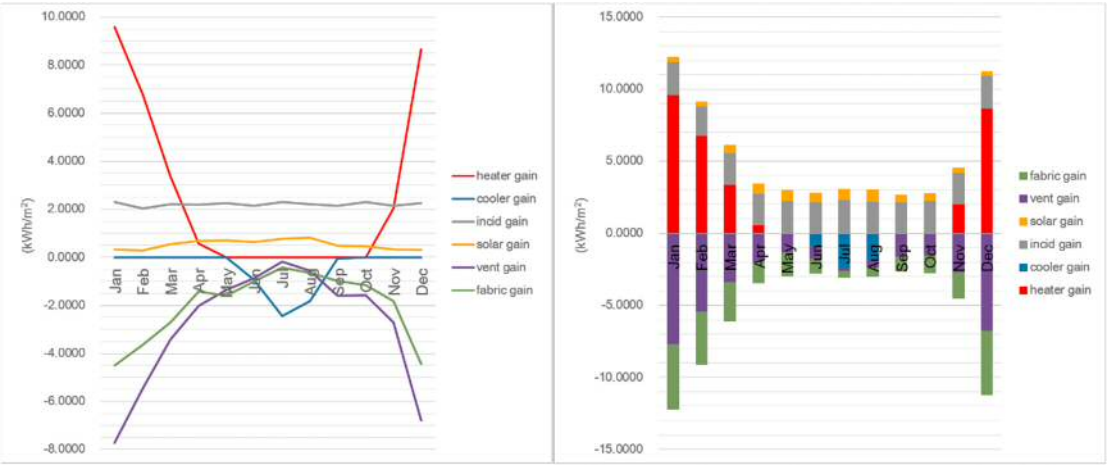

Figure 6. 13: Gain (left) proportion (right) of monthly gain from different heat sources for residential space No.5 of Site No.62

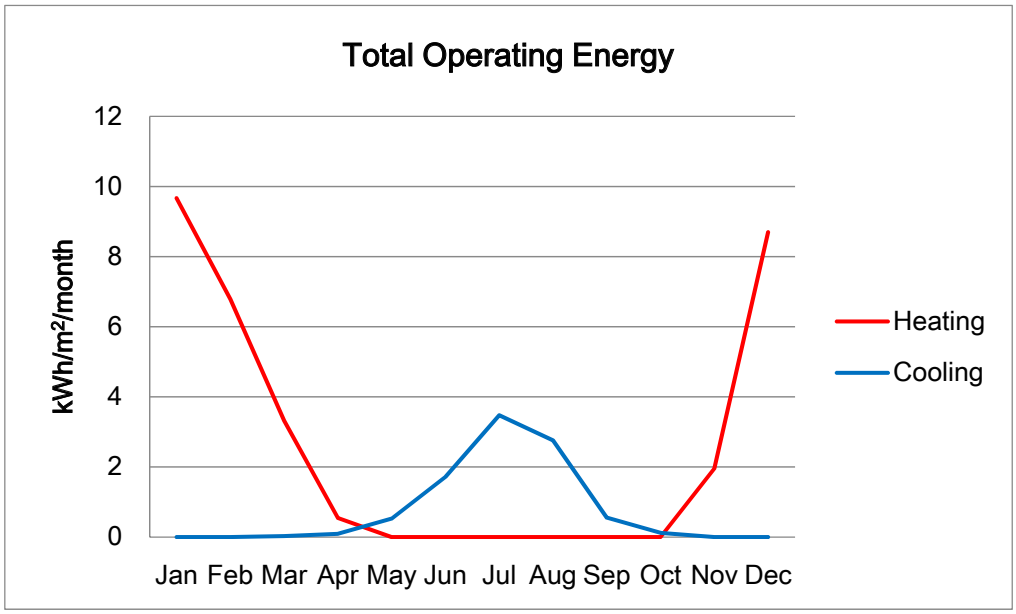

Figure 6. 14: The total operating energy for heating & cooling in site No.62

For the entire project of Site No.62 (Figure 6.14), the peak value of cooling demand in summer occurs in July, which is 3.5 kWh/m^2/month, and exchange time for switching

the heating and cooling appears at the end of April and late October. While the heating demand in winter rises to more than 9.5kWh/m^2/month, which is almost three time of peak value of cooling demand in summer.

6.3.5 Interspersed

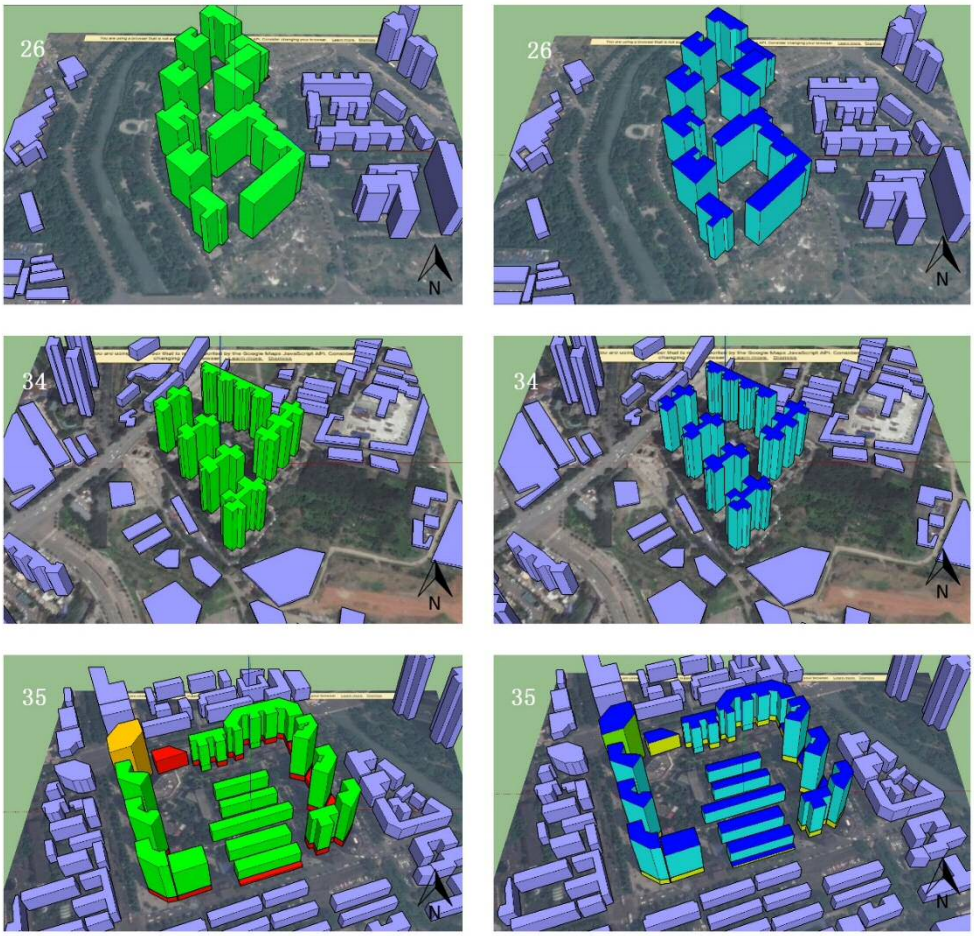

Figure 6. 15: Models of Interspersed Group reconstructed in SketchUp with Virvil Plug-in

Taking Site No.35 as an example for this site group, the simulation results for office building No.1, retail building No.7, and residential building No.11 are shown in Figure 6.18, Figure 6.17, and Figure 6.16, respectively. Incidental gain is the leading heat source for all three buildings, which is around 16kWh/m^2/month in the retail building, 2.2kWh/m^2 monthly in the residential buildings, and 9kWh/m^2 in an office building. And solar gains are as low as one-sixth of incidental gains in each case. Ventilation gain brings a small amount of heat in July and August to retail building No.35 and helps building to release heat in all the other months. While in the other two buildings,

ventilation keeps taking away heat from the building into outdoor all the year. In the three buildings, substantial heat loss due to radiance to the fabric in winter, and in summer times there is still a considerable amount of energy released due to the fabric.

Consequently, for retail building No.11 and office building No.1, the cooling period for retail is long starting from March to the end of December with massive cooling demand up to 18kWh/m^2 per month and 11kWh/m^2 per month, respectively. On the other hand, heating is only needed in January and the end of December in a small amount in both buildings. For residential building No.7, cooling demand is as low as 2kWh/m^2 in July, and the cooling period is just for three months; however, heating demand is substantial in winter and midseason. Reducing the heat loss due to ventilation and fabric could be a possible energy-saving strategy in these seasons.

As shown in Figure 6.19, due to a large number of retail buildings and a massive-volume office building, cooling demand for the entire Site No.62 is massive with an extended operating period and the peak value of 5kWh/m^2/month. Heating demand is over 9kWh/m^2/month in both January and December, and it drops to below 2kWh/m^2/month in April and November.

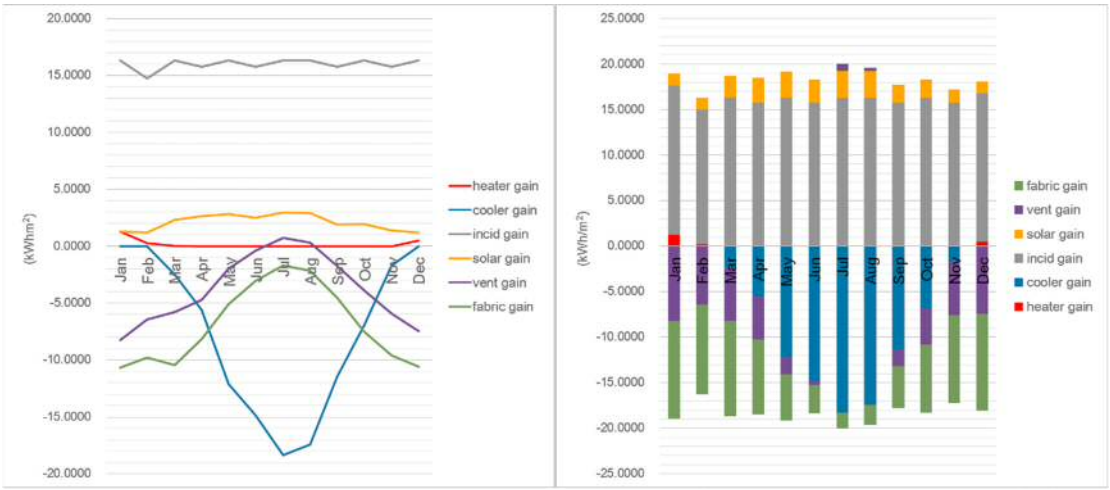

Figure 6. 16: Gain (left) proportion (right) of monthly gain from different heat sources for the retail building No.11 of Site No.35

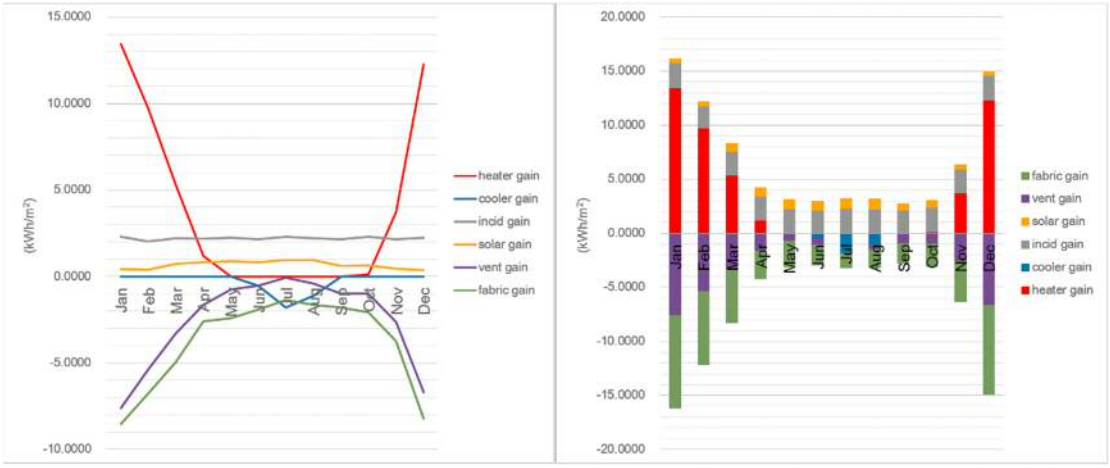

Figure 6. 17: Gain (left) proportion (right) of monthly gain from different heat sources for residential building No.7of Site No.35

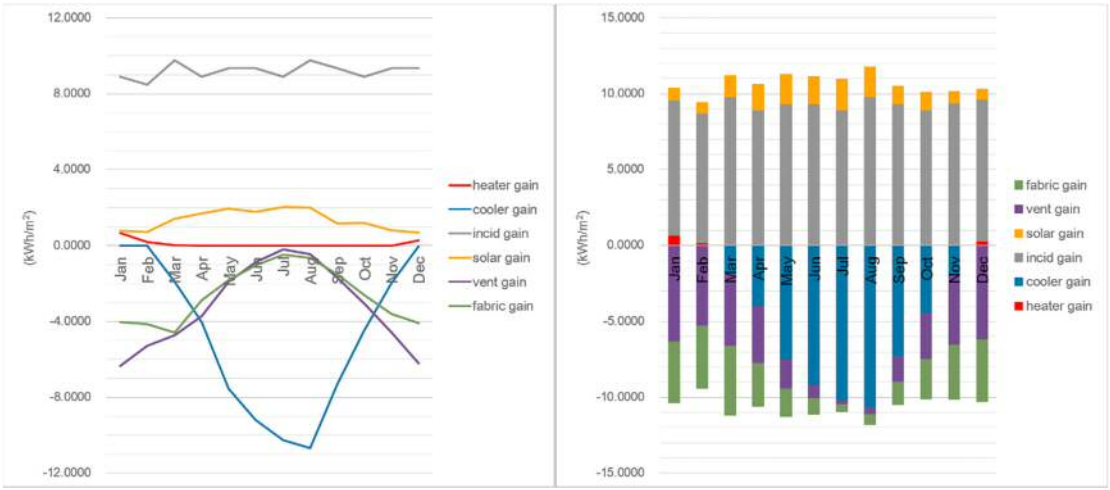

Figure 6. 18: Gain (left) proportion of monthly gain (right) from different heat sources for the No.1 office building of Site No.35

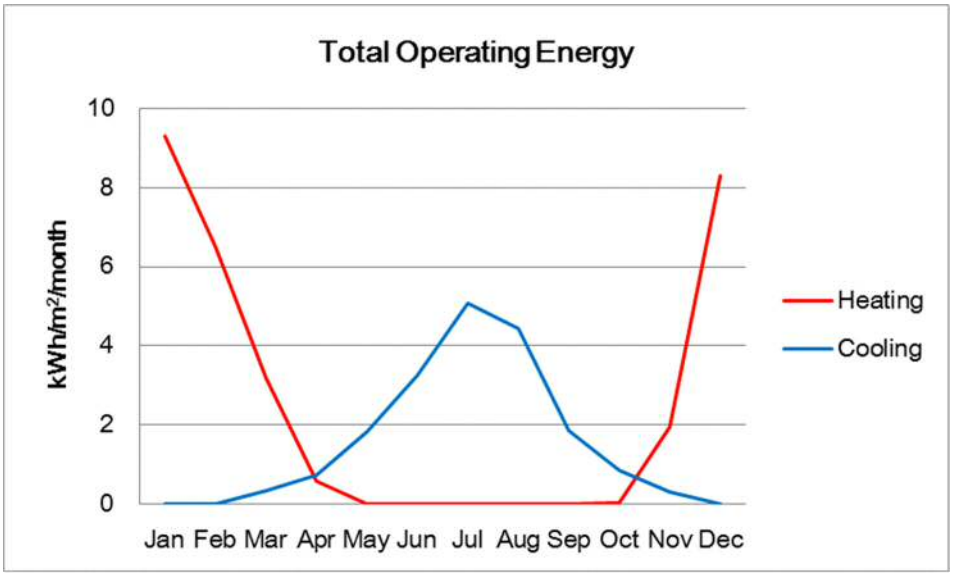

Figure 6. 19: The total operating energy for heating & cooling in site No.35

6.3.6 Court

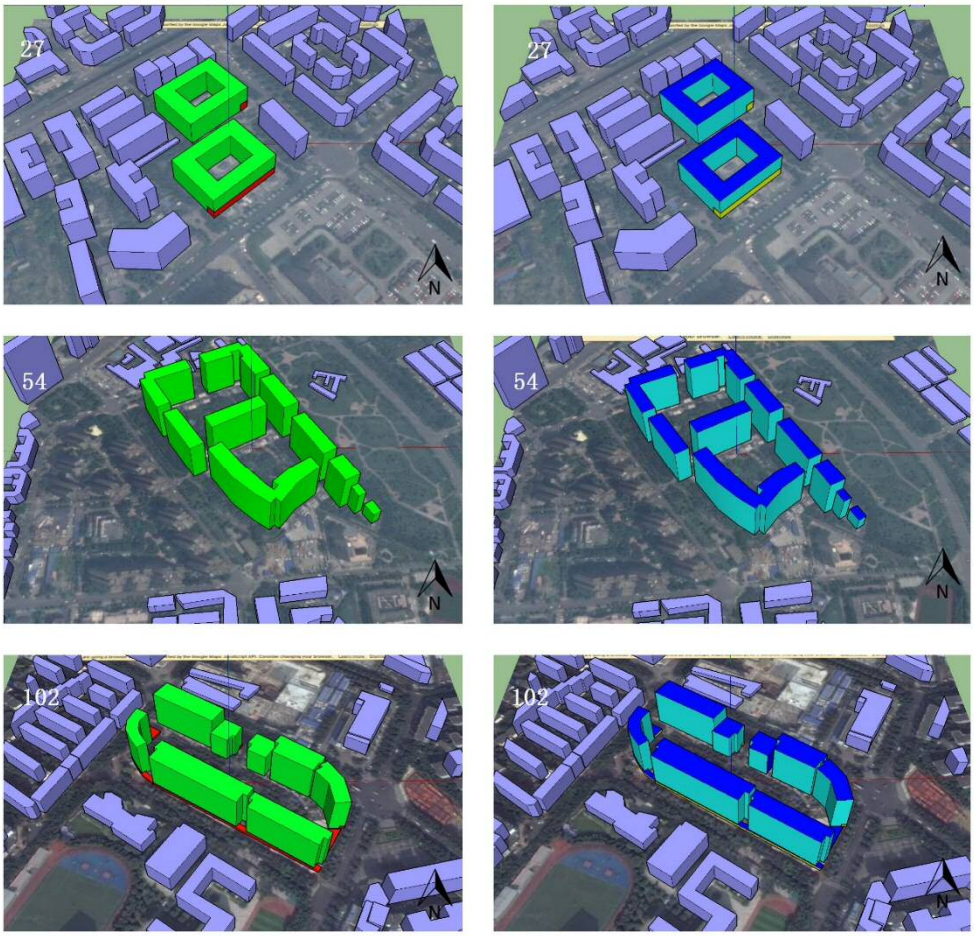

Figure 6. 20: Models of Interspersed Group reconstructed in SketchUp with Virvil Plug-in

Site No.27 is chosen as the example of 'Court Group' for data analysis. The simulation result of the upper floor residential space No.1 is shown in Figure 6.21. The incidental gain is the primary heat source, which is steady at 2kWh/m^2 per month all the year. The solar gain fluctuates below 0.2kWh/m^2 in winter and mid-season and increases to 0.5kWh/m^2 in summer times. On the other hand, the ventilation gain and fabric gain continuously take out heat from buildings all the year, which are up to 8kWh/m^2 per month and 5kWh/m^2 per month in winter, respectively. Moreover, heat is still released through ventilation and fabric in summer: the fabric 'release' drops to 1kWh/m^2 per month in July; in the meanwhile, ventilation 'release' returns zero. Due to all these heat loss, heating demand in the upper floor apartments is up to 10kWh/m^2 per month in January and the operating time for it start from late October to the end of April; cooling demand is relatively low, whose peak value is around 2kWh/m^2 in July.

For the ground floor retail space No.3, the simulation result is shown in Figure 6.22. The incidental gain fluctuates at a high level (16kWh/m^2 per month), and the solar is nearly 3kWh/m^2 in summer and mid-season while it drops to 1kWh/m^2 per month in winter times. Ventilation gain brings in the heat for buildings around 1kWh/m^2 per month in July and August. It helps to release heat from buildings in other months, which is up to 9kWh/m^2 per month in January and December. Lastly, fabric gain follows the trend of ventilation gain all the year and keeps taking out 7kWh/m^2 more heat in each month than ventilation. Finally, a heating period in this retail space starts from April to October, and the highest values of heating demand appear in July and August; on the other hand, heating demand is relatively lower than the cooling demand, and its operating period covers winter months and part of March.

As shown in Figure 6.23, due to a significant portion of residential spaces in this Site No.27, the peak value of cooling demand is more than 2kWh/month in July and the operating period covers summer months starting from May to September. In the rest months, heating is being operated and reaches its peak value-10.3kWh/m^2/month - in early January.

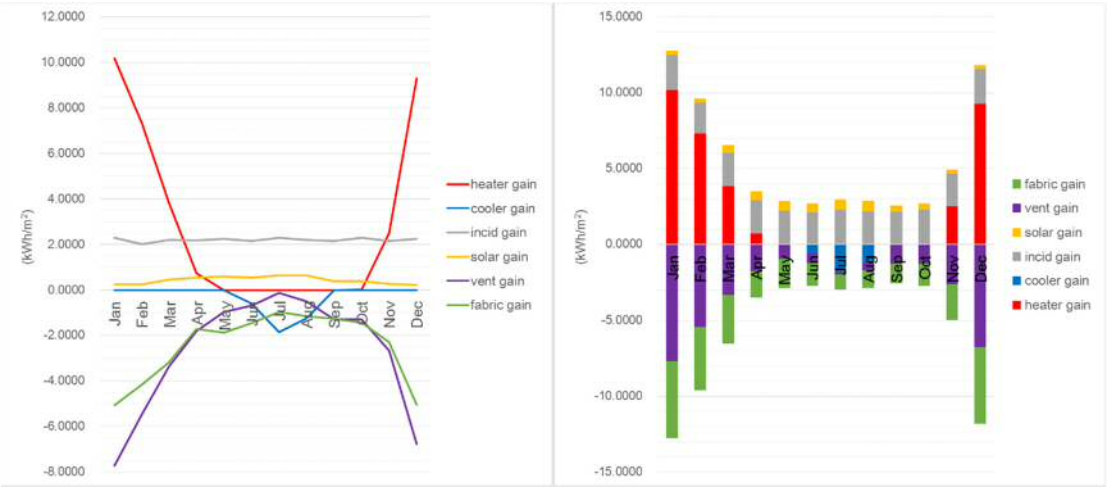

Figure 6. 21: Gain (left) proportion of monthly gain (right) from different heat sources for the No.1 residential building of Site No.27

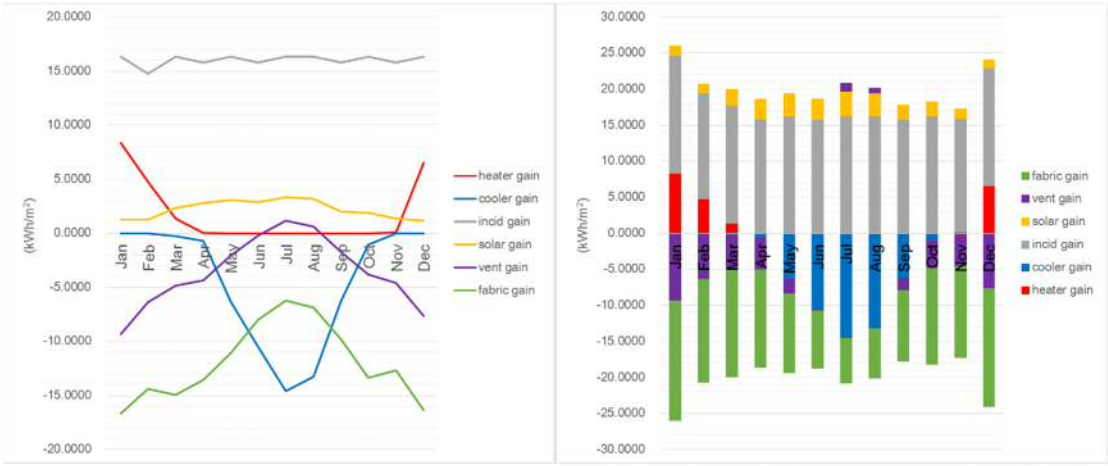

Figure 6. 22: Gain (left) Proportion of monthly gain (right) from different heat sources for the No.1retail building of Site No.27

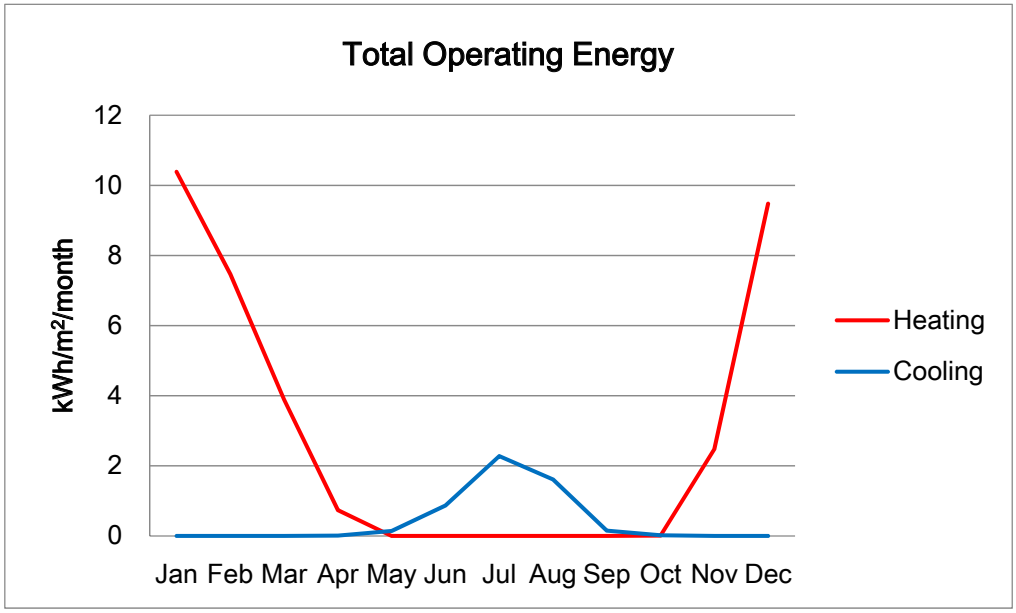

Figure 6. 23: The total operating energy for heating & cooling in site No.27

6.4 Data analysis and discussion

Base on the simulation results, the energy consumption of each building/functional spaces in every 15 target project sites are obtained. According to this series of data, the following findings can be summarised.

6.4.1 The structure of heat sources

The structure of heat sources varies in different buildings with a different function. The impacts due to different gain sources generally remain in each type of buildings in target project sites. The incidental gain overwhelmingly stays at a high level in the full year in all cases, comparing to other heat sources. Solar gain rises to its highest level in the period from March to mid-September in every type of buildings. On the other hand, even the heat loss due to ventilation and fabric is substantial, massive incidental gain and solar gain in retail and office buildings could balance those heat loss. In terms of residential buildings, due to lower incidental gain than the other two types of buildings, a vast amount of heat loss due to ventilation and fabric cause substantial heating demand.

Consequently, cooling demand is relatively low and the operating period (or summer time) is short in residential buildings, comparing to retail and office buildings. For retail and office buildings, summertime is extended from June-to-August to May-to-September. Heat due to ventilation gain increases the cooling load in July and August in most retail buildings. Moreover, at some sites, the cooling demand for retail and office is still high in April and October. Generally speaking, the heat accumulated by incidence, solar, and ventilation are usually rebalanced by air conditioning systems. Therefore, in both types of buildings, heating demand is retained at a very low level, which is nearly zero in most cases. And the heating operating period is limited in the winter time. For residential buildings, heating demand is substantial and the working time is long. Which means there is still a need for heating in mid-seasons, such as March, April and October. However, there is no tradition for heating in dwellings in Chengdu (Li 2012), actual energy consumption for heating in residential buildings is

barely observed. Local residence prefers shutting down windows and wear outdoor clothes when they are living indoor in the winter time.

6.4.2 Possible mitigation strategies

According to the structure of heat gain in buildings with different functions, possible mitigation strategies for energy saving vary. In the summertime, reducing the incidental gain and a solar gain is a practical approach for all types of buildings to cut down the heat accumulated inside of buildings. Furthermore, preventing ventilation gain is another possible method for further reduction of cooling consumption, especially in retail buildings. On the other hand, heat from the different heat source is balanced in most retail and office buildings, but the massive heat loss due to ventilation and fabric cause enormous energy for heating residential indoors. Therefore, preventing these sorts of heat loss could be a potential strategy for maintaining the further livable domestic indoor environment.

6.4.3 Average energy demand for heating/cooling

Through the simulation process, average energy demand for heating/cooling in buildings of 15 target project sites can be obtained (Table 6.1 and Figure 6.24). Heating demand in residential buildings is 32.98 kWh/m^2/year, which is much highest value comparing to the 8.41 kWh/m^2/year in retail buildings and 1.15 kWh/m^2/year in an office building. However, as mentioned in the previous section, heating for domestic indoors is beyond the traditional winter lifestyle in the region, thereby minimising the importance of a large number of heating demand in residential buildings. On the other hand, cooling demand in residential building is only 5.93 kWh/m^2/year, and it is much lower than the other two types of buildings. For retail and office buildings, cooling demand is 61.49 kWh/m^2/year and 57.39 kWh/m^2/year, respectively. Generally speaking, in the 15 sites, both types of public buildings have higher total energy demand for heating/cooling than residential buildings (Figure 6.25 and Figure 6.26), especially for cooling demand. Moreover, the cooling demand is significantly higher than heating demand in most cases of public buildings, except for the retails on Site

No.27 and Site No.102.

6.4.4 Possible design factors impact the structure of energy demand

The other design features, such as building function, plot-layout, building density factors, could be possible factors to impact the structure of energy demand in all types of building:

i) Plot-layout and building energy demand

As illustrated in Figure 6.25 and Figure 6.26, the energy demand varies in sites of different plot-layout. Retails in Tower, Linear and Semi-closed groups have more than 64 kWh/m^2/year energy demand for cooling, and cooling demand in retails of the Interspersed Group have lower than 58 kWh/m^2/year cooling demand. However, Retails in Court is shown with the lowest cooling demand, which is just half of the values in Linear Group. Noticeably, heating demand in retails of Court Group is more than its cooling demand, while the values in other groups are lower than 15 kWh/m^2/year, mostly less than 7 kWh/m^2/year. Moreover, there was no significant variation in energy demand in a residential building with five different layouts: except for lower than 30 kWh/m^2/year values in court group, residential buildings with other four types of plot-layout have around 34 kWh/m^2/year heating demand. Generally speaking, court and linear are shown with the lowest energy demand in both heating and cooling.

Table 6. 1: The result of simulations of heating and cooling demand for all sites.

Full Year Simulation			Building floor area (m^2)	Energy Demand (kWh/m^2/year)	
				Heating	Cooling
Tower	Site-48	1 Residential	8378.30	38.2554	-6.6751
		1 Retail	425.80	44.3693	-26.3508
	Site-59	1 Residential	26933.47	33.7405	-7.2311
		1 Retail	4290.31	6.7277	-63.0636
	Site-66	1 Residential	10815.93	34.1768	-10.0595
		1 Retail	2456.48	0.2684	-72.6747
	Group Mean	Residential	46127.70	34.66	-7.79
		Retail	7172.59	6.75	-64.18
Linear	Site-61	5 Residential	107212.50	32.0350	-5.3427
		5 Retail	5524.30	10.3191	-52.1088
	Site-69	2 Residential	28903.30	34.0797	-6.3771
		3 Retail	7782.23	0.2078	-80.3516
	Site-92	1 Residential	28905.20	30.2819	-7.2599
	Group Mean	Residential	165021.00	32.09	-5.86
		Retail	13306.53	4.41	-68.63
Semi-Closed	Site-25	9 Residential	486986.63	33.2768	-6.5309
		5 Retail	35075.83	0.2119	-72.9283
	Site-62	4 Residential	80516.83	32.0530	-5.5315
		4 Retail	6318.33	17.2501	-57.0961
	Site-97	3 Residential	107851.43	36.4049	-6.1166
		2 Retail	5214.93	8.8084	-19.0222
	Group Mean	Residential	675354.90	33.63	-6.35
		Retail	46609.09	3.48	-64.75
Interspersed	Site-26	9 Residential	237790.50	33.6031	-6.3319
		1 Retail	1013.75	13.0142	-24.7671
	Site-34	6 Residential	270716.60	35.1563	-6.7048
	Site-35	15 Residential	192406.27	37.2616	-6.1734
		18 Retail	25983.77	14.7588	-57.6869
		1 Office	36049.90	1.1476	-57.3904
	Group Mean	Residential	700913.37	35.21	-6.43
		Retail	26997.52	14.69	-56.45
		Office	36049.90	1.15	-57.39
Court	Site-27	2 Residential	66129.37	34.0757	-3.7597
		2 Retail	2009.29	46.5982	-49.1384
	Site-54	10 Residential	453380.70	28.4654	-5.5161
	Site-102	8 Residential	103800.93	33.3291	-5.2364
		9 Retail	2719.43	26.2263	-22.8968
	Group Mean	Residential	623311.00	29.87	-4.78
		Retail	4728.71	34.88	-34.05
Overall		Residential	2210727.97	**32.98**	**-5.93**
		Retail	98814.44	**8.41**	**-61.49**
		Office	36049.90	**1.15**	**-57.39**

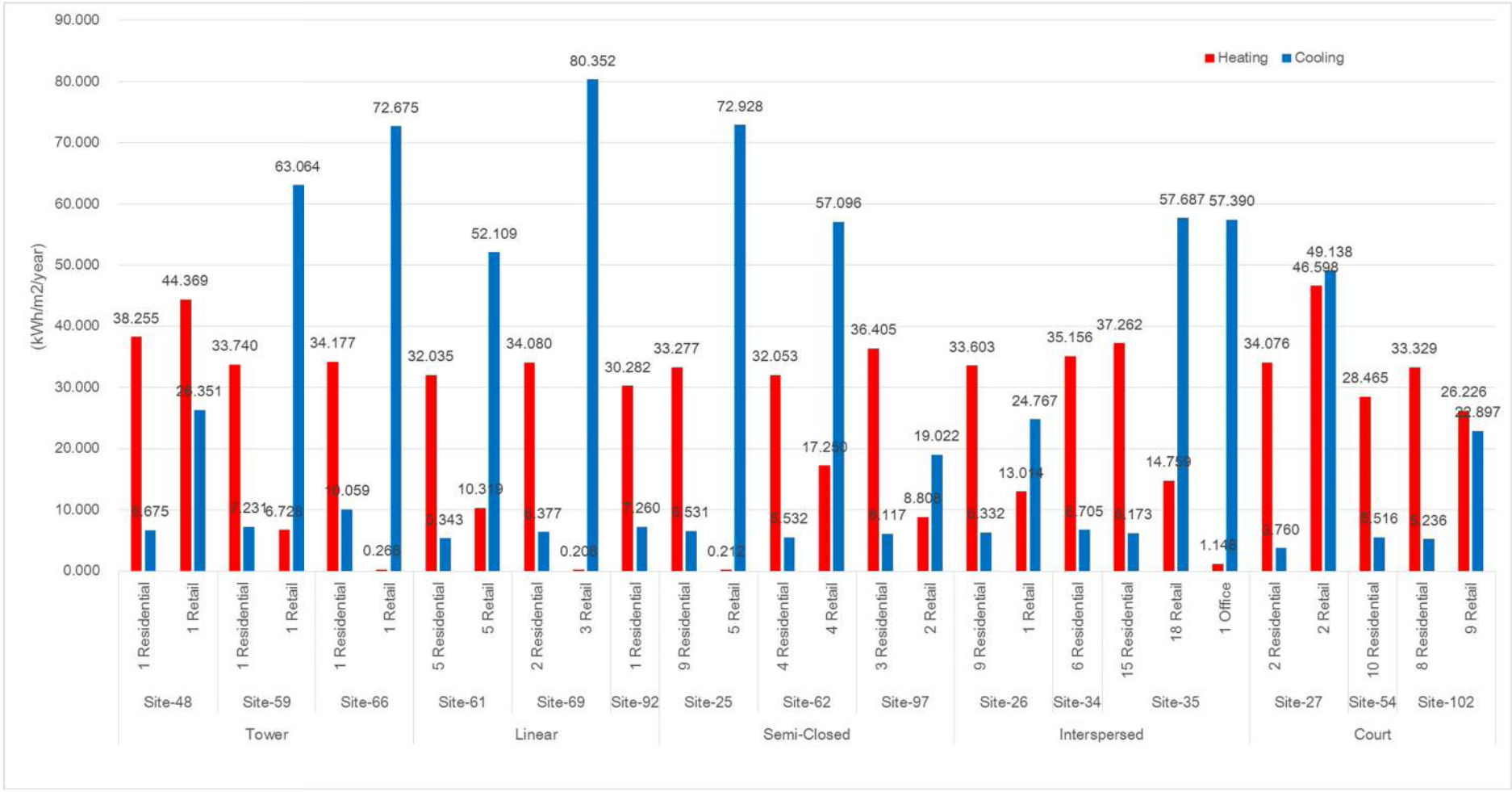

Figure 6. 24: Heating/cooling demand for all buildings from 15 target project site

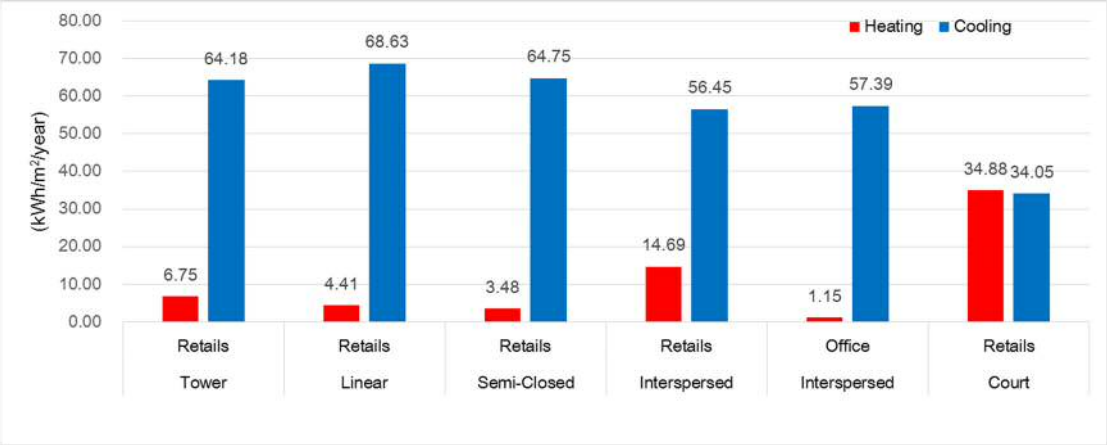

Figure 6. 25: Heating/cooling demand for retails and office from 15 target project sites

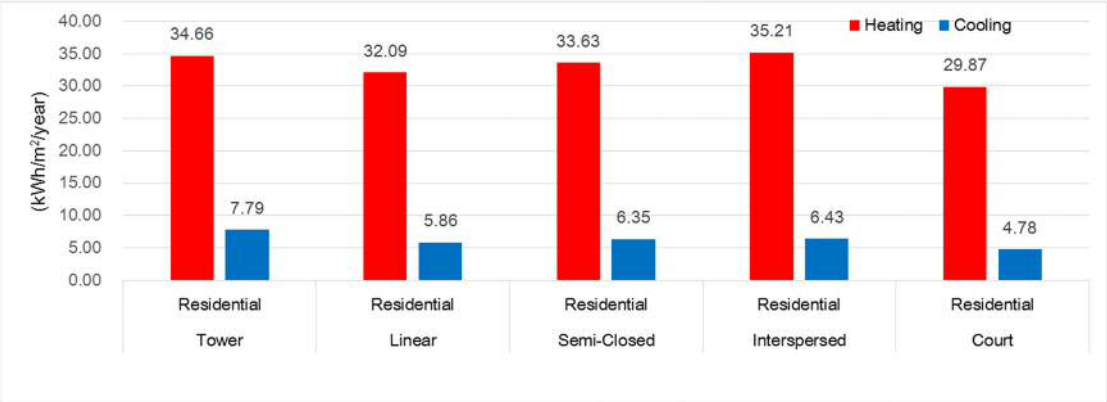

Figure 6. 26: Heating/cooling demand for residential buildings from 15 target project sites

ii) Building density and building energy demand

According to Figure 6.27 and Figure 6.28, there is a strong correlation between each building density factor and energy demand in retail buildings, and the R^2 value in these cases are all more than 5% significant. Notably, the correlation between building height and heating/cooling demand is of more than 30% significance. On the other hand, for the residential buildings, even though the correlation between FAR/BCR and energy demand is of less than 5% significance, building height is shown with strong correlation with heating/cooling (Figure 6.28). The results based on both figures generally indicate that retails and residential buildings in a denser project site could have lower heating demand in winter, on the other hand, cooling load in summer would increase. And this phenomenon is more apparent in public buildings.

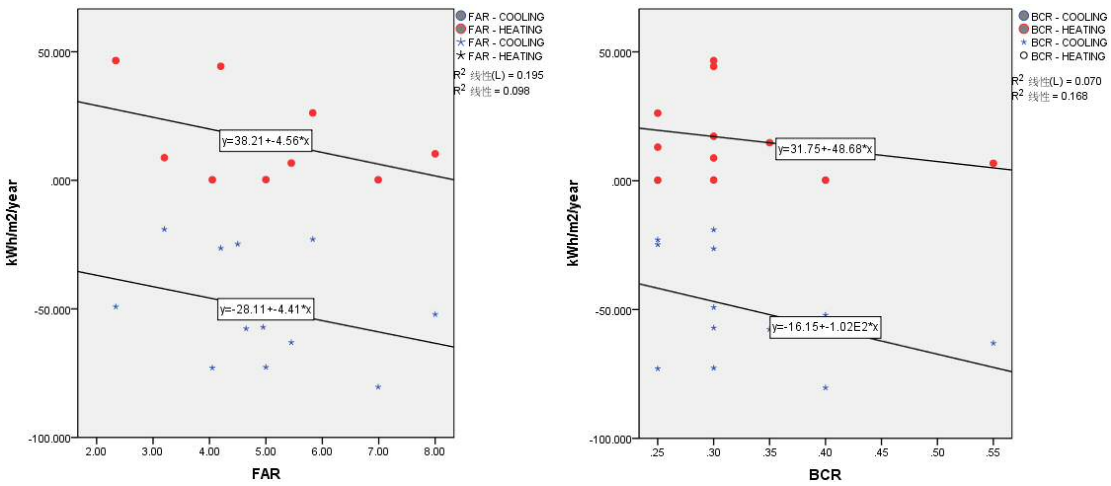

Figure 6. 27: Correlations between FAR (left)/BCR (right) and energy demand in retails

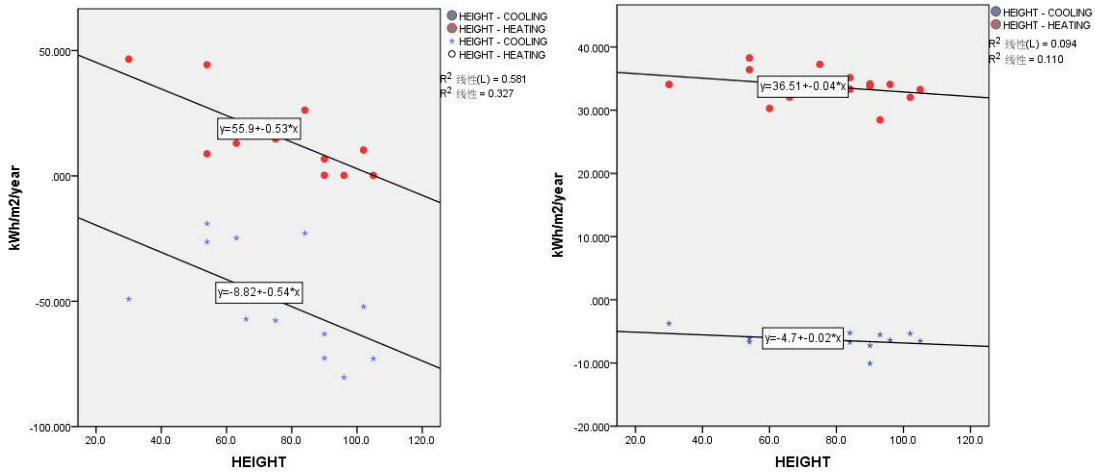

Figure 6. 28: Correlations between building height and energy demand in retails (left) and residential buildings (right)

6.5 Accuracy and validation with survey reference data

Energy demand is the output of all energy applicants, and energy supply means the total energy input that is delivered to the buildings. Considering the factors- the system performance of building services and losses during the distribution of electricity within the buildings, there are differences between energy demand and energy supply (Figure 6.29). Specifically, that difference is due to Coefficient of Performance (COP) in heating/cooling system, and efficiency of other service facilities. In addition, the energy loss during distribution within buildings just accounts for a small amount, and this part of the energy difference is neglected in this study.

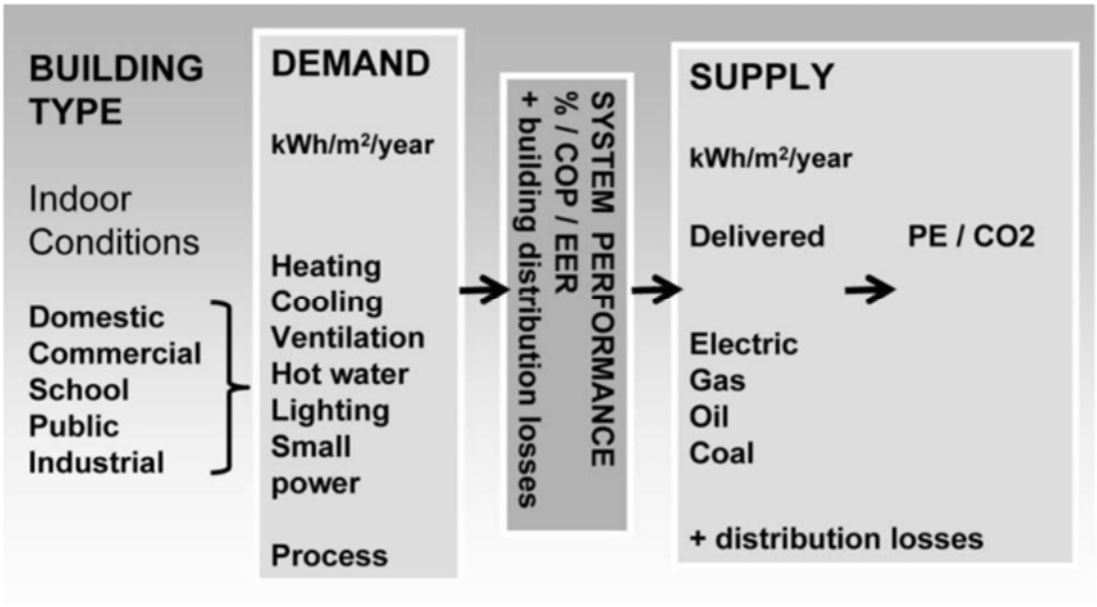

Figure 6. 29: Summary of energy terminology

Source: (Jones et al. 2011)

The simulation provides an approach to investigate energy demand, especially when the field investigation is impractical to carry out. The accuracy of setting and modelling is a key to obtain the precise predictions. In the meanwhile, in this study, the survey of the practical energy consumption on local urban buildings regarding building functions can be used to check the accuracy of this study and validate the simulation results.

In order to obtain the exact energy supplied for heating/cooling, it is necessary to

determine the COP in each scenario. According to national (MOHURD & AQSIQ 2005) and local (MOHURD 2010) codes for thermal performance of civil buildings, standard values of COP are specified according to the geo-condition, building type, and condition of services. As in most buildings in Chengdu, no matter which the function of the building is, work for heating and cooling is mainly completed by split units of AC systems (Li 2012). Therefore, the value for COP can be precisely determined, which is 1.9 and 2.3 in residential buildings for heating and cooling, respectively (MOHURD 2010). On the other hand, in both public buildings, COP is 2.8 for cooling systems and is 1.8 for heating systems (MOHURD & AQSIQ 2005). Then, the energy supplied for heating/cooling is calculated with COPs and simulated energy demand according to building type. The calculation process and results are shown in Table 6.2.

Table 6. 2: Calculation of energy supply for different types of buildings

Building Type	Heating /Cooling	Energy Demand (kWh/m^2/year)	COP (MOHURD 2010) (MOHURD & AQSIQ 2005)	Energy Supply (kWh/m^2/year)
Residential	Heating	32.98	1.9	17.36
	Cooling	-5.93	2.3	-2.58
Retail	Heating	8.41	1.8	4.67
	Cooling	-61.49	2.8	-21.96
Office	Heating	1.15	1.8	0.64
	Cooling	-57.39	2.8	-20.50

Table 6. 3: Comparison between simulated values and survey reference values

Building Type	Sum of Heating and Cooling (kWh/m^2/year)	Survey Refernece Energy Supply of Heaing and Cooling (kWh/m^2/year) (Su et al. 2010)	Percentage of Survey Refernece Total Energy Supply (kWh/m^2/year)
Residential	(No heating traditon) 2.58	(No heating traditon) 2.8	16%
Retail	26.63	30.0	31%
Office	21.13	18.5	30%

On the other hand, the data of practical total building energy consumption in Chengdu was collected through surveys (Su et al. 2010). In the surveys, more than 2000 buildings, including 1292 residential building and 751 public buildings, were investigated, and the monthly usage of electricity for each building were summaries.

Due to the limitations, the surveys were not able to directly collect energy consumption for electricity usage of individual equipment. However, the energy consumption for the AC systems could be calculated by the difference between the minimum monthly usage and the monthly usage of the other months, assuming that the minimum usage was for the total usage excluding the AC systems, while the consumption of the AC system was included in the other months (Su et al. 2010). Therefore, the energy consumption for AC systems and total electric consumption for six types of building were obtained in the surveys. The use of the AC system is indicated in Table 6.10, which is 2.8 kWh/m^2/year residential buildings, 30.0 kWh/m^2/year for a retail building, and 18.5 kWh/m^2/year an office building. The proportion to total consumption is 16%, 31%, and 30%, respectively. The data obtained from the surveys had been validated through further calculations and practical measurements.

Finally, the reference data of surveys are applied to compare with the simulation results. The comparison between modelling and practical measurement can be checked in Table 6.3, which indicates the accuracy of the simulation and validates the simulated energy consumptions. For residential buildings, the simulated consumption for cooling is 2.58 kWh/m^2/year, which is close to the reference value. On the other hand, for retail buildings, the sum of energy consumption for heating and cooling is 26.63 kWh/m^2/year, which is 11.23% lower than the reference value. Lastly, the use of heating and cooling in an office building is 21.13 kWh/m^2/year, which is 14.22% higher than the value obtained from surveys. Generally speaking, according to these comparisons, the simulation results of heating and cooling demand in all three types of buildings are close to the accurate values of a practical situation, thereby confirming the validity of the simulations.

6.6 Energy Simulation for selected 15 projects with additional validated UHI values

6.6.1 Introduction of UHI effect

As one of the most significant influences of UHI on the urban environment, a variation of air temperature profoundly affects the energy demand for space heating cooling and lighting (Chen & Ng 2011)(Stone & Rodgers 2001)(Allegrini et al. 2012). Previous studies (Yao et al. 2011)(Ali-toudert 2009) show that the UHI will increase the peak cooling load of buildings in summer, on the other hand, heating demand is lower if the urban context is well modelled which benefits from the higher outdoor air temperature. Specifically, and every 1°C of outdoor air temperature reduction will achieve 5% energy saving in building energy consumption (Wong et al. 2011). Therefore, mitigating the UHI effects has a significant influence on the total building energy consumption. Also, the UHI effect has a considerable impact on the outdoor thermal comfort and health of citizens (Moonen et al. 2012). Tan's (2010) numerical study reveals that the longer people stay in the 'very hot' environment, higher heat stress will be experienced. Moreover, people are vulnerable to the heat wave; the extreme weather will cause excess deaths rates. In short, there have the needs to consider the UHI effect during the process of prediction for building energy demand (Principles 2011).

Therefore, based on the on-site outdoor air temperature obtained through simulations in the previous chapter, the revised weather file which is considered with the UHI effect will be applied for building energy simulation in this section. Lastly, the results of the simulation with revised weather files will be compared with the original data obtained in the previous phase of this chapter, in order to investigate the impact of outdoor temperature on building energy consumption.

6.6.2 The adjusted simulation tool with modified Weather File

As mentioned in the previous chapter, two-day (one for winter and one for summer) simulation was carried out, the results (Table 6.4, Table 6.5) indicate that local temperature varies at each site. Accordingly, the weather file is modified with the

predicted 24-hour temperature data for each site. Therefore, the weather data for the other 363 days will be applied to the revised weather file for the new simulation of this section without any change. Worthy of the node is that other meteorological parameters, including but not limited to relative humidity, wind speed, air pressure, are still applied with the data from the original data used in the simulation of previous sections. Therefore, the only altered parameter of weather file is air temperature.

Table 6. 4: Hourly temperature on Jan 9, 2005, for each target project site.

Time	25	26	27	34	35	48	54	59	61	62	66	69	92	97	102	Rural
0:00	7.30	7.34	7.30	7.26	7.48	7.34	7.23	7.42	7.32	7.34	7.20	7.43	7.28	7.77	7.45	5.10
1:00	6.95	6.98	7.00	6.91	7.14	7.05	6.86	7.12	6.97	7.01	6.90	7.04	6.96	7.44	7.08	4.90
2:00	6.77	6.79	6.82	6.72	6.95	6.88	6.67	6.94	6.78	6.82	6.74	6.82	6.78	7.25	6.87	4.70
3:00	6.39	6.42	6.50	6.32	6.57	6.59	6.28	6.62	6.39	6.48	6.41	6.42	6.42	6.86	6.43	4.40
4:00	5.90	5.93	6.05	5.81	6.06	6.17	5.77	6.18	5.89	6.01	5.94	5.89	5.94	6.36	5.87	3.80
5:00	5.39	5.41	5.56	5.27	5.52	5.72	5.24	5.70	5.35	5.51	5.44	5.32	5.42	5.82	5.29	3.10
6:00	4.62	4.64	4.86	4.46	4.72	5.08	4.44	5.01	4.55	4.79	4.71	4.51	4.66	5.02	4.41	2.40
7:00	4.18	4.19	4.41	4.01	4.27	4.64	3.99	4.56	4.11	4.33	4.26	4.02	4.20	4.56	3.95	1.30
8:00	3.96	3.94	4.16	3.78	4.03	4.39	3.76	4.31	3.87	4.08	4.02	3.76	3.96	4.32	3.71	0.30
9:00	3.97	3.96	4.21	3.85	4.03	4.36	3.89	4.32	3.89	4.17	4.05	4.01	3.99	4.26	3.82	0.20
10:00	5.08	5.16	5.26	5.05	5.20	5.15	5.15	5.24	5.06	5.32	5.11	5.48	5.06	5.24	5.37	1.90
11:00	6.36	6.40	6.46	6.29	6.39	6.25	6.41	6.39	6.34	6.49	6.32	6.65	6.23	6.43	6.73	4.60
12:00	7.19	7.16	7.13	7.07	7.13	6.98	7.18	7.12	7.17	7.23	7.07	7.35	7.01	7.21	7.40	6.70
13:00	7.77	7.79	7.70	7.72	7.76	7.60	7.83	7.70	7.84	7.82	7.65	7.97	7.63	7.88	7.99	7.80
14:00	8.09	8.16	8.07	8.08	8.12	8.00	8.18	8.08	8.24	8.19	8.03	8.35	8.03	8.26	8.35	8.30
15:00	8.21	8.33	8.25	8.24	8.28	8.20	8.31	8.24	8.39	8.36	8.19	8.49	8.20	8.44	8.48	8.60
16:00	8.20	8.38	8.31	8.31	8.30	8.28	8.30	8.28	8.40	8.40	8.24	8.49	8.26	8.48	8.49	8.60
17:00	8.15	8.28	8.23	8.23	8.23	8.23	8.20	8.22	8.30	8.30	8.16	8.34	8.19	8.43	8.35	8.30
18:00	8.02	8.05	8.05	8.04	8.09	8.07	8.01	8.09	8.11	8.09	8.00	8.08	8.02	8.29	8.13	7.90
19:00	7.70	7.73	7.77	7.71	7.80	7.81	7.68	7.83	7.78	7.80	7.74	7.77	7.74	8.02	7.81	7.50
20:00	7.51	7.53	7.58	7.51	7.62	7.61	7.48	7.64	7.58	7.60	7.55	7.56	7.54	7.83	7.62	7.00
21:00	7.19	7.22	7.31	7.18	7.31	7.36	7.15	7.36	7.24	7.31	7.27	7.26	7.25	7.57	7.28	6.60
22:00	6.99	6.99	7.10	6.96	7.11	7.15	6.93	7.15	7.02	7.09	7.06	7.03	7.03	7.39	7.06	6.30
23:00	6.90	6.89	7.00	6.86	7.01	7.04	6.83	7.05	6.92	6.98	6.96	6.91	6.93	7.29	6.96	6.10
0:00	6.58	6.58	6.71	6.54	6.68	6.78	6.50	6.77	6.58	6.69	6.66	6.58	6.62	6.98	6.59	5.90

Source: Section 5.2.3, Chapter 5

Table 6. 5: Hourly temperature on Aug 21, 2005, for each target project site.

Time	25	26	27	34	35	48	54	59	61	62	66	69	92	97	102	Rural
0:00	28.1	27.8	28.1	27.9	28.2	28.3	28.1	28.1	27.9	28.0	28.3	27.6	28.2	28.4	27.9	24.5
1:00	27.8	27.4	27.8	27.7	28.0	28.1	27.8	27.9	27.6	27.7	28.0	27.2	27.9	28.2	27.6	24.2
2:00	27.7	27.3	27.6	27.5	27.8	27.9	27.6	27.7	27.4	27.6	27.8	27.1	27.7	28.0	27.4	24.0
3:00	27.6	27.2	27.6	27.4	27.7	27.8	27.6	27.6	27.4	27.5	27.7	27.1	27.6	27.9	27.4	23.7
4:00	27.3	26.8	27.2	27.0	27.3	27.5	27.2	27.3	27.0	27.1	27.3	26.6	27.3	27.6	27.0	23.5
5:00	27.3	27.0	27.3	27.2	27.4	27.5	27.3	27.4	27.2	27.2	27.4	26.9	27.4	27.7	27.1	23.3
6:00	27.1	26.7	27.1	26.9	27.2	27.3	27.1	27.1	26.9	27.0	27.2	26.5	27.1	27.5	26.8	23.2
7:00	26.9	26.5	26.9	26.7	27.0	27.1	26.9	26.9	26.7	26.8	27.0	26.4	26.9	27.3	26.7	23.4
8:00	27.5	27.4	27.6	27.5	27.7	27.7	27.6	27.7	27.5	27.6	27.7	27.5	27.7	27.9	27.5	23.7
9:00	28.3	28.5	28.7	28.5	28.7	28.7	28.6	28.7	28.8	28.8	28.7	29.1	28.7	28.8	28.8	24.1
10:00	29.3	29.6	29.7	29.5	29.6	29.6	29.6	29.7	29.8	29.9	29.6	30.3	29.6	29.7	29.8	24.6
11:00	30.3	30.7	30.6	30.6	30.6	30.5	30.6	30.6	30.9	30.9	30.6	31.2	30.5	30.6	30.8	25.3
12:00	31.3	31.6	31.6	31.6	31.6	31.5	31.6	31.6	31.9	31.9	31.5	32.2	31.4	31.6	31.8	26.3
13:00	32.4	32.8	32.6	32.7	32.7	32.6	32.8	32.6	33.0	32.9	32.5	33.3	32.5	32.6	32.9	27.8
14:00	33.2	33.5	33.3	33.4	33.3	33.3	33.5	33.3	33.7	33.7	33.2	34.0	33.2	33.3	33.6	29.9
15:00	33.6	33.9	33.7	33.8	33.7	33.6	33.9	33.6	34.1	34.0	33.5	34.4	33.6	33.7	33.9	31.6
16:00	33.3	33.6	33.4	33.6	33.4	33.4	33.6	33.2	33.8	33.8	33.3	34.2	33.3	33.3	33.7	31.4
17:00	32.7	33.0	32.8	33.0	32.8	32.8	32.9	32.6	33.2	33.2	32.7	33.7	32.8	32.8	33.1	30.8
18:00	31.1	32.2	32.1	31.2	32.1	32.1	31.2	32.0	32.4	32.5	32.0	32.8	32.1	32.2	32.3	30.1
19:00	30.5	30.3	31.4	30.5	31.4	31.4	30.5	31.3	31.5	31.6	31.3	31.6	31.3	31.6	31.4	29.2
20:00	29.7	29.3	30.5	29.6	29.6	30.6	29.7	29.5	30.5	30.6	30.4	30.4	30.4	30.8	30.4	28.3
21:00	29.3	29.0	30.0	29.2	29.2	30.1	29.3	29.2	29.9	30.1	30.0	29.8	29.9	30.4	29.9	27.5
22:00	28.9	28.4	29.5	28.7	28.8	29.6	28.8	28.7	28.3	29.5	29.5	29.1	29.4	29.9	29.3	26.8
23:00	28.4	27.8	28.9	28.1	28.2	28.3	28.2	28.2	27.8	27.9	28.9	27.3	28.8	29.3	28.6	26.2
0:00	28.3	27.9	28.1	28.1	28.3	28.3	28.2	28.2	28.0	28.0	28.8	27.6	28.8	29.2	28.6	25.6

Source: Section 5.2.3, Chapter 5

Table 6. 6: The simulation result of heating/cooling demand considering UHI on two specific days for all sites

Full Year Simulation (with UHI on Jan 9 and Aug 21)			Building floor area (m^2)	Energy Demand (kWh/m^2/year)	
				Heating	Cooling
Tower	Site-48	1 Residential	8378.30	38.1891	-6.8169
		1 Retail	425.80	44.2719	-26.5732
	Site-59	1 Residential	26933.47	33.6773	-7.3566
		1 Retail	4290.31	6.6643	-63.2087
	Site-66	1 Residential	10815.93	34.1172	-10.1967
		1 Retail	2456.48	0.2670	-72.7791
	Group Mean	Residential	46127.70	34.60	-7.92
		Retail	7172.59	6.71	-64.31
Linear	Site-61	5 Residential	107212.50	31.9810	-5.4618
		5 Retail	5524.30	10.2914	-52.2275
	Site-69	2 Residential	28903.30	34.0199	-6.5052
		3 Retail	7782.23	0.2063	-80.4611
	Site-92	1 Residential	28905.20	30.2301	-7.3787
	Group Mean	Residential	165021.00	32.03	-5.98
		Retail	13306.53	4.39	-68.74
Semi-Closed	Site-25	9 Residential	486986.63	33.2212	-6.6486
		5 Retail	35075.83	0.2106	-73.0187
	Site-62	4 Residential	80516.83	31.9964	-5.6529
		4 Retail	6318.33	17.1693	-57.2850
	Site-97	3 Residential	107851.43	36.3329	-6.2597
		2 Retail	5214.93	8.7586	-19.1350
	Group Mean	Residential	675354.90	33.57	-6.47
		Retail	46609.09	3.47	-64.86
Interspersed	Site-26	9 Residential	237790.50	33.5468	-6.4465
		1 Retail	1013.75	12.9598	-24.8866
	Site-34	6 Residential	270716.60	35.1007	-6.8272
	Site-35	15 Residential	192406.27	37.1989	-6.3046
		18 Retail	25983.77	14.6875	-57.8568
		1 Office	36049.90	1.1299	-57.4526
	Group Mean	Residential	700913.37	35.15	-6.55
		Retail	26997.52	14.62	-56.62
		Office	36049.90	1.13	-57.45
Court	Site-27	2 Residential	66129.37	34.0187	-3.8772
		2 Retail	2009.29	46.4824	-49.3950
	Site-54	10 Residential	453380.70	28.4183	-5.6218
	Site-102	8 Residential	103800.93	33.2724	-5.3581
		9 Retail	2719.43	26.1552	-23.0550
	Group Mean	Residential	623311.00	29.82	-4.88
		Retail	4728.71	34.79	-34.25
Overall		Residential	2210727.97	**32.92**	**-6.04**
		Retails	98814.44	**8.37**	**-61.62**
		Office	36049.90	**1.13**	**-57.45**

Moreover, there is no any modification in other default settings of the simulation tool- HTB2/ SketchUp- Virvil Plug-in, including dairy file, internal gain settings, and construction files. Moreover, the models from the original simulations will be applied once again in this revised simulation, and general simulation process follows that of previous original simulation. The result of simulation for the energy consumption of each building/functional spaces in each site are obtained, and it is presented in different forms, in the form of site value, the mean value of the group, and overall value of building function (Table 6.6).

As shown in Table 6.6, the change of temperature on the summer day and the winter day influence daily building energy demand of these specific two-day for all building groups of the 15 target project sites. By comparing the Table 6.6 with Table 6.1, it can be found that heating demand on all sites is slightly reduced, and cooling demand (absolute value) grows in all types of buildings. Specifically, the heating demand in residential buildings is reduced to 32.92 kWh/m^2/year, and its cooling demand has risen to 6.04 kWh/m^2/year. For retails, the cooling demand growths to 61.62 kWh/m^2/year, and energy demand for heating is 8.37 kWh/m^2/year. Lastly, heating demand in office drops to 1.13 kWh/m^2/year, and cooling energy demand is increased to 57.45 kWh/m^2/year.

6.6.3 Data analysis and discussion

Based on the above result obtained from the simulation, it can be summarised that the structure of annual energy demand still varies with the plot-layout and building type. Cooling demand in residential buildings is much lower than that in retails and office building, and the demand for heating in residential building is stronger at the same time. However, as mentioned in the previous section, there is no tradition for heating domestic building, thereby the heating energy of residential buildings could be neglected in this study.

Table 6. 7: Calculation of annual difference in energy demand considering UHI

	Difference of Energy Demand for two days (Jan 9 and Aug 21) (kWh/m^2/year)		Difference of Energy Demand for a year (90 heating days and 77 cooling days) (kWh/m^2/year)	
	Heating	Cooling	Heating	Cooling
Residential	-0.0556	0.1152	-2.4999	4.4357
Retail	-0.0367	0.1307	-1.6533	5.0334
Office	-0.0177	0.0622	-0.7972	2.3954

Table 6. 8: The result of simulations of heating and cooling demand considering UHI in the full year for all sites

Full Year Simulation (UHI full year)			Building floor area (m^2)	Energy Demand (kWh/m^2/year)	
				Heating	Cooling
Tower	Site-48	1 Residential	8378.30	35.2698	-12.1362
		1 Retail	425.80	39.9866	-34.9122
	Site-59	1 Residential	26933.47	30.8964	-12.0609
		1 Retail	4290.31	3.8740	-68.6501
	Site-66	1 Residential	10815.93	31.4950	-15.3427
		1 Retail	2456.48	0.2044	-76.6954
	Group Mean	Residential	46127.70	31.83	-12.84
		Retail	7172.59	4.76	-69.40
Linear	Site-61	5 Residential	107212.50	29.6067	-9.9310
		5 Retail	5524.30	9.0719	-56.6792
	Site-69	2 Residential	28903.30	31.3896	-11.3105
		3 Retail	7782.23	0.1410	-84.5688
	Site-92	1 Residential	28905.20	27.9516	-11.8343
	Group Mean	Residential	165021.00	29.63	-10.51
		Retail	13306.53	3.85	-72.99
Semi-Closed	Site-25	9 Residential	486986.63	30.7754	-11.0619
		5 Retail	35075.83	0.1520	-76.4092
	Site-62	4 Residential	80516.83	29.5075	-10.2056
		4 Retail	6318.33	13.6138	-64.3689
	Site-97	3 Residential	107851.43	33.1644	-11.6287
		2 Retail	5214.93	6.5679	-23.3654
	Group Mean	Residential	675354.90	31.01	-11.05
		Retail	46609.09	2.69	-68.84
ntersperse	Site-26	9 Residential	237790.50	31.0681	-10.7459
		1 Retail	1013.75	10.5665	-29.3655
	Site-34	6 Residential	270716.60	32.6580	-11.4182
	Site-35	15 Residential	192406.27	34.4384	-11.2234
		18 Retail	25983.77	11.5536	-64.2310
		1 Office	36049.90	0.3505	-59.7858
	Group Mean	Residential	700913.37	32.61	-11.14
		Retail	26997.52	11.52	-62.92
		Office	36049.90	0.35	-59.79
Court	Site-27	2 Residential	66129.37	31.5104	-8.2851
		2 Retail	2009.29	41.3882	-59.0155
	Site-54	10 Residential	453380.70	26.3457	-9.5865
	Site-102	8 Residential	103800.93	30.7764	-9.9214
		9 Retail	2719.43	23.0285	-28.9882
	Group Mean	Residential	623311.00	27.63	-8.52
		Retail	4728.71	30.83	-41.75

i) Heating/cooling demand considering UHI effect in a whole year

The results of the revised simulation (Table 6.6) indicates the impact of UHI effect of two specific days on the total yearly energy demand, which hardly reveals the overall influence of UHI effect in a full year. Therefore, the required full year scheme needs further processing.

Based on the local codes (MOHURD 2010), the heating period in winter starts from December 1st to February 28th, and the cooling period is between June 15th to August 31st, which means 90 heating days and 77 cooling days. In order to obtain the increase/reduction in energy demand for the entire 365 days of a year, it is assumed that (Figure 6.30): the increase of cooling demand on the summer day- Aug 21- and the reduction of heating demand on winter day-Jan 9 are the peak values for all heating/cooling days, and the change of heating/cooling demand drops to zero on Dec 1st & Feb 28th and Jun 15th & Aug 31st, respectively. At the same time, the change rate of heating/cooling demand keeps constant.

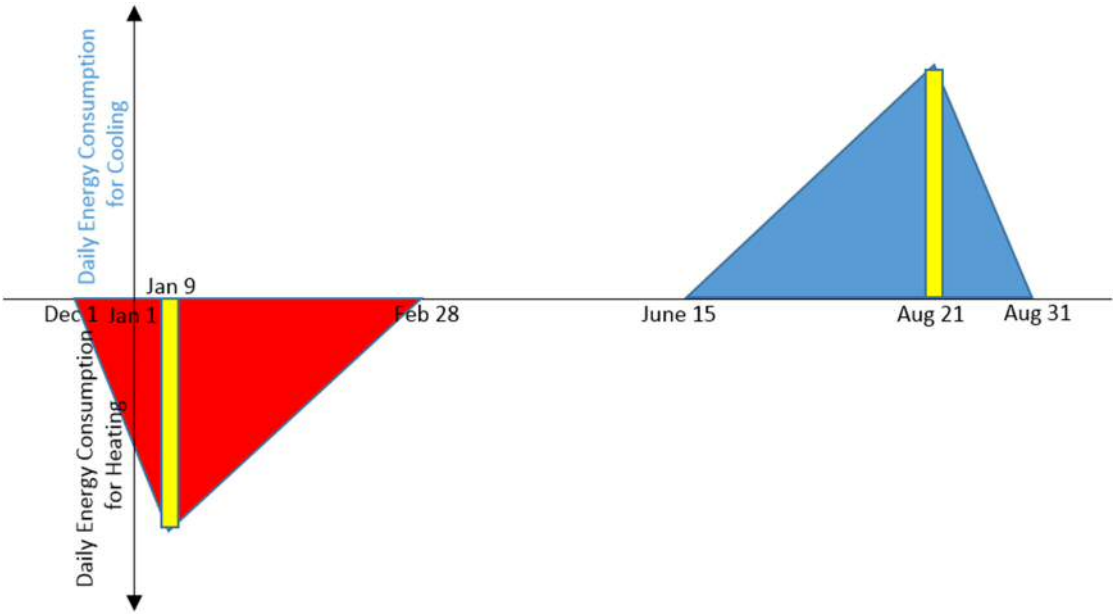

Figure 6. 30: An assumption for distribution of daily energy consumption for heating and cooling

Then, the annual increase in cooling load will be calculated, which is:

$$\Delta E_{annual} = \frac{1}{2}\,\Delta E_{Max-day} \times Days_{operating} \qquad (6.1)$$

Therefore, the overall change in heating/cooling demand in terms of building functional type (Table 6.7) is calculated as followed:

For residential buildings, the increase of cooling energy on Aug 21st is 0.115213 kWh/m^2/year, so the value for all cooling period in residential buildings is:

$$\frac{1}{2} \times 0.115213 \times 77 = 4.4357\ [kWh/\ m^2/year] \quad (6.2)$$

and the value for all heating period in residential buildings is

$$\frac{1}{2} \times (-0.055553) \times 99 = -2.4999\ [kWh/m^2/year] \quad (6.3)$$

the annual value of reduction on in heating demand for retails is

$$\frac{1}{2} \times (-0.036740) \times 99 = -1.653281\ [kWh/m^2/year] \quad (6.4)$$

and an increase in cooling demand for the 77 cooling days is

$$\frac{1}{2} \times 0.130737 \times 99 = 5.033370\ [kWh/m^2/year] \quad (6.5)$$

For an office building, the reduction in heating demand for 99 heating days is

$$\frac{1}{2} \times (-0.036740) \times 99 = -1.653281\ [kWh/m^2/year] \quad (6.6)$$

and the increase in cooling demand for the 77 cooling days is

$$\frac{1}{2} \times 0.130737 \times 99 = 5.033370\ [kWh/m^2/year] \quad (6.7)$$

Following the same hypothesis, the processed results of each site and overall are shown in Table 6.8.

ii) Structure of energy demand and the design features

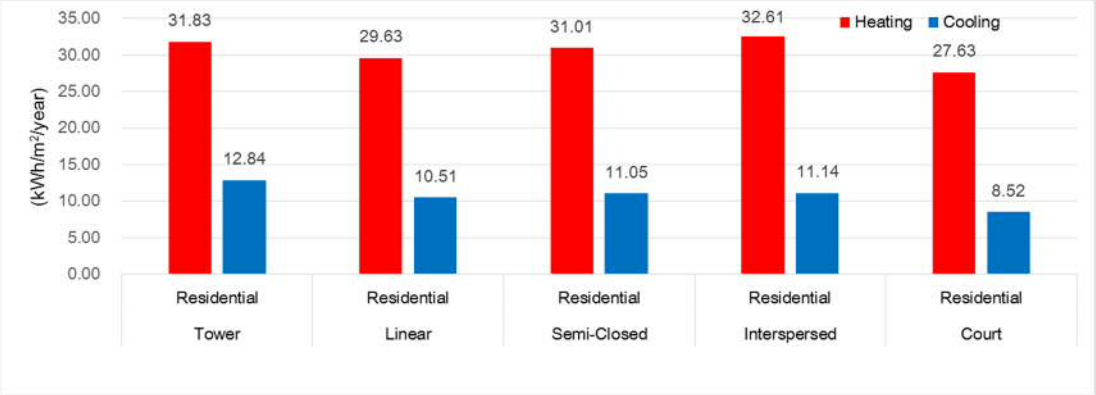

Figure 6. 31: Heating/cooling demand for retails and office from 15 target project sites.

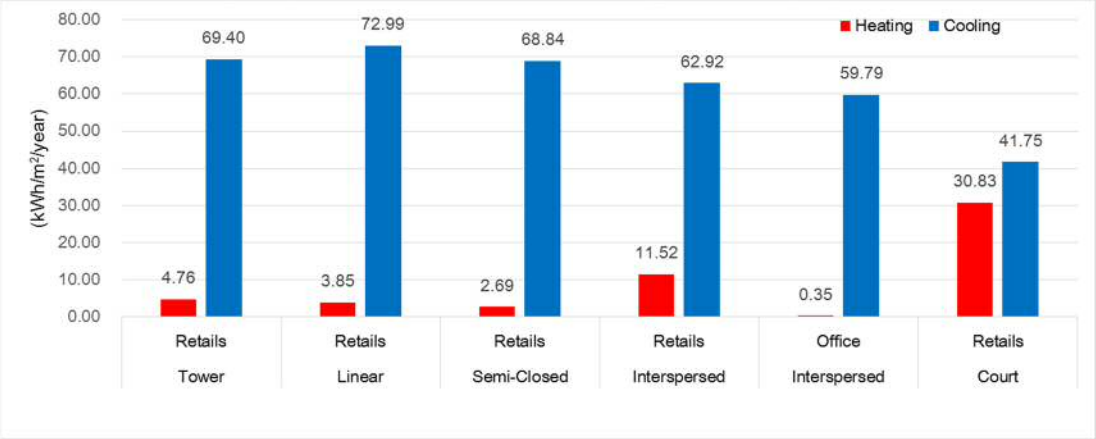

Figure 6. 32: Heating/cooling demand for residential buildings from 15 target project sites

Due to the UHI effect, the cooling demand in public buildings is higher than the total energy demand for heating/cooling in residential buildings (Figure 6.30 and Figure 6.31), and its. Moreover, the cooling demand in public building is much higher than the heating demand, which is more than six times in most cases. As the same pattern of energy demand structure in the previous original simulation, in residential buildings, project sites with linear and court plot-layout has lower heating demand in winter and lower cooling load in summer, especially project sites in court group is recorded the lowest value both in annual heating demand and cooling demand. On the other hand, there is significant variation in energy demand in public buildings with five different layouts. Retails in Tower, Linear and Semi-closed groups have the highest energy demand for cooling. Noticeably, retails in Court are shown with the lowest cooling demand, and the heating demand in office building drops to nearly zero, and its cooling

demand is lower than the retails.

Regarding the correlation between design building density factor and energy demand, the general patterns of correlation between design building density factor and energy demand stay the same as those of the original simulation. According to Figure 6.32 and Figure 6.33, there is still a strong correlation between each building density factor and energy demand in retail buildings with more than 5% significance. On the other hand, for the residential buildings, only building height is shown with strong correlation with heating/cooling. However, the correlation between FAR/BCR and energy demand is weak. In short, the results indicate that a denser project site could have lower heating demand in winter and higher cooling demand in summer, while the absolute value of the change in cooling demand is larger than that in heating demand.

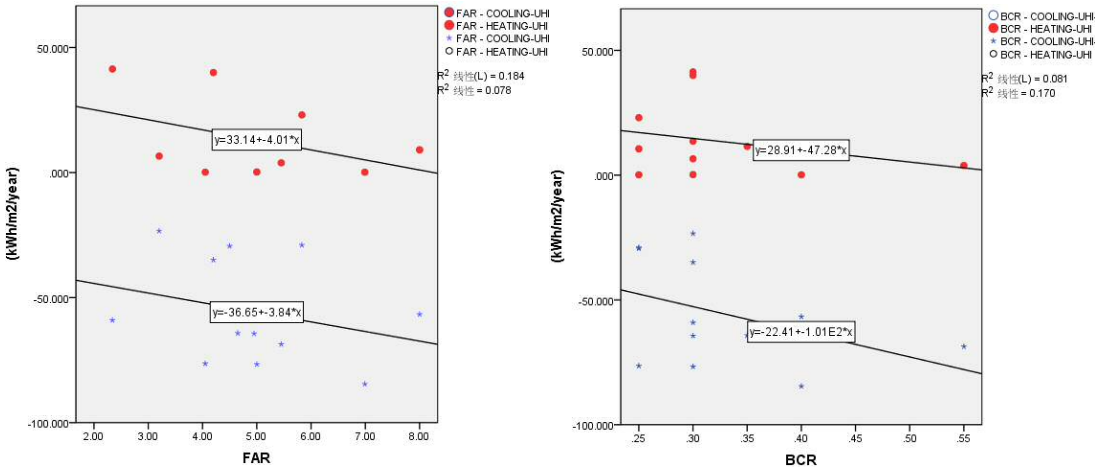

Figure 6. 33: Correlations between FAR (left)/ BCR (right) and energy demand in retails buildings considering UHI on all operating days

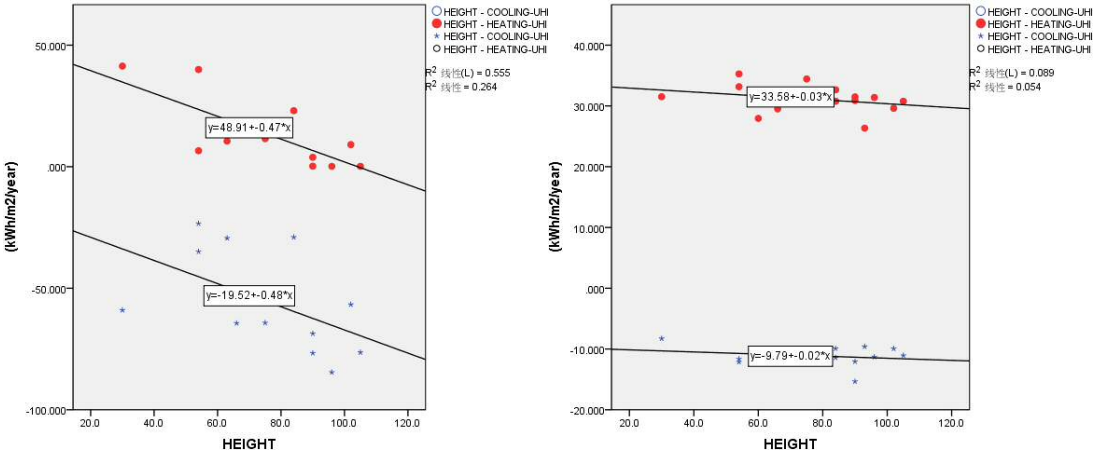

Figure 6. 34: Correlations between HEIGHT and energy demand in retails buildings (left) and residential buildings (right) considering UHI on all operating days

6.7 Data comparison of results obtained from two cases

6.7.1 Comparison of energy demand between UHI scenario and original scenario

As shown in Figure 6.34, the comparison regarding the annual energy demand on each site between the original condition and revised condition with UHI effect based is carried out. According to the comparison, the heating/cooling demand varies in all target sites. In summer, cooling demand in most residential buildings is witnessed with more than 60% increase from the original baseline values. Noticeably, UHI effect doubles the cooling demand in two residential buildings on Site No.27 with court plot-layout. However, the increase due to UHI effect in most public buildings is less than 10%, only retails at site No.26, site No.27 and site No.102 have more than 20% increase in cooling demand.

On the other hand, UHI effect reduces heating demand in the wintertime. Specifically, the reduction in most retails is more than 20%, and some retail (Site No.59 and Site No.69) even achieve more than 30% reduction. Moreover, the UHI effect in winter cuts down nearly 70% heating energy demand for an office building on Site No.35, which is located in a block with an interspersed plot-layout. Moreover, the warmer winter days reduce less than 10% of the heating demand in most domestic buildings. In short, the cooling demand in residential buildings is more sensitive to the UHI effect. However, the higher outdoor temperature in winter time has a significant impact on the heating demand in public buildings.

Lastly, the correlation between the energy demand change rate and all the other building design features- Plot- layout, FAR, BCR, HEIGHT- is of less than 5% significance, which indicates that these design features are not sensitive to the value of variation in heating/cooling demand due to UHI effect. However, the lifestyle, or building function in other words, is a decisive factor which impacts the influence of UHI effect on building energy demand.

Figure 6. 35: Change rate of heating/cooling demand for all buildings from 15 target project sites

6.7.2 Comparison of energy supply between simulation results and reference values

As discussed in the early sections, the energy supply is the practical energy input for all energy consumers, for example, AC systems in this study. The COP, coefficient of performance, is applied to the calculation of energy supply based on energy demand. Moreover, the COP varies in different building equipment's, and under different working conditions. Based on the local (MOHURD 2010) and national (MOHURD & AQSIQ 2005) code, standard values for COP are chosen for calculations according to the types of AC systems and the geo-regions.

Therefore, the difference in energy demand for a year (Table 6.9) is divided by the corresponding value of COP, then the difference of annual energy supply is obtained. As shown in Table 6.9, total energy supply for heating/cooling is increased by 1.93 kWh/m^2/year, 0.88 kWh/m^2/year, and 0.41 kWh/m^2/year, in residential buildings, retails and office, respectively.

Table 6. 9: Calculation of energy supply for different types of buildings considering UHI effect on all operating days

	COP (MOHURD & AQSIQ 2005) (MOHURD 2010)		Difference of Energy Supply for a year (90 heating days and 77 cooling days)(kWh/m^2/year)		Sum of Difference of Energy Supply (Heating and Cooling) for a year (kWh/m^2/year)
	Heating	Cooling	Heating	Cooling	No heating for residential
Residential	1.9	2.3	-1.316	1.929	1.93
Retail	1.8	2.8	-0.918	1.798	0.88
Office	1.8	2.8	-0.443	0.856	0.41

Table 6. 10: Extra energy supply due to UHI, baseline values, and reference values

	A. Sum of Difference of Energy Supply (Heating and Cooling) for a year (kWh/m^2/year)	B. Simulated Energy Supply for Heaing and Cooling (without UHI) (kWh/m^2/year)	$\frac{A}{B} \times 100\%$	C. Survey Refernece Energy Supply of Heaing and Cooling (kWh/m^2/year) (Su et al. 2010)	$\frac{A}{C} \times 100\%$
Residential	1.93	2.58	74.92%	2.8	68.93%
Retail	0.88	28.97	3.04%	30.0	2.93%
Office	0.41	21.45	1.91%	18.5	2.22%

Table 6. 11: Comparison between energy supply with UHI and the reference value

	A. Sum of Difference of Energy Supply (Heating and Cooling) for a year (kWh/m^2/year)	B. Simulated Energy Supply for Heaing and Cooling (without UHI) (kWh/m^2/year)	D. Energy Supply for Heaing and Cooling (with UHI) (kWh/m^2/year)	C. Survey Refernece Energy Supply of Heaing and Cooling (kWh/m^2/year) (Su et al. 2010)	$\frac{D-C}{C} \times 100\%$
Residential	1.93	2.58	4.51	2.8	60.93%
Retail	0.88	28.97	29.85	30.0	-0.50%
Office	0.41	21.45	21.86	18.5	18.18%

Next, as shown in Table 6.10, the energy consumed for domestic cooling demand due to UHI in a full year has grown by 74.92% compared to the original simulated value, which is 68.93% of the reference energy consumed for cooling in residential buildings. Moreover, the UHI effect increases the total heating/cooling supply in retails by 3.04% compared to the original simulation result, and it equals 2.93% of the reference value obtained from the survey. The increase in energy supply in office building accounts 1.91% of the baseline value of heating/cooling, which equals 2.22% of the reference value for office buildings.

Lastly, the total energy supply for heating/cooling system is shown in Table 6.11, which is 4.51 kWh/m^2/year for residential, 29.85 kWh/m^2/year for retail, and 21.86 kWh/m^2/year for office. According to the calculation of deviation, the revised simulation enlarge the difference between the predicted values and the practical reference values in both domestic buildings and office, which are 60.93% and 18.18% higher than the reference, respectively. However, in comparison to residential and office, the predicted heating/cooling supply under UHI conditions in retail (Table 6.11, D) is more accurate, which is 0.5% lower than survey reference values.

To sum up, residential buildings have much higher sensibility on the UHI effect in terms of energy supply. The warmer air temperature leads more than a 70% increase of heating/cooling consumption in the domestic building. And this extra energy consumption means an outstanding growth in domestic expense on living. While on the other hand, even there has a substantial reduction in heating consumption in public buildings, the increase in cooling demand still dominates the overall trend of variation in energy structure. Considering the large floor are in those public buildings, the extra 2%-3% cost per square metre for energy consumption could be a severe threat to the operating profit margin because more than 30% proportion of the total electricity consumption is taken by AC systems (Table 6.3).

6.8 Summary

In this chapter, the research objects have been achieved.

> *To summarise building energy features of the city-block-scale building groups in China, to explore the influence of both design features of the urban configuration and microclimate on building energy performance;*

This chapter investigates the basic data of energy demand and supply through a simulation and literature review. The process not only indicates the variation in the energy performance of different building groups but also analyses the relationship between design variables and building energy demand. Moreover, it provides a baseline for building energy performance for further analysis. Secondly, the revised simulation predicts the adjusted energy performance considered with air temperature variation. Therefore, the variation in energy demand/supply due to alteration in microclimate was obtained by comparing the results obtained from the two stages simulations. By comparing with the practical statistic data obtained by surveys (Su et al. 2010), *the simulation results of all target sites are shown with high reliability, thereby confirming the validity of the research products in this chapter*.

6.8.1 Building energy performance and building function

The structure of heat source varies in different building function types. The incidental gain dominates the heat gain in all cases of this study, which accounts for more than 60% of total heat gain in residential buildings and more than 80% of the total in public buildings. Moreover, the heat provided by the massive incidental gain balances most of the heat loss due to ventilation and fabric transmittance in public buildings in the winter time. On the contrary, *the heat released into fabric through transmittance in summer could benefit reducing the indoor heat in all building types in the summertime*. However, ventilation in summer would bring heat into the most public building and keep neutral in heat-gain/loss in residential. Therefore, *blocking-up the heat transmission by ventilation could avoid extra heat gathered in public building in summer*. In short, the

active controlling the heat gain/loss due to ventilation and gain accordingly could rebalance the indoor thermal environment.

In most residential buildings, there have the needs for cooling only in June, July and August, and the demand is lower compared that at the same time in public buildings. However, the cooling need for retails and offices still exists in April and October. Even the demand for heating in winter is massive in residential buildings, local tradition of living style cut off almost all energy consumption on heating in real practice. Moreover, the need for heating in public buildings in winter time stays at a low level, which is less than 10 kWh/m^2/year in most cases.

Based on the simulation results, average heating demand in residential building is more than three times higher than that in retail buildings, and office building has the lowest demand and shortest operating time for heating. On the other hand, cooling demand in non-domestic buildings is around 60 kWh/m^2/year, which is ten times of that in residential buildings. In general, *the total energy demand for heating/cooling is higher than that in domestic buildings*, in which cooling demand accounts for the significant portion.

6.8.2 The impact of the other variables on building energy demand

The results obtained in this chapter reveal that then energy demand is influenced by forms of plot-layout. For public buildings, the three site forms- tower, linear and Semi-closed- are recorded with more than 64 kWh/m^2/year cooling demand, which is nearly double of that in retails with a form of court. Interspersed and the court has the lower demand for cooling, but the heating demand in these two forms of sites is much higher than the other three types, especially for the later which has 34.88 kWh/m^2/year heating demand.

Moreover, *the demand for heating and cooling in public building shows a strong correlation with design variables-FAR, BCR and HEIGHT*; the significance is more than 30% in correlation with HEIGHT. However, *for residential buildings, the energy demand*

is shown strong correlation only with HEIGH. The results of correlations indicate that *sites with higher building density will reduce the heating demand in winter, but it will have more need for cooling in summer in return*.

6.8.3 The impact of UHI effect on energy demand in Chengdu

By applying weather data adjusted with on-site air temperature obtained from Chapter 5, the energy demand in 15 target project sites has been changed due to the warmer outdoor environment. According to the comparison between the demand with UHI effect and the baseline value, in general, *cooling demand is increased (more than 60% in most residential buildings) and heating demand is reduced (more than 20% in most retails) in all sites*. By comparing the change rate in buildings with different function, cooling demand is sensitive to the rising temperature only in residential buildings, and warmer winter will cause a higher rate of reduction in heating demand in public buildings. However, the change rate of energy demand due to UHI effects is not sensitive to other design variables.

Generally speaking, t*he UHI effect through a year increase the total energy consumption for heating/cooling, which means the amount of extra energy for heating is higher than the value saved in heating in all buildings*. For residential buildings, outstand increase per unit area in cooling due to UHI effect will result in more than 70% extra cost on the electricity bill. In the meanwhile, due to large floor area in public buildings and the outstand proportion of total energy consumption occupied by AC systems, the 2%-3% increase in energy use could significantly raise the cost for business operations.

Chapter Seven

CONCLUSIONS AND RECOMMENDATIONS

7.1 Introduction

This chapter concludes the overall discussions and findings in this research. Moreover, this chapter answers the following research questions:

> *'What is the relationship between the microclimate evaluations and building energy performance, what are best strategies planning in city-block-scale real estate projects in China from the perspectives of both mitigating the variation in microclimate and optimising building energy consumption?'*

> *'What are indicators and guidelines for planning city-block-scale building groups?'*

This chapter then makes recommendations for the future work on planning high-rise building group. Lastly, it explains the limitations of this study and summaries the contribution of the study and suggestions for possible future research.

7.2 Contributions of this study

In Chapter 2, three research gaps were identified after reviewing the existing literature on the planning a block-scale building group:

1. The lack of research on outdoor temperature and building energy consumption at the city-block level;

2. The absence of research on the impact of multi-variable on microclimate and building energy performance;

3. The scarcity of research on design strategies for mitigating building energy demand and optimising outdoor thermal comfort in large-scale building groups in China.

The study focused on the three research gap aiming to fill them, making theoretical contributions.

Moreover, by using the periodical MODIS satellite data being converted into the UHI intensity map, a new approach to observe the local temperature in a long-time period for multi-scale subjects has been concluded. Both overall long-term conditions and specific details of urban air temperature can be obtained.

Moreover, due to its relatively high resolution of the processed UHI maps, local variation regarding microclimate at any place within the urban area change will be investigated directly. This innovated methodology provides a new option of a method to analyse the microclimate conditions for building scale research subjects. Lastly, the study will provide a comprehensive understanding on microclimate and building energy consumption in large-scale building group real estates to the relevant stakeholders-scholars, policy-makers, designers and clients- and assist them to understand the evaluation of microclimate and building energy consumption, in order to achieve low-carbon development at city-block scale.

7.3 Conclusions

As addressed in Chapter 1, this research aims:

> ***'to investigate the impact of multi-design variables on microclimates and the building energy performance of large-scale buildings in South-West China, through the application of GIS mapping and modelling.'***

The findings of this research are arranged into the following seven topics:

7.3.1 Review of planning high-rise building groups at a city-block scale

i) Building performance and outdoor thermal performance are two core issues to achieve goals of low-carbon eco development in building industry in China.

As discussed in Chapter 2, toward global climate change, actions have been taken to reduce greenhouse gas emissions. Many urban development concepts have adopted world-widely with concerns on mitigation of environmental impaction. Among these concepts, the low-carbon eco-city stands out, which has been proved to a practical

theory for urban development. Moreover, the majority of the assessment and evaluation systems of different urban development theories address the similar issues, among which energy performance and thermal environment become core issues for planning building group at a city-block scale. Even regardless of the importance of mitigation of emissions, there is such a strong need to implement energy efficiency policies and optimise outdoor thermal comfort toward the energy crisis and environment protection.

ii) Urban form parameters and design features impact microclimate and building energy performance.

Firstly, chapter 2 reviewed the microclimate from an architectural point of view, which describes the outdoor thermal environment and influences on building energy performance (Erell et al. 2011). In an urban microclimate, an energy balance exists everywhere, which can be expressed as an equation with energy flows and heat fluxes. Solar radiation is considered as the only source of radiant energy input to the atmosphere system (Oke 2002a). In an urban microclimate, except for the influence of weather conditions, the solar radiation is significantly impacted by obstruction of buildings. Moreover, due to the urbanisation process, the geometry and thermal property of the surface in cities have been modified, which affects the transmission and distribution of different heat fluxes in the urban microclimate (Oke 1982). Due to the modification of surface and anthropogenic heat produced by human activities, microclimate features, including air temperature, humidity, and wind, are all affected. As the heat is gathered and accumulated in the urban surface, the urban temperature is raised to higher than that in a rural area, which is named as the phenomenon of urban heat island.

As the most remarkable effect of urban heat island, temperature rising causes the degradation in the urban built environment, including a reduction in ventilation rates, air pollution harmful gases in photochemistry higher emission (Cardelino & Chameides 1990) (Oke 1997), and outdoor thermal discomfort. On the other hand, as the primary

cause for urban heat island effect is the modification in surface and atmosphere during urbanisation process, three groups of factors can be summarised to explain the micro mechanism behind this effect. Which include the temporary effect variables (wind speed, cloud cover, humidity), permanent effect variables (city size, population, green area, urban forms and surface materials), and cyclic effect variables (anthropogenic heat and solar radiations) (Rizwan et al. 2008). At a city-block scale, design factors, including urban form, greenery, water bodies, and albedo of the surface, play critical roles in mitigating UHI effect. Accordingly, UHI mitigation strategies can be implemented by optimising urban geometry, increasing the green and water coverage, and using high albedo surface materials.

Moreover, urban form influences building energy performance in both direct and indirect ways (Ratti et al. 2005) (Ewing & Rong 2008) (Strømann-Andersen & Sattrup 2011) (Lee & Lee 2014). By providing choices in urban geometry, building size and function, urban form determines the solar accessibility and internal gains, thereby shaping the basic pattern of building energy structure. On the other hand, the urban form influences the UHI effect, which alters outdoor temperature resulting in the variation in building energy demand.

Finally, regarding to the concerns on mitigation strategies for UHI effect and building energy consumption at a city-block scale, relevant urban form parameters and design features can be summarised: floor area ratio, building coverage ratio, building height, green coverage ratio (including water bodies), plot layout, building function, which was indicators forming guidelines for planning city-block-scale building groups.

iii) Reviewing the building industry in Chengdu

Chengdu is a big city with strategic importance located in south-west China; it has been one of a few most prosperous cities in China since ancient times. Accordingly, the population in Chengdu has always been significant. Based on the specific geo and climate condition, its building typology and urban morphology have been developed with unique patterns. A foursquare courtyard with very deep eaves was a standard form

for both public and residential buildings in history. Since 1978, when reform and opening-up policy was implemented, the economy of China has been proliferating. Urbanisation rate is increasing in every region of China. In order to adjust the massive demand due to rapid urban development, ambitious development plans have been launched, resulting in massive investments in mega-scale urban construction and regeneration projects. The foursquare courtyards are gradually being replaced with parallel slab buildings, and finally high-rise buildings, in order to solve the problem of massive demand due to the increasing population, as well as the increasing land price. Since the New Century, high-rise buildings have been widespread and becomes the dominant form in the building industry. It alters the city skyline, thereby shaping the new form of an urban neighbourhood in Chengdu.

According to the types of function, the majority of high-rise buildings in Chengdu can be categorised into residential buildings and public buildings (including retails, office, and hotels). As the energy demand varies in buildings with different function, the heating/cooling period is different between residential buildings and public buildings. For example, the cooling demand lasts a whole year in most public buildings, but it is only needed in the summertime. Depending on different plot layout, Chapter 2 summarised five types of high-rise building group: Tower, Linear, Semi-closed, Interspersed, and court.

iv) Review of existing research microclimate and building energy in the context of Chengdu

Regarding the issues raised in microclimate and building energy performance in high-rise building group blocks, existing local research in Chengdu still focused on single measures at the very late stage of design. Achieving higher ventilation rate and improving insulation levels were only measures of early strategies for energy efficiency, which could not achieve satisfying results. On the other hand, single measures, such as increasing green area and installing pools, are the only choice for reducing the outdoor temperature. Therefore, a multi-measure strategy of energy efficiency at early

design stages needs to be investigated.

7.3.2 A new approach for observing the local temperature of multi-scale subjects in a long-time period: high-resolution remote sensing and long-period UHI observing

In chapter 4, the high-resolution imagines for UHI intensity of the entire region of Chengdu were used, which presents a practical approach for observing the long-term urban temperature at different scales. The imagines of UHI map were derived from the remote sensing data provided by Chengdu plateau Meteorological Institute of China Meteorological Bureau, obtaining and being processed through DVB-S system broadcasts of China National Satellite Meteorological Center and Huayun MODIS satellite remote sensing data receiving and processing system (Zhang & Zhou 2013). All the data was recorded under a clear sky condition during the period between 2005 and 2010. After the data was processed in a method of the Split-Window Algorithm (Zhang & Zhou 2013), 52,358 meters × 51,244 metre- equivalent UHI imagines of Chengdu were obtained. By categorising the imagines according to the date recorded, UHI maps of monthly average values were obtained.

According to these six monthly intensity maps, several intensity centres of UHI-summer can be identified, which were located around the inner rings of this urban area. In specific, north-east corner of the Second Ring, south-west corner of the Third Ring is UHI intensity centre in summer. In winter month, lower UHI intensity was recorded in the centre of the First Ring. Moreover, several intensity centres of UHI-summer could be identified, which were located around the inner rings of this urban area. Study results in this chapter show a significant correlation between the distance (D) from the site to the city centre and UHI intensity in summer and winter. The longer distance away from the site to the city centre, the more decrease in the UHI intensity in summer. However, in winter, UHI intensity peaks at the area around 13km away from the city centre. Moreover, within the 13km range, the UHI intensity fell when the site was approaching the city centre, which proved ‘black hole’ in winter UHI map of Chengdu. This phenomenon is called the urban cool island, which can be results of the over-

shading effect of the dense and tall buildings and winter foggy weather. This effect found in this study corroborates findings- the daytime negative UHI in urban core- by Wong et al. (2011) and Futcher et al. (2013).

In general, a more than 6°C urban heat island was recorded, which corresponded the findings from other studies (Yang 1988) (Dan et al. 2011) (Zhang & Zhou 2013). The highest measured site-mean UHI reached 6.94°C in summer (on site No.63) and 2.26°C in winter (on site No.34). Note that the strongest UHI in Chengdu occurs in August, due to humid, calm and clear weather conditions. This phenomenon was due to the area's low height to floor area ratio (H/A) (2nd lowest) and high green area coverage (GCR) (2nd highest) (Table 3.10). On site 34, the highest winter UHI intensity was recorded, where the Green Coverage Ratio was third highest among the 103 sites.

By comparing with the on-site UHI values, the zonal UHI intensity was shown with background effect on each selected site at a statistic scale. The zonal UHI intensity for each zone was positively related to the average value of all sites within the zone area. However, due to the massive variation of UHI intensity among sites within the same zone, zonal UHI was proved to not decisive enough to accurately determine a site-specific UHI intensity at a city-block scale.

7.3.3 A method to analyse and predict the microclimate of building group at a city-block scale: ENVI-Met numerical modelling.

To investigate the diurnal variation of air temperature and other microclimate variables on a summer day and a winter day, confirms the effect of urban settlement on urban microclimate, Chapter 5 of this study conducted predictions of 15 selected projects from the original 103 target sites, as well as evaluations cooling effect of green coverage and water bodies. Based on the findings in Chapter 5, it had been provided that open spaces with massive solar exposure had higher air temperatures in summer daytime in Chengdu. Moreover, the shading effect of tall buildings effectively reduced the air temperature in the summertime. Moreover, air temperature and relative humidity were found with a relationship of compensating each other in Chengdu. Hotter areas

have dry air; the relative humidity is high where the air temperature is low.

On the other hand, the urban settlement is the key to determine the pattern of wind distribution in Chengdu. In open spaces without obstacles, wind can flow through these spaces at a relatively high speed. It gets stronger where the pattern of the path is suddenly changed, especially at the opening of the tall building group and street with building rows on both sides. In this study, however, local wind with relatively low speed, which ranged from 1.0m/s to 3.5m/s, played a minor role in determining the local air temperature at a microclimate scale.

Through the prediction of ENVI-Met, city-block scale sites in forms of the interspersed and the court were recorded with lower UHI in summer and higher UHI in winter. On the other hand, building groups with interspersed and court plot layout were proved to have lower summer UHI and higher winter UHI, which had been verified in Chapter 4 through analysis of remote sensing observation.

In the summertime, building height was highly related to UHI intensity, compared to another design variable. Though tall buildings can provide shading effect to reduce the air temperature at the points closed to them, the over-all on-site UHI intensity was proved to be raised with the increase in building height. In winter time, building density variables had a weak relationship with UHI. However, GCR was shown a strong relationship with UHI. Sites with high GCR tent to be warmer, which revealed a similar finding from the study in chapter 4 through remote sensing observations. According to the results of simulations, green areas are recorded with lower air temperature, which can increase the relative humidity locally with a magnitude around 1%.

Further study on modification of surface elements, including vegetation and water bodies was conducted in this chapter. It was proved that it was possible to cool the microclimate of city-block sites by generally increasing in green coverage ratio with the only grassland. It confirmed that this modification provides up to an hourly temperature reduction of 0.32°C, which corroborates the potential cooling effect of 0.5- 5°C by green

area (Oke 1989). Moreover, this cooling process was also proved to increase the overall relative humidity in the daytime. In the meanwhile, it was found that the cooling effect of water bodies settled within city-block sites reduced up to 0.1°C air temperature within the range of 5 metres from the water body in the daytime, a more extensive water coverage can offer the more significant effect of on-site cooling.

It recommended that a combination of grass, tall trees and water bodies could offer an additional solution for an optimised on-site cooling strategies thereby encouraging multiple cooling mechanisms, including evapotranspiration, shading, and direct heat exchange.

Finally, it can be summarised that urban settlement, including planning of plot layout of building group, and building height and density, plays a significant role in determining urban microclimate at city-block scale. Moreover, planning outdoor elements by adding sufficient coverage of multiple types of vegetation and water elements offers notable improvement for urban microclimate in Chengdu, which can be an additional solution of mitigating on-site UHI effect.

7.3.4 ENVI-met model validation

To validate the simulations results, the calculated data based on reliable the information was obtained from the long-period remote sensing. Based on the results of the comparison between the simulated data and reliable calculated data on a summer day, the average error during the simulation period of twenty-four hours was found to be around 1.00°C. The trend of the simulated atmospheric temperature curves was shown similar with the calculated ones (Figure 5.25), and the correlation coefficient, R^2, between simulated and calculated temperature, ranged from 0.788 to 0.897 (Figure 5.25). On the other hand, on a winter day, the average error between the simulated and calculated values ranged from 0.02°C to 0.64°C. It showed a significant correlation between the two groups of values, which achieved above 0.93 of the correlation coefficient (R^2) in any case of correlations (Figure 5.27). Thus, the simulated and calculated T_a in winter time are strongly correlated, thereby validating

the accuracy of simulation values obtained from ENVI-Met simulations. Therefore, T_a through two different methods- the ENVI-Met simulation and calculations derived from data obtained from weather stations- are well correlated, which indirectly presents the reliability and accuracy of ENVI-Met simulations regarding atmospheric temperatures in Chengdu.

7.3.5 A method to analyse and predict building energy performance of building group at a city-block scale: HTB2- Virvil Plug-in numerical modelling.

To answer the research question, Chapter 6 aimed to simulate energy demand and derive the energy supply in two stages of simulations. In the first stage of the simulation process, prototypes were set up to investigate the building energy performance and energy use. In the second stage, the outdoor environment varied regarding UHI values, and this was adopted by adjusting the weather data for the second simulation. Through the two stages of simulation, the impact of variation of outdoor microclimate on building energy performance was investigated and analysed. Moreover, the influence of design factors on building energy performance was discussed.

The structure of heat source varied in different building function types. The incidental gain dominates the heat gain in all cases of this study, which accounted for more than 60% of total heat gain in residential buildings and more than 80% of the total in public buildings. Moreover, the heat provided by the massive incidental gain balanced most of the heat loss due to ventilation and fabric transmittance in public buildings in the winter time. On the contrary, the heat released into fabric through transmittance in summer could benefit reducing the indoor heat in all building types in the summertime. However, ventilation in summer would be brought heat into the most public building and kept neutral in heat-gain/loss in residential. Therefore, blocking-up the heat transmission by ventilation could avoid extra heat gathered in public building in summer. In short, the active controlling the heat gain/loss due to ventilation and gain accordingly could rebalance the indoor thermal environment.

In most residential buildings, there had the needs for cooling only in June, July and

August, and the demand was lower compared that at the same time in public buildings. However, the cooling need for retails and offices still existed in April and October. Even the demand for heating in winter was massive in residential buildings, local tradition of living style cut off almost all energy consumption on heating in real practice. Moreover, the need for heating in public buildings in winter time stayed at a low level, which was less than 10 kWh/m^2/year in most cases.

Based on the simulation results, average heating demand in residential building was more than three times higher than that in retail buildings, and office building has the lowest demand and shortest operating time for heating. On the other hand, cooling demand in non-domestic buildings is around 60 kWh/m^2/year, which was ten times of that in residential buildings. In general, the total energy demand for heating/cooling was higher than that in domestic buildings, in which cooling demand accounted for the significant portion. The results obtained in this chapter revealed that then energy demand was influenced by forms of plot-layout. For public buildings, the three site forms- tower, linear and Semi-closed- were recorded with more than 64 kWh/m^2/year cooling demand, which is nearly double of that in retails with a form of court. Interspersed and the court had lower demand for cooling, but the heating demand in these two forms of sites was much higher than the other three types, especially for the later which has 34.88 kWh/m^2/year heating demand.

Moreover, the demand for heating and cooling in public building showed a strong correlation with design variables-FAR, BCR and HEIGHT; the significance was more than 30% in correlation with HEIGHT. However, for residential buildings, the energy demand was shown strong correlation only with HEIGH. The results of correlations indicated that sites with higher building density would reduce the heating demand in winter, but it would have more need for cooling in summer in return.

7.3.6 Understanding the influence of modification in microclimate conditions towards building energy performance at a city-block scale

By applying weather data adjusted with on-site air temperature obtained from Chapter

5, the energy demand in 15 target project sites has been changed due to the warmer outdoor environment. According to the comparison between the demand with UHI effect and the baseline value, in general, cooling demand is increased (more than 60% in most residential buildings) and heating demand is reduced (more than 20% in most retails) in all sites, which corroborates the finding in Athens by Fung et al. (2006). By comparing the change rate in buildings with different function, cooling demand is sensitive to the rising temperature only in residential buildings, and warmer winter will cause a higher rate of reduction in heating demand in public buildings. However, the change rate of energy demand due to UHI effects is not sensitive to other design variables.

Generally speaking, the UHI effect through a year increase the total energy consumption for heating/cooling, which means the amount of extra energy for heating is higher than the value saved in heating in all buildings. For residential buildings, outstand increase per unit area in cooling due to UHI effect will result in more than 70% extra cost on the electricity bill. In the meanwhile, due to large floor area in public buildings and the outstand proportion of total energy consumption occupied by AC systems, the 2%-3% increase in energy use could significantly raise the cost for business operations.

7.3.7 HTB2-Vivil Plug-in Model Validation

Considering the factors- the system performance of building services and losses during the distribution of electricity within the buildings, there are differences between energy demand and energy supply. In order to obtain the exact energy supplied for heating/cooling, it was necessary to determine the COP in each scenario. According to national (MOHURD & AQSIQ 2005) and local (MOHURD 2010) codes for thermal performance of civil buildings, standard values of COP were specified according to the geo-condition, building type, and condition of services. On the other hand, the data of practical total building energy consumption in Chengdu was collected through surveys (Su et al. 2010). In the surveys, more than 2000 buildings, including 1292 residential

building and 751 public buildings, were investigated, and the monthly usage of electricity for each building were summaries. However, the energy consumption for the AC systems could be calculated by the difference between the minimum monthly usage and the monthly usage of the other months, assuming that the minimum usage was for the total usage excluding the AC systems, while the consumption of the AC system was included in the other months (Su et al. 2010). Therefore, the energy consumption for AC systems and total electric consumption for six types of building were obtained in the surveys.

Finally, the reference data of surveys were applied to compare with the simulation results. The comparison between modelling and practical measurement could be checked in Table 6.3, which indicated the accuracy of the simulation and validates the simulated energy consumptions. Generally speaking, according to these comparisons, the simulation results of heating and cooling demand in all three types of buildings were close to the accurate values of a practical situation, thereby confirming the validity of the simulations.

7.4 Guidelines for planning building group at a city-block scale

Based on the finding and conclusions, the potential guidelines for optimising microclimate performance and building energy performance at a city-block scale can be summarised as follows:

1. Choice of the site should consider the effect of over-shading by surrounding buildings in Chengdu. The study shows that the city centre, where the urban density is low and with large open spaces suffered high UHI intensity in summer low UHI intensity in winter. The fact was that surrounding skyscrapers could not obstruct high-angle sunlight in summer, but the massive solar heat was storage together with surrounding buildings by blocking wind, absorbing the heat, and releasing massive anthropogenic heat. On the other hand, surrounding buildings blocked the low-angle sunlight leaving the site over-shaded cold and

uncomfortable.

2. Choice of building density should be based on the overall impact on microclimate. The study shows that the high density of the site tends to have higher outdoor air temperatures and higher building energy consumption, especially for public buildings. Even it was found that the taller buildings could provide over-shading, but just within a limited range, the overall outdoor temperature of the entire site would increase as the building height was getting taller.

3. Choice of plot layout should be considered with the microclimate and building energy performance. The study shows that the building groups with interspersed and court plot layout were achieved with lower heating and cooling energy consumption, while at the same time, with a reduced UHI intensity in summer and increased UHI intensity in winter.

4. The study presents the fact that modification of the ground surface with greening and water bodies has a considerable impact on the outdoor thermal environment. In a humid urban environment, like in Chengdu, increasing green coverage ratio and installing water bodies within site can alter the thermal properties of the surface on site, resulting in the desired effects of reduction of air temperature and building energy consumption. Moreover, taller trees are suggested to provide sufficient shading effect; larger area of water bodies with short distance to buildings is also suggested.

7.5 Limitations

The limitations of this study are summarised as follows:

In the surveys on information of 103 selected project sites, the accessibility and accuracy of database available are not entirely satisfied. Different numbers of the same construction parameter from different database occasionally appeared. Therefore, the accuracy of the basic parameters for the 103 sites needed to be improved, which might

cause lower satisfactory on findings.

Considering the accessibility on some critical data, for example, the history records of building energy consumption in a specific building, assumptions or derived data were made for the study, which might cause further errors and reduce the accuracy of the findings.

Lastly, due to the limitation of the period, this study could not address a further broader scope. Anthropogenic heat should be considered, which has significant influence in a busy and crowded city like Chengdu.

7.6 Recommended future studies

As the scope of this study is limited, many issues raised. Further investigation of the findings is still needed. The following suggestions are recommended for future research:

1. The simulation tool ENVI-Met is missing the consideration of vertical long-wave flux divergence (Bruse et al. 2002) (Taleghani et al. 2015), which may lead to a more significant error in the prediction results. Moreover, simulations lack the internal gain within buildings and anthropogenic heat, which may increase the error. Therefore, it is better to choose another platform with more calculation mechanism built in, if conditions permit.

2. For a future design project, it is suggested to use ENVI-Met or other platforms with a complete thermal modelling system as a design tool to assess the environmental performance of a design proposal thereby assisting a practical design project.

3. Considering the limited availability of data from satellite remote sensing, collecting the continuous imagines over a long period becomes impossible. However, the related future work could be suggested to be carried out with a group of aircraft that can be operated at low altitude for a long time. For example, a cluster

unmanned aerial vehicle (UAV). In this way, continuous observation over a large area becomes possible.

4. The findings of this study can be checked with different urban environment conditions in order to continuously improve the accuracy of the conclusions.

Reference

1. (NOAA), N.O. and A.A., 1998. Integrated Surface Data (ISD) database. Available at: https://www.ncdc.noaa.gov/isd/products [Accessed April 20, 2018].
2. Ackerman, B., 1985. Temporal March of the Chicago Heat Island. *Journal of Applied Meteorology*, 24(6), p.547. Available at: http://ams.allenpress.com/perlserv/?request=get-abstract&doi=10.1175%2F1520-0450(1985)024%3C0547:TMOTCH%3E2.0.CO%3B2.
3. Adebayo, Y.R., 1991. “Heat island” in a humid tropical city and its relationship with potential evaporation. *Theoretical and applied climatology*, 43(3), pp.137–147.
4. Adolphe, L., 2001. A simplified model of urban morphology: application to an analysis of the environmental performance of cities. *Environment and Planning B: Planning and Design*, 28(2), pp.183–200. Available at: http://epb.sagepub.com/lookup/doi/10.1068/b2631.
5. Agricultural, C. et al., 2015. Wavelet Analysis of API Changes of Chengdu About 10 Years. *Chinese Agricultural Science Bulletin*, 31(14), pp.200–205.
6. Ahmed, V., Opoku, A. & Aziz, Z., 2016. *Research methodology in the Built Environment*, Oxon: Routledge.
7. Akbari, H., 2009. *Cooling our Communities: A Guidebook on Tree Planting and Light-Colored Surfacing*,
8. Akbari, H., Rosenfeld, A.H. & Taha, H., 1990. *Summer heat islands, urban trees, and white surfaces*,
9. Alexander, C. et al., 1985. *The production of houses*, Oxford University Press on Demand.
10. Ali-toudert, F., 2009. Energy Efficiency of Urban Buildings: Significance of Urban Geometry, Building Construction and Climate Conditions. *The seventh International Conference on Urban Climate, Yokohama, Japan*, (July), pp.29–32.
11. Ali-Toudert, F. & Mayer, H., 2006. Numerical study on the effects of aspect ratio and orientation of an urban street canyon on outdoor thermal comfort in hot and dry climate. *Building and Environment*, 41(2), pp.94–108.
12. Allegrini, J., Dorer, V. & Carmeliet, J., 2012. Influence of the urban microclimate in street canyons on the energy demand for space cooling and heating of buildings. *Energy and Buildings*, 55, pp.823–832. Available at: http://linkinghub.elsevier.com/retrieve/pii/S0378778812005221.
13. Amaratunga, D. et al., 2002. Quantitative and qualitative research in the built environment: application of “mixed” research approach. , 51(1), pp.17–31. Available at: http://www.adolphus.me.uk/emx/research_design/meth_be_files/p17.htm.
14. Ambrosini, D. et al., 2014. Evaluating mitigation effects of urban heat islands in a

historical small center with the ENVI-Met®climate model. *Sustainability (Switzerland)*, 6(10), pp.7013–7029.

15. Anderson, W.P., Kanaroglou, P.S. & Miller, E.J., 1996. Urban form, energy and the environment: a review of issues, evidence and policy. *Urban studies*, 33(1), pp.7–35.
16. Andreou, E., 2013. Thermal comfort in outdoor spaces and urban canyon microclimate. *Renewable Energy*, 55, pp.182–188.
17. Anon, 2013. Climate of Chengdu. Available at: http://www.docin.com/p-570863276.html [Accessed April 20, 2018].
18. Arnfield, a. J. & Grimmond, C.S.B., 1998. An urban canyon energy budget model and its application to urban storage heat flux modeling. *Energy and Buildings*, 27(1), pp.61–68.
19. Arnfield, A.J., 2003. Two decades of urban climate research: A review of turbulence, exchanges of energy and water, and the urban heat island. *International Journal of Climatology*, 23(1), pp.1–26.
20. Asia, K.I. and Y.T., 2016. APEC Low-Carbon Model Town Project Progress and.pdf. *Modern Environmental Science and Engineering*, 1(8).
21. Asia Pacific Energy Research Centre, 2014. *The Concept of the Low-Carbon Town in the APEC Region:Third Edition*, Tokyo.
22. Avissar, R., 1996. Potential Effects of Vegetation on the Urban Thermal Environment. *Atmospheric Environment*, 30(3), pp.437–448.
23. Beyer, P., 2010. *Mixed-Use Zoning*, Available at: http://www.aging.ny.gov/LivableNY/ResourceManual/Index.cfm.
24. Bickman, L. & Rog, D.J., 2009. *The SAGE Handbook of Applied Social Research*,
25. Boumans, R.J.M. et al., 2014. Developing a model for effects of climate change on human health and health-environment interactions: Heat stress in Austin, Texas. *Urban Climate*, 8, pp.78–99. Available at: http://dx.doi.org/10.1016/j.uclim.2014.03.001.
26. BPIE, 2010. Discussing methodology and challenges within the recast Energy Performance of Buildings Directive. In *Cost Optimality*. Brussels, Belgium.
27. Breheny, M., 1996. Centrists, decentrists and compromisers: views on the future of urban form. In *The compact city: A sustainable urban form*. pp. 13–35.
28. Brest, C.L., 1987. Seasonal Albedo of an Urban/Rural Landscape From Satellite Observations. *Journal of Applied Meteorology and Climatology*, 26, pp.1169–1187.
29. Bruse, M. et al., 2002. *Measurements and model simulations in WP MICRO*, Bochum, Germany.
30. Bruse, M. & Fleer, H., 1998. Simulating surface-plant-air interactions inside urban environments with a three dimensional numerical model. *Environmental Modelling and*

Software, 13(3–4), pp.373–384.

31. Bueren, E. van, Bohemen, H. van & Visscher, L.I.H., 2012. *Sustainable Urban Environments*, London New York: Springer. Available at: http://ebooks.cambridge.org/ref/id/CBO9781107415324A009%0Ahttp://www.ncbi.nlm.nih.gov/pubmed/25246403%0Ahttp://www.pubmedcentral.nih.gov/articlerender.fcgi?artid=PMC4249520%0Ahttp://arxiv.org/abs/1011.1669%0Ahttp://dx.doi.org/10.1088/1751-8113/44/8/085201.

32. Building Research Establishment (BRE), 2011. BREEAM 2011. Available at: https://www.breeam.com/.

33. Burton, E., Jenks, M. & Williams, K., 2003. *The compact city: a sustainable urban form?*, Routledge.

34. Butcher, K., 2006. *CIBSE Guide A Environmental Design* 7th Revise., Chartered Institution of Building Services Engineers.

35. CAAS, 2010. *Technical Specification for Concrete Structure of Tall Buildings*, Beijing.

36. Cardelino, C.A. & Chameides, W.L., 1990. Natural hydrocarbons, urbanization, and urban ozone. *Journal of Geophysical Research: Atmospheres*, 95(D9), pp.13971–13979. Available at: http://dx.doi.org/10.1029/JD095iD09p13971.

37. CCREA, 2013. The number of commercial complexes in Chengdu reaches 122. *Chengdu Commercial Real Estate Alliance*. Available at: http://news.winshang.com/html/019/3943.html [Accessed April 20, 2018].

38. CDMPB, 2012. *Supplementary Provisions for Planning Management of Large Urban Complex Projects in Downtown Chengdu*, Chengdu, China: Chengdu Municipal Planning Bureau. Available at: http://www.cdgh.gov.cn/hbdt/768.htm.

39. Chang, C.R., Li, M.H. & Chang, S.D., 2007. A preliminary study on the local cool-island intensity of Taipei city parks. *Landscape and Urban Planning*, 80(4), pp.386–395.

40. Changnon, S.A. & Kunkel, K.E., 1996. Impacts and responses to the 1995 heat wave: A call to action. *Bulletin of the American …*, 77(7), pp.1497–1506. Available at: http://journals.ametsoc.org/doi/abs/10.1175/1520-0477%281996%29077%3C1497%3AIARTTH%3E2.0.CO%3B2%0A(null).

41. Chen, H., Jia, B. & Lau, S.S.Y., 2008. Sustainable urban form for Chinese compact cities: Challenges of a rapid urbanized economy. , 32, pp.28–40.

42. Chen, L. et al., 2012. Sky view factor analysis of street canyons and its implications for daytime intra-urban air temperature differentials in high-rise, high-density urban areas of Hong Kong: a GIS-based simulation approach. *International Journal of Climatology*, 32(1), pp.121–136. Available at: http://doi.wiley.com/10.1002/joc.2243.

43. Chen, L. & Ng, E., 2011. Quantitative urban climate mapping based on a geographical database: A simulation approach using Hong Kong as a case study. *International Journal of Applied Earth Observation and Geoinformation*, 13(4), pp.586–594.

44. Chen, L., Zeng, J. & Zhou, B., 2009. Ecological Process and Sustainable Development of Urban Spatial Morphology in Chengdu. *Architectural Journal*, (12), pp.14–17.

45. Chen, Q. et al., 2009. Urban heat island effect research in Chengdu city based on MODIS data. *3rd International Conference on Bioinformatics and Biomedical Engineering, iCBBE 2009*, pp.1–5.

46. Chen, Y. et al., 2011. Estimating the relationship between urban forms and energy consumption: A case study in the Pearl River Delta, 2005–2008. *Landscape and Urban Planning*, 102(1), pp.33–42. Available at: http://linkinghub.elsevier.com/retrieve/pii/S0169204611001381.

47. Cheng, V. et al., 2006. Urban Form , Density and Solar Potential. *PLEA2006 - The 23rd Conference on Passive and Low Energy Architecture, Geneva, Switzerland*, (September), pp.6–8.

48. Chengdu Meteorological Bureau (CDMB), 2016. Chengdu's monthly weather throughout the year. Available at: http://www.tianqi.com/qiwen/city_chengdu/ [Accessed April 20, 2018].

49. Chengdu Municipal Bureau of Statistics, 2001. *Annual Data of Chengdu*, Chengdu. Available at: http://www.cdstats.chengdu.gov.cn/sjck/cdnj/2001_0.htm.

50. Chengdu Municipal Commission of Economy and Information Technology, 2017. *Chengdu City Energy Development Planning in the 13th Five-Year*, Chengdu. Available at: http://www.cdgy.gov.cn/cdsjxw/c132946/2017-04/25/content_2d4f462a322c4b0aafbecd5adbb01724.shtml.

51. Chengdu Municipal Planning Bureau, 2017. *Draft for Chengdu Urban Master Plan (2016-2035)*, Chengdu. Available at: https://wenku.baidu.com/view/850418cc846a561252d380eb6294dd88d0d23d18.html.

52. Chengdu Upwards, 2017. Will the 677 Metre Tianfu Center Become the Center of Chengdu in the Future? Available at: http://cd.house.163.com/17/1204/02/D4PFPSUO02241EF1.html [Accessed April 20, 2018].

53. Cheval, S. & Dumitrescu, A., 2009. The July urban heat island of Bucharest as derived from modis images. *Theoretical and Applied Climatology*, 96(1–2), pp.145–153.

54. China Meteorological Bureau Tsinghua University, 2005. *China Standard Weather Data for Analyzing Building Thermal Conditions* April 2005., Beijing: China Building Industry Publishing House.

55. China Ministry of Construction, N.S. of the P.R. of C., 2006. *Assessment Standard for Green Building*,

56. China Ministry of Construction, N.S. of the P.R. of C., 2005. *Design Standard for Energy Efficiency of Public Buildings*,

57. Chow, W.T.L. & Roth, M., 2006. Temporal dynamics of the urban heat island o

Singapore. *International Journal of Climatology*, 26(26), pp.2243–2260.

58. Christen, A. & Vogt, R., 2004. Energy and radiation balance of a central European City. *International Journal of Climatology*, 24(11), pp.1395–1421.

59. Christensen, A.J., 2005. *Dictionary of Landscape Architecture and Construction*, McGraw-Hill.

60. Ciscar, J.C. & Dowling, P., 2014. Integrated assessment of climate impacts and adaptation in the energy sector. *Energy Economics*, 46, pp.531–538. Available at: http://dx.doi.org/10.1016/j.eneco.2014.07.003.

61. CMBS, 2011. *Chengdu Statistical Yearbook (2010)*, Chengdu. Available at: http://www.cdstats.chengdu.gov.cn/htm/detail_1550.html.

62. CMBS, 2015. *Chengdu Statistical Yearbook (2014)*, Chengdu.

63. CMBS, 2016. *Chengdu Statistical Yearbook (2015)*,

64. CMBS, 2017. *Chengdu Statistical Yearbook (2016)*, Chengdu.

65. CMBS, 2018. *China Statistical Yearbook （2017）*, Beijing. Available at: http://www.stats.gov.cn/tjsj/ndsj/2017/indexch.htm.

66. Cohen, P., Potchter, O. & Matzarakis, A., 2012. Daily and seasonal climatic conditions of green urban open spaces in the Mediterranean climate and their impact on human comfort. *Building and Environment*, 51, pp.285–295. Available at: http://dx.doi.org/10.1016/j.buildenv.2011.11.020.

67. Commission of the European Communities (CEC), 1990. *Green Paper on The Urban Environment*, Brussels.

68. Compagnon, R., 2004. Solar and daylight availability in the urban fabric. *Energy and Buildings*, 36(4), pp.321–328.

69. Correa, E. et al., 2012. Thermal comfort in forested urban canyons of low building density. An assessment for the city of Mendoza, Argentina. *Building and Environment*, 58, pp.219–230.

70. Coutts, A.M. et al., 2016. Temperature and Human Thermal Comfort Effects of Street Trees Across Three Contrasting Street Canyon Environments. *Theoretical and Applied Climatology*, 126(3–4), p.815.

71. Crawley, D. & Aho, I., 1999. Building environmental assessment methods: applications and development trends. *Building Research & Information*, 27(4/5), pp.300–308.

72. Creswell, J.W., 2002. *Research design : qualitative, quantitative, and mixed methods approaches* 2nd ed., SAGE Publications.

73. Crotty, M., 1998. *The foundations of social research: Meaning and perspective in the research process*, Sage.

74. Crowley, T.J., 2000. Causes of Climate Change Over the Past 1000 Years. *SCIENCE*,

289(5477), pp.270–277.

75. Cui, L. & Shi, J., 2012. Urbanization and its environmental effects in Shanghai, China. *Urban Climate*, 2, pp.1–15. Available at: http://dx.doi.org/10.1016/j.uclim.2012.10.008.

76. Curl, J.S., 2006. *The Oxford Dictionary of Architecture and Landscape Architecture* 2 edition., UK, USA: Oxford University Press.

77. Dan, S. et al., 2011. Analysis of Impact of Urban Development on Heat Island Effect in Chengdu City. *Environmental science & technology*, 34(7), pp.180–185.

78. Dan, S. & Dan, B., 2001. Analysis of urban heat island using remote sensing. In *the 22nd Asian Conference on Remote Sensing*. Singapore.

79. Daniels, T.L., 2009. American Environmental Planning From City Beautiful to Sustainability. *Journal of the American Planning Association*, 75(2), pp.178–192.

80. Delgarm, N. et al., 2016. Multi-objective optimization of the building energy performance: A simulation-based approach by means of particle swarm optimization (PSO). *Applied Energy*, 170, pp.293–303. Available at: http://dx.doi.org/10.1016/j.apenergy.2016.02.141.

81. Deng, X., 2016. A simulation of impact of micro- climate change and neighbourhood morphology on building energy demand. *Archidoct*, pp.48–61. Available at: http://www.enhsa.net/archidoct/Issues/vol3_iss2/ArchiDoct_vol3_iss2 04 A simulation of impact of microclimate change Deng.pdf.

82. Dhakal, S., 2009. Urban energy use and carbon emissions from cities in China and policy implications. *Energy Policy*, 37(11), pp.4208–4219. Available at: http://dx.doi.org/10.1016/j.enpol.2009.05.020.

83. Dousset, B. & Gourmelon, F., 2003. Satellite multi-sensor data analysis of urban surface temperatures and landcover. *ISPRS Journal of Photogrammetry and Remote Sensing*, 58(1–2), pp.43–54.

84. DRAHOŠ, M. & Drahoš, R., 2012. Influence of Meteorological Conditions on Propagation of Sound.

85. Du, W., 2003. Consumer Survey of Residential Market in Chengdu in 2002. *Chinese and Foreign Real Estate Guide*, 9, pp.17–17. Available at: http://www.cqvip.com/read/read.aspx?id=7978243.

86. Du, X., Bokel, R. & van den Dobbelsteen, A., 2014. Building microclimate and summer thermal comfort in free-running buildings with diverse spaces: A Chinese vernacular house case. *Building and Environment*, 82, pp.215–227. Available at: http://linkinghub.elsevier.com/retrieve/pii/S0360132314002741.

87. Ebinger, Jane; Vergara, W., 2011. *Climate impacts on energy systems: key issues for energy sector adaptation*,

88. Eliasson, I., 1996. Urban nocturnal temperatures, street geometry and land use. *Atmospheric Environment*, 30(3), pp.379–392.

89. Erell, E., Pearlmutter, D. & Williamson, T., 2011. *Urban Microclimate: Designing the Spaces Between Buildings*, Taylor & Francis.

90. Ewing, R., Pendall, R. & Chen, D., 2002. *Measuring Sprawl and its Impact*, Washington, D.C.

91. Ewing, R. & Rong, F., 2008. The impact of urban form on U.S. residential energy use. *Housing Policy Debate*, 19(1), pp.1–30.

92. Fabbri, K. et al., 2017. Outdoor Comfort: The ENVI-BUG tool to Evaluate PMV Values Output Comfort Point by Point. In *Energy Procedia*. pp. 510–519.

93. Fang, Y., Chen, G. & Li, W., 2001. Approaches of Eco-city Construction in Chengdu. *Urban Envrionment & Urban Ecology*, 14(2), pp.50–53.

94. Feng, Y., 2004. Thermal design standards for energy efficiency of residential buildings in hot summer/cold winter zones. *Energy and Buildings*, 36(12), pp.1309–1312.

95. Feng, Y., 2015. URBAN MORPHOLOGY AND MICROCLIMATE : REVIEW OF PERFORMANCE-BASED SIMULATION APPROACHES. , pp.93–94.

96. Ferrara, M. et al., 2014. A simulation-based optimization method for cost-optimal analysis of nearly Zero Energy Buildings. *Energy and Buildings*, 84, pp.442–457. Available at: http://dx.doi.org/10.1016/j.enbuild.2014.08.031.

97. Ferreira, J., Pinheiro, M.D. & De Brito, J., 2014. Portuguese sustainable construction assessment tools benchmarked with BREEAM and LEED: An energy analysis. *Energy and Buildings*, 69, pp.451–463. Available at: http://dx.doi.org/10.1016/j.enbuild.2013.11.039.

98. Forster, C., 2006. The challenge of change: Australian cities and urban planning in the new millennium. *Geographical Research*, 44(2), pp.173–182.

99. Fröhlich, C. & Lean, J., 1998. The Sun's Total Irradiance: Cycles, Trends and Related Climate Change Uncertainties since 1976. , 25(23), pp.4377–4380.

100. Fung, W. et al., 2006. Impact of urban temperature on energy consumption of Hong Kong. *Energy*, 31(14), pp.2623–2637. Available at: http://linkinghub.elsevier.com/retrieve/pii/S0360544206000119.

101. Futcher, J.A., Kershaw, T. & Mills, G., 2013. Urban form and function as building performance parameters. *Building and Environment*, 62, pp.112–123. Available at: http://linkinghub.elsevier.com/retrieve/pii/S0360132313000449.

102. Futcher, J.A. & Mills, G., 2013. The role of urban form as an energy management parameter. *Energy Policy*, 53, pp.218–228. Available at: http://linkinghub.elsevier.com/retrieve/pii/S0301421512009652.

103. Galster, G. et al., 2001. Wrestling Sprawl to the Ground-Defining and Measuring an Elusive Concept. *US Geological Survey professional paper*, (1726), pp.55–58. Available at: http://cat.inist.fr/?aModele=afficheN&cpsidt=20240464 [Accessed October 4, 2015].

104. Gao, B. et al., 2009. Analysis on the characteristic of Air-conditioning load in residential buildings in Chengdu. *Refrigeration and Air Condingning*, 23(06), pp.19–22.

105. Giannaros, T.M. et al., 2013. Numerical study of the urban heat island over Athens (Greece) with the WRF model. *Atmospheric Environment*, 73, pp.103–111. Available at: http://linkinghub.elsevier.com/retrieve/pii/S1352231013001726.

106. Gill, J. & Johnson, P., 2010. *Research Methods for Managers*, Sage.

107. Givoni, B., 1989. *Urban design in different climates*,

108. Goh, K.C. & Chang, C.H., 1999. The relationship between height to width ratios and the heat island intensity at 22:00 h for Singapore. *International Journal of Climatology*, 19(9), pp.1011–1023.

109. Golany, G.S., 1996. Urban Design Morphology and Thermal Performance. *Atmospheric Environment*, 30(3), pp.455–465.

110. Google, 2014. SketchUp. Available at: https://www.sketchup.com/ [Accessed April 20, 2015].

111. Gray, R. & Gleeson, B., 2007. Energy Demands of Urban Living : What Role for Planning. In *3rd National Conference on the State of Australian Cities*. pp. 28–30.

112. Grazi, F. & van den Bergh, J.C.J.M., 2008. Spatial organization, transport, and climate change: Comparing instruments of spatial planning and policy. *Ecological Economics*, 67(4), pp.630–639.

113. Grimmond, C.S.B. & Souch, C., 1994. Surface Description for Urban Climate Studies: A GIS Based Methodology. *Geocarto International*, 9, pp.47–59. Available at: http://www.informaworld.com/openurl?genre=article&doi=10.1080/10106049409354439&magic=crossref%7C%7CD404A21C5BB053405B1A640AFFD44AE3%5Cnhttp://dx.doi.org/10.1080/10106049409354439.

114. Grosso, M., 1998. Urban form and renewable energy potential. *Renewable energy*, 15(1–4 pt 1), pp.331–336.

115. Guo, J., Sun, M. & Li, G., 2008. Climatic Characteristics of High Temperature and Muggy and Comfort Degree Assessment in Summer in Sichuan Basin 环境与健康杂志. *Journal of Environment and Health*, 25(1), pp.45–48.

116. Guo, Z., 2005. Prevention of Tall Building Syndrome. *Healthy Life*, pp.20–20.

117. Haapio, A., 2012. Towards sustainable urban communities. *Environmental Impact Assessment Review*, 32(1), pp.165–169. Available at: http://dx.doi.org/10.1016/j.eiar.2011.08.002.

118. Hachem, C., Athienitis, A. & Fazio, P., 2012. Evaluation of energy supply and demand in solar neighborhood. *Energy and Buildings*, 49, pp.335–347. Available at: http://linkinghub.elsevier.com/retrieve/pii/S0378778812000989.

119. Hafner, J. & Kidder, S.Q., 1999. Urban Heat Island Modeling in Conjunction with

Satellite-Derived Surface/Soil Parameters. *Journal of Applied Meteorology*, 38(4), pp.448–465. Available at: http://journals.ametsoc.org/doi/abs/10.1175/1520-0450%281999%29038%3C0448%3AUHIMIC%3E2.0.CO%3B2.

120. Hamada, S. & Ohta, T., 2010. Seasonal variations in the cooling effect of urban green areas on surrounding urban areas. *Urban Forestry and Urban Greening*, 9(1), pp.15–24. Available at: http://dx.doi.org/10.1016/j.ufug.2009.10.002.

121. Hamilton, I., Davies, M. & Steadman, P., 2009. Onsite energy yield and demand in the urban built form: Balancing yield and demand to achieve zero carbon communities. , (June), pp.22–24. Available at: http://discovery.ucl.ac.uk/1349527/.

122. Hamin, E.M. & Gurran, N., 2009. Urban form and climate change: Balancing adaptation and mitigation in the U.S. and Australia. *Habitat International*, 33(3), pp.238–245.

123. He, J., 2015. *Research on energy consumption and energy saving of city complex in Chengdu*. Harbin Institute of Technology.

124. He, X. et al., 2014. Study on Dynamic Landscape Pattern of Green Space in Downtown of Chengdu City. *Forestry Science in the West*, (5).

125. Holden, E. & Norland, I.T., 2005. Three Challenges for the Compact City as a Sustainable Urban Form: Household Consumption of Energy and Transport in Eight Residential Areas in the Greater Oslo Region. *Urban Studies*, 42(12), pp.2145–2166. Available at: http://eds-1a-1ebscohost-1com-1ebsco.han.buw.uw.edu.pl/eds/pdfviewer/pdfviewer?vid=27&sid=4786ab56-79c2-4393-9621-1f4e976faeff@sessionmgr4001&hid=4113.

126. Honjo, T. & Takakura, T., 1990. Simulation of Thermal Effects of Urban reen Areas on Their Surrounding Areas. *Energy and Buildings*, 16, pp.443–446.

127. Höppe, P., 1999. The physiological equivalent temperature - A universal index for the biometeorological assessment of the thermal environment. *International Journal of Biometeorology*, 43(2), pp.71–75.

128. Howard, E., 1965. *Garden cities of to-morrow (Vol. 23)* (New rev., Eastbourne: Mit Press.

129. Howard, L., 1833. *The climate of London, vols. I–III*, London: Harvey and Dorton.

130. Huang, J., Lu, X.X. & Sellers, J.M., 2007. A global comparative analysis of urban form: Applying spatial metrics and remote sensing. *Landscape and Urban Planning*, 82(4), pp.184–197. Available at: http://linkinghub.elsevier.com/retrieve/pii/S0169204607000588.

131. Huang, Y. & Sun, Y., 2012. Judgement Characteristics and Quantitative Index of Suitable Block Scale. *Journal of South China University of Technology (Natural Science Edition)*, 40(9), pp.131–138.

132. Huang, Z., 1981. Traditional Houses and Others in Chengdu. *Architectural Journal*, 11(11), pp.50–53.

133. Huttner, S., Bruse, M. & Dostal, P., 2008. Using ENVI-met to simulate the impact of global warming on the microclimate in central European cities. *5th Japanese-German Meeting on Urban Climatology*, pp.307–312. Available at: https://www.researchgate.net/profile/Michael_Bruse/publication/237304053_Using_ENVI-met_to_simulate_the_impact_of_global_warming_on_the_mi-_croclimate_in_central_European_cities/links/00b4952c59e958040e000000.pdf.

134. Intergovernmental Panel on Climate Change (IPCC), 2007. *The Working Group III Contribution to the IPCC Fourth Assessment Report Climate Change 2007: Mitigation of climate change*., Cambridge: Cambridge University Press.

135. IPCC, 2001. *Climate change 2001 : Impacts, Adaptation, and Vulnerability*, Available at: https://www.ipcc.ch/ipccreports/tar/wg2/pdf/wg2TARchap1.pdf.

136. IPCC, 2014. *Climate Change 2014: Mitigation of Climate Change*, Available at: http://www.ipcc.ch/report/ar5/wg3/.

137. Jacobs, J.M., Cairns, S. & Strebel, I., 2007. The Red Road High-rise as a Black Box. , 44(3), pp.609–629.

138. Jauregui, E., 1990. Influence of a large urban park on temperature and convective precipitation in a tropical city. *Energy and Buildings*, 15(3–4), pp.457–463.

139. Jenks, M., 2000. *Achieving sustainable urban form*, Taylor & Francis.

140. Jones, P.J. et al., 2011. *LCRI-CISDI Low Carbon Master Plan Guideance*, Welsh School of Architecture, Cardiff University. Available at: http://orca.cf.ac.uk/id/eprint/49347.

141. de Jong, M. et al., 2015. Sustainable-smart-resilient-low carbon-eco-knowledge cities; making sense of a multitude of concepts promoting sustainable urbanization. *Journal of Cleaner Production*, 109, pp.25–38. Available at: http://dx.doi.org/10.1016/j.jclepro.2015.02.004.

142. De Jong, M. et al., 2015. Sustainable-smart-resilient-low carbon-eco-knowledge cities; Making sense of a multitude of concepts promoting sustainable urbanization. *Journal of Cleaner Production*, 109, pp.25–38.

143. Jonsson, P.E.R., 2004. Vegetation as an Urban Climate Control in the Subtropical City of Gaborone, Botswana. *INTERNATIONAL JOURNAL OF CLIMATOLOGY*, 1322, pp.1307–1322.

144. Kato, S. & Yamaguchi, Y., 2005. Analysis of urban heat-island effect using ASTER and ETM+ Data: Separation of anthropogenic heat discharge and natural heat radiation from sensible heat flux. *Remote Sensing of Environment*, 99(1–2), pp.44–54.

145. Kawashima, S., 1990. Effects os vegetation on surface temperatures in urban and suburban areas in winter. *Energy and Buildings*, 15–16, pp.465–469.

146. Kellett, R. et al., 2013. A systems approach to carbon cycling and emissions modeling at an urban neighborhood scale. *Landscape and Urban Planning*, 110, pp.48–58. Available

at: http://www.sciencedirect.com/science/article/pii/S0169204612002733.

147. Kikegawa, Y. et al., 2006. Impacts of city-block-scale countermeasures against urban heat-island phenomena upon a building's energy-consumption for air-conditioning. *Applied Energy*, 83(6), pp.649–668.

148. Kim, Y.-H. & Baik, J.-J., 2002. Maximum Urban Heat Island Intensity in Seoul. *Journal of Applied Meteorology*, 41(6), pp.651–659.

149. Kłysik, K. & Fortuniak, K., 1999. Temporal and spatial characteristics of the urban heat island of Łódź, Poland. *Atmospheric Environment*, 33(24–25), pp.3885–3895.

150. Knight, A. & Ruddock, L., 2008. *Advanced Research Methods in the Built Environment*, Oxford: Blackwell Publishing Ltd. Available at: https://www.academia.edu/8012398/Andrew_Knight_Les_Ruddock_Advanced_Research_Methods_in_the_Built_Environment.

151. Kolokotroni, M., Giannitsaris, I. & Watkins, R., 2006. The effect of the London urban heat island on building summer cooling demand and night ventilation strategies. *Solar Energy*, 80(4), pp.383–392.

152. Kolokotroni, M. & Giridharan, R., 2008. Urban heat island intensity in London: An investigation of the impact of physical characteristics on changes in outdoor air temperature during summer. *Solar Energy*, 82(11), pp.986–998. Available at: https://www.sciencedirect.com/science/article/pii/S0038092X08001084 [Accessed July 18, 2018].

153. Korthals Altes, W.K. & Tambach, M., 2008. Municipal strategies for introducing housing on industrial estates as part of compact-city policies in the Netherlands. *Cities*, 25(4), pp.218–229.

154. Kuang, X., Chen, J. & Sun, C., 2015. Evaluation of Ventialtion Effectiveness of Block Scale Urban Green Belt Based on Computer Simulation. *Urban Development Studies*, 22(9), pp.91–95.

155. Kuzi, 2017. A Brief Look at the Evolutionary History of the High Buildings in Chengdu. Available at: http://www.sohu.com/a/207199526_687733 [Accessed April 20, 2018].

156. Landsberg, H.E., 1981. *The urban climate (Vol. 28)*, Academic press.

157. Lao, C., 2015. Analysis and forecast of energy and electric power in Sichuan in 2014~2015. In G. Yang, ed. *Analysis and forecast of Sichuan's economic situation in 2015 (2015 Edition) / Sichuan Blue Book*. Chengdu: Social Science Literature Press, p. 412. Available at: http://www.doc88.com/p-7384580069861.html.

158. Lau, K.K.-L. et al., 2017. Defining the environmental performance of neighbourhoods in high-density cities. *Building Research and Information*, 0(5), pp.1–12. Available at: https://doi.org/10.1080/09613218.2018.1399583.

159. Lechtenböhmer, S. & Schüring, A., 2011. The potential for large-scale savings from insulating residential buildings in the EU. *Energy Efficiency*, 4(2), pp.257–270.

160. Lee, H.-Y., 1993. An Application of NOAA AVHRR Thermal Data to the Study of Urban Heat Islands. *Atmospheric Environment*, 27(1), pp.1–13.

161. Lee, S. & Lee, B., 2014. The influence of urban form on GHG emissions in the U.S. household sector. *Energy Policy*, 68, pp.534–549. Available at: http://linkinghub.elsevier.com/retrieve/pii/S0301421514000299.

162. Lee, T.-W., Lee, J.Y. & Wang, Z.-H., 2012. Scaling of the urban heat island intensity using time-dependent energy balance. *Urban Climate*, 2, pp.16–24. Available at: http://linkinghub.elsevier.com/retrieve/pii/S2212095512000120.

163. Lei, Z. & Nanyang, Y., 2017. Study on the Energy Conservation Scheme of Achieving 65% Goals of Energy Efficiency in Residential Buildings in Chengdu. *Refrigeration and Air Conditioning*, 31(6), pp.636–641.

164. Leung, C.W. et al., 2010. Measuring the neighborhood environment: Associations with young girls' energy intake and expenditure in a cross-sectional study. *International Journal of Behavioral Nutrition and Physical Activity*, 7.

165. Lewis, P.T. & Alexander, D.K., 1990. HTB2: A flexible model for dynamic building simulation. *Building and Environment*, 25(1), pp.7–16.

166. Li, C. et al., 2012. A new zero-equation turbulence model for micro-scale climate simulation. *Building and Environment*, 47, pp.243–255. Available at: http://linkinghub.elsevier.com/retrieve/pii/S036013231100223X.

167. Li, C. et al., 2014. Interaction between urban microclimate and electric air-conditioning energy consumption during high temperature season. *Applied Energy*, 117, pp.149–156. Available at: http://linkinghub.elsevier.com/retrieve/pii/S0306261913009641.

168. Li, H. et al., 2007. Study on Retrieval Urban Land Surface Temperature with Multi-source Remote Sensing Data. *JOURNAL OF REMOTE SENSING*, 11(6), pp.891–898.

169. Li, J., 2007. *Study on the spatial distribution of Chengdu Industrial Park*. Southwestern University of Finance and Economics.

170. Li, J. & Colombier, M., 2009. Managing carbon emissions in China through building energy efficiency. *Journal of Environmental Management*, 90(8), pp.2436–2447.

171. Li, J. & Shui, B., 2015. A comprehensive analysis of building energy efficiency policies in China: Status quo and development perspective. *Journal of Cleaner Production*, 90, pp.326–344. Available at: http://dx.doi.org/10.1016/j.jclepro.2014.11.061.

172. Li, M., 2006. *A Study on the Price of Economical Houses*. Sichuan University.

173. Li, S., 2012. Analysis of Building Energy Consumption and Energy Saving Ways in Chengdu. *Sichuan Architecture*, 32(2), pp.43–45.

174. Li, X. & Yeh, A.G.-O., 2004. Analyzing spatial restructuring of land use patterns in a fast growing region using remote sensing and GIS. *Landscape and Urban Planning*, 69(4), pp.335–354. Available at:

http://linkinghub.elsevier.com/retrieve/pii/S0169204603002500.

175. LI, X. & ZENG, H., 2015. The Urban Form Evolution and Historical Regional Features Exploration of Chengdu City. *Journal of Human Settlements in West China*, 6, p.21.

176. Lin, B. & Zhu, J., 2017. Energy and carbon intensity in China during the urbanization and industrialization process: A panel VAR approach. *Journal of Cleaner Production*, 168, pp.780–790.

177. Lin, C. & Wang, X., 1990. Surveys of the urban heat island archipelago in west Sichuan Plain with the meteorogical satellite information. *Remote Sensing Information*, (1), pp.10–13.

178. Lin, J., 2002. *Rooted in the Mainland -- Regionalism of Urban Housing Design in Chengdu*. Chongqing University.

179. Liu, G., Wu, Z. & Hu, M., 2012. Energy Consumption and Management in Public Buildings in China: An Investigation of Chongqing. *Energy Procedia*, 14(2011), p.1. Available at: http://linkinghub.elsevier.com/retrieve/pii/S1876610211043037.

180. Liu, J. et al., 2009. Study on Energy Consumption Audit and Energy-saving Retrofit Potential for a High-rise Building in hot Summer and Cold Winter Zone. *Building Science*, 25(10), pp.21–26.

181. Liu, R., 2016. *Study on Micro Environmental Characteristics and Passive Design Method of Residential Buildings in Chengdu*. Southwest Petroleum University.

182. Liu, W. & Qin, B., 2016. Low-carbon city initiatives in China: A review from the policy paradigm perspective. *Cities*, 51, pp.131–138.

183. Liu, X. & Sweeney, J., 2012. Modelling the impact of urban form on household energy demand and related CO2 emissions in the Greater Dublin Region. *Energy Policy*, 46, pp.359–369. Available at: http://linkinghub.elsevier.com/retrieve/pii/S0301421512002753.

184. Liu, Z., 2015. China's Carbon Emissions Report 2015. *Belfer Center for Science and International Affair*, (May), pp.1–15. Available at: http://belfercenter.org/publication/25417%5Cnhttp://hks.harvard.edu/centers/mrcbg/programs/sustsci/documents/papers/2015-02.

185. Liu, Z. et al., 2013. Energy policy: A low-carbon road map for China. *Nature*, 500(7461), pp.143–145.

186. Liu, Z. et al., 2009. Low-carbon city: Concepts, international practice and implications for China. *Urban Studies*, 16(6), pp.1–7.

187. Lo, C.P., Quattrochi, D.A. & Luvall, J.C., 1997. Application of high-resolution thermal infrared remote sensing and GIS to assess the urban heat island effect. *International Journal of Remote Sensing*, 18(2), pp.287–304.

188. Long, W.D., 2005. Proportion of energy consumption of building sector and target of

building energy efficiency in China. *China Energy*, 27(10), pp.23–27.

189. Lowry, J.H. & Lowry, M.B., 2014. Comparing spatial metrics that quantify urban form. *Computers, Environment and Urban Systems*, 44, pp.59–67. Available at: http://linkinghub.elsevier.com/retrieve/pii/S0198971513001142.

190. Luederitz, C., Lang, D.J. & Wehrden, H. Von, 2013. A systematic review of guiding principles for sustainable urban neighborhood development. *Landscape and Urban Planning*, 118, pp.40–52. Available at: http://dx.doi.org/10.1016/j.landurbplan.2013.06.002.

191. Luo, J., 2005. *A Study on the Planning Design of Healthy Envrionment in High-rise Residence*. Qinghua University.

192. Luo, P. et al., 2006. An Analysis of Ecological Footprint in Chengdu and Ecological Environment Protection. *Eco Environment and Tourisim Development*, 23(3), pp.103–107. Available at: http://en.cnki.com.cn/Article_en/CJFDTOTAL-DZKG200602023.htm.

193. Ma, X. et al., 2016. Association between temperature and mortality in three cities in China. *Basic & Clinical Medicine*, 36(6), pp.805–810.

194. Marsh, A., 2010. Ecotect. Available at: www.autodesk.com/ecotect [Accessed April 20, 2013].

195. Masson, V., 2006. Urban surface modeling and the meso-scale impact of cities. *Theoretical and Applied Climatology*, 84(1–3), pp.35–45.

196. Matson, M. et al., 1978. Satellite Detection of Urban Heat Islands. *Monthly Weather Review*, 106(12), pp.1725–1734. Available at: http://journals.ametsoc.org/doi/abs/10.1175/1520-0493%281978%29106%3C1725%3ASDOUHI%3E2.0.CO%3B2.

197. Matzarakis, A., Mayer, H. & Iziomon, M.G., 1999. Applications of a universal thermal index: Physiological equivalent temperature. *International Journal of Biometeorology*, 43(2), pp.76–84.

198. Meadows, D., 1998. *Indicators and Information Systems for Sustainable*, Available at: http://www.comitatoscientifico.org/temi SD/documents/@@Meadows SD indicators.pdf.

199. Middel, A. et al., 2014. Impact of urban form and design on mid-afternoon microclimate in Phoenix Local Climate Zones. *Landscape and Urban Planning*, 122, pp.16–28.

200. Mideksa, T.K. & Kallbekken, S., 2010. The impact of climate change on the electricity market: A review. *Energy Policy*, 38(7), pp.3579–3585. Available at: http://dx.doi.org/10.1016/j.enpol.2010.02.035.

201. MOHURD, 2010. *Design Standard for Energy Efficiency of Residential Buildings in Hot Summer and Cold Winter Zones*, Beijing, China: MOHURD. Available at: http://www.china-nengyuan.com/tech/74560.html.

202. MOHURD, 2017. *Thermal Design Code for Civil Building GB50176-2016*,

203. MOHURD & AQSIQ, 2011. *Design Code for Residential Buildings*, Beijing, China.

204. MOHURD & AQSIQ, 2005. *Design standard for energy efficiency of public buildings*,

205. MOHURD & AQSIQ, 2015. *Design Standard for Energy Efficiency of Public Buildings*, Beijing.

206. MOHURD & AQSIQ, 1993. *Thermal Design Code for Civil Building GB50176-93*,

207. Moonen, P. et al., 2012. Urban Physics: Effect of the micro-climate on comfort, health and energy demand. *Frontiers of Architectural Research*, 1(3), pp.197–228.

208. Morakinyo, T.E. & Lam, Y.F., 2016. Simulation study on the impact of tree-configuration, planting pattern and wind condition on street-canyon's micro-climate and thermal comfort. *Building and Environment*, 103, pp.262–275. Available at: http://dx.doi.org/10.1016/j.buildenv.2016.04.025.

209. Moreno-garcia, M.C., 1994. Intensity and form of the urban heat island in Barcelona. *International Journal of Climatology*, 14(6), pp.705–710.

210. National Bureau of Statistics, 2015. *China Energy Statistics Yearbook 2015* Department of Energy Statistics, ed., Beijing: China Statistics Press.

211. NDRC & MOHURD, 2016. *Development Plan of Chengdu-Chongqing City Group 2016*,

212. Neuman, M., 2005. The Compact City Fallacy. *Journal of planning education and research*, 25(1), pp.11–26.

213. Ng, E. et al., 2012. A study on the cooling effects of greening in a high-density city: An experience from Hong Kong. *Building and Environment*, 47(1), pp.256–271. Available at: http://dx.doi.org/10.1016/j.buildenv.2011.07.014.

214. Ng, E. et al., 2011. Improving the wind environment in high-density cities by understanding urban morphology and surface roughness: A study in Hong Kong. *Landscape and Urban Planning*, 101(1), pp.59–74. Available at: http://linkinghub.elsevier.com/retrieve/pii/S0169204611000326.

215. Ng, E., Wong, N.H. & Han, M., 2005. Parametric studies of urban design morphologies and their implied environmental performance. In *Tropical Sustainable Architecture: Social and Environmental Dimensions*. London: Architectural Press.

216. Niu, J., 2004. Some Significant Environmental Issues in High-rise Residential Building Design in Urban Areas. *Energy and Buildings*, 36(12), pp.1259–1263.

217. Offerle, B. et al., 2006. Intraurban Differences of Surface Energy Fluxes in a Central European City. *Journal of Applied Meteorology and Climatology*, 45(1), pp.125–136. Available at: http://journals.ametsoc.org/doi/abs/10.1175/JAM2319.1.

218. Oke, T., 1989. The micrometeorology of th Urban Forest. *Jstor*, 324, pp.335–349.

219. Oke, T.R., 2002a. *Boundary layer climates*, Routledge. Available at:

http://linkinghub.elsevier.com/retrieve/pii/S036013230700251X%5Cnhttp://www.future-cities.eu/uploads/media/report_Urban_Climatic_Map_of_Arnhem_City_02.pdf%5Cnhttp://linkinghub.elsevier.com/retrieve/pii/S0360132309000766%5Cnhttp://doi.wiley.com/10.1002/joc.

220. Oke, T.R., 2002b. *Boundary layer climates* Second edi., Taylor & Francis.

221. Oke, T.R., 1981. Canyon geometry and the nocturnal urban heat island: Comparison of scale model and field observations. *Journal of climatology*, 1(3), pp.237–254.

222. Oke, T.R., 1973. City size and the urban heat island. *Atmospheric Environment Pergamon Pres*, 7, pp.769–779. Available at: http://www.sciencedirect.com/science/article/pii/0004698173901406.

223. Oke, T.R., 1984. Methods of urban climatology. In *25th International Geographical Congress*. Zurich: Geographisches Institut, ETH.

224. Oke, T.R., 1974. *Review of urban Climatology 1968-1973*,

225. Oke, T.R., 1988. Street design and urban canopy layer climate. *Energy and Buildings*, 11(1–3), pp.103–113.

226. Oke, T.R., 1982. The energetic basis of the urban heat island. *QUARTERLY JOURNAL OF THE ROYAL METEOROLOGICAL SOCIETY*, 108(455), pp.1–24.

227. Oke, T.R., 1997. Urban climates and global environmental change. In R. Thompson & A. Perry, eds. *Applied climatology: Principles & practices*. pp. 273–287.

228. Oke, T.R., 2011. Urban heat island. In *The Handbook of Urban Ecology*. pp. 120–131.

229. Okeil, A., 2010. A holistic approach to energy efficient building forms. *Energy and Buildings*, 42(9), pp.1437–1444. Available at: http://linkinghub.elsevier.com/retrieve/pii/S0378778810000903.

230. Oldfield, P., Trabucco, D. & Wood, A., 2008. Five Energy Generations of Tall Buildings: A Historical Analysis of Energy Consumption in High Rise Buildings. In *CTBUH 8th World Congress*.

231. Ong, B.L., 2003. Green Plot Ratio: An Ecological Measure for Architecture and Urban Planning. *Landscape and Urban Planning*.

232. Onishi, A. et al., 2010. Evaluating the Potential for Urban Heat-island Mitigation by Greening Parking Lots. *Urban Forestry & Urban Greening*, 9(4), pp.323–332. Available at: http://linkinghub.elsevier.com/retrieve/pii/S1618866710000403.

233. Pearlmutter, D., Berliner, P. & Shaviv, E., 2007. Integrated modeling of pedestrian energy exchange and thermal comfort in urban street canyons. *Building and Environment*, 42(6), pp.2396–2409.

234. Pearlmutter, D., Krüger, E.L. & Berliner, P., 2009. The role of evaporation in the energy balance of an open-air scaled urban surface. *International Journal of Climatology*, 29(6), pp.911–920.

235. Peng, Z., 2011. *A Research on Facade Design of Residential Based on the Requirment of Energy-saving in Buildings*. Southwest Jiaotong University.

236. Perini, K. et al., 2017. Modeling and simulating urban outdoor comfort: Coupling ENVI-Met and TRNSYS by grasshopper. *Energy and Buildings*, 152, pp.373–384.

237. Phillips, D.C. & Burbules, N.C., 2000. *Postpositivism and educational research*, Rowman & Littlefield.

238. Pigeon, G. et al., 2007. Anthropogenic heat release in an old European agglomeration (Toulouse, France). In *International Journal of Climatology*. pp. 1969–1981.

239. PMGCD, 2011. PMGCD Regional Planning Working Papers, 2011/10. *The Overall Planning of Chengdu City*.

240. Pongracz, R., Bartholy, J. & Dezso, Z., 2006. Remotely sensed thermal information applied to urban climate analysis. *Advances in Space Research*, 37(12), pp.2191–2196.

241. Potchter, O., Cohen, P. & Bitan, A., 2006. Climatic behavior of various urban parks during hot and humid summer in the Mediterranean city of Tel Aviv, Israel. *International Journal of Climatology*, 26(12), pp.1695–1711.

242. Principles, P., 2011. *Computer Modelling for Sustainable Urban Design*, Available at: http://www.tandfebooks.com/isbn/9781849775403.

243. Qiao, Z., Tian, G. & Xiao, L., 2013. Diurnal and seasonal impacts of urbanization on the urban thermal environment: A case study of Beijing using MODIS data. *ISPRS Journal of Photogrammetry and Remote Sensing*, 85, pp.93–101.

244. Qin, Z. et al., 2001. Mono-window Algorithm for Retriev ing Land Surface Temperature from Landsat TM 6 data. *Acta Geographica Sinica*, 56(4), pp.456–466.

245. Qiu, B., 2009a. From Green Building to Low Carbon Eco-City. *Urban Studies*, 7, pp.1–11.

246. Qiu, B., 2009b. The Transformation Trends of Urban Development Model in China. *Urban Studies*, 8, pp.1–6.

247. Quattrochi, D.A. et al., 2000. High Spatial Resolution Airborne Multispectral Thermal Infrared Remote Sensing Data for Analysis of Urban Landscape Characteristics.

248. Radhi, H., Fikry, F. & Sharples, S., 2013. Impacts of urbanisation on the thermal behaviour of new built up environments: A scoping study of the urban heat island in Bahrain. *Landscape and Urban Planning*, 113, pp.47–61. Available at: http://linkinghub.elsevier.com/retrieve/pii/S0169204613000200.

249. Raji, B., Tenpierik, M.J. & van den Dobbelsteen, A., 2015. The impact of greening systems on building energy performance: A literature review. *Renewable and Sustainable Energy Reviews*, 45, pp.610–623. Available at: http://linkinghub.elsevier.com/retrieve/pii/S1364032115000994.

250. Rastogi, A. et al., 2017. Impact of different LEED versions for green building certification

and energy efficiency rating system: A Multifamily Midrise case study. *Applied Energy*, 205, pp.732–740.

251. Ratti, C., Baker, N. & Steemers, K., 2005. Energy consumption and urban texture. *Energy and Buildings*, 37(7), pp.762–776.

252. Register, R., 1993. *Ecocity Berkeley: building cities for a healthy future*, North Atlantic Books.

253. Remenyi, D. et al., 1998. *Doing research in business and management: an introduction to process and method*, Sage.

254. Ren, W. et al., 2014. Study on of Remote Sensing Monitoring and Evolution Characteristics of Urban Expansion Chengdu City. *Journal of Gansu Sciences*, 26(2), pp.15–21.

255. Resch, E. et al., 2016. Impact of Urban Density and Building Height on Energy Use in Cities. *Energy Procedia*, 96, pp.800–814.

256. Rizwan, A.M., Dennis, L.Y.C. & Liu, C., 2008. A review on the generation, determination and mitigation of Urban Heat Island. *Journal of Environmental Sciences*, 20(1), pp.120–128. Available at: http://www.sciencedirect.com/science/article/pii/S1001074208600194.

257. RIZWAN, A.M., DENNIS, L.Y.C. & LIU, C., 2008. A review on the generation, determination and mitigation of Urban Heat Island. *Journal of Environmental Sciences*, 20(1), pp.120–128.

258. Robinson, D., 2006. Urban morphology and indicators of radiation availability. *Solar Energy*, 80(12), pp.1643–1648. Available at: http://linkinghub.elsevier.com/retrieve/pii/S0038092X06000612.

259. Rode, P., 2014. Cities and Energy: Urban Morphology and Heat Energy Demand. *LSE Cities*, pp.227–249. Available at: https://lsecities.net/publications/reports/cities-and-energy-urban-morphology-and-heat-energy-demand/.

260. Rode, P. & Burdett, R., 2011. Cities : investing in energy and resource efficiency. In C. Ed., ed. *Towards a green economy: pathways to sustainable development and poverty eradication*. United Nations Environment Programme: United Nations Environment Programme, pp. 453–492. Available at: http://www.unep.org/greeneconomy/greeneconomyreport/tabid/29846/default.aspx.

261. Rosenfeld, A.H. et al., 1995. Mitigation of urban heat islands: materials, utility programs, updates. *Energy and Buildings*, 22(3), pp.255–265.

262. Roth, M., 2002. Effects of cities on local climates. *Proceedings of Workshop of IGES/APN Mega-City Project*, 2002(January 2002), pp.1–13.

263. Roth, M., Oke, T.R. & Emery, W.J., 1989. Satellite-derived urban heat islands from 3 coastal cities and the utilization of such data in urban climatology. *Int. J. Remote Sens.*, 10, pp.1699–1720. Available at: http://dx.doi.org/10.1080/01431168908904002.

264. Run, M., Yu, C. & Wang, B., 2002. Research on High-rise Building and Its Urban Ecological Environment. *Industrial Construction*, 32(3), pp.16–18.

265. Saito, I., Ishihara, O. & Katayama, T., 1990. Study of the effect of green areas on the thermal environment in an urban area. *Energy and Buildings*, 15(3–4), pp.493–498.

266. Salata, F. et al., 2016. Urban microclimate and outdoor thermal comfort. A proper procedure to fit ENVI-met simulation outputs to experimental data. *Sustainable Cities and Society*, 26, pp.318–343.

267. Santamouris, M., 2013. *Energy and climate in the urban built environment*, Routledge.

268. Sarkar, A., Energy, L. & Block, U., 2009. Low Energy Urban Block : Morphology and planning guidelines. In *45th ISOCARP Congress*. pp. 1–10.

269. Saunders, M., Lewis, P. & Thornhill, A., 2008. *Research Methods for Business Students*,

270. SCDOHURD, 2012. *Design Standard for Energy Efficiency of Residential Buildings in Sichuan Province*, China: Sichuan Department of Housing and Urban and Rural Construction.

271. Schlesinger, M.E. & Ramankutty, N., 1992. Implications for Global Warming of Intercycle Solar Irradiance Variations. *Nature*, 360, pp.330–333.

272. Schwartz, Y. & Raslan, R., 2013. Variations in results of building energy simulation tools, and their impact on BREEAM and LEED ratings: A case study. *Energy and Buildings*, 62, pp.350–359. Available at: http://dx.doi.org/10.1016/j.enbuild.2013.03.022.

273. Shashua-Bar, L. & Hoffman, M.E., 2000. Vegetation as a climatic component in the design of an urban street. *Energy and Buildings*, 31(3), pp.221–235. Available at: http://www.sciencedirect.com/science/article/pii/S0378778899000183.

274. Shashua-Bar, L., Pearlmutter, D. & Erell, E., 2011. The influence of trees and grass on outdoor thermal comfort in a hot-arid environment. *International Journal of Climatology*, 31(10), pp.1498–1506.

275. Shashua-Bar, L., Tsiros, I.X. & Hoffman, M.E., 2010. A modeling study for evaluating passive cooling scenarios in urban streets with trees. Case study: Athens, Greece. *Building and Environment*, 45(12), pp.2798–2807.

276. Shashua-Bar, L., Tzamir, Y. & Hoffman, M.E., 2004. Thermal Effects of Building Geometry and Spacing on the Urban Canopy Layer Microclimate in a Hot-humid Climate in Summer. *International Journal of Climatology*, 24(13), pp.1729–1742.

277. Simon, H., 2016. *Modeling urban microclimate:Development, implementation and evaluation of new and improved calculation methods for the urban microclimate model ENVI-met*. Uniersity of Mainz. Available at: http://www.envi-met.info/lists/lt.php?id=ZkwBC0hUAE8CCFtR.

278. Skelhorn, C., Lindley, S. & Levermore, G., 2014. The impact of vegetation types on air and surface temperatures in a temperate city: A fine scale assessment in Manchester,

UK. *Landscape and Urban Planning*, 121, pp.129–140.

279. Smith, C. & Levermore, G., 2008. Designing urban spaces and buildings to improve sustainability and quality of life in a warmer world. *Energy Policy*, 36(12), pp.4558–4562. Available at: http://linkinghub.elsevier.com/retrieve/pii/S0301421508004825.

280. Sonne, J.K. & Vieira, R.K., 2000. Cool Neighborhoods: The Measurement of Small Scale Heat Islands. *Proceedings ACEEE Summer Study on Energy Efficiency in Buildings*, 1(Heisler), pp.1307–1318. Available at: http://aceee.org/files/proceedings/2000/data/papers/SS00_Panel1_Paper26.pdf%0Ahttp://www.scopus.com/scopus/inward/record.url?eid=2-s2.0-0034581275&partnerID=40&rel=R7.0.0.

281. State Council of the PRC, 1998. Notice of the State Council on Further Deepening the Reform of Urban Housing System and Accelerating Housing Construction. Available at: https://wenku.baidu.com/view/d89d86c04028915f804dc2ac.html [Accessed April 20, 2018].

282. Steadman, P., Hamilton, I. & Evans, S., 2014. Energy and urban built form: an empirical and statistical approach. *Building Research & Information*, 42(1), pp.17–31. Available at: http://www.tandfonline.com/doi/abs/10.1080/09613218.2013.808140.

283. Steemers, K., 2003. Energy and the city: Density, buildings and transport. *Energy and Buildings*, 35(1), pp.3–14.

284. Steyn, D.G. et al., 1981. On scales in meteorology and climatology. *Climatological Bulletin*, 39, pp.1–8.

285. Stone, B. & Rodgers, M.O., 2001. Urban Form and Thermal Efficiency: *How the Design of Cities Influences the Urban Heat Island Effect*. *Journal of the American Planning Association*, 67(2), pp.186–198. Available at: http://www.tandfonline.com/doi/abs/10.1080/01944360108976228.

286. Strømann-Andersen, J. & Sattrup, P. a., 2011. The urban canyon and building energy use: Urban density versus daylight and passive solar gains. *Energy and Buildings*, 43(8), pp.2011–2020. Available at: http://linkinghub.elsevier.com/retrieve/pii/S0378778811001605.

287. Stupka, R. & Kennedy, C., 2010. Impact of Neighborhood Density on Building Energy Demand and Potential Supply via the Urban Metabolism. *2010 ACEEE Summer Study on Energy Efficiency in Buildings*, 2020, pp.239–252. Available at: http://www.aceee.rste040vlmp01.blackmesh.com/files/proceedings/2010/data/papers/2262.pdf.

288. Su, H. et al., 2010. Investigation of energy consumption of public buildings in Chengdu. *Sichuan Building Science*, 36(4), pp.291–294.

289. Sundborg, A., 1950. Local Climatological Studies of the Temperature Conditions in an Urban Area. *Tellus*, 2(3), pp.222–232. Available at: http://www.tellusa.net/index.php/tellusa/article/view/8544.

290. Taha, H. et al., 1992. Causes and effects of heat islands: sensitivity to surface parameters and anthropogenic heating. *Lawrence Berkeley Lab. Rep*, (29864).

291. Taha, H., 1997a. *Modeling the impacts of large-scale albedo changes on ozone air quality in the South Coast Air Basin*,

292. Taha, H. et al., 1988. Residential cooling loads and the urban heat island—the effects of albedo. *Building and environment*, 23(4), pp.271–283.

293. Taha, H., 1997b. Urban climates and heat islands: albedo, evapotranspiration, and anthropogenic heat. *Energy and Buildings*, 25(2), pp.99–103. Available at: http://linkinghub.elsevier.com/retrieve/pii/S0378778896009991.

294. Takebayashi, H. & Moriyama, M., 2012. Relationships between the properties of an urban street canyon and its radiant environment: Introduction of appropriate urban heat island mitigation technologies. *Solar Energy*, 86(9), pp.2255–2262.

295. Taleghani, M. et al., 2015. Outdoor thermal comfort within five different urban forms in the Netherlands. *Building and Environment*, 83, pp.65–78. Available at: http://dx.doi.org/10.1016/j.buildenv.2014.03.014.

296. Tan, J. et al., 2010. The urban heat island and its impact on heat waves and human health in Shanghai. *International Journal of Biometeorology*, 54(1), pp.75–84.

297. Taylor, T.A., 2010. *Guide to LEED 2009 estimating and preconstruction strategies*, New Jersey: John Wiley & Sons.

298. Tian, Y. & Jim, C.Y., 2012. Development potential of sky gardens in the compact city of Hong Kong. *Urban Forestry and Urban Greening*, 11(3), pp.223–233. Available at: http://dx.doi.org/10.1016/j.ufug.2012.03.003.

299. Todhunter, P.E., 1990. Microclimatic variations attributable to urban-canyon asymmetry and orientation. *Physical geography*, 11(2), pp.131–141.

300. Tomlinson, C.J. et al., 2012. Derivation of Birmingham's summer surface urban heat island from MODIS satellite images. *International Journal of Climatology*, 32(2), pp.214–224.

301. Torrens, P.M. & Alberti, M., 2000. *Measuring Sprawl*, Available at: http://discovery.ucl.ac.uk/1370/1/paper27.pdf.

302. Tourism Administration Network of Chengdu, 2017. A Brief Introduction on Chengdu. Available at: http://www.cdta.gov.cn/show-87-27748-1.html.

303. Tran, H. et al., 2006. Assessment with satellite data of the urban heat island effects in Asian mega cities. *International Journal of Applied Earth Observation and Geoinformation*, 8(1), pp.34–48.

304. Tsai, Y.H., 2005. Quantifying Urban Form: Compactness versus 'Sprawl.' *Urban studies*, 42(1), pp.141–161.

305. Turak, T., 1985. Remembrances of the Home Insurance Building. *Journal of the Society*

of Architectural Historians, 44(1), pp.60–65.

306. U.S. Green Building Council (USGBC), 2016. Checklist: LEED v4 for Building Design and Construction. *5 Apr 2016*. Available at: https://www.usgbc.org/resources/leed-v4-building-design-and-construction-checklist [Accessed January 1, 2017].

307. UN-DESA, 2008. *Sustainable Cities, Human Mobility and International Migration*,

308. UN-HABITAT, 2011. *Global Report on Human Settlements 2011: Citites and Climate Change*, London: Gutenberg Press. Available at: http://www.zaragoza.es/contenidos/medioambiente/onu/538-eng-ed2011.pdf.

309. UNFCCC, 2016. *Adoption of the Paris Agreement*, Available at: http://unfccc.int/resource/docs/2015/cop21/eng/l09r01.pdf.

310. UNFCCC, 2015. Report of the Conference of the Parties on its twenty-first session, held in Paris from 30 November to 13 December 2015. *Addendum-Part two: action taken by the Conference of the Parties*, 01194(January), pp.1–36. Available at: http://unfccc.int/resource/docs/2015/cop21/eng/10a01.pdf.

311. Unger, J., 2008. Connection between urban heat island and sky view factor approximated by a software tool on a 3D urban database. *International Journal of Environment and Pollution*, 36(1–3), pp.59–80.

312. Unger, J., 2004. Intra-urban relationship between surface geometry and urban heat island: review and new approach. *Climate Research*, 27, pp.253–264.

313. Unwin, D.J., 1980. The Synoptic Climatology of Birmingham's UHI, 1965-74. *Weather*, 35(2), pp.43–50.

314. Upmanis, H. & Chen, D., 1999. Influence of geographical factors and meteorological variables on nocturnal urban-park temperature differences-a case study of summer 1995 in Goteborg, Sweden. *Climate Research*, 13(2), pp.125–139.

315. Vardoulakis, E. et al., 2013. The urban heat island effect in a small Mediterranean city of high summer temperatures and cooling energy demands. *Solar Energy*, 94, pp.128–144. Available at: http://linkinghub.elsevier.com/retrieve/pii/S0038092X13001564.

316. Voogt, J.A. & Oke, T.R., 2003. Thermal remote sensing of urban climates. *Remote Sensing of Environment*, 86(3), pp.370–384.

317. Wan, Z., Zhang, Y., Zhang, Q. and Li, Z.L., 2004. Quality assessment and validation of the MODIS global land surface temperature. *International journal of remote sensing*, 25(1), pp.261–274.

318. Wan, Z. and Dozier, J., 1996. A Generalized Split- Window Algorithm for Retrieving Land-Surface Temperature from Space. *IEEE Transactions on geoscience and remote sensing*, 34(4), pp.892–905.

319. Wan, H., 2004. *Eco-cities Paradigm Research*. Beijing Normal University.

320. Weather Underground, 2014. History of Weather Data. Available at:

https://www.wunderground.com/ [Accessed June 6, 2016].

321. Wei, F., Fgeng, Z. & Hu, J., 1997. Population Viability Analysis Computer Model of Giant Panda Population in Wuyipeng, Wolong Natural Reserve, China. *Bears: Their Biology and Management*, 9(ArticleType: research-article / Issue Title: Part 2: A Selection of Papers from the Ninth International Conference on Bear Research and Management, Grenoble, France, October 1992 / Full publication date: 1997 / Copyright © 1997 International Association o), pp.19–23. Available at: http://www.jstor.org/stable/3872656.

322. Weng, Q., 2001. A remote sensing – GIS evaluation of urban expansion and its impact on surface temperature in the Zhujiang Delta , China. *Int. J. Remote Sensing*, 22(10), pp.1999–2014.

323. Weng, Q., Lu, D. & Schubring, J., 2004. Estimation of land surface temperature-vegetation abundance relationship for urban heat island studies. *Remote Sensing of Environment*, 89(4), pp.467–483.

324. Wiedenhofer, D., Lenzen, M. & Steinberger, J.K., 2013. Energy requirements of consumption: Urban form, climatic and socio-economic factors, rebounds and their policy implications. *Energy Policy*, 63, pp.696–707.

325. Wilson, B., 2013. Urban form and residential electricity consumption: Evidence from Illinois, USA. *Landscape and Urban Planning*, 115, pp.62–71. Available at: http://linkinghub.elsevier.com/retrieve/pii/S0169204613000601.

326. Winter, C.J., 1994. Solar cities. *Renewable energy*, 4(1), pp.15–26.

327. Wolsink, M., 2016. “Sustainable City” requires ’recognition’-The example of environmental education under pressure from the compact city. *Land Use Policy*, 52, pp.174–180. Available at: http://dx.doi.org/10.1016/j.landusepol.2015.12.018.

328. Wong, N.H. et al., 2011. Evaluation of the impact of the surrounding urban morphology on building energy consumption. *Solar Energy*, 85(1), pp.57–71. Available at: http://linkinghub.elsevier.com/retrieve/pii/S0038092X10003294.

329. Wong, N.H. & Chen, Y., 2008. *Tropical urban heat islands: climate, buildings and greenery*, Routledge.

330. Wong, N.H. & Yu, C., 2005. Study of green areas and urban heat island in a tropical city. *Habitat International*, 29(3), pp.547–558.

331. Wootton-Beard, P. et al., 2016. Review: Improving the Impact of Plant Science on Urban Planning and Design. *Buildings*, 6(4), p.48. Available at: http://www.mdpi.com/2075-5309/6/4/48.

332. WSA, 2015. VirVil SketchUp Extension. Available at: http://u001.arch.cf.ac.uk/plugin/ [Accessed April 20, 2015].

333. Wu, S. & Yang, G., 2013. Research and Design of Greeninghouse on Climate Conditions-with the Disscussion of Greeninghouse Desigh which is to Acclimatise to Regional of Chengdu Climatic Features as an Example. *Architecture & Culture*, (11),

pp.128–131.

334. Wu, Y., 2016. History of High-rise Building in China. Available at: https://wenku.baidu.com/view/7ae56f536529647d262852c2.html [Accessed April 20, 2018].

335. Wu, Z., 2012. Investigation Report on High-rise Housing Market in Chengdu. Available at: http://www.doc88.com/p-576886374920.html [Accessed April 20, 2018].

336. Xia, J., Dan, S. & Chen, G., 2007. Analysis of relation between trend of heat island effect and urban development in Chengdu. *JOURNAL OF CHENGDU UNIVERSITY OF INFORMATION TECHNOLOGY*, 22(Suppl.), pp.6–11.

337. Xie, L. & Sun, Q., 2007. The Existing Problems and Countermeasures of the Affordable Housing in Chengdu. *Journal of Chengdu University (SOCIAL SCIENCE EDITION)*, (3), pp.60–62.

338. Xin, F., 2008. *Study on the problems of affordable housing and low rent housing in Chengdu*. Southwestern University of Finance and Economics.

339. Xing, Y., 2015. *Passive Technology and Energy Performance Analysis of Chengdu Residential Building*. Xi'an University Of Architecture And Technology.

340. Xing, Y., Jones, P. & Donnison, I., 2017. Characterisation of nature-based solutions for the built environment. *Sustainability (Switzerland)*, 9(1).

341. Xu, H. et al., 2007. Remote Sensing Analysis of Urban Heat Island Effect in Chengdu Plain. *Envrionmental Science and Technology*, 30(8), pp.21–23.

342. Xu, L. et al., 2013. Building energy saving potential in Hot Summer and Cold Winter (HSCW) Zone, China—Influence of building energy efficiency standards and implications. *Energy Policy*, 57, pp.253–262. Available at: http://linkinghub.elsevier.com/retrieve/pii/S030142151300075X.

343. Xu, P. et al., 2013. Commercial building energy use in six cities in Southern China. *Energy Policy*, 53, pp.76–89. Available at: http://linkinghub.elsevier.com/retrieve/pii/S0301421512008592.

344. Xu, W. et al., 2007. Analysis of Coordinated Development between Eco-environment and Socio-economy in Chengdu City. *Journal of Catastrophology*, 22(1), pp.129–133.

345. Xu, X. et al., 2012. The impact of place-based affiliation networks on energy conservation: An holistic model that integrates the influence of buildings, residents and the neighborhood context. *Energy and Buildings*, 55, pp.637–646.

346. Yaghoobian, N. & Srebric, J., 2015. Influence of Plant Coverage on the Total Green Roof Energy Balance and Building Energy Consumption. *Energy and Buildings*, 103, pp.1–13.

347. Yamashita, S. et al., 1986. On relationships between heat island and sky view factor in the cities of Tama River basin, Japan. *Atmospheric Environment (1967)*, 20(4), pp.681–686.

348. Yang, B., 1988. Research on the Urban Hot Island Effect in Chengdu. *Journal of Chengdu Meteorological Institute*, 7(2), pp.50–59.

349. Yang, F., Lau, S.S.Y. & Qian, F., 2011. Urban design to lower summertime outdoor temperatures: An empirical study on high-rise housing in Shanghai. *Building and Environment*, 46(3), pp.769–785. Available at: http://linkinghub.elsevier.com/retrieve/pii/S0360132310003021.

350. Yang, S.R. & Lin, T.P., 2016. An integrated outdoor spaces design procedure to relieve heat stress in hot and humid regions. *Building and Environment*, 99, pp.149–160. Available at: http://dx.doi.org/10.1016/j.buildenv.2016.01.001.

351. Yang, X., 2000. Studies on History and Present of the Downtown of Chengdu City. In *Anthology of architectural history*. pp. 36–52.

352. Yang, Y., 2008. *Study on Urban Block Scale*. Southeast University.

353. Yao, R. et al., 2017. Temporal trends of surface urban heat islands and associated determinants in major Chinese cities. *Science of the Total Environment*, 609, pp.742–754.

354. Yao, R., Luo, Q. & Li, B., 2011. A simplified mathematical model for urban microclimate simulation. *Building and Environment*, 46(1), pp.253–265. Available at: http://linkinghub.elsevier.com/retrieve/pii/S0360132310002246.

355. Yin, H., 2007. *Study on the Spatial Form of Small and Medium-sized High-Rise residential buildings -- Taking Chengdu as an example*. Southwest Jiaotong University.

356. Yu, C. & Hien, W.N., 2006. Thermal benefits of city parks. *Energy and Buildings*, 38(2), pp.105–120. Available at: http://linkinghub.elsevier.com/retrieve/pii/S0378778805000794.

357. Yu, J., Yang, C. & Tian, L., 2008. Low-energy envelope design of residential building in hot summer and cold winter zone in China. *Energy and Buildings*, 40(8), pp.1536–1546.

358. Yu, L., 2014. Low carbon eco-city: New approach for Chinese urbanisation. *Habitat International*, 44, pp.102–110.

359. Yuen, B. et al., 2006. High-rise Living in Singapore Public Housing. , 43(3), pp.583–600.

360. Zang, X., 2013. The Construction of Technical Indicator System for Eco-Cities at Blocks Scale. *Urban Planning Forum*, (4), pp.81–87.

361. Zengcui, M., 2010. *The Preliminary Research on the Integration of Building Complex with Urban Space*. Tianjin University.

362. Zhang, C., 2008. On the Health Design of Modern High-rise Building. *Shanxi Architecture*, 34(27), pp.79–80.

363. Zhang, C. & Zhang, L., 2013. Research on Construction of Low-carbon City in Chengdu. *Reform of Economic System*, pp.37–42.

364. Zhang, H. et al., 2014. Analysis of the Relationship between Urban Heat Island Effect and Urban Expansion in Chengdu, China. *JOURNAL OF GEO-INFORMATION SCIENCE*, 16(1), pp.70–78.

365. Zhang, J., 2013. A study of the relationship between urban form and environmental performance for three urban block typologies in Paris. , 45, pp.170–179. Available at: http://www.scopus.com/inward/record.url?eid=2-s2.0-84876847777&partnerID=40&md5=9d6125fbd4c81fe8c4fb09b74526fd54.

366. Zhang, J. et al., 2012. Evaluating environmental implications of density: A comparative case study on the relationship between density, urban block typology and sky exposure. *Automation in Construction*, 22, pp.90–101. Available at: http://linkinghub.elsevier.com/retrieve/pii/S0926580511001233.

367. Zhang, J., Wang, Y. & Wang, Z., 2007. Change analysis of land surface temperature based on robust statistics in the estuarine area of Pearl River (China) from 1990 to 2000 by Landsat TM / ETM + data. , 28(10), pp.2383–2390.

368. Zhang, S.-Q.. b & Zhou, C.-Y.., 2013. Spatiotemporal distribution characteristics and causes of sunny days' heat island effect in Chengdu City of Southwest China. *Chinese Journal of Applied Ecology*, 24(7), pp.1962–1968. Available at: http://www.scopus.com/inward/record.url?eid=2-s2.0-84882980792&partnerID=40&md5=8c697238c23c3fa164bab7828c1c232b.

369. Zhang, W. & Cheng, W., 2016. A Research on Dynamic Changes of the Summer Heat Island Effect in Chengdu. *Hubei Agricultural Sciences*, 55(4), pp.883–886.

370. Zhang, Z. & Tang, J., 2014. *An Overview of China's Regional Culture - Sichuan Volume* 1st ed. Z. Zhang & J. Tang, eds., Beijing: Zhong Hua Book Company.

371. Zhao, C. et al., 2011. Urban planning indicators, morphology and climate indicators: A case study for a north-south transect of Beijing, China. *Building and Environment*, 46(5), pp.1174–1183. Available at: http://linkinghub.elsevier.com/retrieve/pii/S0360132310003616.

372. Zhao, Q., Li, P. & Zhou, P., 2002. Geochemical Features of Ecologic Environment in Chengdu City. *Acta Geologica Sichuan*, 22(4), pp.231–235.

373. Zhao, T., 2010. *Investigation on Energy Consumption and Analysis on Energy Effciency for Residential Buildings in Chengdu*. University of West China.

374. Zhou, J., 2006. The Energy Consumption Problem of the High-rise Building and Its Countermeasre. *Chongqing Architecture*, 10(5), pp.18–22.

375. Zhou, N., He, G. & Williams, C., 2012a. China's Development of Low-Carbon Eco-Cities and Associated Indicator Systems. , (July), p.39.

376. Zhou, N., He, G. & Williams, C., 2012b. China ' s Development of Low - Carbon Eco-Cities and Associated Indicator Systems. , (July).

377. Zhou, Y., 2011. Investigation of Out-door Space and Neighborhood of High Residential

Buildings in Chengdu. *Value Project*, 30(25), pp.306–306.